Tuning the Sulfonyl Fluoride Warhead towards New Proteasome Inhibitors: Alpha-substituted Sulfonyl Fluorides and Vinyl Sulfonyl Fluorides

Lcda. Química Natalia Herrero Álvarez

Thesis submitted in fulfilment of the requirements for the degree of Doctor of Philosophy

School of Chemistry

College of Science and Engineering

University of Glasgow

June 2017

Abstract

Sulfonyl fluorides have recently been described as “privileged warheads” in chemical biology due to the right balance of reactivity and stability that these electrophiles possess. Peptido sulfonyl fluorides (ß-PSFs) have shown to be particularly potent as proteasome inhibitors in recent years. Tuning the reactivity of the sulfonyl fluoride electrophilic trap may be crucial for modulating its biological action.

The first part of this thesis describes the design and synthesis of peptido sulfonyl fluoride derivatives containing a substituent on the alpha position with respect to the sulfonyl fluoride electrophilic trap. Therefore, the chemical reactivity and biological activity of α-substituted sulfonyl fluorides (αSFs) were studied. Comparison with the previously described ß-substituted sulfonyl fluorides (ßSFs) was performed as an attempt to get a deeper insight into the importance of the immediate structural environment of the sulfonyl fluoride moiety. αSFs proved to be more reactive than ßSFs towards nucleophilic substitution, including hydrolysis. However, it could not be clarified as yet if and how this is translated to the bio-activity of the resulting α-PSFs since the poor solubility of these molecules precluded a proper evaluation.

The second part of this thesis describes the synthesis of a vinyl sulfonyl fluoride moiety as a new dual warhead class. The consecutive attack of the two nucleophiles of the proteasome active threonine on the double bond and the sulfonyl fluoride was proposed as the inhibition mechanism which should lead to the formation of a seven-membered covalent adduct. *In vitro* studies were designed in order to test this hypothesis. Although the formation of the proposed seven-membered ring structure could not be unambiguously demonstrated with the chosen model systems, the crystal structure confirmed this formation within enzymatic environment. Incorporation of vinyl sulfonyl fluoride warhead into peptide backbones (PVSF) resulted in strong proteasome inhibitors (IC_{50} = 99 and 218 nM).

Declaration

I declare that, except where explicit reference is made to the contribution of others, the substance of this thesis is the result of my own work and has not been submitted for any other degree at the University of Glasgow or any other institution.

Natalia Herrero Alvarez

Prof Rob M. J. Liskamp

Parts of this thesis have been published:

Herrero Alvarez, N.; van de Langemheen, H.; Brouwer, A. J.; Liskamp, R. M. J. "Potential peptidic proteasome inhibitors by incorporation of an electrophilic trap based on amino acid derived α-substituted sulfonyl fluorides" *Bioorganic Med. Chem.* **2017**, 25 (19), 5055-5063.

Herrero Alvarez, N.; Brouwer, A. J.; Ciaffoni, A.; van de Langemheen, H.; Liskamp, R. M. J. "Proteasome inhibition by new dual warhead containing peptido vinyl sulfonyl fluoride" *Bioorganic Med. Chem.* **2016**, *24* (16), 3429–3435.

Acknowledgements

Firstly, I would like to thank my supervisor Prof. Rob Liskamp for giving me the great opportunity to undertake this research project. His continuous support and encouragement throughout my time as a PhD student have been invaluable.

I would like to thank all the past and present members of the Liskamp group for providing a great work environment and sharing with me the ups and downs of doing a PhD. Such a different combination of characters made it very pleasant in and outside the lab. Also I thank the members of the Clark group for adopting me, for the stimulating discussions and for countless pub evenings.

Very special thanks to Anna for her determination to always see the bright side of life, for being not only pretty but also naive. It has been a pleasure to share with her the passion for food and wine. And also to Tina for her constant reminder that we are not conventional people.

I would like to mention the friends, who for various and unexpected reasons, happened to share chapters of their lifes with me in Glasgow. Thanks to Tamara and Edu, Mar, Ana and Alvaro; for their company and support, for bringing a bit of sunshine with them and making my time in here definitely better.

Thanks to Grazia for building up our little safe place, our refuge, a place to call home. 4 years of laughter and tears, stories and secrets, afternoon acoustic, soups and spaghettis. Because we owe everything to spaghettis.

My most sincere gratitude goes to Kirsten, Michael and Aurélien, my other family. Without them these four years would have never been the same and Glasgow would have never been my home. Thanks to Kirsten for sharing with me true happiness and pain along the way, the best definition of friendship. No one would have ever understood me better than her in a “hating day”. Thanks to Michael for his immense patience listening to my dramas, for his priceless company and for Chinese Sunday nights. Thanks to Aurélien for all the moments of pure laughter, for Arran, for being such a great heavy princess and particularly for giving me the best birthday cheese ever seen.

A Raik, mi compañero, mi equipo. For sharing with me every little step of these four years, hell and heaven, beginning to end. For driving me crazy in every possible sense, for the lemonades and for recovering my smile. Thanks for staying, for making it with me through the day and specially for making sure tomorrow will never be the same, it will be better.

A mis padres, por su apoyo incondicional en cada paso del camino, que no ha sido fácil, por nunca dejar de creer en mí. Por compartir conmigo cada logro y cada derrota, por las alegrías y las noches en vela, por enseñarme a ganar y a perder. Por ayudarme a convertirme en la mujer que soy hoy, porque sin ellos esto no habría sido posible, este éxito conseguido con tanto esfuerzo es tan suyo como mío. Gracias.

List of Abbreviations

aa	amino acid
Ac	acetyl
AESBF	4-(2-aminoethyl)benzenesulphonyl fluoride
AMC	7-Amido-4-methylcoumarin
aq.	aqueous
ATP	adenosine triphosphate
Bn	benzyl
Boc	*tert*-Butyloxycarbonyl
BOP	(Benzotriazol-1-yloxy)tris(dimethylamino)phosphonium hexafluorophosphate
calc.	calculated
Cbz	carboxybenzyl
cCP	constitutive proteasome core particle
CP	proteasome core particle proteasome core particle
DBU	1,8-diazabicyclo[5.4.0]undect-7-ene
DCC	dicyclohexylcarbodiimide
DCE	dichloroethane
DCU	dicyclohexyl urea
DEAD	diethyl azodicarboxylate
DEPT	distortionless enhancement by polarisation transfer
DiPEA	*N*,*N*-diisopropylethylamine
DME	dimethoxyethane
DMF	*N*,*N*-dimethylformamide
DMSO	dimethyl sulfoxide
d*r*	diastereomeric ratio
EDC	*N*-(3-Dimethylaminopropyl)-*N*′-ethylcarbodiimide
ee	enantiomeric excess
equiv.	equivalent
ESI	electrospray ionisation
FDA	US Food and Drug Administration

Fmoc	fluorenylmethyloxycarbonyl
HCTU	2-(6-Chloro-1-H-benzotriazole-1-yl)-1,1,3,3-tetramethylaminium hexafluorophosphate
HFIP	hexafluoroisopropanol
HOBt	1-hydroxybenzotriazole
HPLC	high pressure chromatography
HRMS	high resolution mass spectroscopy
IC_{50}	half maximal inhibitory concentration
*i*CP	immunoproteasome core particle
IFN	interferon
IPA	isopropanol
K*i*	constant of inhibition
*m*CPBA	meta-chloroperoxybenzoic acid
Me	methyl
MHC	major histocompatibility complex
Morph	morpholino
Ms	mesyl
NBS	*N*-bromosuccinimide
n-hex	*n*-hexane
NMM	*N*-methylmorpholine
Nu	nucleophile
P	protecting group
PBS	phosphate-buffered saline
PE	petroleum ether
Ph	phenyl
PMSF	phenylmethyl sulfonyl fluoride
P_n	substrate residue
PSF	peptido sulfonyl fluoride
quant.	quantitative
R	generalised group
Rpn	regulatory particle non-ATPase
Rpt	regulatory particle tripleA-ATPase

RT	room temperature
S	substrate binding pocket
SAR	structure-activity relationship
SF	sulfonyl fluoride
S_N	nucleophilic substitution
TBDMS	*tert*-butyldimethylsilyl
TBDPS	*tert*-butyldiphenylsilyl
TFA	trifluoroacetic acid
THF	tetrahydrofuran
ThrN	nuclephilic amine of the catalytic threonine
ThrO	nuclephilic hydroxyl of the catalytic threonine
TLC	thin layer chromatography
Tris	trisaminomethane
UPS	Ubiquitin-Proteasome System
VSF	vinyl sulfonyl fluoride

Table of Contents

1. Introduction

Proteases are one of the largest families of enzymes found in nature.[1] They selectively catalyse the hydrolysis of peptide bonds by mediating a nucleophilic attack on the carbonyl carbon of the scissile amide bond. To this end, the residues which configure the active site of the enzyme either directly perform the nucleophilic attack (enzyme-activated nucleophile) or assist it by activating a nucleophilic water molecule (enzyme-bound water).[2]

Based on the exact mechanism of cleavage and the active residues affecting it, proteases are divided into four major classes: aspartic-, serine-, cysteine- and metallo-proteases (**Figure 1**).[3] **a**) Aspartic proteases: two aspartic residues form a catalytic diad. The ionised Asp activates a water molecule which acts as the nucleophile and the unionised Asp donates a proton to the nitrogen of the scissile amide bond. **b**) Serine proteases: the serine residue provides a hydroxyl group which is activated by an Asp and a His residue, effecting the nucleophilic attack. **c**) Cysteine proteases: the cysteine residue provides a thiol group which is activated by a His residue. The resulting thiolate is highly nucleophilic and performs the attack. **d**) Metallo-proteases: a zinc cation, which is tetrahedrally coordinated, activates a water molecule by ligation. The nucleophilic attack is performed by the zinc-bound water.

Serine proteases represent almost one-third of all proteases[4] and nearly 1% of all proteins in mammals.[5]

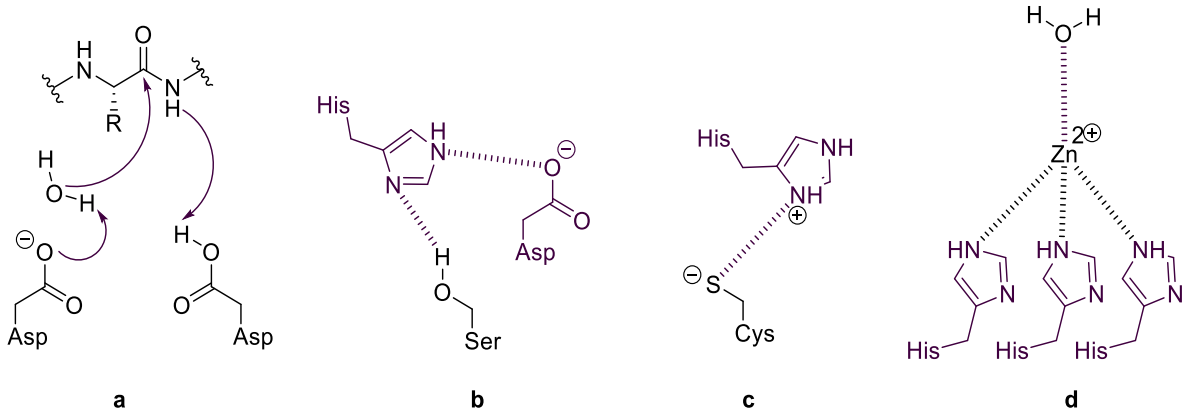

Figure 1 Active site amino acid residues in the four major classes of proteases.

Proteases regulate protein synthesis and turnover. They are therefore involved in many physiological processes such as digestion, blood coagulation, cell growth and migration, tissue arrangement, immunological defence, inflammation, healing and apoptosis.[6]

1.1 26S Proteasome and the Ubiquitin-Proteasome System

The 26S proteasome is a multisubunit protease composed of a core particle (CP), termed as the 20S proteasome, and two regulatory particles (RP), denoted as 19S particles, which cap the central core particle at both ends.[7] This large complex of over 2.5 MDa is responsible for the degradation of proteins by an ATP-dependent process *via* the Ubiquitin-Proteasome System (UPS).[8]

The UPS is the main cytosolic proteolytic system in eukaryotic cells and is therefore essential for the maintenance of protein homeostasis, i.e. the steady level of protein concentrations in the cell as a result of a strictly regulated rate of synthesis and degradation.[9] Selective degradation of proteins *via* this pathway is a highly controlled process regulated at multiple levels by a complex machinery of enzymes which mediate the ubiquitination of the target substrate for proteasomal recognition. A poly-ubiquitin chain is attached to the target substrate by the E1, E2 and E3 enzyme cascade. The tagged protein is recognised and unfolded by the regulatory particles (RP) of the 26S proteasome and hydrolysed to smaller peptides by the core particle (CP). Ubiquitin units are recycled by deubiquitylating enzymes (DUBs) (**Figure 2**).[10]

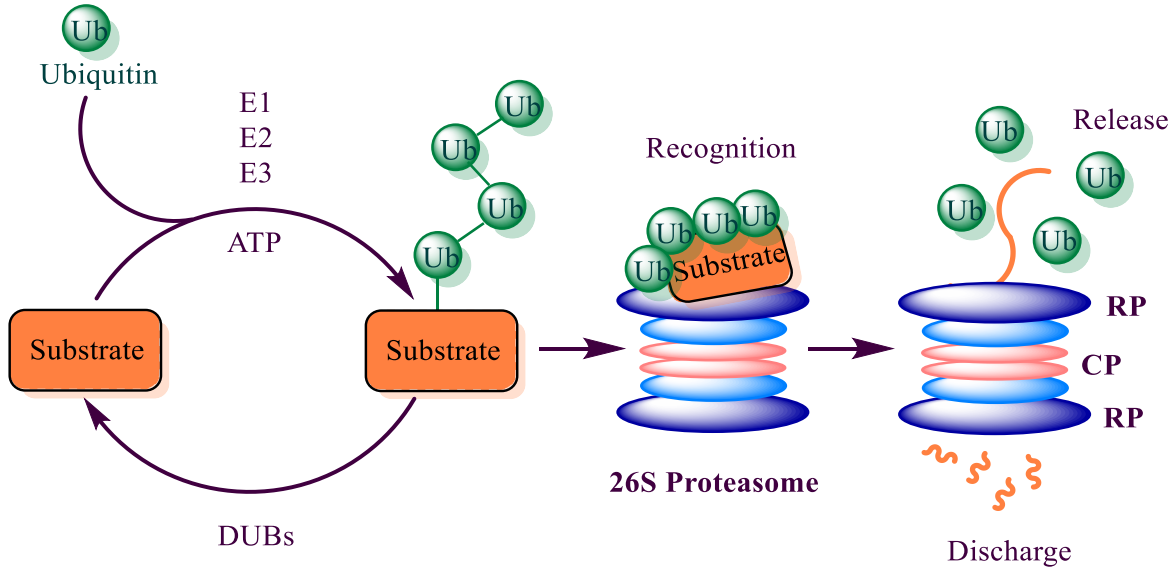

Figure 2 Protein degradation *via* the Ubiquitin-Proteasome System.

The signalling cascade starts with the activation of the 76 amino acid protein ubiquitin by the ubiquitin-activating enzyme (E1). This ATP consuming reaction results in the formation of a thioester bond between a conserved cysteine residue of E1 and the terminal carboxyl glycine residue of ubiquitin. Activated ubiquitin is then transferred by a transthiolation reaction onto a cysteine residue of an E2 enzyme, which is a member of the ubiquitin carrier protein family. Finally, ubiquitin is further transferred from E2 to E3 through the generation of a third thioester bond and subsequently covalently attached to the substrate upon formation of an isopeptide bond between the ubiquitin glycine residue and a lysine residue of the protein substrate. Alternatively, ubiquitin can also be directly transferred from E2 to the substrate when it is forming a complex with E3. This ubiquitination process is repeated, generating a poly-ubiquitin chain which is recognised by the 26S proteasome as the signal of the tagged protein to be degraded. Out of the 7 lysine residues within ubiquitin only Lys48-based chains are recognised by the 26S proteasome as proteolytic signals; modifications of the other six residues are involved in non-proteolytic functions of this protein. Although most substrates require poly-ubiquitin chains to be formed and non-forked chains are believed to be more favourable for substrate degradation, the precise number of ubiquitin moieties and the structure of the chain required remain unclear. After proteasomal hydrolysis, ubiquitin is recycled by deubiquitylating enzymes (DUBs).[11,12,13]

Each enzyme class of the UPS pathway is mechanistically distinct and comprises a diverse series of enzymes, each of which presents specificity for only one or very few substrates, resulting in the selective tagging and degradation of specific intracellular proteins.[14]

Ubiquitin-activating enzymes E1

Eight E1 enzymes have been identified in humans to initiate the activation of ubiquitin, exhibiting structural domains which are highly conserved within the family. All E1 enzymes present an adenylation domain, a catalytic cysteine domain which displays the cysteine residue involved in the thioester linkage between the enzyme and the ubiquitin, and a carboxyl-terminal ubiquitin-fold domain which engages E2.[15]

Ubiquitin conjugating enzymes E2

This family of enzymes comprises of many structurally and functionally heterogeneous proteins, all of them characterised by the presence of a conserve domain which contains the active cysteine residue essential for binding to ubiquitin. Each E2 recognises a small number of E3s and their specific substrate.[16]

Ubiquitin-protein ligases E3

The human genome encodes for hundreds of E3 enzymes and they are the most diverse group of proteins of the UPS system. The three major classes of E3 enzymes are named after their catalytic domains HECT, RING or U-box. These defining motifs confer the different types of E3 distinct modes of action, making them key components for the target specificity of the degradation pathway.[17]

Deubiquitylating enzymes DUBs

The DUBs are cysteine proteases which disassemble the polyubiquitin chains by cleaving the thioester and amide bonds between the glycine residue of the ubiquitin subunit and proteins. This recycle the ubiquitin subunits for their conjugation to new substrates [18]

1.2 19S Regulatory Particle: the Proteasome Base and the Proteasome Lid

The 19S regulatory particle of the proteasome is a multifunctional complex formed by 19 subunits and subdivided into two asymmetric assemblies: the base and the lid. The 19S RP is responsible for substrate recognition, unfolding, translocation and deubiquitination.[19]

The lid particle contains 9 subunits, although the function of only one of them (Rpn11) has been identified. Rnp11 is a DUB protein and performs the separation of the ubiquitin moieties from the substrate. This early step is crucial for the translocation of the substrate into the core particle of the proteasome and therefore for the degradation process.[19]

The base particle contains 10 subunits: two scaffolding proteins (Rpn1 and Rpn2), which confer structural stability to the proteasome, two ubiquitin receptors (Rpn10 and Rpn13), which regulate substrate recognition and deubiquitination and 6 ATPases (Rpt1-6), which are involved in substrate unfolding; hydrolysing ATP by pulling the substrate to the channel that leads to the core praticle.[19]

1.3 20S Proteasome: the Proteolytic Core Particle

The 20S core particle of the proteasome (CP) is a barrel-shaped protease complex which forms the core and proteolytic chamber of the 26S complex. It is composed of 28 protein subunits, which are arranged as four homo-heptameric rings α_7-β_7-β_7'-α_7' exhibiting a D7 symmetry. The two outer rings are formed by the α-subunits whilst the two inner rings are formed by the β-subunits (**Figure 3**).[20]

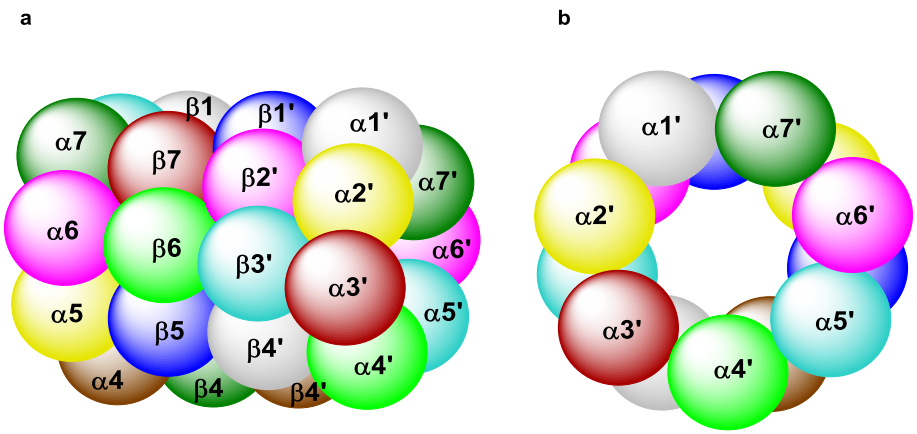

Figure 3 Representation of the 28 subunits of the eukaryotic 20S core particle of the proteasome. **a)** Side view of the 20S. **b)** Top view of the α-ring.

Both α-subunits and ß-subunits are structurally similar and contain a sandwich motif of two antiparallel ß-sheets which are flanked by α-helices on the top and the bottom (**Figure 4**). The four rings form a central channel with three large compartments which control substrate translocation to the proteolytic chamber of the 20S complex. Two of the cavities are placed at the interface within the α- and ß-rings and the third one, which presents a maximum diameter of 53 Å, is shaped by the ß-rings.[21]

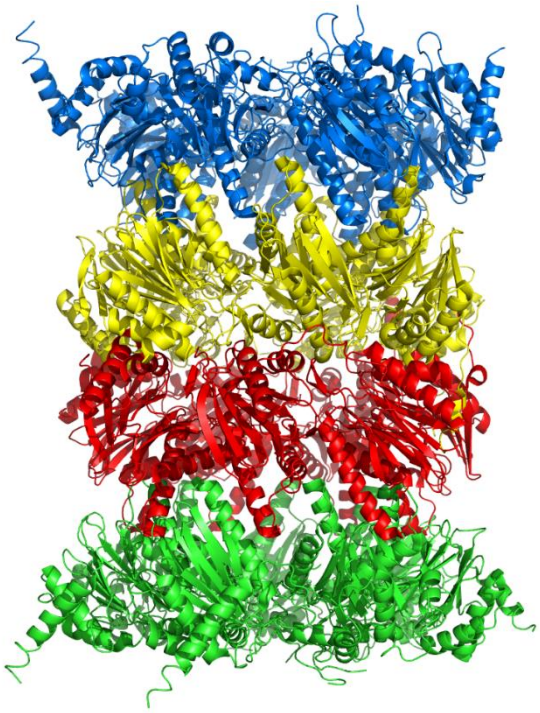

Figure 4 Crystal structure of 20S human proteasome at 2.6 Å resolution (PDB: 4R3O).

The α-subunits are proteolytically inactive and serve as outer gates for the inner compartment, forming a passage of approximately 13 Å at both ends of the barrel. The α-helices of these subunits interact with the 19S regulatory complex and control the opening of the channel. The *N*-terminal tails of the α-helices of the α-subunit are inserted into the pore and their structural rearrangement, which is triggered by binding of regulatory proteins to the CP, stabilise the open state.[22]

The ß-subunits make up the proteolytic chamber in the central cavity of the 20S complex. Only three of the seven ß-subunits are catalytically active: ß1, ß2 and ß5. These three proteolytic centres have different cleavage specificities which endow the proteasome with the capability to perform peptide bond hydrolysis after the majority of amino acids.[23]

The distinct cleavage patterns of the active ß-subunits are determined by the structure of the substrate binding pockets.[24] Based on their proximity to the active site the pockets are termed as non-primed (S_1, S_2, $S_{3,}$...,) and primed (S_1', S_2', $S_{3,}$'...,). The substrate residues which interact with these pockets are termed as P_1, P_2, $P_{3,}$..., and P_1', P_2', P_3',..., accordingly (**Figure 5**).

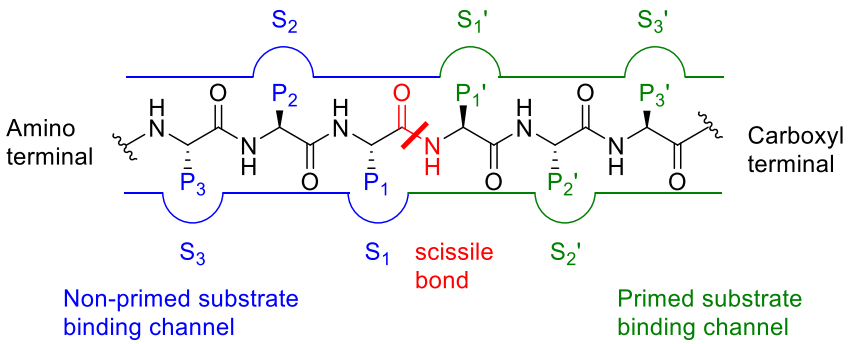

Figure 5 Standard nomenclature for substrate residues and their corresponding binding sites.

The architecture of the pockets is shaped by the active site residues and defines the size and character of the binding amino acid side chains accepted. The S_1 pocket has the largest effect on cleavage specificity due to its proximity to the scissile bond, whilst the S_2, S_3,..., sites are less discriminatory. In contrast, the influence of the interactions between the non-primed residues with the leaving group of the substrate have not been accurately understood to date.[24]

The unique cleavage preferences of the β1-, β2- and β5-subunits of the proteasome are predominantly attributed to residue 45 of the corresponding S_1 sites. In fact, their S_2 pockets do not possess specificity features and the S_3 pockets are large cavities in all three subunits.[25]

β1-subunit

The S_1 pocket of the β1-subunit presents Arg45 which stabilises acidic substrate side chains and therefore endows this subunit with a caspase-like activity. Additionally this active centre also displays some degree of branched chain amino acid preferring (BrAAP) activity.[25]

β2-subunit

Gly45 of the β2-subunit provides this active centre with a spacious S_1 pocket, which is delimited at the bottom by a glutamate residue. This subunit preferentially binds very large residues with a basic character at P_1, displaying the trypsin-like activity of the proteasome. [25]

β5-subunit

The β5-subunit possesses a chymotrypsin-like activity as a result of its S1 pocket conformation, which is mainly attributed to the Met45. As a result, it favours cleavage after hydrophobic residues. Nevertheless, this subunit also exhibits branched chain amino acid preferring (BrAAP) and small neutral amino acid preferring (SNAAP) activity.[25]

Despite their distinctive substrate-binding channel assembly and substrate specificity the three subunits share the same catalytic mechanism for peptide bond hydrolysis, which is characterised by the presence of an *N*-terminal threonine as the active nucleophile. Therefore, the proteasome belongs to the family of Ntn (*N*-terminal nucleophile) hydrolases.[26]

The Ntn hydrolases are proteases with an unusual folding. They are encoded as inactive precursors and expose the amino-terminal catalytic residue by intramolecular autocatalytic processing of the peptide bond preceding the nucleophilic residue. The functional group performing the nucleophilic attack is activated by proton transfer to the free *N*-terminus.[27]

The *N*-terminal threonine (Thr1) possessed by the β1-, β2- and β5-subunits has a hydroxyl group that, upon activation by a proton acceptor *via* hydrogen bonds, performs the nucleophilic attack onto the carbonyl carbon of a peptide bond. The proposed proton transfer between the oxygen atom and the nitrogen atom of the threonine results in the formation of an acyl-ester intermediate. Finally the acyl-ester bond is hydrolysed by a molecule of water regenerating the threonine residue (**Scheme 1**).[28]

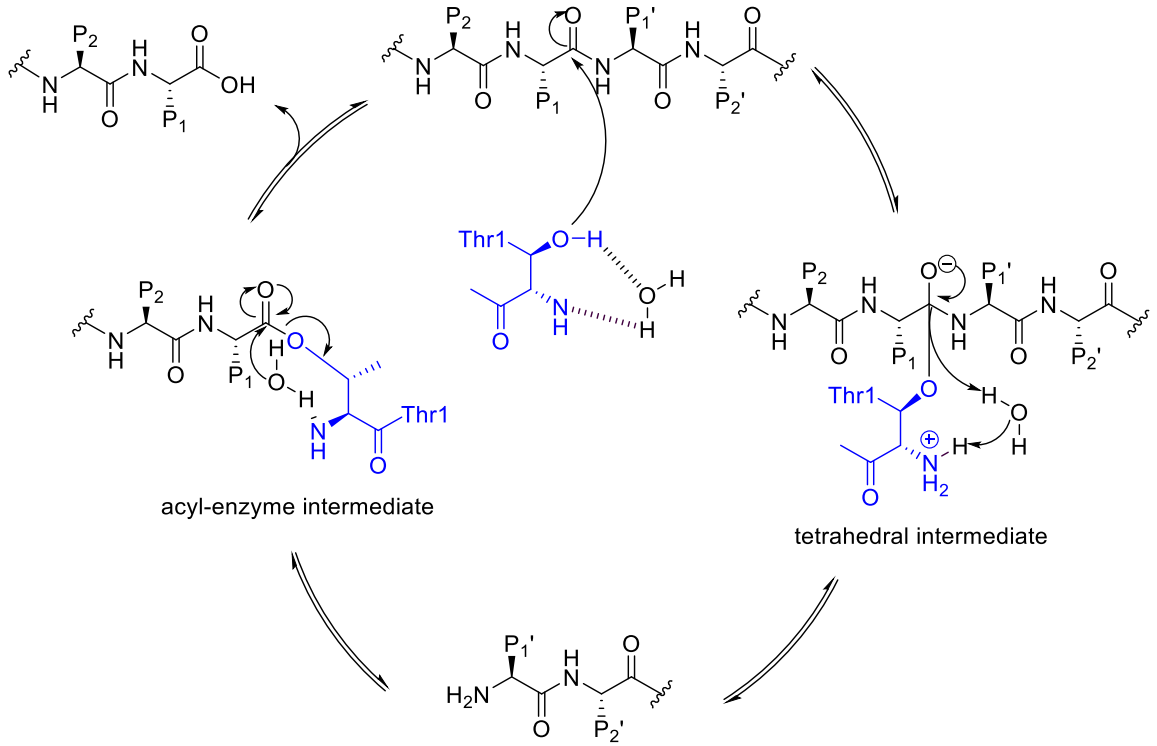

Scheme 1 Proposed mechanism for substrate hydrolysis by the 20S proteasome.

Recent studies have suggested the Lys33 side chain as an alternative candidate for deprotonating the hydroxyl group of the threonine. This new model proposes a catalytic triad formed by threonine, lysine and aspartate/glutamate. The amino group of the lysine is proposed to act as the proton acceptor and is thought to be analogously activated *via* hydrogen bonding by the aspartate; increasing its pk_{aH}. The charged amino terminus of threonine then donates a proton to the amide nitrogen of the peptide substrate and in its deprotonated state it activates a water molecule for the hydrolysis of the acyl-enzyme (**Scheme 2**). This mechanism would explain the autocatalytic processing of the β-subunit precursors. Since the amino terminus of the threonine is part of the peptide bond to be cleaved in the

immature active sites, it is not yet exposed and available to take part in the splicing. [29]

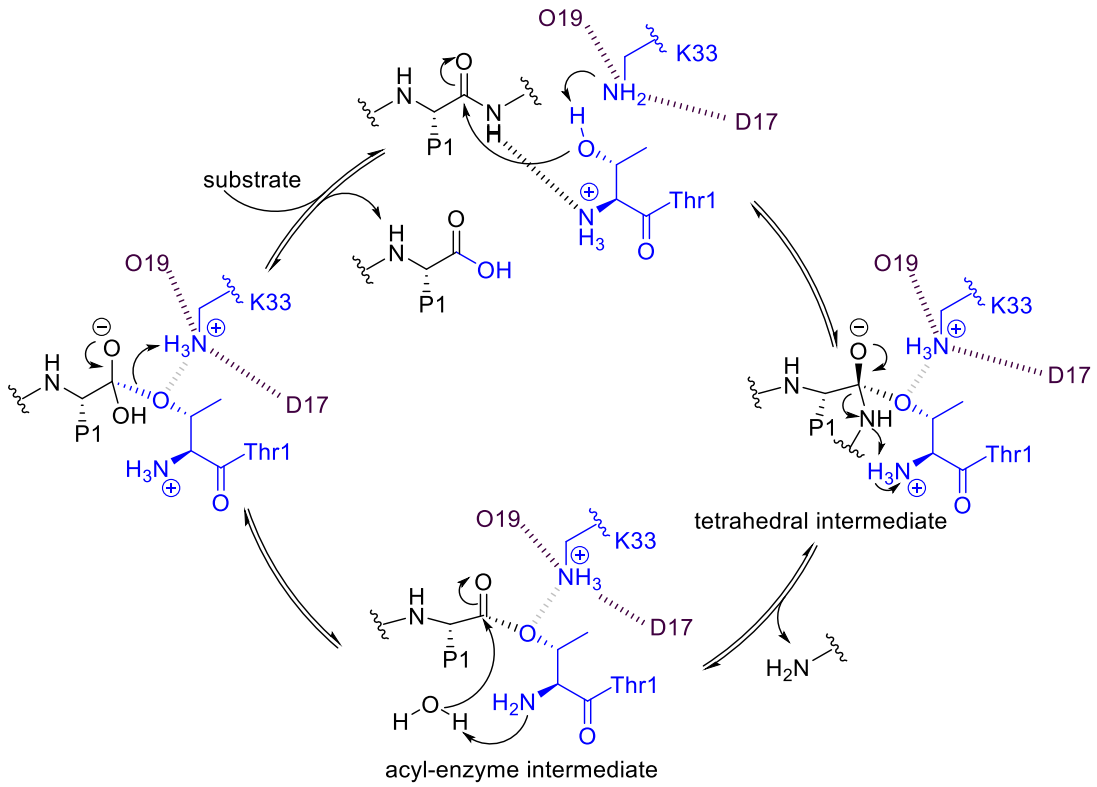

Scheme 2 Recently proposed substrate hydrolysis mechanism in the 20S proteasome.

β3, β4, β6 and β7-subunits

The remaining β-subunits (β3, β4, β6 and β7) are proteolytically inactive but contribute to the hydrolysis process by being directly involved in the formation of the substrate binding channels. The inactivity of the β3, β4, β6-subunits is due to the lack of the catalytic *N*-terminal threonine which performs the nucleophilic attack. In the case of the β7-subunits, which conserve the active nucleophile, the absence of the necessary bond cleavage during the maturation process results in a glycine-capped threonine.[30]

1.4 Tissue Specific Proteasomes

Proteasomes present a highly conserved structure; however, substantial variations exist in terms of subunit composition, activity and tissue distribution. In

mammalian systems three different types of 20S proteasome have been reported: constitutive, immune and thymoproteasome. These different properties and functions are the result of the replacement of the active β-subunits.[31]

While the constitutive proteasome (cCP) is expressed in all tissues, the immunoproteasome (iCP) is predominately found in hematopoietic cells, particularly in lymphocytes and monocytes, and the thymoproteasome (tCP) is exclusively located in cortical thymic epithelial cells.[32]

The Immunoproteasome

The main role of the immunoproteasome is the generation of antigenic peptides for presentation to the immune system by major histocompatibility complex class I molecules (MHC-I).[33] The MHC-I class molecules are proteins anchored to the surface of all nucleated cells and play an essential role in the acquired immune system.[34] The antigenic peptides, which are typically 8-11 amino acids long, are derived from the degradation of endogenous or pathogenic proteins by the immunoproteasome. These peptides are presented to cytotoxic T cells (CTLs) on the surface of MHC-I molecules encoded in the cell surface triggering immune responses.[33]

The immunoproteasome subunits, also known as interferon inducible subunits (β1i, β2i and β5i), are predominantly expressed in hematopoietic cells. However, they can replace their constitutive counterparts in non-immune cells upon cytokine stimulation by interferon-γ (IFN-γ) and tumour necrosis factor- α (TNF-α). In addition to antigen processing, the immunoproteasome is also involved in T cell differentiation and the control of cytokine production.[35] Therefore, its function is not restricted to the immune system but extended to inflammatory processes and viral infections.[36]

The high sequence homology between cCP and iCP subunits of the proteasome complexes results in substantial overlapping of their substrate preference and the same mechanism of hydrolysis. Despite this, differences in specificity have been observed because of the presence of different amino acid residues assembling their corresponding binding pockets.[37]

The S_1 pocket of β1i is smaller and more hydrophobic than the corresponding pocket in β1c and therefore favours branched non polar side chains (Leu, Val or Ile) instead of negatively charged residues. Additionally, β1i accommodates

smaller and more polar amino acids in the S_3 site due to a less spacious and more polarised pocket.[37]

Similarly, the ß5i subunit presents a more spacious S_1 pocket than the ß5c and binds less structurally demanding amino acids. Furthermore, the S_2 pocket of this subunit is shallower, while the opposite holds true for the S_3 pocket.[37]

In contrast, subunits ß2c and ß2i present almost identical binding pockets, which suggests that ß2i may play an additional functional role.[37]

The Thymoproteasome

The thymoproteasome is responsible for the generation of $CD8^+$ T cells during the positive selection of developing thymocites in the cortical thymic epithelial cells.[38] The proteolytic 20S core particle of the thymoproteasome (tCP) is homologous to the immunoproteasome (iCP) since it incorporates the inducible subunits ß1i and ß2i, and only replaces the unique subunit ß5t, which is essential for its function. The S1 pocket of ß5t is mostly composed of hydrophilic residues, unlike those present in ß5c and ß5i, resulting in decreased chymotrypsin-like activity.[38]

1.5 Proteasome as an Anticancer Target

As the main pathway for protein degradation in eukaryotes, the ubiquitin-proteasome system (UPS), regulates critical cellular processes as diverse as cell cycle control, transcription, protein quality control and apoptosis. Therefore, it is also involved in many pathological conditions in which these physiological processes become dysregulated.[39]

Since normal functioning of the UPS is essential for cell survival, disruption of this process leads to many biological consequences. This includes the accumulation of aberrant and polyubiquitinated proteins which are toxic to the cell and subsequently induce apoptosis.[40]

Apoptosis, also known as programmed cell death, is a controlled form of cellular death which is fundamental for multicellular organisms. It is an ATP-dependent process in which the cell is shrunk, condensed and partitioned into membrane-

bound apoptotic bodies which are phagocytosed by surrounding cells.[41] The involvement of the UPS in apoptosis occurs through multiple pathways, most prominently in mediating the degradation of pro-apoptotic factors and regulatory proteins which participate in this form of cellular death.[42]

Nuclear factor-kappa B (NF-*k*B)

NF-*k*B is a pro-survival transcription factor which mediates immune and inflammatory responses and activates genes which encode cytokines, chemokines and anti-apoptotic factors. Activation of NF-*k*B requires the UPS proteolysis of the inhibitor factor I*k*Bα. Inhibition of this degradation results in a higher level of I*k*Bα, leading to a reduced biosynthesis of the NF-*k*B-dependent molecules, which are implicated in cells survival signalling pathway, and triggers cell death.[43]

Tumour suppressor p53

The tumour suppressor p53 is a short-lived transcription factor which down-regulates anti-apoptotic proteins, such as the BCL-2 family, whilst also inducing the synthesis of several pro-apoptotic proteins. Expression of p53 is largely regulated by MDM2, an E3 ligase which modulates its degradation rate. The impeded degradation results in stabilisation and accumulation of p53 and therefore favours apoptosis.[44]

Cyclins and cyclin-dependent kinases (CDKs)

Progression of the cell cycle is determined by the successive activation of cyclin-dependent protein kinases (CDKs) upon heterodimerisation by cyclin proteins. Levels of the different CDKs remain constant during the cell cycle and it is the quantity of cyclin proteins which change in a phase-specific manner during the cell cycle acting as the rate limiting factor. Their degradation by the UPS is normally a prerequisite for the cell cycle to progress. Inhibition of this process leads to dysregulation of cyclin turnover and consequently of cyclin-dependent kinase activity. This results in the arrest of the cell cycle at the G2/M and G1/S check points and induces cell death.[45]

Cancer cells are characterised by an accelerated proliferation rate due to altered or defective cell cycle proteins and their inability to undergo apoptosis. As a result, these cells accumulate damaged proteins at a much higher rate than

normal cells and therefore have an increased dependency on the proteasomal degradation.[46] Consequently, inhibition of UPS activity has been considered an attractive therapeutic anti-cancer target during the last decade. Although not all cells respond in the same way to this inhibition, the blockage of the UPS pathway has been shown to induce apoptosis preferentially in neoplastic cells with reduced cytotoxicity in normal cells.[47] The UPS can be blocked at various points but most of the presently available inhibitors directly target the 20S proteasome. This is currently a clinically validated chemotherapy modality for the treatment of specific types of cancer.[14]

1.6 Other Biological Implications of the Proteasome

The UPS pathway is involved in a broad range of physiological processes and as a result the system has been implicated not only in cancer but also in the pathogenesis of several other diseases. These pathologies include neurodegenerative diseases such as Alzheimer's, Huntington's and Parkinson's disease which result from the accumulation of toxic proteins. They are also implicated in genetic disorders such as cystic fibrosis and hereditary forms of hypertension.[48]

The proteasome is connected to the stimulation of inflammatory responses by degradation of the inhibitory factor IκB, necessary for the activation of the transcription factor NF-κB, which is responsible for the expression of many inflammatory mediators. Thus, many inhibitors of the proteasome have shown anti-inflammatory effects.[49]

The important role of the immunoproteasome in the cellular immune response as the main producer of antigenic peptides has led to the studied of its inhibitors as strong candidates for the treatment of autoimmune disorders such as rheumatoid arthritis and multiple sclerosis, as well as potential drugs for the treatment of transplant rejection.[50] The recent discoveries regarding the selective inhibition of the immunoproteasome represent a promising approach for the treatment of cancers related to immune system cells, such as lymphomas, where the

immunoproteasome is the predominant proteasome species.[51] Finally, the effects of proteasome inhibitors are being studied for the treatment of and various viral and parasitic infections.[52]

1.7 Proteasome Inhibitors

The identification of the proteasome as an effective therapeutic anticancer target led to the development of numerous synthetic compounds based on the structural diversity of natural proteasome inhibitors.

Typically, proteasome inhibitors are peptide-based and contain an electrophilic trap that reacts with the hydroxyl group of the *N*-terminal threonine to form a covalent bond.[53] Depending on the nature of the electrophile and the type of bonding, these inhibitors can be classified as reversible or irreversible. Additionally, there are non-covalent inhibitors, known as "tight-binding inhibitors", that, without forming a covalent complex with the active nucleophile, also present a long target residence time.[54] Although the peptide backbones are designed to control the subunit selectivity, the reactive warheads determine the target specificity and biological stability of the inhibitors.[55]

The major classes of warheads used for covalent proteasome inhibition are aldehydes, boronates, vinyl sulfones, ß-lactones and α', ß'-epoxyketones. [56] Recently, the new classes of α-ketoaldehydes and α-ketoamides have been introduced to the pool.[55]

Due to the very reactive nature of aldehydes low selectivity for the proteasome is achieved. Additionally, they also co-inhibit serine and cysteine proteases. Aldehydes react reversibly with the active threonine, forming hemiacetals, which present a high dissociation rate (**Scheme 3**). Furthermore, their oxidation to inactive carboxylic acids inside the cells results in their efflux by the multi-drug resistance carrier.[56]

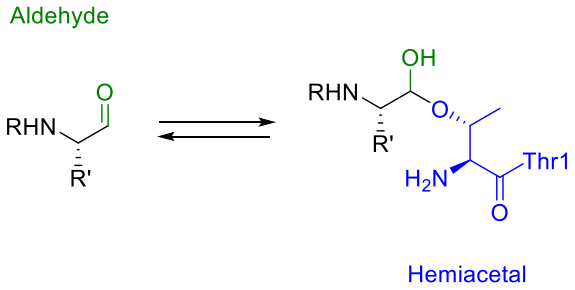

Scheme 3 Aldehyde warhead and its reaction with the catalytic threonine.

Boronates are very potent inhibitors of the proteasome.[39] They form reversible tetrahedral adducts with the active threonine but their dissociation rate is so low that the inhibition can be considered irreversible (**Scheme 4**). Boronates were initially designed as serine protease inhibitors but due to the stabilisation of the tetrahedral adduct by hydrogen bonding with the *N*-terminal amino group of the threonine, the boronic acid moiety presents a higher selectivity for the proteasome.[57]

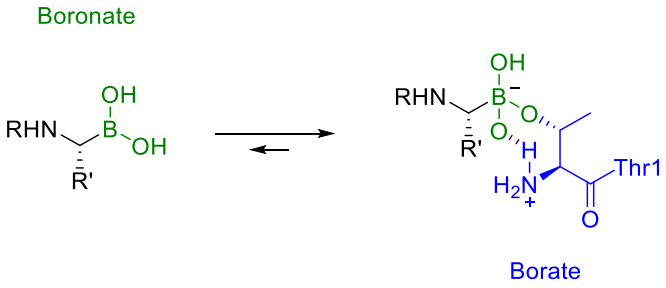

Scheme 4 Boronate warhead and its reaction with the catalytic threonine.

Vinyl sulfones were initially designed for the inhibition of cysteine proteases. The active threonine reacts covalently with the vinyl moiety in a 1,4- Michael addition of the hydroxyl group to the double bond (**Scheme 5**).[25] Although they display lower selectivity and potency than epoxyketones, vinyl sulfones are widely used due to their easy synthesis and good stability. Their specificity can be controlled by modification of the peptide backbone.[58]

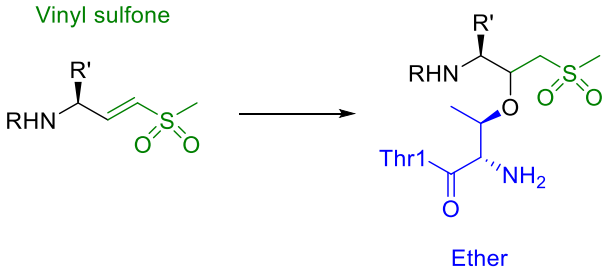

Scheme 5 Vinyl sulfone warhead and its reaction with the catalytic threonine.

β-Lactones are non-peptidic natural products. Reaction of the threonine with the β-lactone ring results in the formation of an acyl-enzyme ester (**Scheme 6**). Hydrolysis of this adduct leads to the regeneration of the threonine.[51]

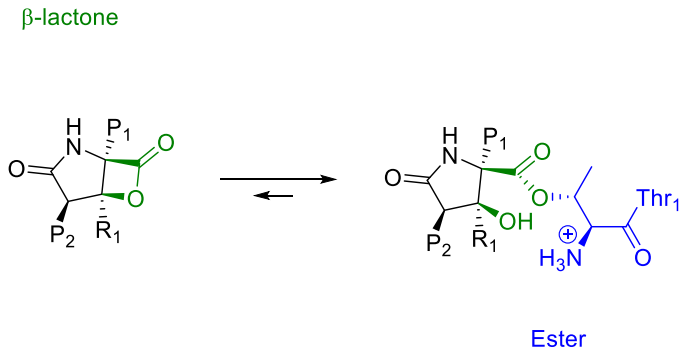

Scheme 6 β-Lactone warhead and its reaction with the catalytic threonine.

The α', β'-epoxyketones are the most potent proteasome inhibitors known to date. This warhead initially reacts through the carbonyl group in a similar manner to aldehyde warhead, forming a hemiacetal. Subsequently, a second nucleophilic attack of the N-terminal amino group of the threonine opens the epoxide intramolecularly, resulting in the irreversible formation of a six-membered morpholino ring (**Scheme 7**). The dual character of the α', β'-epoxyketone moiety accounts for its great selectivity for the proteasome. Given that the morpholino formation requires an *N*-terminal nucleophile this warhead, in contrast with the rest, does not inhibit other proteases.[59]

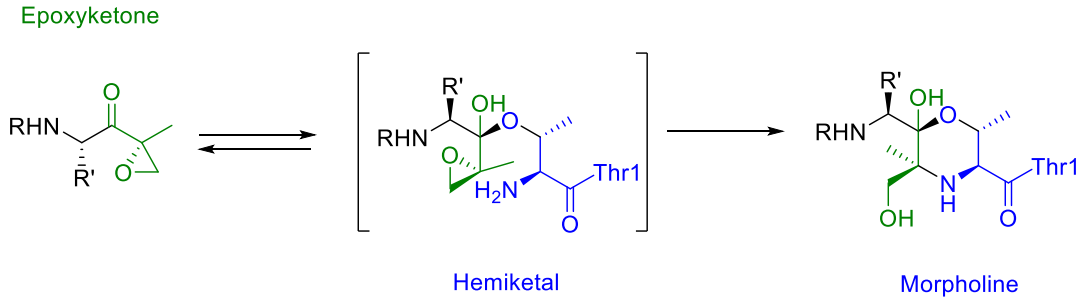

Scheme 7 Epoxyketone warhead and its reaction with the catalytic threonine.

The α-ketoaldehydes, like the α', ß'-epoxiketones, react with the active threonine in a two-step process, exploiting the characteristic mechanism of the proteasome. However, the formation of a reversible carbinolamine intermediate, which undergoes a condensation reaction, results in an oxazine ring with a Schiff base bond (**Scheme 8**). This warhead represents a unique type of highly selective and reversible covalent inhibitors.[60]

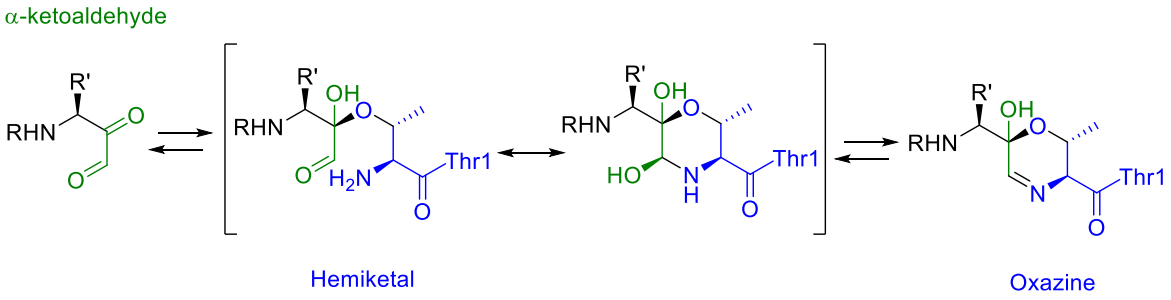

Scheme 8 α-Ketoaldehyde warhead and its reaction with the catalytic threonine.

Unfortunately, α-ketoaldehydes showed a significantly decreased inhibitory potential, For this reason Groll and co-workers replaced the ketoaldehyde functionality was by an α-ketoamide. The α-ketoamide forms only one covalent bond through its ketone moiety and stabilises its phenyl amide terminus by van der Waals interactions within the proteasomal substrate binding channels (**Scheme 9**).[55]

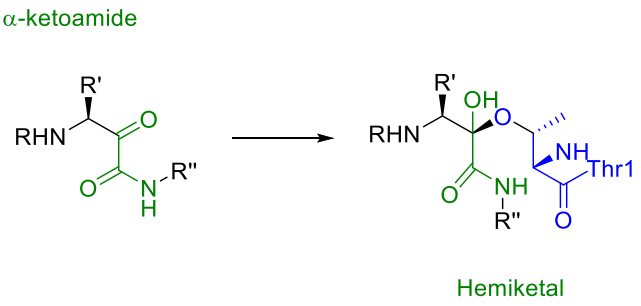

Scheme 9 α-Ketoamide warhead and its reaction with the catalytic threonine.

1.7.1 Proteasome Inhibitors in Clinic

The boronic acid Bortezomib (**1**) (Velcade™) (**Figure 6**) is a potent and selective proteasome inhibitor. It was the first of its class to enter clinical trials, being approved by the US Food and Drug Administration (FDA) in 2003 for the treatment of relapsed multiple myeloma.[61]

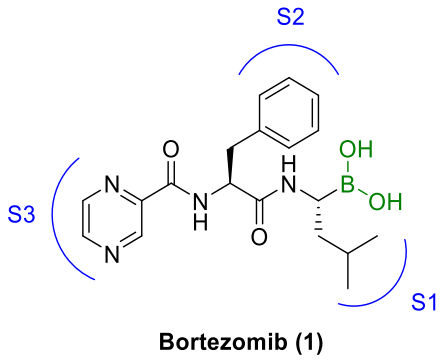

Bortezomib (1)

Figure 6 Structure of the inhibitor Bortezomib (**1**).

Multiple myeloma is a hematologic type of cancer characterised by the accumulation of malignant plasma cells in the bone marrow. Although it is treatable with chemotherapy and radiotherapy, it remains incurable due to the proliferation of resistant tumour cells.[62] Multiple myeloma cells display a particularly enhanced NF-κB activity which is responsible for their chemoresistance. Furthermore, cells possess an increased expression of the immunoproteasome and have shown a great sensitivity towards proteasome inhibition.[63,64]

Bortezomib (**1**) is administered intravenously and binds reversibly but with slow dissociation to the proteasome; targeting the β5-subnit of both the constitutive and immunoproteasome (β5c IC_{50} = 7 nM, β5i IC_{50} = 4 nM).[65] Its antitumour activity has been attributed to inhibition of the NF-κB pathway which hampers tumour growth and cell survival.[66,67] Despite the initial success of Bortezomib treatments, the high activity of this inhibitor against other proteases is associated with several off-target effects, including severe peripheral neuropathy, which has been detected in more than 30% of the patients.[68] Additionally, prolonged treatments lead to the development of drug resistance.[69]

The peptide epoxyketone Carfilzomib (**2**) (Kyprolis®) (**Figure 7**) was approved by the FDA in 2012 as a second generation proteasome inhibitor for the treatment of multiple myeloma resistant to a previous Bortezomib chemotherapy. Hematologic tumour cells are more responsive to Carfilzomib than solid tumours. This irreversible inhibitor preferentially targets the β5-subunit of the constitutive proteasome (β5c IC_{50}: 6 nM; β5i IC_{50}: 33 nM).[70] The high specificity of Carfilzomib for the proteasome over other proteases, in contrast with Bortezomib, results from the unique inhibition mechanism of the epoxyketone moiety, as a result, less side effects have been recorded during clinical trials.[71]

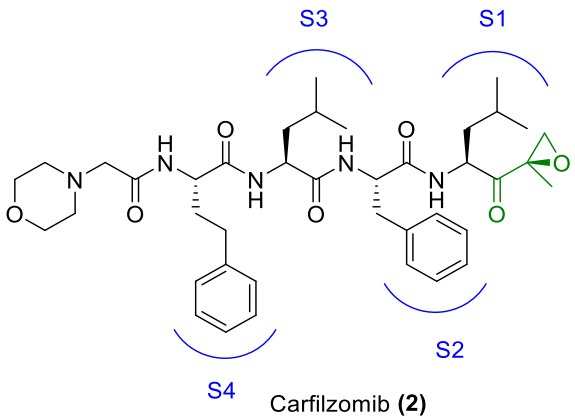

Figure 7 Structure of the inhibitor Carfilzomib (**2**).

Ixazomib (**4**) (Ninlaro®) (**Scheme 10**) was approved by the FDA in November 2015 for the treatment of multiple myeloma patients who have been treated with at least one other inhibitor agent. It is a citrate boronate ester which hydrolyses to the biologically active boronic acid in the gastrointestinal tract and plasma; making it the first orally administered proteasome inhibitor. The better blood

distribution of this small molecule has been linked to a higher antitumor activity.[72] The potency of Bortezomib and Ixazomib for the β1, β2 and β5-subunits are comparable. However, Ixazomib presents a shorter dissociation half-life which results in better tissue penetration and so far the side effects reported are not severe. Ixazomib is also in phase I-II clinical trials for the treatment of other diseases such as graft-versus-host disease and lupus nephritis.[73]

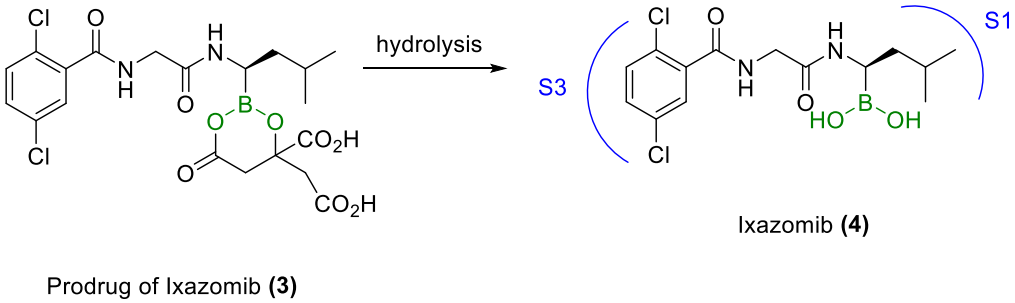

Scheme 10 Structure of the inhibitor Ixazomib (**4**).

Oprozomib (**5**) (OXN 0912) (**Figure 8**) is an orally available analogue of Carfilzomib which is currently in phase I-II clinical trials for the treatment of multiple myeloma and solid tumours.[74] No data from these studies have been reported yet.[75]

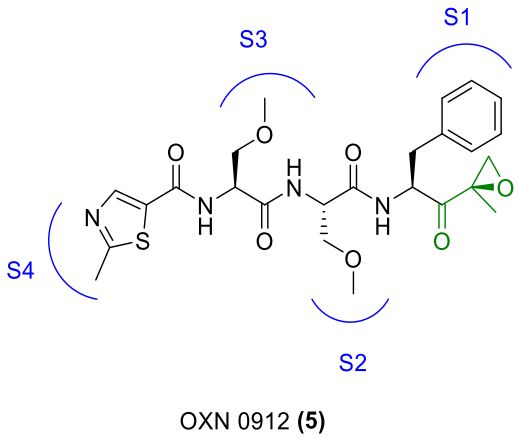

Figure 8 Structure of the inhibitor Oprozomib (**5**) (OXN 0912).

The pronounced improvement on reactivity and target selectivity obtained by the epoxyketone derived inhibitors has meant this bivalent motif has attracted a great amount of attention. Further investigations into the "advantaged" mechanism of action of the epoxyketone warhead with the active threonine have subsequently

occurred. A very recent study by Schrader[76] reported the formation of a 7-membered ring as the inhibition adduct. This adduct is believed to be formed by a nucleophilic attack of the ThrN onto the ß-carbon of the epoxide hemiketal intermediate (**Scheme 11**). This finding differs from the earlier stated mechanism (**Scheme 7**) which proposed the formation of a six-membered morpholino ring by an epoxide opening reaction at the α-carbon.[59]

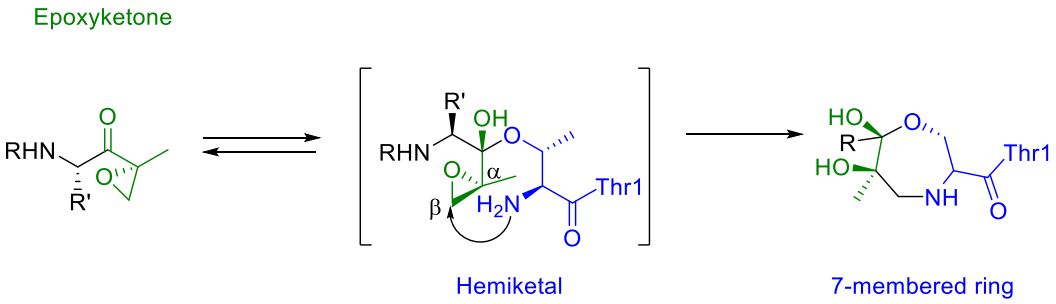

Scheme 11 Mechanism of inhibition of the epoxyketone warhead proposed by Schrader.

1.7.2 Subunit Specific Inhibitors

All of the previously described inhibitors and most of the ongoing clinical candidates are designed to target the ß5-subunit of the proteasome, although several of them also coinhibit the ß1 and ß2-subunits at higher concentrations.[56] The ß5-subunit is considered to be rate limiting for protein degradation.[77] Consequently, inhibition of the ß5-subunit results in the highest levels of cytotoxic effects.[70] Recent studies have instead shown that the simultaneous inhibition of either the ß1 or the ß2-subunit is necessary to achieve an optimal anti-neoplastic response.[78,79]

Acquired cell resistance for proteasome inhibitors is a huge drawback for their use in chemotherapy. The cellular mechanism for this resistance includes over expression of the proteasome and the enhancement of the proteolytic activity of the remaining active subunits.[50] Together with the undesirable off-target effects,

these points have strongly motivated the development of compounds with specificity towards a particular ß subunit.[8]

Furthermore, the discrimination between the counterparts of the different types of proteasomes has been identified as the main challenge in the design of the next generation of inhibitors. Since they are involved in distinct biological functions their inhibitors could offer distinctive clinical applications.[80]

In particular, the selective inhibition of the immunoproteasome subunits has been investigated in recent years as a potential treatment for autoimmune disorders.[51] Distinguishing between CP and iCP catalytic subunits is also important in neoplasms related to immune cells such as lymphomas, where the iCP is the predominant proteasome species.[80]

ONX 0914 (**6**) is the first inhibitor that selectively targets the ß5i-subunit and is currently in preclinical trials (**Figure 9**). It has been shown to stop the progression of inflammatory disorders by reducing the production of pro-inflammatory cytokines such as IL-6 and TNF. Its high affinity for ß5i is explained by the presence of a more bulky group at the P1 position, which is not well accepted in the less spacious S1 pocket of the ß5c-subunit. As a result, ONX 0914 is effective at much lower concentrations than non-specific inhibitors.[51]

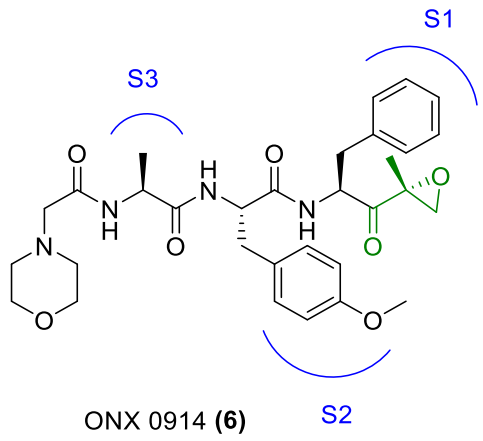

Figure 9 Structure of the inhibitor ONX 0914 (**6**).

1.8 Sulfonyl Fluorides

Methanesulfonyl fluoride **7** (MSF) (**Figure 10**) was first described as a potent insecticide by Schrader in 1952. Some years later, Myers and Kemp,[81] reported the inhibition of rat-brain cholinesterase by MSF and suggested the sulfonylation of an active residue of the enzyme as the mechanism of inhibition. In 1962, Fahrney and Gold[82] extended this research to aromatic sulfonyl fluorides, reporting phenylmethane sulfonyl fluoride **8** (PMSF) (**Figure 10**) as an inhibitor of α-chymotrypsin enzyme. Additionally, they proposed the formation of a complex between the sulfonyl fluoride and the active residue before the sulfonylation reaction.

MSF **(7)** PMSF **(8)**

Figure 10 Structures of methanesulfonyl fluoride **7** (MSF) and phenylmethane sulfonyl fluoride **8** (PMSF).

Further investigations into the mechanism of sulfonyl fluorides within the active sites of different enzymes were performed by Vaz and Schoellman.[83] They used 5-dimethylaminonaphthalene-1-sulfonyl fluoride **9** (Dns-fluoride) (**Figure 11**) as a fluorescent reporter group for the reaction with α-chymotrypsin. Isolation of the dye-protein complex proved the reaction to occur selectively with the hydroxyl group of the active serine residue.

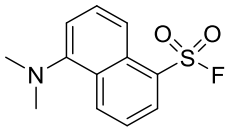

Dns-fluoride **(9)**

Figure 11 Structure of Dansyl Fluoride (**9**).

Despite the high selectivity of sulfonyl fluorides towards serine proteases, no clear discrimination between similar members of this family was reported. Interest in these compounds as potential therapeutic agents led to their incorporation into small peptides as a first attempt to enhance selectivity.[84]

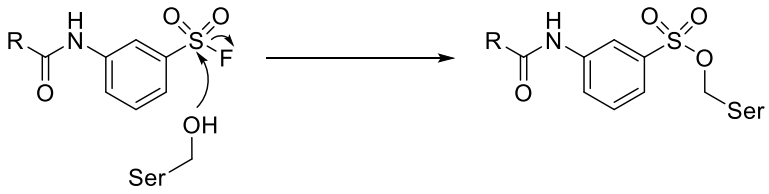

Scheme 12 Inhibition mechanism of serine proteases by sulfonyl fluorides.

Since then, sulfonyl fluorides have been extensively studied as inhibitors of serine proteases (**Scheme 12**). The crystal structure of different sulfonyl fluorides in complex with serine proteases such as α-chymotrypsin, γ-chymotrypsin, elastase and subtilisine have been obtained; helping to elucidate the configuration of the active centres of these enzymes.[1] However, the availability of functionalised sulfonyl fluorides was mainly restricted to aromatic sulfonyl fluorides, limiting the extrapolation of the conclusions of the studies.

1.8.1 Sulfonyl Fluorides in other Areas of Chemical Biology

Sulfonyl Fluorides have recently been described as "privileged warheads in chemical biology" due to the right balance of reactivity and stability that these electrophiles possess.[85]

The size and the electronegativity of the fluorine atom provides the sulfur (VI) fluoride bonds with a remarkable stability compared to other sulfonyl halides.[86] The sulfonyl-fluoride bond in SO_2-F is remarkably strong with a homolytic bond dissociation energy of 229 ± 20 kJmol^{-1}.[87] The cleavage of this bond occurs solely in a heterolytic manner contributing to the resistance of this functional group to

reduction. Sulfonyl fluorides also show a high stability to nucleophilic substitution, including hydrolysis.[88] Furthermore, they also present a great passivity towards thermolysis.[86]

These distinctive properties account for the special reactivity of the $-SO_2$-F unit which demands very specific conditions. One of the main contributors to the activation of this electrophile is the stabilisation of the fluoride as a leaving group by proton solvation.[89] The important role of the hydrogen bonding network and the stabilisation of the fluoride anion in an aqueous environment enhances the reactive potential of the sulfonyl fluoride in biological systems, such as a protein binding sites.[86] Additionally, the controlled reactivity of the sulfonyl fluoride electrophile allows specific substitution reactions to be performed at other electrophiles contained in the molecule, making further functionalisation possible without altering the $-SO_2$-F group.

This unique reactivity-stability profile, along with the synthetic accessibility of sulfonyl fluorides, has been exploited by medicinal chemists in different areas of chemical biology, including their incorporation into fluorescence probes and the synthesis of inhibitors of a wide range of enzymes.

Sulfonyl fluoride based activity probes that label specific residues in proteins are used to map their binding sites. Examples of this are the 5′-fluorosulfonylbenzoyl adenosine **10**, which labels NAD and ATP binding sites in proteins[90] and 5'-p-fluorosulfonylbenzoyl-1,N^6-ethenadenosine **11** (**Figure 12**), which targets active site nucleophiles of the tyrosine kinase family.[91]

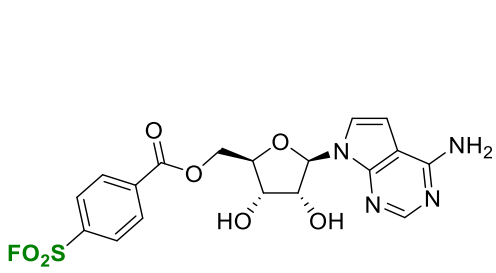

10

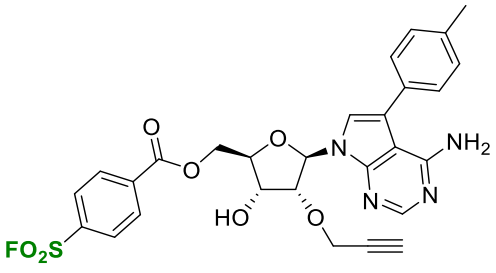

11

Figure 12 Structures of 5′-fluorosulfonylbenzoyl adenosine **10**[90] and 5'-p-fluorosulfonylbenzoyl-1,N^6-ethenadenosine **11**.[91]

Examples of small molecules containing the sulfonyl fluoride warhead for covalent modification of active amino acid residues include inhibitors of the fatty acid amide hydrolase **12**[92] and antagonists of the human A_3 adenosine receptor **13**[93] (**Figure 13**).

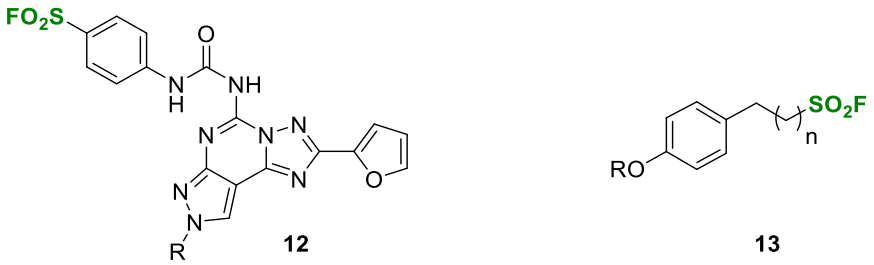

Figure 13 General structures of compounds **12**[92] and **13**.[93]

In addition, incorporation of the sulfonyl fluoride moiety into a library of 1,3,4-oxadiazoles **14** (**Figure 14**) for the stabilisation of the transthyretin protein resulted in the formation of fluorescent conjugates **15** upon reaction with the ε-amino group of an active lysine residue suggesting the use of these molecules as potential imaging agents.[94]

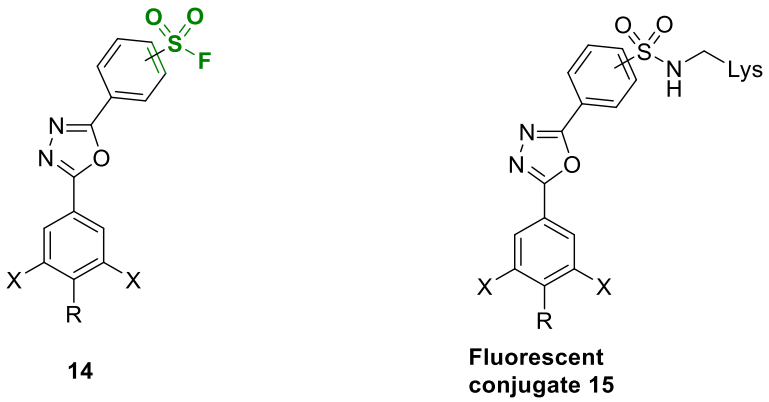

Figure 14 Structure of a 1,3,4-oxadiazole **14** and the fluorescent conjugate **15** formed by reaction with the lysine residue at the active site.[94]

1.8.2 Previous Work in the Liskamp Group

PMSF **8** and AEBSF **16** (**Figure 15**), a more physiologically stable derivative, are commonly used in protease inhibitor cocktails to prevent protein degradation when working with cell lysates. Based on this reactivity the Liskamp group decided to synthesise amino acid based sulfonyl fluorides with the aim of enhancing the properties of the sulfonyl fluoride warhead and its applicability as a selective serine protease inhibitor.[95]

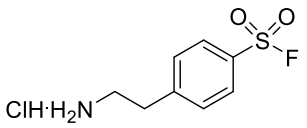

AEBSF **(16)**

Figure 15 Structure of 4-benzenesulfonyl fluoride hydrochloride (AEBSF).

The first synthesis that was performed targeted a simple sulfonyl fluoride derived from Taurine **17**. Cbz-protection of the taurine *N*-terminus in water led to the sodium sulfonate salt **18**, which was reacted with a phosgene solution to obtain the sulfonyl chloride **19**. The taurine derived sulfonyl fluoride **20** was obtained by treatment of the sulfonate salt **18** with DAST in CH_2Cl_2 or by reaction of the sulfonyl chloride **19** with potassium fluoride and 18-crown-6 in acetonitrile (**Scheme 13**).

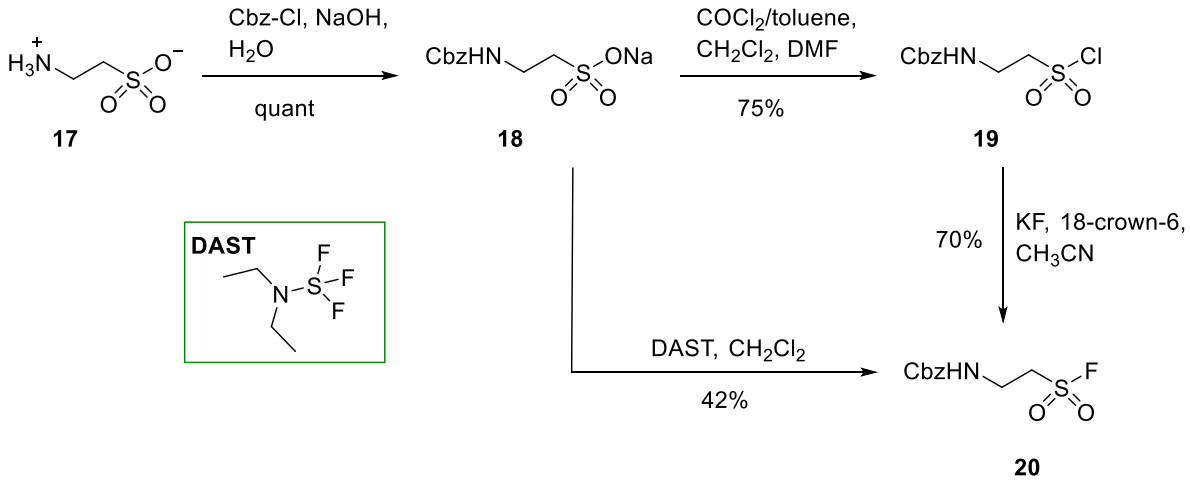

Scheme 13 Synthesis of taurine-derived sulfonyl fluoride **20**.

After the development of this synthetic pathway, the route was further extended to furnish different side chain-containing amino acids (**Scheme 14**). The Cbz-protected amino acids **21a-e** were reduced to the corresponding alcohols **22a-e** in a two-step reaction with *iso*butylchloroformate and sodium borohydride. Treatment of the alcohols with methanesulfonyl chloride and NMM subsequently afforded the corresponding mesylates **23a-e**. Thioacetates **24a-e** were obtained by reaction with *in situ* prepared caesium thioacetate and oxidised to the corresponding sulfonate salts **25a-e** using aqueous hydrogen peroxide and subsequent treatment with sodium acetate. The salts were transformed into sulfonyl chlorides **26a-e** with a solution of phosgene in acetonitrile. Finally, the substitution reaction with potassium fluoride and 18-crown-6 in acetonitrile delivered the sulfonyl fluoride derivatives **27a-e**, which were also obtained after the corresponding treatment of the sodium salts with DAST in CH_2Cl_2. Yields for the different steps of the synthesis are summarised in **Table 1**.

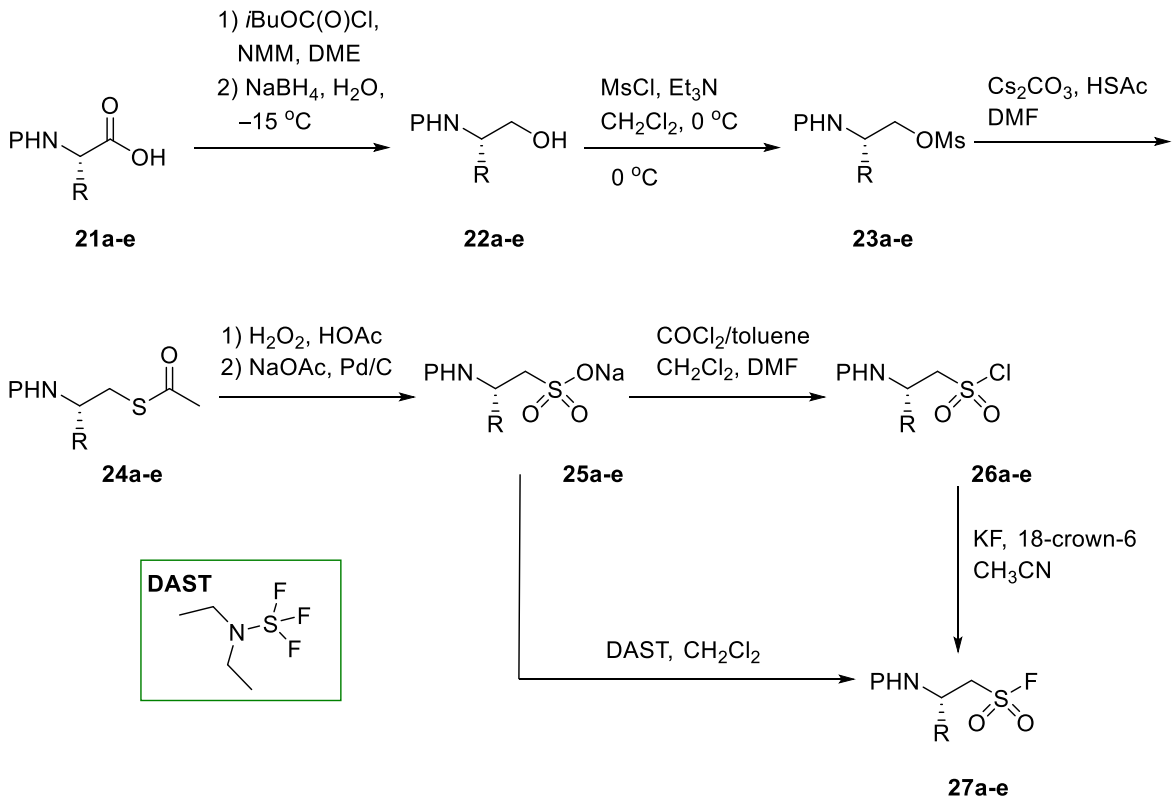

Scheme 14 Synthesis of amino acid-based sulfonyl fluorides starting from N-protected amino acids.

Table 1 Yields (%) for the synthesis of sulfonyl fluorides **27a-e** starting from N-protected amino acids. P = Protecting group.

	P	R	Amino	22	23	24	26	27
a	Cbz	CH_3	Ala	82	91	61	65	65
b	Cbz	$CH(CH_3)_2$	Val	50	65	51	-	40
c	Cbz	$CH_2CH(CH_3)_2$	Leu		58	44	45	76
d	Cbz	CH_2Ph	Phe	80	86	87	67	62
e	Fmoc	$CH(CH_3)_2$	Val	90	86	71	30	-

To evaluate the potency of the amino acid-based sulfonyl fluorides as irreversible inhibitors of serine proteases a biological assay was performed with selected compounds **20** and **27a-f** (**Figure 16**) using α-chymotrypsin since this enzyme is the best characterised member of this class.[96]

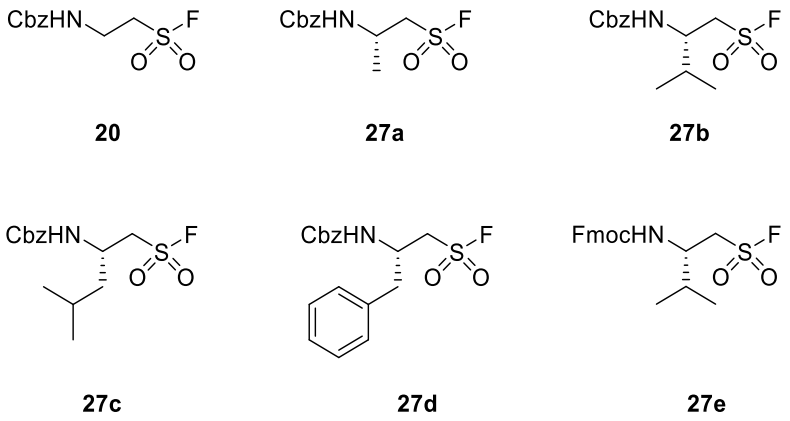

Figure 16 Structures of sulfonyl fluorides **20** and **27a-f**.

As expected aliphatic sulfonyl fluorides displayed the weakest inhibition whilst Cbz-Phenylalanine **27d** was the best inhibitor in the series (K_i = 22 µM, k_{inact} = 0.33 min^{-1}). These results correlate with the fact α-chymotrypsin preferentially binds aromatic residues. Additionally, modifying the protecting group has little influence on the inhibition since similar results were obtained for both Fmoc- and Cbz-Valine. (**Table 2**)

Table 2 Inhibitor constants and $k_{inactivation}$ values of selected sulfonyl fluorides (**20** and **27a-f**) and PMSF.

Sulfonyl fluoride	R	K_i (µM)	K_{inact} (min^{-1})
27a	Cbz-Ala	No inhibition	nd
27e	Fmoc-Val	No inhibition	nd
27c	Cbz-Leu	341 ± 35.6	0.053 ± 0.0017
27b	Cbz-Val	255 ± 6.8	0.043 ± 0.006
20	Cbz-Gly	104 ± 10.7	0.13 ± 0.006
27d	Cbz-Phe	22 ± 1.6	0.33 ± 0.03
PMSF (8)		13 ± 0.8	0.32 ± 0.04

Considering the size of these small molecule inhibitors, the obtained affinities were very favourable. Further improvement by modification of the side chains and extension of the sequences to improve selectivity had therefore high potential.

This encouraged the group to use amino acid-based sulfonyl fluorides as novel electrophilic traps to target the proteasome.

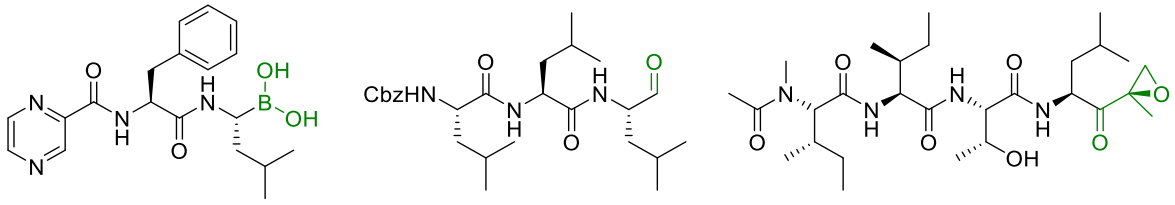

Bortezomib **(1)** MG-132 **(28)** Epoxomicin **(29)**

Figure 17 Structures of Bortezomib (**1**), Cbz-Leu$_3$-aldehyde (**28**, MG132), and Epoxomicin (**29**).

In collaboration with Groll (Technische Universität München) and Overkleeft (University of Leiden) a library of peptido sulfonyl fluoride (PSF) inhibitors was synthesised using the peptidic sequences of the known proteasome inhibitors Bortezomib (**1**) , MG132 (**28**) and Epoxomicin (**29**) (**Figure 17**) by replacing their electrophilic groups with the sulfonyl fluoride moiety. Furthermore, additional modifications were performed at the N-terminus.[97]

The synthetic strategy began with the deprotection of the amino group of the amino acid derived sulfonyl fluoride followed by coupling with the corresponding Boc-protected amino acid with BOP and DiPEA. Cycles of deprotection and coupling were then repeated until the completion of the desired peptide sequence (**Scheme 15**).[97]

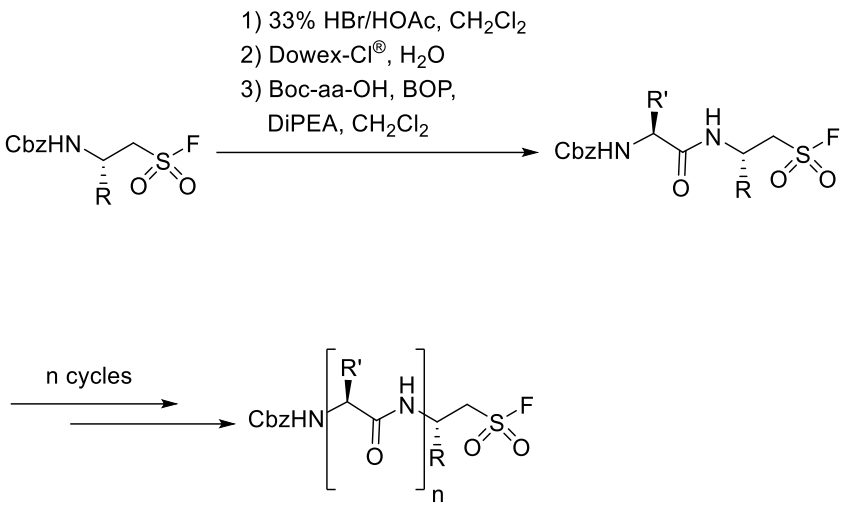

Scheme 15 Systematic synthesis of Peptido Sulfonyl Fluorides (PSF).

Although the syntheses of the PSF were carried out successfully, synthesising the *N*-terminal peptide backbone first and coupling the amino acid derived sulfonyl fluoride in the last step displays may be a better alternative to avoid the degradation of the sulfonyl fluoride electrophile during repeated coupling and work-up steps. [97]

In this study the activity of the PSF inhibitors was determined by a competitive labelling reaction with a fluorescent proteasome probe; the inhibitory potency was determined for the best compounds (PSF **30-39**) (**Figure 18**) in an enzymatic assay. The IC_{50} values (**Table 3**) obtained were between 7 nM and 1.7 µM, validating the PSFs as very potent proteasome inhibitors. Three of the tested PSFs (**32**, **34** and **37**) showed lower values than Epoxomicin and were therefore evaluated *in vivo* using HEK cells and found to have good membrane penetration.[97]

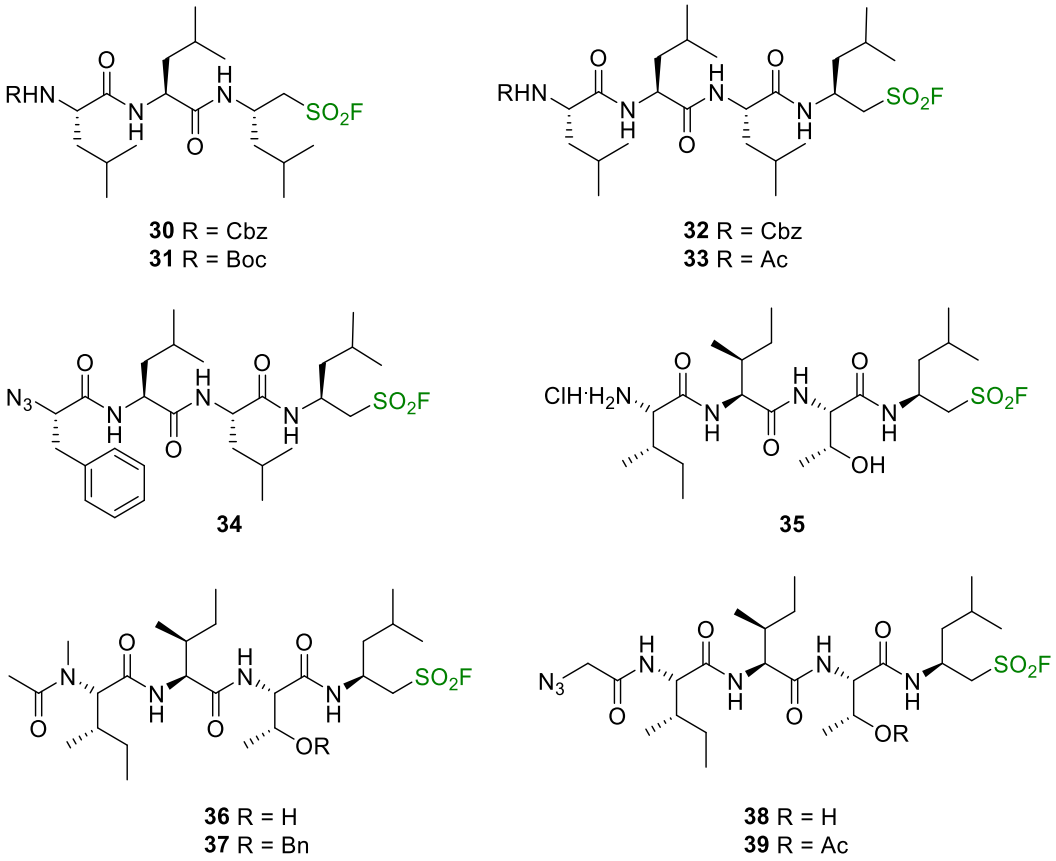

Figure 18 Structure of PSF **30-39**.

Table 3 IC_{50} values of Sulfonyl Fluorides and Epoxomicin for the proteasome β5-subunit.

Compound	IC_{50} (nM)
Epoxomicin (29)	261 ± 37
30	350 ± 70
31	1750 ± 48
32	7 ± 2
33	300 ± 40
34	110 ± 30
35	800 ± 200
36	250 ± 70
37	1150 ± 400
38	40 ± 10
39	1570 ± 340

Additionally, a set of peptido sulfonyl fluorides were studied for their antimalarial activity by Mordmüller, showing inhibition in the low nanomolar range against both multidrug-resistant and –sensitive laboratory strains. The most potent sulfonyl fluoride **32** suppressed growth of *Plasmodium berghei in vivo* and showed no cytotoxicity in HeLa and HEK 293 (non-carcinoma human embryonal kidney) cell lines up to 500 µM. Unfortunately, it presented signs of toxicity in mice.[98]

The exact mechanism of inhibition of the proteasome by the sulfonyl fluoride electrophile was investigated in collaboration with Groll and his group.[99] For this study, peptido sulfonyl fluoride analogues of the inhibitors Carfilzomib (**2**) and ONX 0914 (**6**) were synthesised; replacing the epoxyketone warhead with the sulfonyl fluoride moiety (PSF **40**, PSF **41**). An additional PSF **42** derivative was synthesised by extending the PSF **41** sequence by the addition of a homo-phenylalanine residue (**Figure 19**).

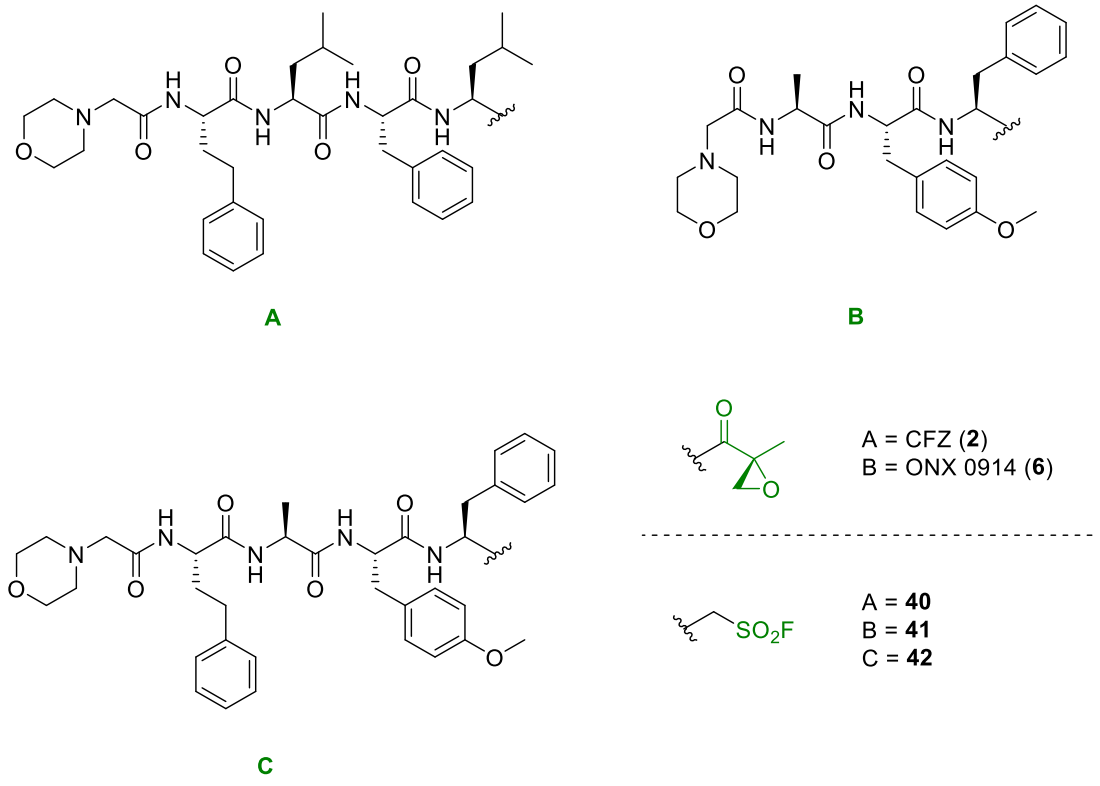

Figure 19 Structures of Carfilzomib (**2**), ONX 0914 (**6**) and the PSF analogues **40**, **41** and **42**.

The PSF **40** was used for crystal soaking experiments with yeast proteasome (yCP). Furthermore, time-resolved intact protein mass spectra analysis was carried out in order to identify short-lived reaction intermediates. The PSF **40** only reacted

with the β5-subunit whilst β1 and β2 remained unmodified. The obtained crystal structures (**Figure 20**) revealed the formation of an aziridine with the active threonine. This intramolecular cyclisation was confirmed by the inverted stereoconfiguration of the methyl group in the (*S*,*S*)-aziridine-T1 product, which implies an S_N2 reaction.[99]

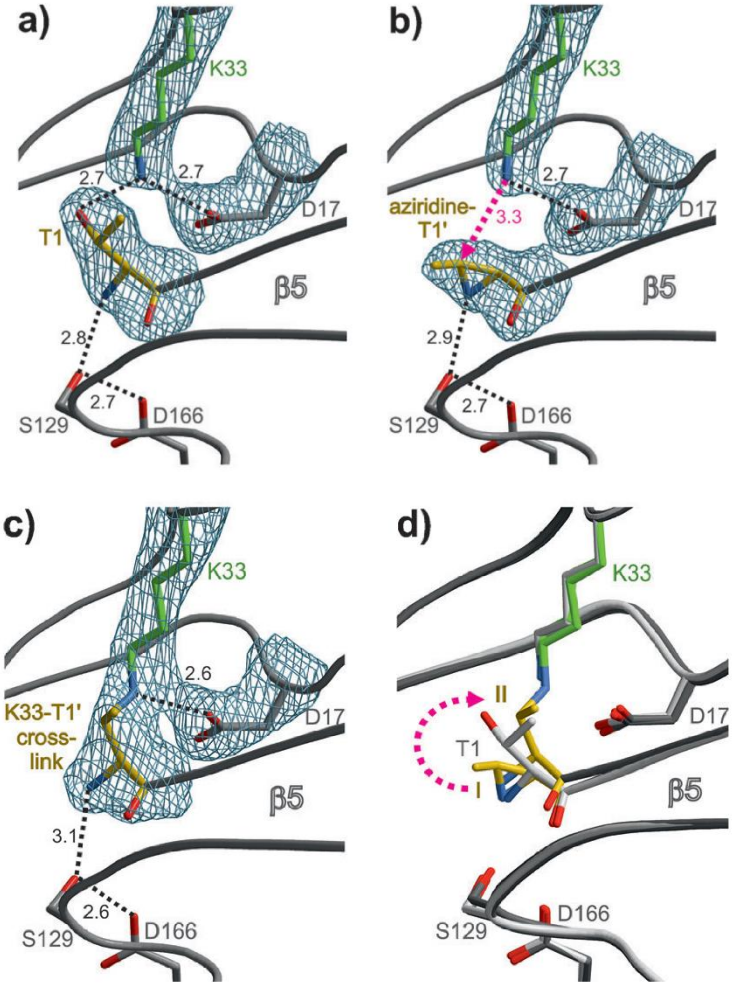

Figure 20 X-ray analysis of the β5 active site after time-dependent soaking experiment of yCP crystal with PSF **40**. **a)** Subunit β5 with unmodified Thr (T1). **b)** Aziridine-T1 formation. **c)** Lys33-T1 crosslink formation. **d)** Superposition of the three structures.[99]

Further soaking experiments were conducted in order to analyse the stability of the aziridine. These results revealed a S_N2 ring-opening reaction by attack of the amino group of the Lys33 residue, resulting in an intramolecular crosslink and proving the presence of a polarity-inversed threonine intermediate. Based on the identified reaction intermediates, a three-step mechanism resulting in the crosslink of the proteasome active site was proposed (**Scheme 16**).[99]

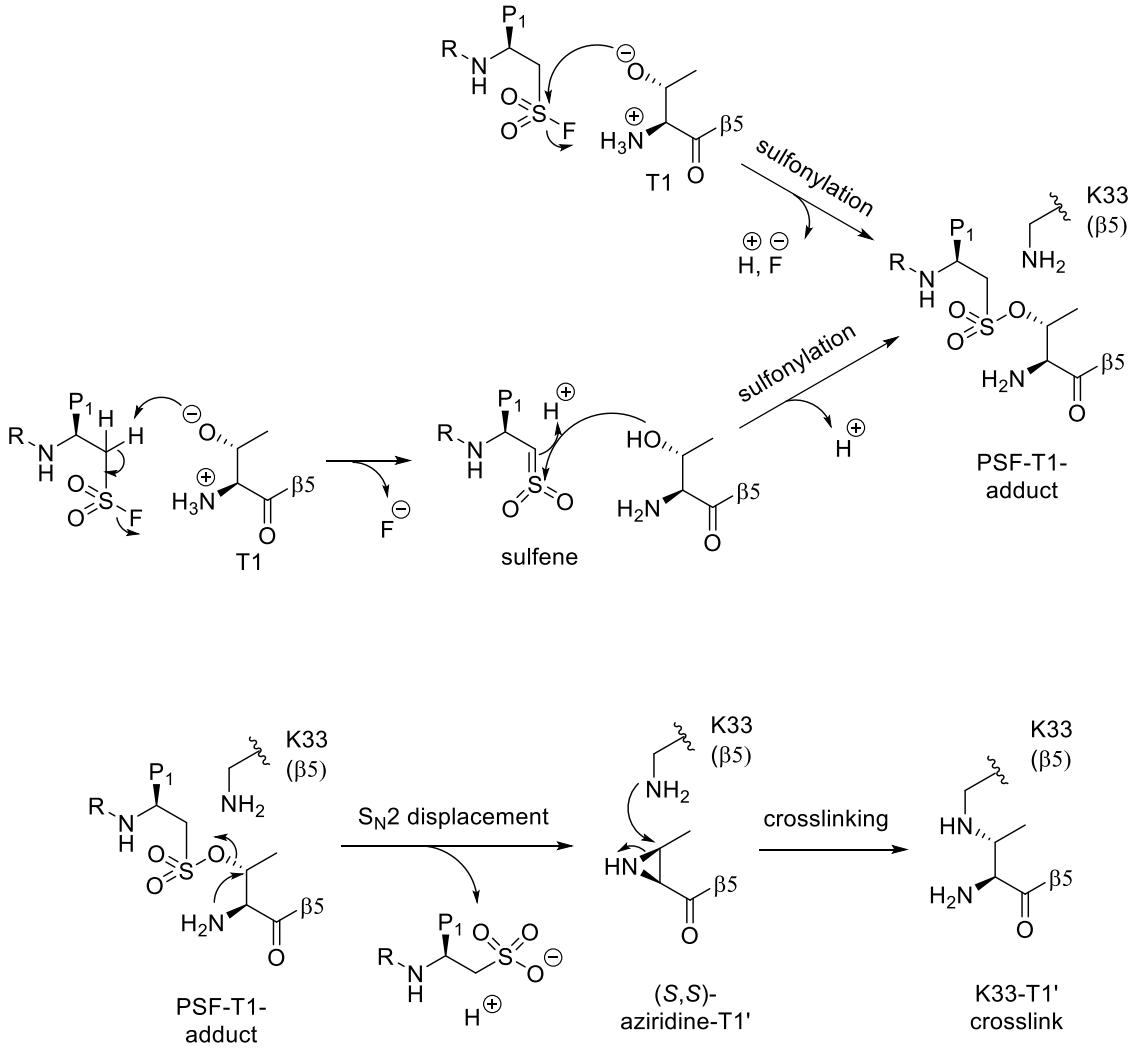

Scheme 16 Proposed three-step inhibition mechanism of the PSF compounds at the proteasomal active site of subunit β5.

In principle, the formation of the sulfonate adduct with Thr can occur by either direct nucleophilic attack of ThrO onto the electrophilic sulphur centre or by sulfene formation after proton abstraction. Sulfonylation is followed by an intramolecular S_N2 displacement by ThrN to yield the aziridine which is then opened to form an intramolecular crosslink. This previously unobserved mode of action suggests that PSF compounds (the only peptidic proteasome inhibitors known so far whose electrophilic trap is shifted by a methylene) are able to take advantage of the double nucleophilicity of the terminal threonine.[99]

The exploitation of this unique binding mode in order to increase selectivity towards the β5 subunit of the immunoproteasome over the corresponding subunit

of the constitutive proteasome was investigated. For this purpose, PSF **40**, **41** and **42** were evaluated against various CP types. The ratio between the IC_{50} was used to determine the selectivity of the compounds (**Table 4**).[99]

PSF **40** proved to be a very potent inhibitor but displayed no discrimination between the different ß5 subunits. Both PSF **41** and **42** exhibited a high selectivity towards ß5i but PSF **42** presented a 10-fold improvement in potency.[99]

The cytotoxic profiles of the PSFs were determined in viability assays against THP - 1, which express high amounts of immunoproteasome and HeLa cells and compared to the epoxyketone based inhibitors. The results obtained indicated low off-target binding profiles for the PSFs **41** and **42**, and lower toxicity than ONX 0914.[99]

Table 4 *In vitro* IC_{50} values (nM) against the ß5 subunit of various CP types.

Compound	IC_{50} yß5	IC_{50} ß5c	IC_{50} ß5i	IC_{50} ß5c/ ß5i
40	21 ± 2	28 ± 2	54 ± 10	0.5
41	15420 ± 635	28460 ± 1305	1134 ± 146	25
42	1775 ± 476	3927 ± 550	139 ± 34	28

The specificity of the PSFs to target the iCP, together with their low cytotoxicity, make these compounds potential anti-inflammatory inhibitors.

1.9 Aim of the Thesis

The aim of this thesis was to study the effect of the structural modification of the sulfonyl fluoride electrophile containing molecules. The right balance of reactivity and stability represents the key for rational design and optimisation of inhibitors. Understanding how these modifications translate into different chemical reactivity and/or biological action was pursued by chemical synthesis and systematic biochemical evaluations.

2. Synthesis, Reactivity and Biological Evaluation of Alpha-substituted Sulfonyl Fluorides

Parts of this chapter have been accepted for publication:

Herrero Alvarez, N.; van de Langemheen, H.; Brouwer, A. J.; Liskamp, R. M. J. "Potential peptidic proteasome inhibitors by incorporation of an electrophilic trap based on amino acid derived α-substituted sulfonyl fluorides" *Bioorganic Med. Chem.*

The sulfonyl fluoride moiety has been proven to be an outstanding warhead for the covalent modification of enzymes.[86] The special chemistry of this electrophile is highly dependent on its immediate structural environment, therefore, providing the possibility of tuning its reactivity.

Promising results have been obtained by the peptido sulfonyl fluorides (PSFs) as powerful proteasome inhibitors. PSFs have shown a high specificity for the ß5 subunit as well as an exceptional mechanism of inhibition. [97,99] Therefore, as an attempt to get a deeper insight in how structural modifications affect the potency and selectivity of the sulfonyl fluoride inhibitors, it was decided to synthesise sulfonyl fluoride derivatives containing a substituent on the alpha position (αPSFs) with respect to the sulfonyl fluoride electrophilic trap (**Figure 21**).

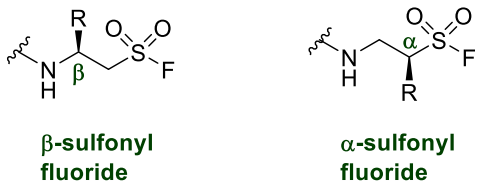

Figure 21 Structures of ß- and α-sulfonyl fluorides.

2.1 Aims of the Project

The aims of this project were the synthesis of alpha substituted sulfonyl fluoride derivatives (α-SFs) as potential peptidic proteasome inhibitors and the study of their chemical behaviour and biological activity. Additionally, the comparison with the beta substituted sulfonyl fluorides (ß-SFs) was desired in order to understand how the shift of the substituent from the ß to the α-position adjacent to the SF moiety correlates with the reactivity and the biological effect of these compounds (Structure Activity Relationship).

This chapter describes four main points: 1) the design of the synthetic route for these new molecules, 2) the reactivity and stability studies carried out with both α- and ß-SF, 3) the incorporation of the electrophilic trap into peptide sequences and 4) the efforts towards the biological testing of the final inhibitors.

2.2 Synthetic Route: a Racemic Approach

The approach of the Liskamp group for the synthesis of amino acid derived sulfonyl fluorides **45** was based on the introduction of the thioacetate moiety **44** into natural amino acids **43** which could be further oxidised to a sulfonate and subsequently fluorinated, retaining the corresponding side chains and not affecting the chiral centre (**Scheme 17**).[95]

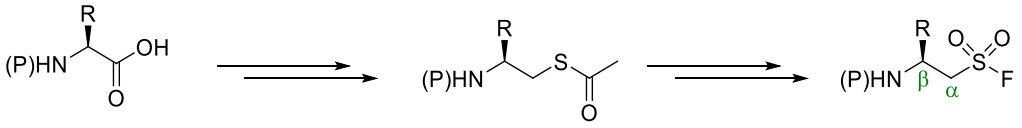

43 **44** **45**

Scheme 17 Synthesis route for amino acid derived ß-sulfonyl fluorides. P = Protecting group. R = amino acid side chain.

Whereas the ß-substituted derivatives were easily accessible starting from proteinogenic amino acids, the α-substituted sulfonyl fluorides presented a higher synthetic challenge since additional manipulation is required in order to shift the side chain to the desired α-position with respect to the sulfur atom.

The chosen strategy to achieve the α-substituted sulfonyl fluorides involved the ring opening of a suitable epoxide **48** and the introduction of the amino functionality to access the corresponding amino alcohol **47** (**Scheme 18**). This amino alcohol contains the side chain at the future alpha position and could be further functionalised towards the sulfonyl fluoride *via* the corresponding thioacetate **46**.

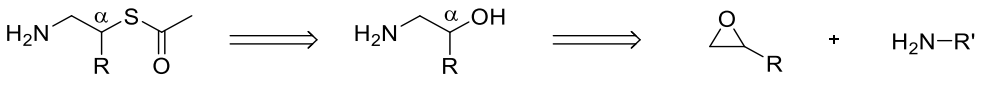

46 **47** **48** **49**

Scheme 18 Retrosynthetic strategy for alpha-substituted sulfonyl fluorides.

2.2.1 Ring opening of epoxides

Commercial racemic epoxides with intrinsic amino acid side chains were used for the initial development of the synthetic route.

The first attempt to open the epoxide was carried out with a calcium triflate catalysed aminolysis (**Scheme 19**).[100] Propylene oxide **50** was reacted with benzylamine in the presence of 50 mol % of the catalyst in acetonitrile. The corresponding *N*-benzyl amino alcohol **51** was obtained in 85% yield. Removal of the benzyl group was desirable at this stage for two main reasons. Firstly, the necessary conditions for benzyl deprotection appeared incompatible with the sulfonyl fluoride functionality, particularly when involving palladium chemistry, due to the tendency of the sulfur to inactivate catalysts.[101] Additionally, Cbz has proven to be the most suitable protecting group over the synthesis of sulfonyl fluorides and their incorporation into peptide sequences due to its stability under the employed conditions and ease to removal with strong acids when required. Therefore, the benzylprotected amino alcohol was subjected to removal of the benzyl group by treatment with the more active Pearlman's catalyst and hydrogen at 1 atm.[102] However, the deprotection reaction failed under the selected conditions and after 3 days only starting material was detected by TLC (**Scheme 19**).

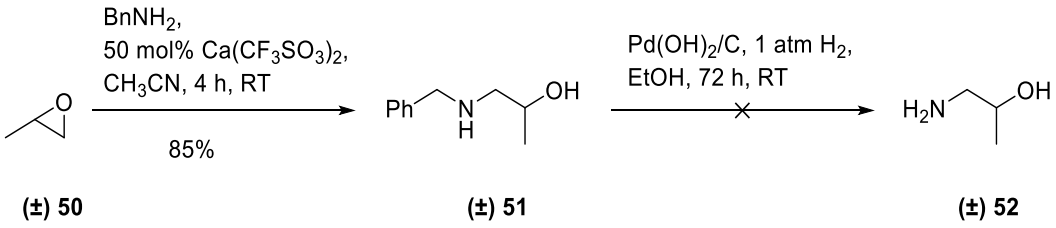

Scheme 19 Calcium triflate-catalysed aminolysis of epoxide and *N*-debenzylation.

In a second attempt, trying to circumventing the hydrogenolysis step, (±) propylene oxide **50** (R = CH_3) and (±) benzyloxirane **53** (R = CH_2Ph) were treated with a 30% solution of ammonia in water.[103] This alternative reaction resulted in a satisfactory and simple method to access the corresponding amino alcohols **52** and **54**. Amino alcohols were directly protected with benzyl chloroformate (Cbz-

Cl) and triethylamine, following standard procedures,[104] affording Cbz-amino alcohols **55** and **56** in 50% and 90% yield, respectively (**Scheme 20**).

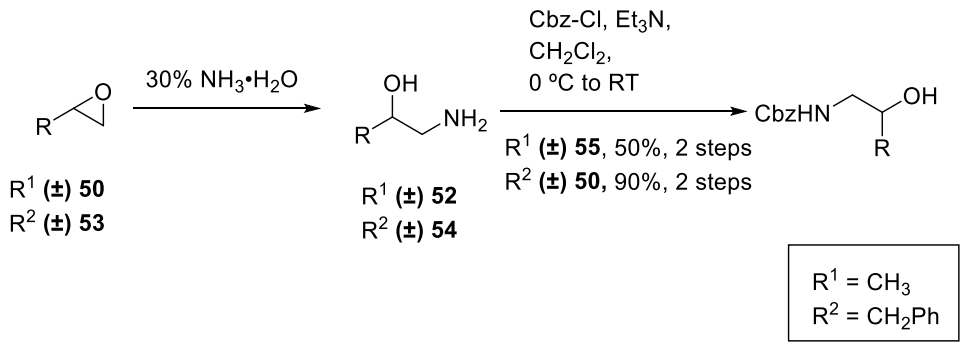

Scheme 20 Ammonia ring opening of the epoxide and Cbz protection of the amino alcohol.

2.2.2 Introduction of the thioacetate group

Subsequent introduction of the thioacetate group was crucial for the success of the synthesis in order to prepare the sulfonyl fluoride moiety. Originally, it was attempted to synthesise the thioacetates **59** and **60** from the mesylates **57** and **58**, taking advantage of the good leaving group character (**Scheme 21**).[95] Mesylates were obtained by reaction of the alcohols **55** and **56** with methanesulfonyl chloride and triethylamine in CH_2Cl_2 in good yields. Following, mesylates were treated with a mixture of thioacetic acid and Cs_2CO_3 in DMF. A range of stoichiometries of reagents were explored (up to 3 equivalents) without clean and full conversion to the corresponding thioacetates. Instead the substitution reaction resulted in a mixture of residual mesylate and several unidentified by-products. Although this procedure was successful for the preparation of the beta-substituted sulfonyl fluorides, it could not be applied in the synthesis of the alpha-substituted sulfonyl fluorides. A possible explanation might be the less favourable S_N2 substitution reaction as a result of the higher steric hinderance of the secondary methylsulfonates.

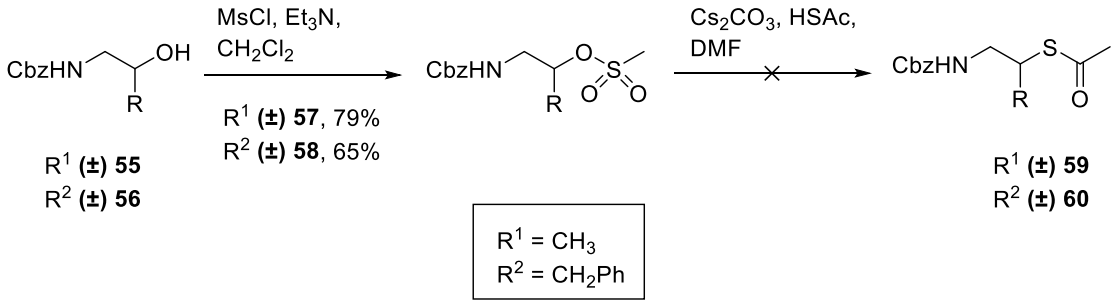

Scheme 21 Attempt to synthesise thioacetate derivatives *via* a mesylate approach.

In a second approach, the thioacetate **60** was directly synthesised by a Mitsunobu reaction (**Scheme 22**).[105] The *N*-terminal protected amino alcohol **56** was treated with triphenylphosphine, diisopropylazodicarboxylate (DIAD) and thioacetic acid in THF. Even though this reaction generated numerous byproducts it resulted in a convenient method to obtain the secondary thioacetate in reasonable yield.

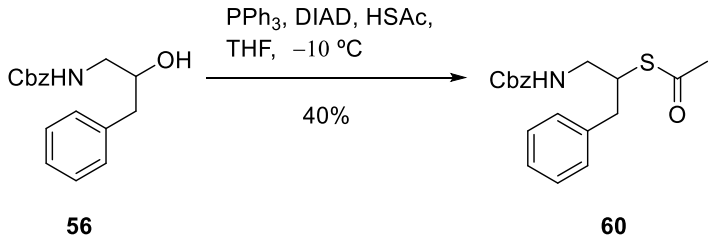

Scheme 22 Successful attempt to synthesise the thioacetates by a Mitsunobu reaction.

2.2.3 Accessibility to epoxides

Finally, terminal alkenes were investigated to access non-commercial epoxides as a potential source to gain access to different amino acid side chains. Firstly, the terminal olefin 4-methyl-1-pentene **61** was converted to the corresponding bromohydrin **62** with NBS in water and preparation of the amino alcohol **64** was attempted *via* a two-step one-pot reaction strategy with a 30% aqueous ammonia solution.[103] However, formation of the epoxide under these conditions was not

observed probably due to the insufficient basicity of ammonia to deprotonate the alcohol (**Scheme 23**).

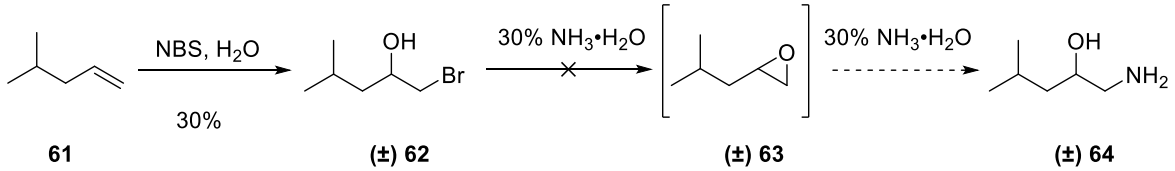

Scheme 23 Bromohydrin formation and amino alcohol preparation by a two-step one-pot reaction strategy.

In a second attempt, the terminal alkene **61** was epoxidised with meta-chloroperoxybenzoic acid in CH_2Cl_2 (**Scheme 24**). ^1H NMR of the crude showed the successful formation the desired epoxide **63** which was directly opened by use of the 30% aqueous ammonia solution. The obtained amino alcohol **64** was directly used in the next reaction without further purification and therefore yield was not recorded.

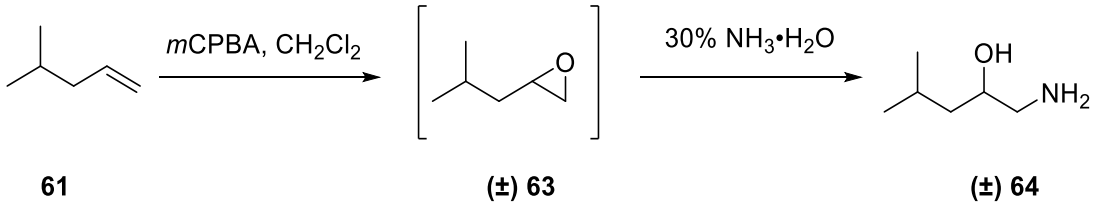

Scheme 24 Epoxidation reaction with mCPBA and ring opening epoxide.

2.2.4 Final proposed synthesis

Two racemic α-substituted derivatives, with side chains corresponding to leucine and phenylalanine, were successfully synthesised, starting either from the commercial epoxide **(±) 53** or by *m*CPBA epoxidation of the terminal alkene **61** (**Scheme 25**). Ring opening of the epoxide with a 30% aqueous ammonia solution allowed the introduction of the amino functionality at the least hindered carbon, affording the amino alcohols **(±) 64** and **(±) 54** which were directly protected with benzyl chloroformate and triethylamine in CH_2Cl_2. The Cbz-protected amino

alcohols **(±) 56** and **(±) 65** were then transformed to the corresponding thioacetates **(±) 60** and **(±) 66** by a Mitsunobu reaction. Further oxidation to the sulfonic acids was performed using a 33% aqueous solution of hydrogen peroxide in acetic acid and the desired sodium sulfonate salts **(±) 67** and **(±) 68** were obtained *in situ* after treatment with sodium acetate in water. Finally, fluorination with morpholinodifluorosulfinium tetrafluoroborate (XtalFluor-M®, **69**)[106] with $Et_3N{\cdot}3HF$ as a promoter in CH_2Cl_2 led to the desired α-substituted sulfonyl fluorides **(±) 70** and **(±) 71**.

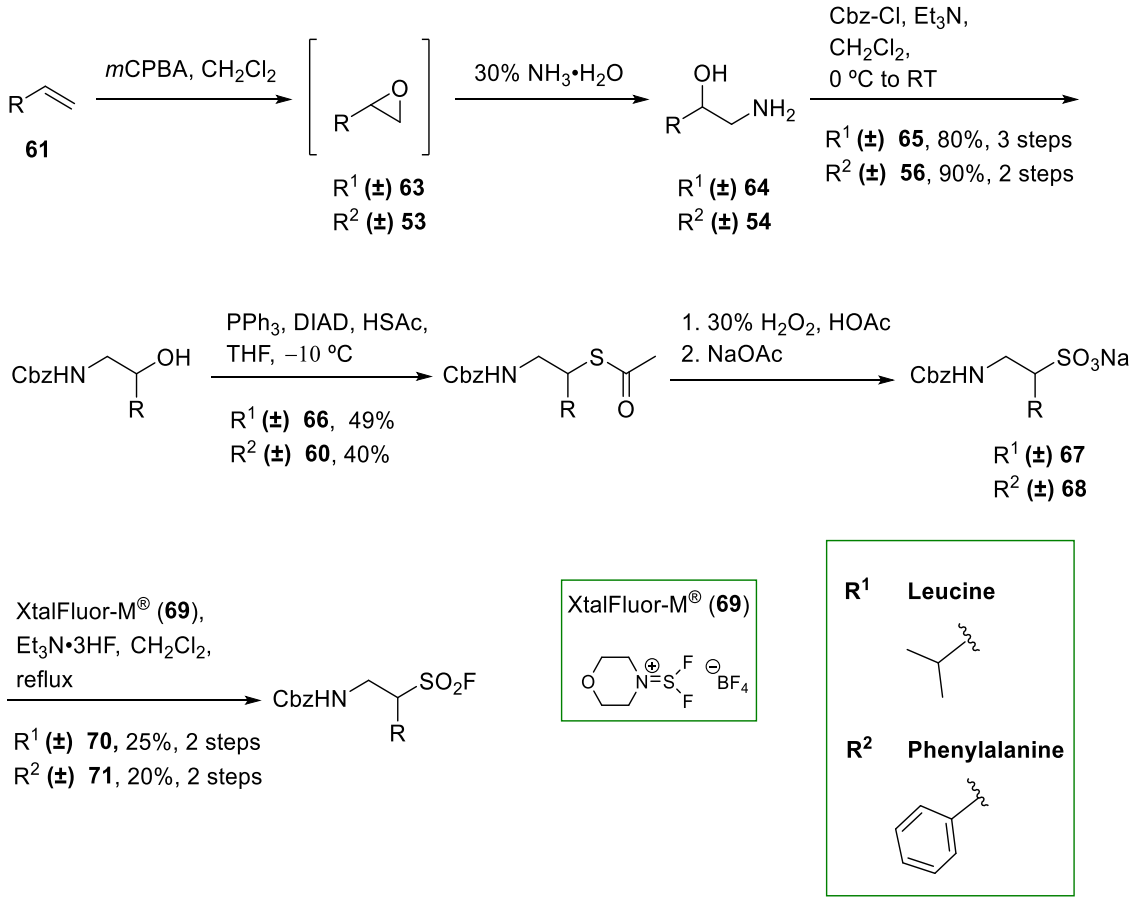

Scheme 25 Designed synthetic route for alpha-substituted sulfonyl fluorides.

2.3 Preliminary Biological Testing

At this stage it was decided to perform a preliminary biological testing of these new sulfonyl fluorides in order to evaluate their potential as serine protease inhibitors.

The enzyme α-chymotrypsin was selected for this purpose as previous experiments with the beta-substituted sulfonyl fluorides resulted in high inhibition.[96] The racemic α- and the enantiopure ß-Cbz-Phenylalanine derivatives, **(±) 71** and **27d,**[96] were selected for this assay due to the enzyme preference for aromatic residues.

A colorimetric assay was carried out by Arwin Brouwer (Utrecht University) (**Figure 22**). Both α-substituted **(±) 71** and ß-substituted **27d** (12.5 μM) were pre-incubated with α-chymotrypsin (1.0 μM) for 1h in an aqueous phosphate buffered saline (PBS) (0.05 M, pH 7.0), before the addition of the substrate Bz-Tyr-pNA **72** (0.25 mM). Subsequently, the liberation of p-nitroaniline **74** from Bz-Tyr-pNA was measured at λ = 405nm over 30 min and used to determine the residual enzyme activity.

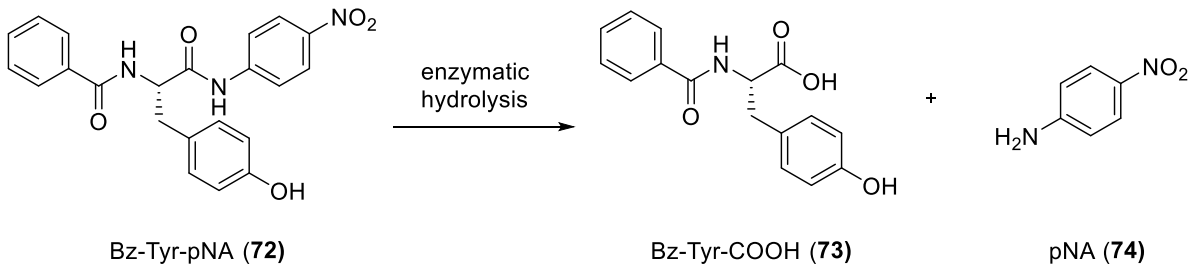

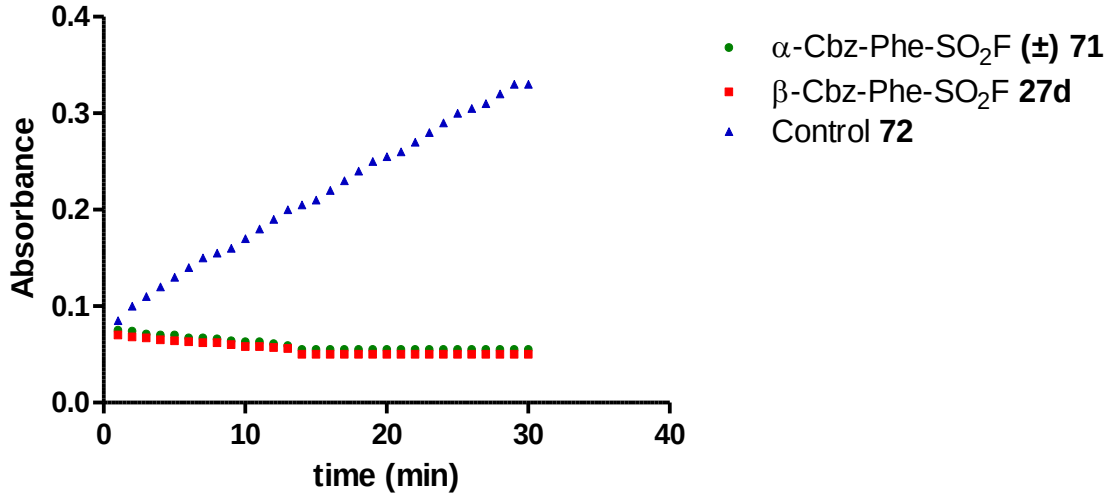

Figure 22 α-Chymotrypsin enzyme assay by monitoring the release of pNA **74** for comparison of the inhibitory activity of sulfonyl fluorides **(±) 71** and **27d**. [Enzyme] = 1.0 μ, [Substrate] = 0.25 mM, [SF] = 12.5 μM.

Satisfactorily, the α-substituted sulfonyl fluoride **(±) 71** was capable of decreasing the activity of α-chymotrypsin under these assay conditions and displayed an equal potency to the ß-substituted sulfonyl fluoride **27d**.

2.4 Enantioselective Synthesis of α-substituted Sulfonyl Fluorides

In light of the preliminary biological results, it was decided to attempt an enantioselective synthesis of the α-substituted sulfonyl fluoride warhead for its incorporation into potential inhibitors of the 20S proteasome.

Since the epoxide was identified as a key synthon in the synthesis of amino alcohols with the side chain in the desired α-position, it was envisioned to prepare the chiral epoxides from natural amino acids (**Scheme 26**).[107] This strategy would allow the use of amino acids **75** as a source of both chirality and proteinogenic side chains, including the more challenging functionalised residues, avoiding the need for further synthetic manipulations. In this approach α-bromo acids **76** can be obtained, which after subsequent reduction and treatment with base of bromo-alcohol **77** will afford epoxide **78**.

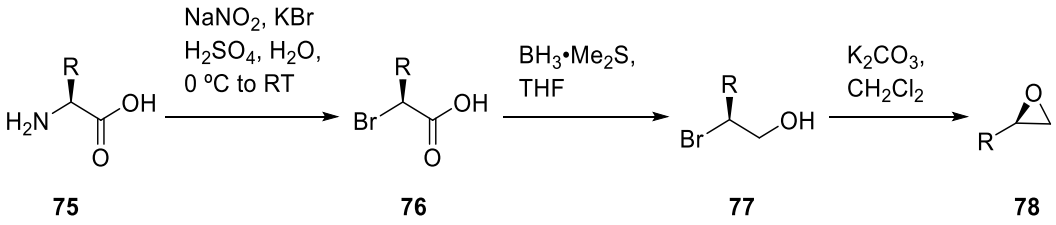

Scheme 26 Proposed synthetic route for preparation of chiral epoxide **78**. R = Amino acid side chains.

Thus, after diazotisation of amino acid **75** the corresponding bromoacid **76** could be obtained, with retention of the configuration by a double inversion mechanism (**Scheme 27**). Nitrous acid is generated *in situ* from sodium nitrite and sulfuric acid and decomposes to nitrosonium ion upon protonation and loss of water. The lone pair of the amino group of the amino acid attacks then onto the reactive

electrophile NO^+ forming the diazonium salt which immediately loses nitrogen gas to give an α-lactone. The lactone is finally opened by the bromide ion resulting in the bromoacid.

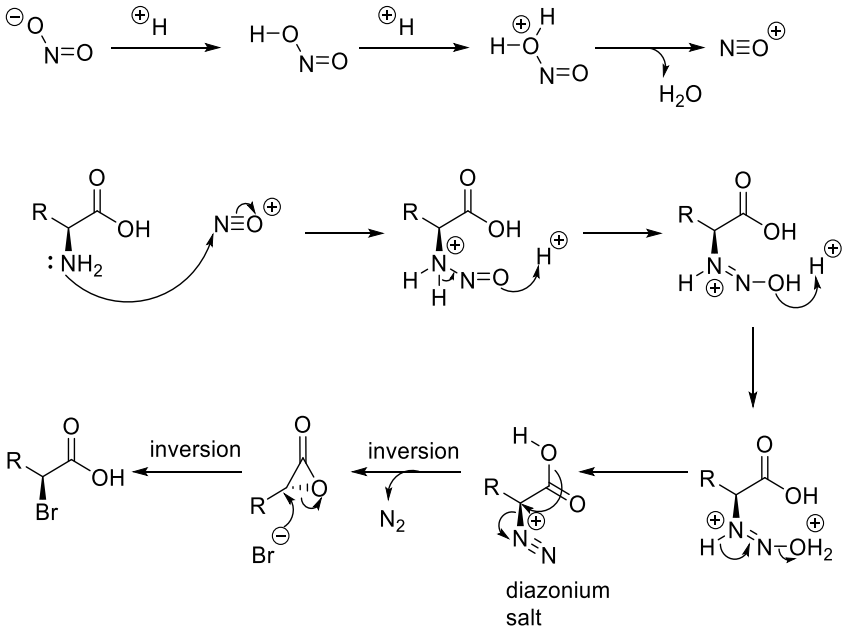

Scheme 27 Diazotisation mechanism. The diazonium salt, formed upon attack of the amine onto the reactive electrophile NO^+, results in the formation of an unstable α-lactone, subsequently opened by the bromide anion.

Following this approach the amino acid Leucine **79** was transformed to the bromoacid **80.** However, isolation of the bromoalcohol **82** was cumbersome due to the formation of side-products during the diazotisation reaction as no previous purification step of the bromoacid **80** was performed. Therefore, it was decided to include an additional step to form the corresponding ester **81**, which facilitated the purification process (**Scheme 28**).[108] The reduction of the unreactive ester was achieved by treatment with $NaBH_4$ in the presence of LiCl to generate $LiBH_4$ *in-situ*.[109]

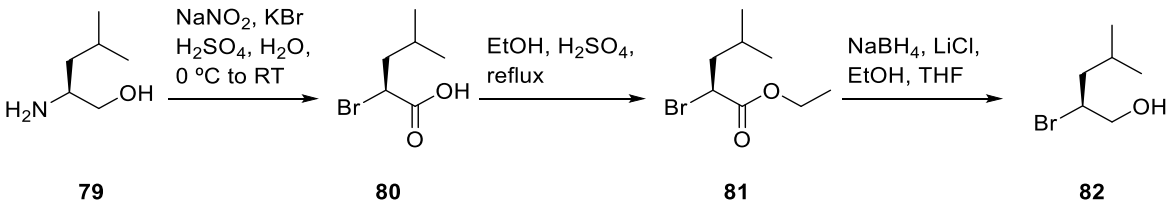

Scheme 28 Two-step formation of the alcohol **82** through the ester **81**.

Next intramolecular epoxidation of the resulting bromoalcohol **82** was attempted by treatment with potassium carbonate.[107] However, only unreacted starting material was observed by ^{1}H NMR and TLC and no generation of the desired epoxide **63** was detected, thus, the required reaction conditions had to be optimised (**Table 5**). The use of 18-crown-6 ether to complex the potassium cations resulted in formation of the product in good yield (50%). Best results were obtained using caesium carbonate[110] as a base due to the higher solubility in organic solvents with no need for any additive.

Table 5 Reaction conditions for the epoxide formation.

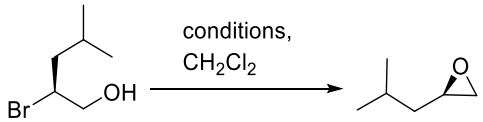

82 **63**

Entry	Base (equiv)	Additive (equiv)	Conversion[a]
1	K_2CO_3 (2)	-	0%
2	K_2CO_3 (2)	18-crown-6 (0.3)	50%
3	Cs_2CO_3 (2)	-	90%

a: Conversion based on ^{1}H NMR of the crude mixture

Since the chiral epoxide could be prepared using this route, it was applied to two different substrates: leucine and phenylalanine (**Scheme 29**). Leucine **79** and phenylalanine **83** were converted into the corresponding α-bromoacids **80** and **84** by treatment with $NaNO_2$ and KBr in an aqueous acid media. Subsequent esterification under acidic conditions provided the esters **81** and **85**, which were further reduced in the presence of $NaBH_4$, LiCl and ethanol in THF, delivering the bromoalcohols **82** and **86** in acceptable yields. Treatment of the bromo-alcohols with Cs_2CO_3 in CH_2Cl_2 generated the chiral epoxides **63** and **53**, which were immediately ring-opened by aqueous ammonia. Protection of the amino group of the obtained amino alcohols **64** and **54** with the Cbz-group afforded **65** and **56** in decent (over 3 steps) yields of 64 and 80%, respectively. Alanine derived Cbz-protected amino alcohol **55** was obtained upon protection of the commercially

available (*R*)-1-amino-2-propanol **87**. The secondary alcohols were converted to the corresponding thioacetates by a Mitsunobu reaction. Purification of the resulting thioacetates **66**, **60** and **59** was difficult and reduced the yields considerably. The oxidation of the thioacetates using aqueous hydrogen peroxide (33% w/w) and acetic acid followed by treatment with sodium acetate led to the corresponding sodium sulfonates **67**, **68** and **88**, which were subjected to the final fluorination reaction with XtalFluor-M® **69**, affording the desired α-substituted sulfonyl fluorides **70**, **71** and **89** in acceptable yields.

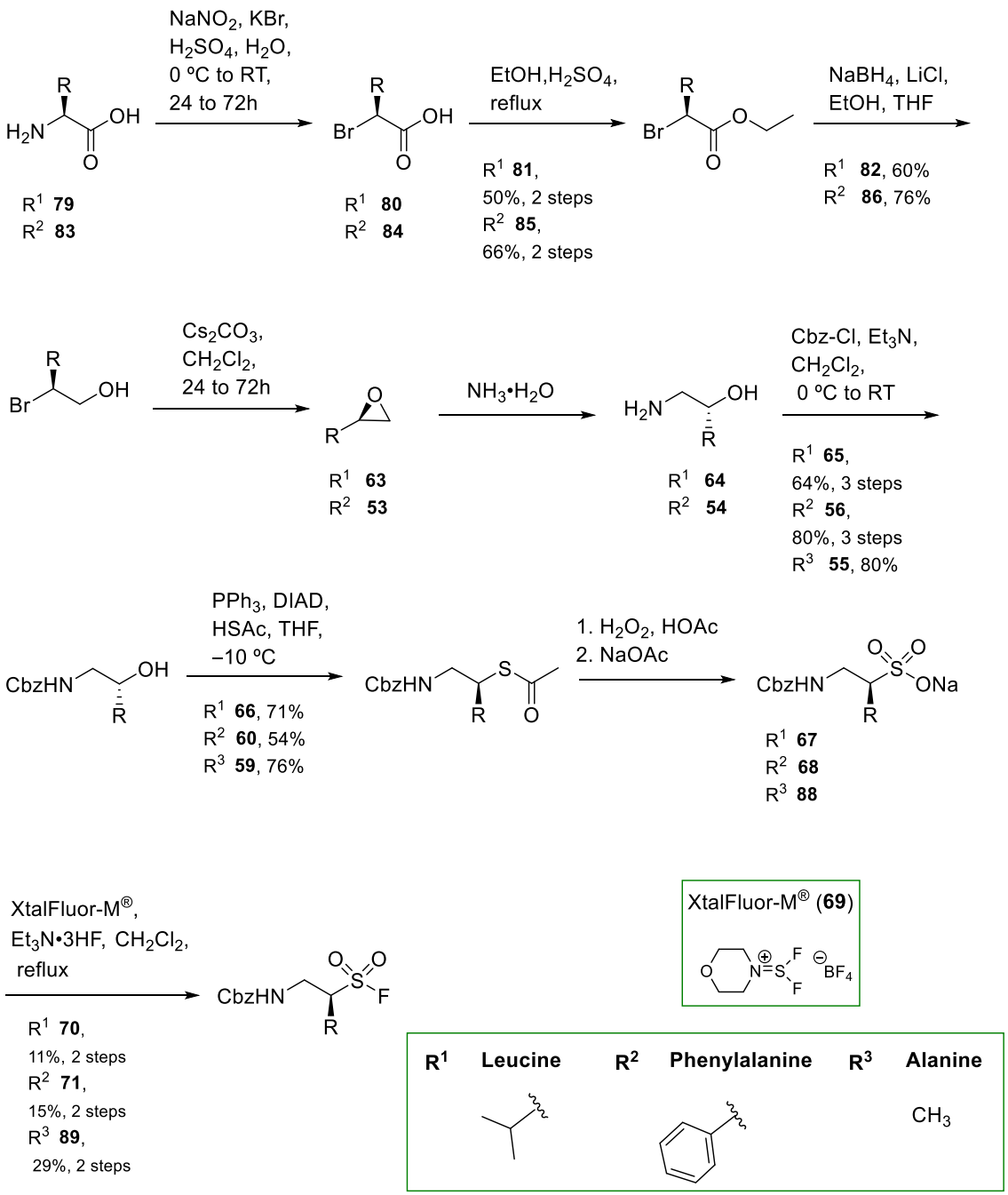

Scheme 29 Enantiopure synthetic route of alpha-substituted sulfonyl fluorides.

2.4.1 Revision of the fluorination reaction

Introduction of the fluorine starting from the sulfonate salts resulted in moderate yields and it proved to be particularly challenging with the α-substituted substrates. Therefore, it was decided to perform further investigations into this reaction, which resulted in the identification of a main side-product as the methyl sulfonate esters **90** and **91** (**Scheme 30**). Over the course of this research it was discovered the contamination of the supplied CH_2Cl_2 with MeOH.

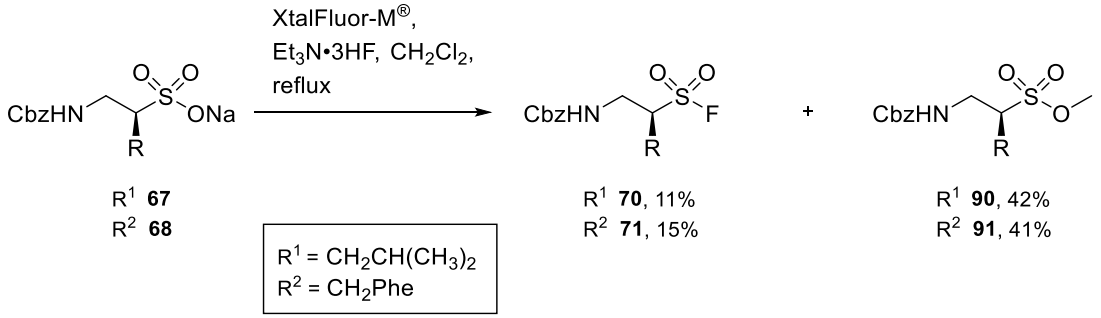

Scheme 30 Fluorination reaction using sodium salts **67** and **68** as substrates and CH_2Cl_2 as solvent.

Conveniently, the methyl ester **90** could be cleaved with tetrabutylammonium iodide in acetone,[111] providing a tetrabutylammonium salt **92** which is a suitable substrate for a repeated fluorination reaction. In a first attempt to avoid the methyl ester formation and to establish the possible relation between the CH_2Cl_2 and this side reaction DCE was selected as a solvent. These new conditions resulted in a dramatic increase of the yield from 11% to 57% (**Scheme 31**).

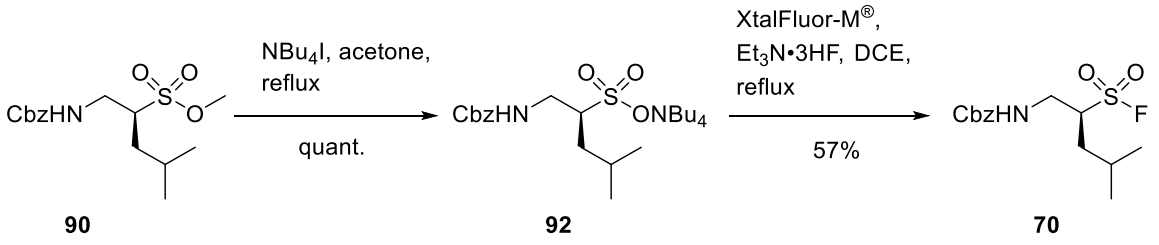

Scheme 31 Methyl ester cleavage and fluorination reaction using tetrabutylammonium salt **92** as substrate in DCE.

The fluorination reaction using DCE as a solvent was then repeated with the sodium salts **67** and **68** as substrates in order to reproduce the increase of yields (**Scheme 32**). Since formation of the sulfonate ester was not observed, the yield of the reaction was higher than the obtained under the original conditions. Nevertheless, the increment was not as high as when using the tetrabutylammonium salt **92**. This might be due to the impurity of the sodium salt, which as contains intermediate species formed during the oxidation reaction difficult to remove by chromatographic procedures. Additionally, the better solubility of the tetrabutylammonium salt in organic solvents could be an important factor. These results suggested the necessity for a less problematic oxidation of the sulfonates as well as the suitability of converting the corresponding sulfonic acids directly into tetrabutylammonium salts.

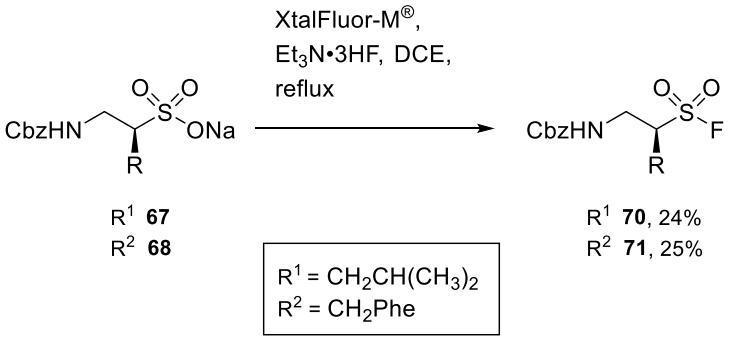

Scheme 32 Fluorination reaction using sodium salts **67** and **68** as substrate in DCE.

2.4.2 Enantiomeric Excess determination

Peptido amino acid-derived sulfonyl fluorides are designed to maximise the interactions with the enzyme binding pockets by mirroring the same residues as the natural substrates. Therefore, obtaining the right configuration of the amino acid-derived side chains is crucial to mimic the natural peptidic ligand.

The enantiopure synthesis of the α-substituted sulfonyl fluorides started from *L*-amino acids and involved several stereochemistry inversions. The optical purity of the intermediates was measured and compared with literature values when available. However, determination of the enantiomeric excess, especially for new molecules, was desirable.

Due to the possible reactivity of the sulfonyl fluoride moiety towards the surface functionalities of the stationary phase of the chiral normal-phased HPLC columns, it was decided to determine the enantiomeric excess of the amino acid-derived thioacetate. The thioacetate is obtained by a Mitsunobu reaction, which is the last step in the synthesis involving an inversion of the configuration as well as the last intermediate subjected to purification prior to the fluorination reaction. For this purpose the racemate of the leucine-derived thioacetate **(±) 66** was analysed using numerous combinations of different HPLC columns and mobile phase gradients. Analysis were performed by Mr Frank McGeoch. However, no base line resolution was achieved under the used conditions. As a result, the enantioselectivity of the synthesis could not be established at this point with the available resources.

The best resolution was obtained with an OD-H column and 98:2 hexane:IPA as mobile phase (**Figure 23**).

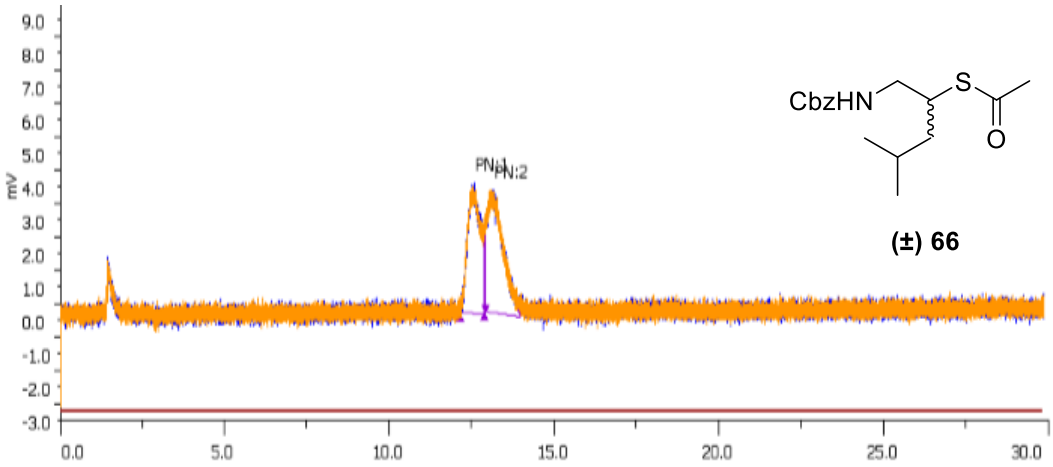

Figure 23 Chiral HPLC analysis of the racemate Cbz-Leu-$SOCH_3$ **66** with an OD-H column using a 98:2 hexane:IPA as mobile phase.

2.4.3 Functionalised amino acid side chains

After the successful synthesis of three α-substituted sulfonyl fluorides (**70**, **71** and **89**) containing a non-functionalised side chain, preparation of a functionalised amino acid derivative was attempted to prove it was possible to access more complex side chains (**Scheme 33**).

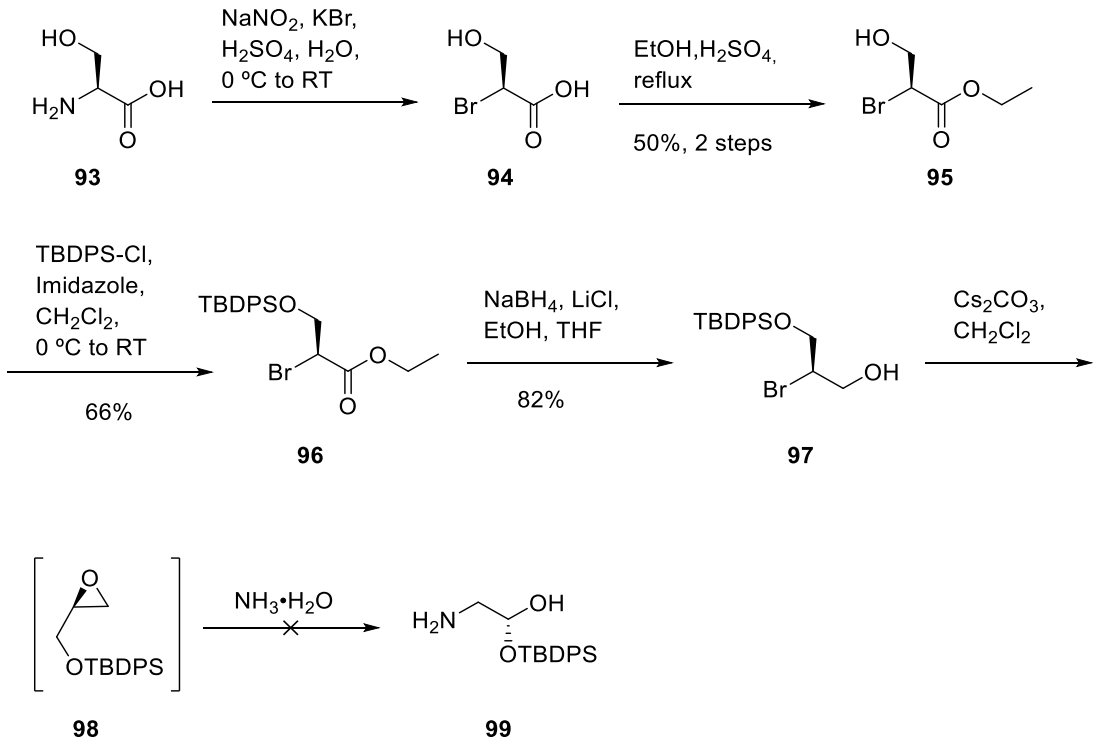

Scheme 33 Synthetic route towards a functionalised α-substituted sulfonyl fluoride.

It was envisioned that the same synthetic route could be applied when using an appropriate protecting group. For this purpose, serine **93** was subjected to a diazotisation reaction and the resulting bromoacid **94** converted to the corresponding bromoester **95**. After this step, the hydroxyl functional group was protected with *tert*-butyldiphenylsilyl (TBDPS), since this group was expected to be compatible with the different conditions applied during the synthesis.[112] The protected ester **96** was then further reduced to the alcohol **97**, which was subjected to epoxidation. Although formation of the epoxide **98** was detected by

TLC and LC-MS analysis, the corresponding amino alcohol **99** was never obtained upon the ring opening epoxide reaction.

This suggested that the protecting group strategy adopted during the synthesis of this derivative was unsuitable for the completion of the route. Therefore, this derivative was not further pursued and investigation of a more suitable group/groups was postponed.

2.5 Reactivity Studies

At this stage we wished to obtain a general idea of the chemical reactivity of the alpha-substituted sulfonyl fluoride warhead with respect to nucleophiles and whether this behavior was different from the beta-substituted sulfonyl fluorides.

For this α-substituted sulfonyl fluorides **70** and **71** were compared with ß-substituted sulfonyl fluoride **27c** by reaction with a small set of nucleophiles chosen to represent the main categories of active residues existent in enzymes (amines, thiols and alcohols). (**Table 6**)

As expected, the α-substituted warhead does not differ from the ß-substituted with respect to their specificity toward the different nucleophiles. Both types of sulfonyl fluorides do react with amine nucleophiles such as piperidine and benzylamine. However, α-substituted sulfonyl fluorides gave rise to more sulfonamide product formation after 24 h. In addition, both categories of sulfonyl fluorides do not react with thiols such as benzylmercaptan and mercaptoethanol, even in the presence of a base (DiPEA).

Table 6 Reactivity of sulfonyl fluorides towards different nucleophiles. Reactions were performed using 2.2 eq of the respective nucleophile in CH_2Cl_2 over 24h. Results show the yields of the isolated products after silica column chromatography.

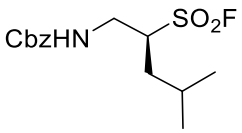

α-Leu

70

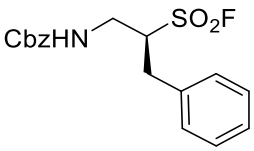

α-Phe

71

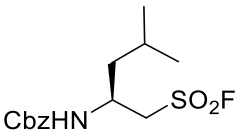

β-Leu

27c

Entry	Piperidine	Benzylamine	Benzylmercaptan	Mercaptoethanol
70	72%	25%	No reaction[a,b]	No reaction[a,b]
71	70%	30%	No reaction[a,b]	No reaction[a,b]
27c	40%	10%[c]	No reaction[a,b]	No reaction[a,b]

a : in the absence of base
b : in the presence of 2.2 eq of DiPEA
c : based on starting material recovery

Nucleophilic substitution at sulfonyl fluorides may occur by an elimination-addition pathway involving formation of a sulfene intermediate after proton abstraction or by direct substitution of the fluorine atom or. There is substantial controversy in the literature regarding whether the direct substitution occurs in a concerted manner or in a stepwise process *via* a trigonal bipyramidal intermediate (TBPI).(**Scheme 34**). Isotopic exchange experiments to detect this intermediate have failed to provide clear evendicences.[113] By contrast, the sulfene type intermediate is firmly supported for sulfonyl halides bearing acidic protons in the α-position.[86]

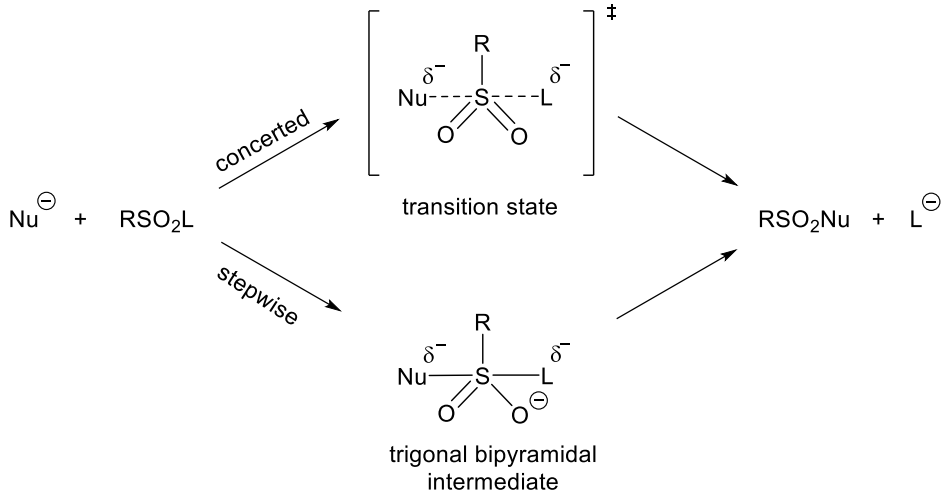

Scheme 34 Two possible mechanisms for the nucleophilic substitution at the sulfonyl center.

Deuterium exchange experiments with the ß-SF were carried out in the Liskamp group (unpublished data) suggested the sulfene pathway, however, direct substitution could not be completely ruled out.

The indication of a possible higher reactivity of the α-substituted warhead cannot be directly attributed to the formation of a sulfene intermediate since abstraction of the α-proton with respect to the -SO_2F in **70** is assumed to be more difficult than in **27c**. Nevertheless, the more substituted sulfene would be thermodynamically more stable.

An explanation for these results may be found assuming a trigonal bipyramidal intermediate in the direct substitution pathway, which could offer relieve of strain going from ca 109º angles in the starting material to ca 120º and therefore allowing steric acceleration (**Scheme 35**).[114,115]

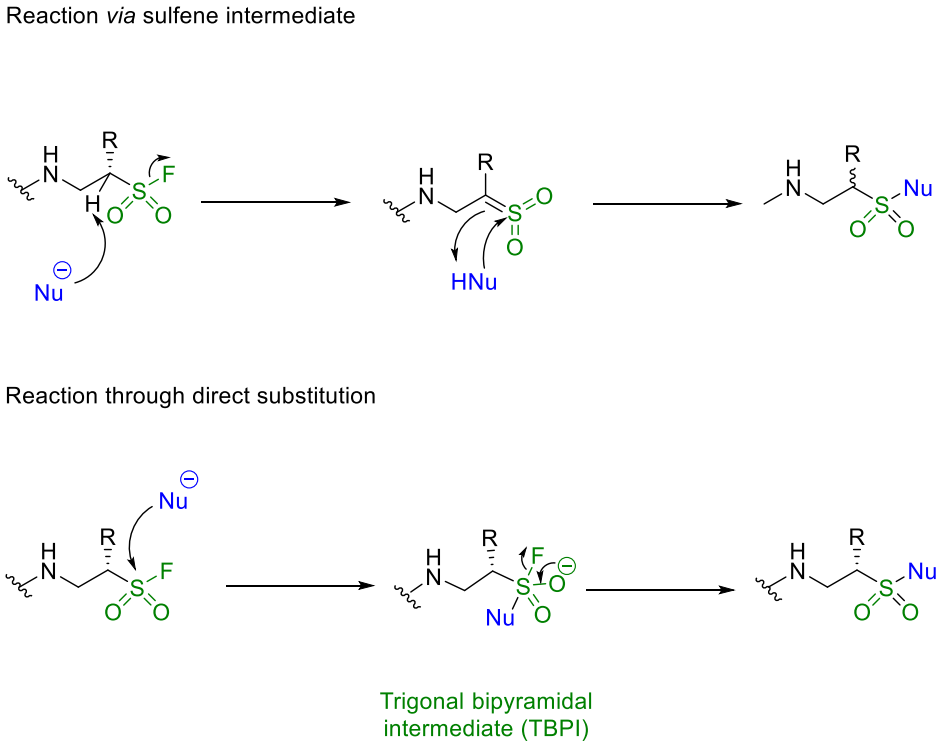

Scheme 35 Possible mechanisms of nucleophilic substitution for α-substituted SF.

1.9 Incorporation of Alpha-substituted Sulfonyl Fluorides towards Potential Proteasome Inhibitors

To evaluate the inhibitory activity of the alpha-substituted sulfonyl fluorides and to compare this with the results previously obtained in the group for the beta-substituted sulfonyl fluorides, they were incorporated into peptide sequences derived from PSF **30**, **32** and **40**.[97]

2.6.1 Synthesis of peptide sequences

Cbz-Leu-Leu-OH **103** (Cbz-Leu$_2$-OH) and Cbz-Leu-Leu-Leu-OH **107** (Cbz-Leu$_3$-OH) sequences were synthesised in solution in a few steps from the common intermediate methyl ester **100**, obtained after treatment of L-leucine **79** with thionyl chloride in MeOH (**Scheme 36**). Respective couplings with Cbz-Leu-OH **101**

and Boc-Leu-OH **104** using BOP and DiPEA in CH_2Cl_2 led to Cbz-Leu$_2$-OMe **102** and Boc-Leu$_2$-OMe **105.** Subsequent removal of the Boc-group with TFA in CH_2Cl_2, followed by an additional coupling reaction with Cbz-Leu-OH **101** using BOP and DiPEA in CH_2Cl_2 afforded Cbz-Leu$_3$-OMe **106.** Carboxylic acids **103** and **107** were obtained after saponification of the methyl esters **102** and **106** with Tesser's base (dioxane/methanol/4N NaOH, v/v/v 4/5/1) and semi-preparative reversed-phase HPLC purification.[97]

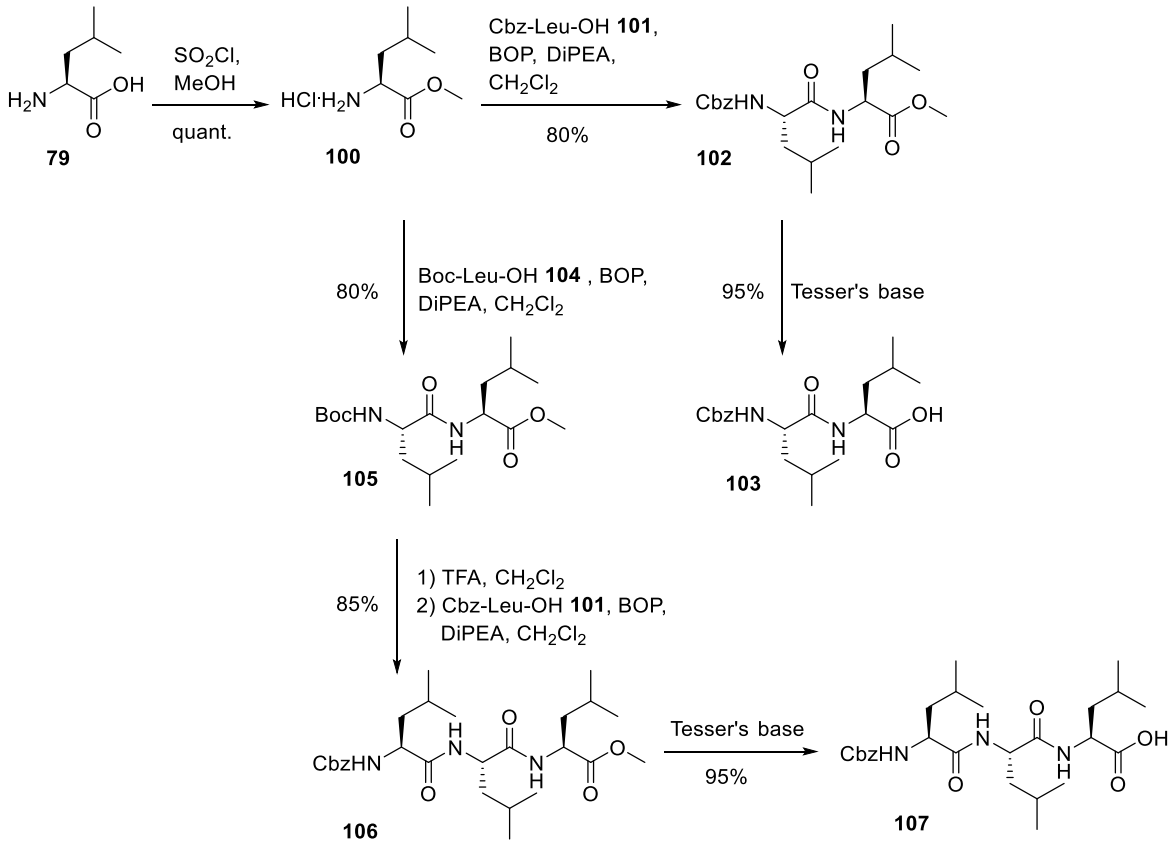

Scheme 36 Synthesis in solution of Cbz-Leu$_2$-OH **103** and Cbz-Leu$_3$-OH **107**.

A morpholino-*h*Phe-Leu-Phe-OH **116** sequence was prepared by solid phase peptide synthesis using Fmoc-chemistry. 2-Cl-Tritylchloride resin was loaded with the first amino acid **108** using DiPEA in CH_2Cl_2. Successive cycles of Fmoc-deprotection, using a 20% solution of piperidine in DMF and coupling with the corresponding Fmoc-protected amino acids (**110**, **112** and **114**), using HCTU and DiPEA in CH_2Cl_2 delivered peptide **115**. The carboxylic acid **116** was obtained after cleavage of **115** from the resin using a 30% solution of HFIP and semi-preparative reversed-phase HPLC purification (**Scheme 37**).[99]

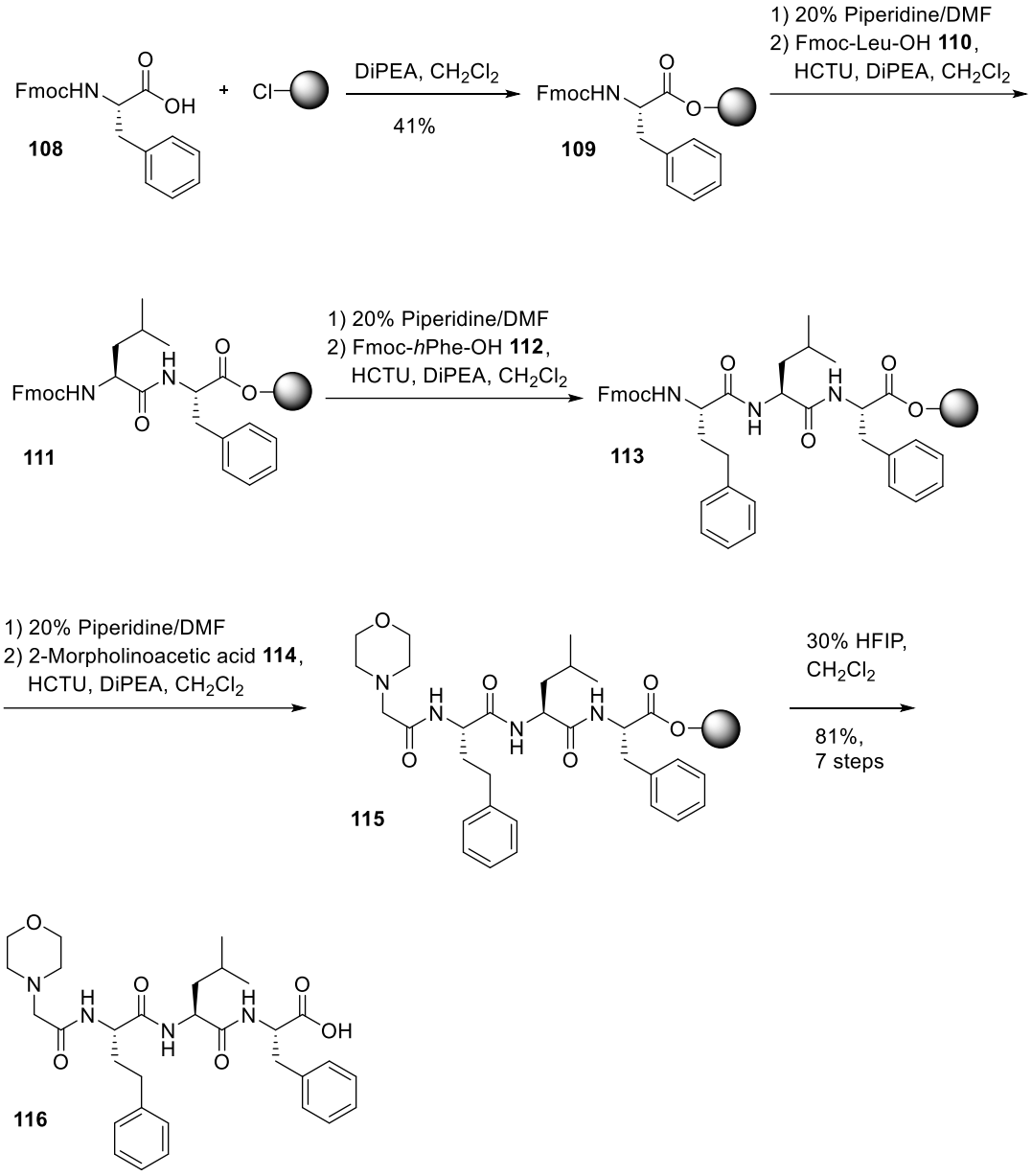

Scheme 37 Solid phase peptide synthesis of Morph-*h*Phe-Leu-Phe-OH **116**

.

2.6.2 Deprotection of the amino acid derived sulfonyl fluorides

As previously discussed, the preparation of peptides as free C-terminal acids followed by coupling with the amino acid derived sulfonyl fluoride to the *N*-terminus in the last step was preferable. This strategy allows to subject the sulfonyl fluoride electrophile to the minimum number of reactions.

Considering the coupling conditions applied for the incorporation of the sulfonyl fluoride warhead into the different peptide backbones, the possibility of racemisation due to the acidity of the alpha proton induced by the sulfonyl fluoride functionality was the first issue to address. Therefore, a coupling reaction using neutral conditions was desirable.

As a consequence the first challenge was the removal of the Cbz-protecting group. The standard procedure is the treatment with a 33% solution of HBr in acetic acid, which provides the HCl salt of the amine **118** upon treatment with an ion exchange resin. This method demands the use of a base during the coupling. Trying to circumventing this problem, the cleavage was attempted by hydrogenation in the presence of a 10% Pd/C as an approach to directly obtain the free amine **117**. However, the hydrogenation did not proceed and starting material **89** was completely recovered after the reaction, probably due to catalyst poisoning by the sulfur.[101] Fortunately, following a recent literature procedure, it was possible to obtain the free amine **117** using HBr in acetic acid followed by treatment of the HCl salt **118** with Zn powder in THF (**Scheme 38**).[116]

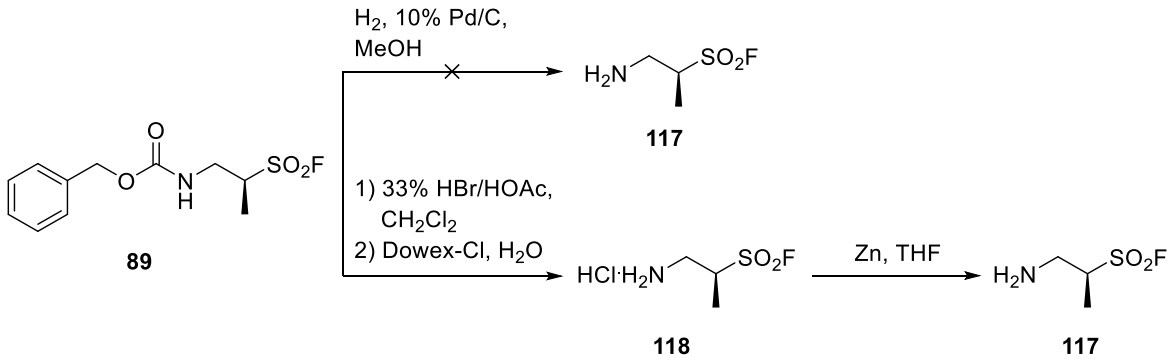

Scheme 38 Different attempts of Cbz-deprotection of sulfonyl fluoride **89**.

2.6.3 Incorporation of the sulfonyl fluoride warhead into the peptide sequences

Inhibitor synthesis was achieved using a DCC mediated-coupling of the peptide backbones in the presence of 6-chloro-HOBt (HOBt-Cl), with the previously liberated amine of the corresponding warheads **118** and **119** (**Scheme 39**). This method provides essentially neutral conditions. The final peptido sulfonyl fluoride inhibitors **120-125** were obtained after semi preparative reversed-phase HPLC purification in rather low yields. This might be due to possible side reactions both before and upon coupling. It is particularly important to mention that the high reactivity of α-SFs towards amines, previously discussed, would be consistent with a reaction between the free *N*-terminus generated by the treatment with Zn and the sulfonyl fluoride moiety prior to the coupling. However, at this stage avoiding the need for basic conditions was the priority and therefore the obtained yields were considered acceptable and sufficient to continue with the rest of the studies.

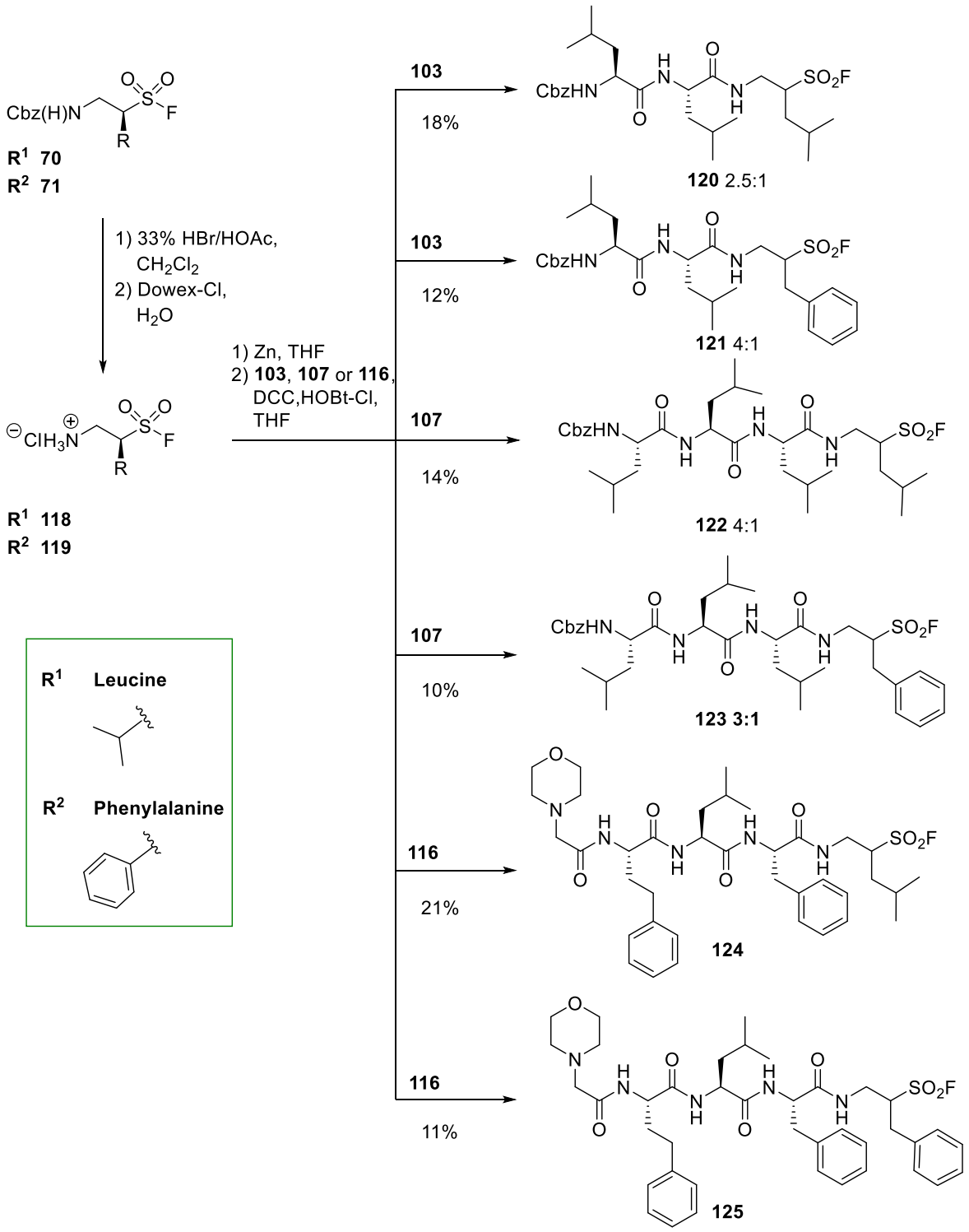

Scheme 39 Incorporation of the α-substituted sulfonyl fluorides to yield inhibitors **120-125**. Diasteroisomeric ratios were calculated by ^{1}H NMR when possible.

2.6.4 Diastereoselectivity of the synthesis

Despite the neutral conditions employed for the coupling of the warheads **70** and **71** with the respective peptide sequences **103**, **107** and **116**, all inhibitors **120-125** were obtained as mixtures of diasteroisomers (**Scheme 39**). The ratios of the mixtures were calculated by ^{1}H NMR based on the proportion of the α-proton next to the sulfonyl fluoride when possible. In light of these results, it was decided to investigate the influence of the coupling reaction on the epimerisation.

The racemic warheads **(±) 70** and **(±) 71** were coupled to Cbz-Leu$_2$-OH **103** sequence under basic conditions, using BOP and DiPEA in CH_2Cl_2, as controls for resolution studies (**Scheme 40**).

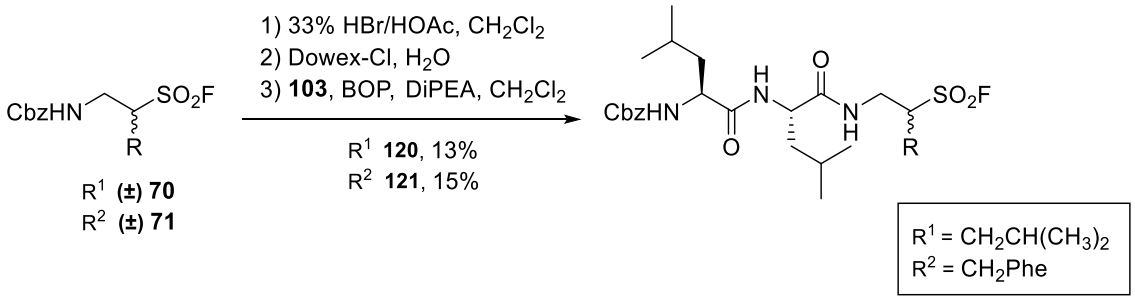

Scheme 40 Coupling reaction with the racemic warheads **70** and **71** using basic conditions.

Additionally, the warhead **71** obtained by the enantiopure synthetic route was coupled to Cbz-Leu$_2$-OH **103** sequence under basic conditions, using BOP and DiPEA in CH_2Cl_2 (**Scheme 41**) for comparison with the coupling performed with the same warhead **71** under neutral conditions.

.

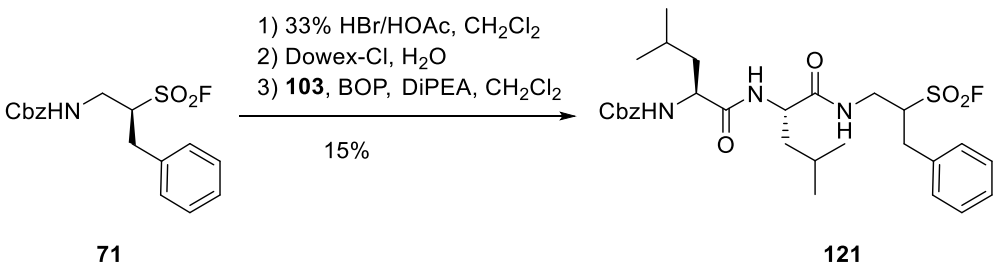

Scheme 41 Coupling reaction with the chiral warhead **71** using basic conditions.

The diasteroisomeric mixtures of inhibitor **121** obtained by the different reaction conditions were evaluated by analytical HPLC. Unfortunately, no base line resolution of the diasteroisomers could be achieved with the available HPLC columns (**Figure 24, 25 and 26**).

However, similar ratios of the diasteroisomers were observed both under basic (**Figure 25**) and neutral conditions (**Figure 26**) when using the chiral warhead **71.** This suggested that the epimerisation was probably not taking place during the coupling step but was the result of the synthesis of the warhead. A possibly explanation might be the increased acidity of the α-proton induced by the introduction of the sulfonyl fluoride moiety. On the other hand, an enantiopurity lost might occur over the different reactions involving configuration inversion. Unfortunately, this could not be proved since the *ee* could not be conclusively established. Consequently, the research was continued with the inhibitors as diasteroisomeric mixtures.

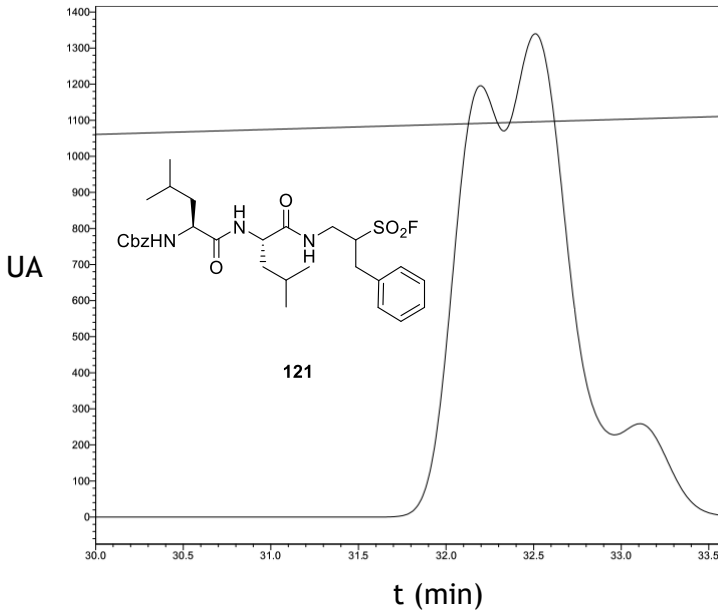

Figure 24 Analytical HPLC analysis of compound **121** obtained by coupling of the racemate **(±) 71** with **103** under basic conditions.

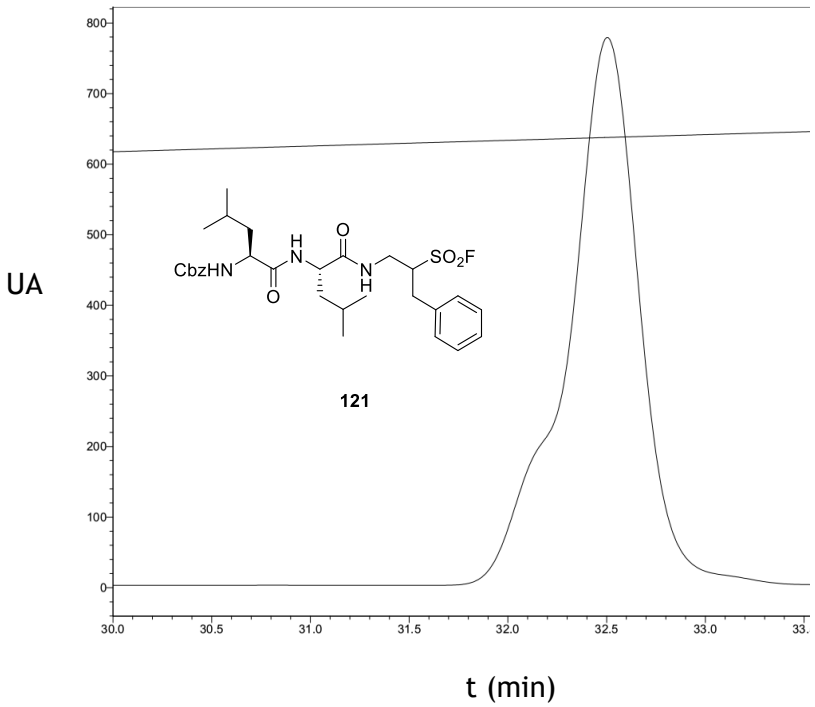

Figure 25 Analytical HPLC analysis of compound **121** obtained by coupling of the chiral **71** with **103** under basic conditions.

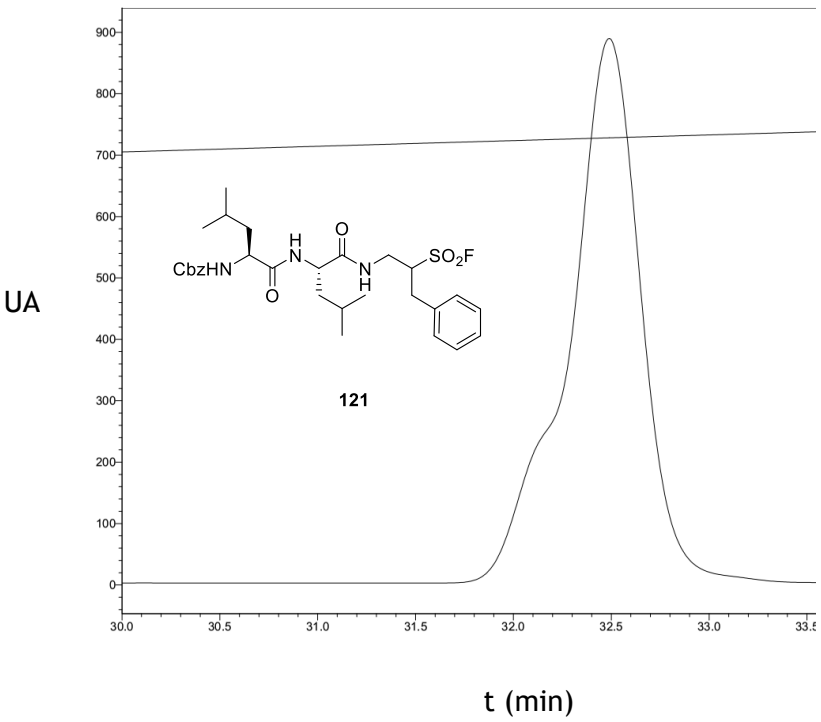

Figure 26 Analytical HPLC analysis of compound **121** obtained by coupling of the chiral **71** with **103** under neutral conditions.

2.7 Buffer Stability Studies

Since the ultimate environment for the inhibitors will be a biological system, the behaviour of α-PSFs **120** and **122** and the ß-PSF inhibitors **30** and **32** in an aqueous buffer was evaluated at different pHs (**Figure 27**).

For this study the different inhibitors were dissolved in DMSO and diluted into aqueous phosphate buffered saline (PBS) at pH 6.5, 7.4 and 8.0. The degree of hydrolysis under these conditions was monitored by analytical HPLC over 12 hours. The measurement of the first injection was taken as the reference peak and the remaining percentage of inhibitor was plotted against the time (**Figure 28**).

Although all the tested compounds exhibited considerable aqueous stability, the α-PSFs **120** and **122** appeared to be more prone to undergo hydrolysis than their ß-PSF counterparts **30** and **32**. Surprisingly, hydrolysis of **120** at acidic pH was initially fast and remained at a constant rate afterwards. Half of the concentration of the α-PSFs **120** and **122** was consumed at the different pHs after 5-7 hours, whereas the ß-PSF inhibitors **30** and **32** were more stable, and depending on the pH their half-life varied between 10-12 hours.

However, it is important to note that remarkable solubility issues were encountered while performing the experiments as reflected by some of the drastic decreases of the remaining peptide in solution over the first hour. These issues will be further discussed in the next section.

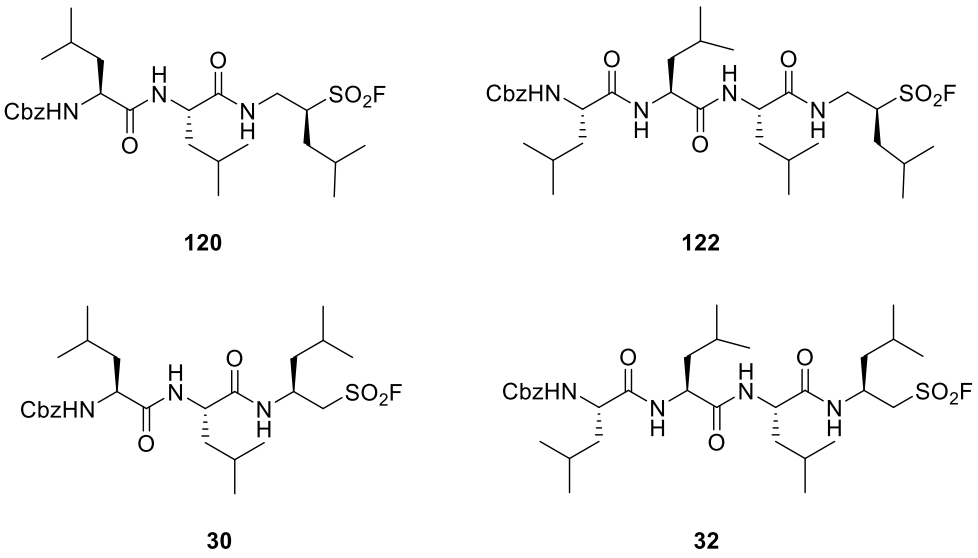

Figure 27 Compounds **120**, **122**, **30** and **32**.

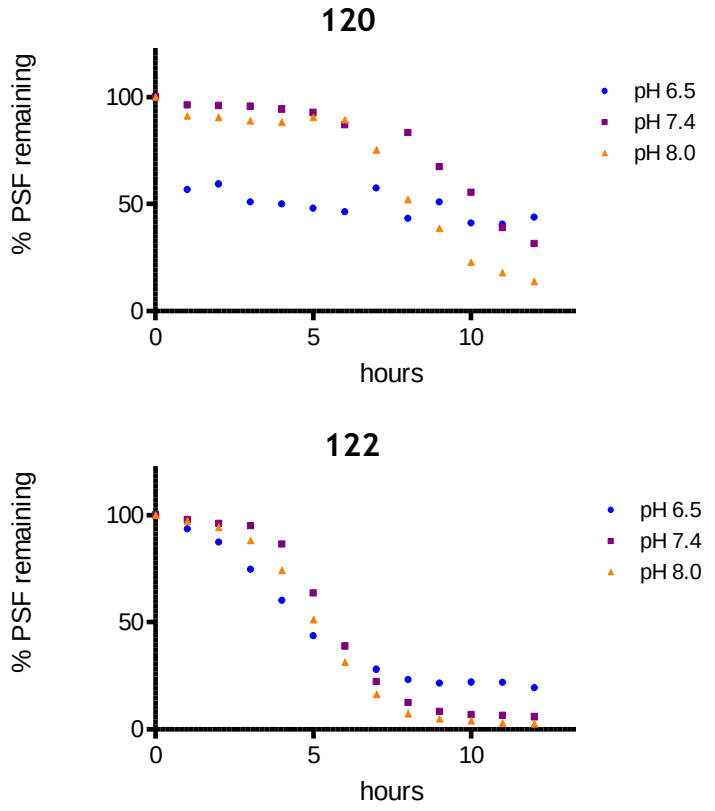

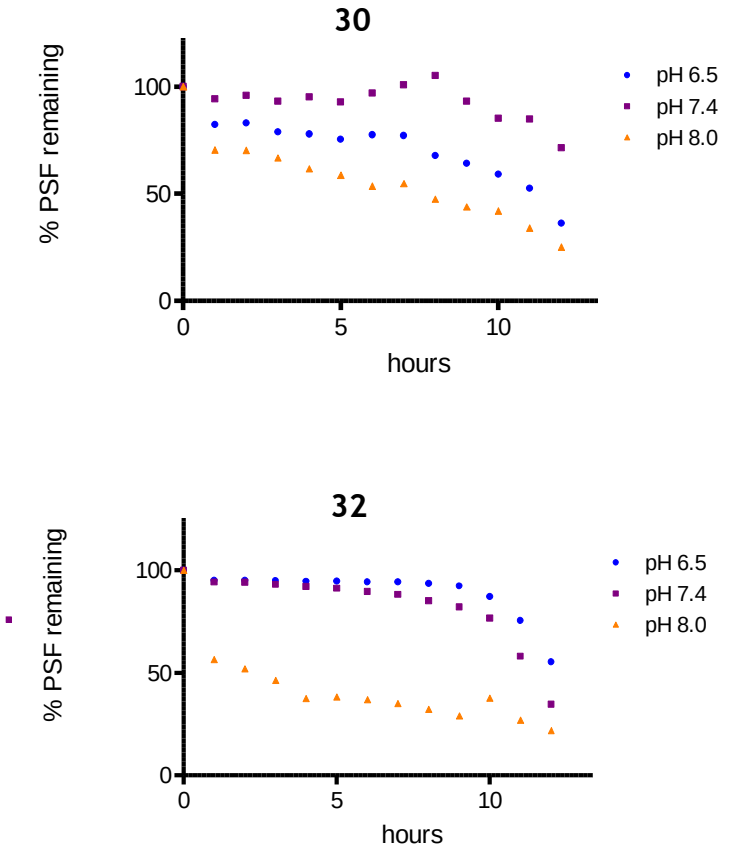

Figure 28 Buffer stability studies of compounds **120**, **122**, **30** and **32** at pH 6.5, 7.4 and 8.0. First measurement (t = 0) is assumed to be 100 % of peptide in solution.

2.8 Biological Evaluation

In order to determine inhibition of proteasomal activity by α-substituted peptido sulfonyl fluorides, the enzyme hydrolysis of the fluorogenic substrate Suc-LLVY-AMC **126** was monitored at λ_{exc} = 360 nm and λ_{em} = 460 nm after incubation of the enzyme with the compounds **120-125** in a range from 0.002 µM-400 µM (**Scheme 42**). Epoxomicin (**29**) and ß-PSF **32** were used as control inhibitors. Assays were performed in TRIS buffer at pH = 7.4. Different assay conditions are summarised in **Table 7**.

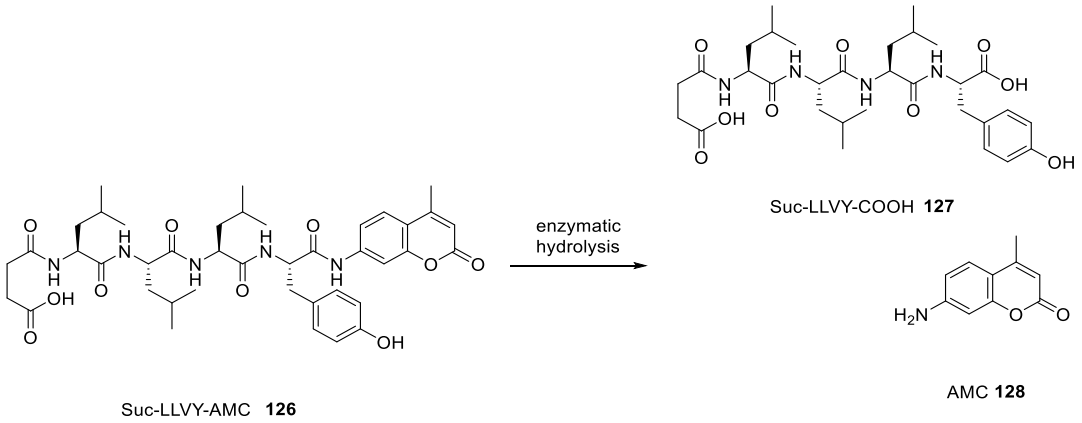

Scheme 42 Hydrolysis of Suc-LLVY-AMC **126** and release of AMC (7-Amido-4-methylcoumarin) **128**.

Table 7 Assay conditions used in the determination of the proteasomal inhibition by compounds **102-125**.

Entry	DMSO (% v/v)	Incubation time (h)	Temperature (ºC)
1	9	1	25
2	9	2	25
3	9	3	25
4	9	1	30
5	9	1	35
6	20	1	25

In a first attempt, compounds were dissolved in DMSO and added to the enzyme solution, achieving a final DMSO concentration of 9%. After 1h incubation at 25 ºC, the substrate **126** was added and the fluorescence was measured. Unexpectedly, the inhibitors showed no proteasome inhibition in the used concentration range. Strangely, an aleatory response which seemed to be independent of the concentration was observed (**Figure 29**).

Considering that the sulfonyl fluoride was proposed to be a slow reacting warhead during the inhibition mechanism studies,[99] the incubation time with the enzyme was increased to 2 and 3h, but no improvement was obtained (data not shown).

In view of the solubility issues already experienced during the buffer stability studies (**Section 2.7**), it was believed that the tested compounds could be partially precipitating from solution distorting the measurement of their proteasome inhibitory activities. Inhibitors had proven to be stable at pH = 7.4 for more than 5 hours and therefore, the stability of the compounds during the assay was not considered the problem. The assay temperature was increased to 25, 30 and 35 ºC respectively, as an attempt to favour the solution of the inhibitors. Unfortunately, inhibitory activity was detected and no trend in the response could be established (data not shown).

In the last attempt, assays were repeated increasing the final percentage of DMSO. However, it was impossible to obtain normal sigmoid inhibition curves for any of the α-substituted peptido sulfonyl fluoride inhibitors **120-125** even when using up to 20% (**Figure 30**) This concentration is much higher than the maximum percentage recommended to avoid denaturing the enzyme[117] and therefore, further increases on the DMSO content were not performed.

Possible explanations for this anomalous behaviour include a complete lack of activity of the compounds in the above used concentration range. This might be a result of the shift of the amino acid side chain on the α-position with respect to the sulfonyl fluoride warhead which might not be well tolerated by the proteasome. The inability of the potential inhibitors **120-125** to provide a proper alignment of the P1, P2 etc. residues and consequently to fit properly into the proteasome binding site may result in a lack of affinity. On the other hand, the poor solubility of these compounds may have prevented an adequate measurement. Assayed concentration ranges may not have been actually realised as a result of the precipitation of the compounds from the solution.

Unfortunately, due to these limiting factors it was impossible to draw definitive conclusions about the proteasome inhibitory activity of the α-PSFs **120-125**.

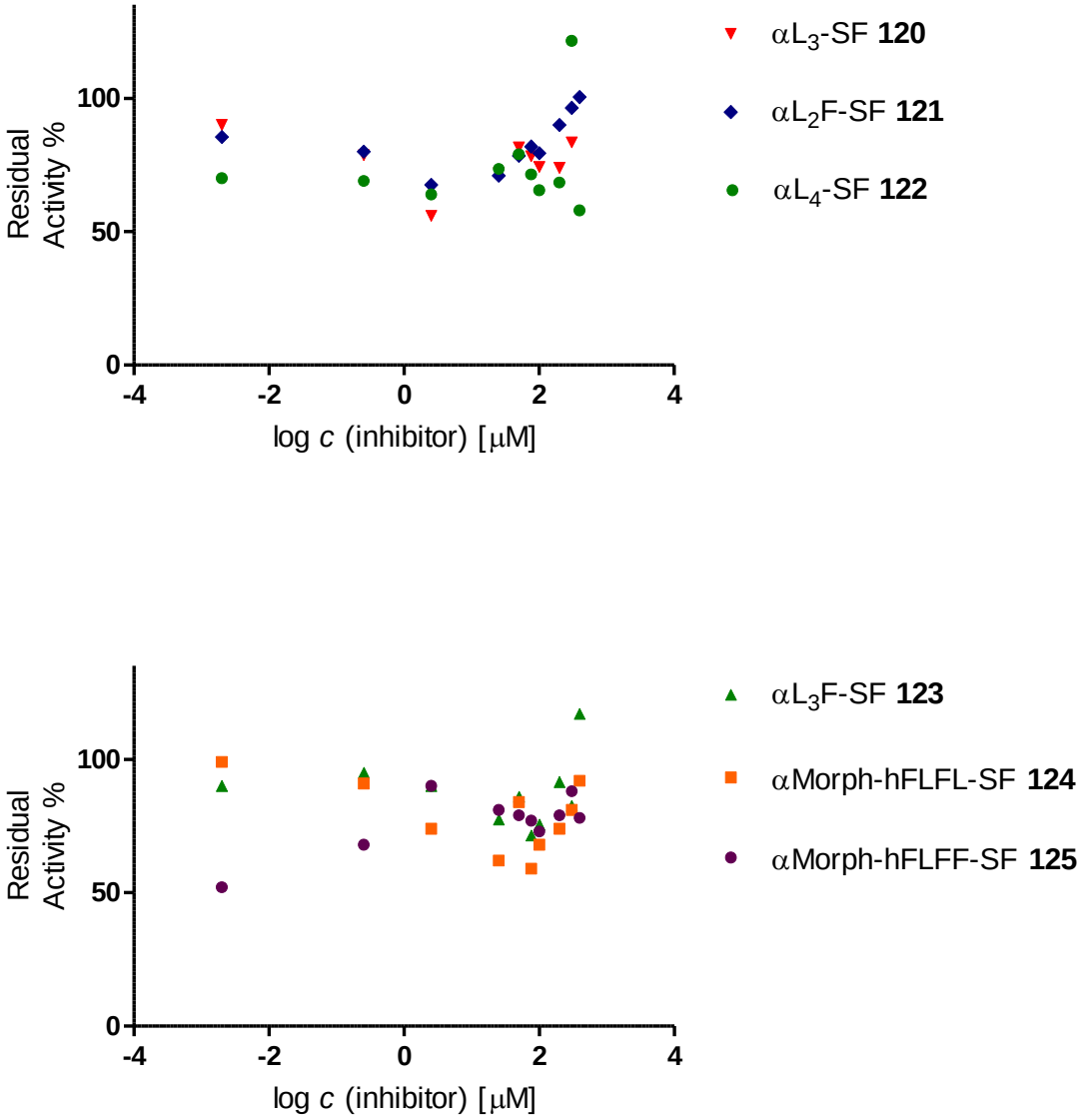

Figure 29 Inhibitory response of compounds **120-125** using 9% DMSO and 1h incubation time at 25 ºC. No trend observed.

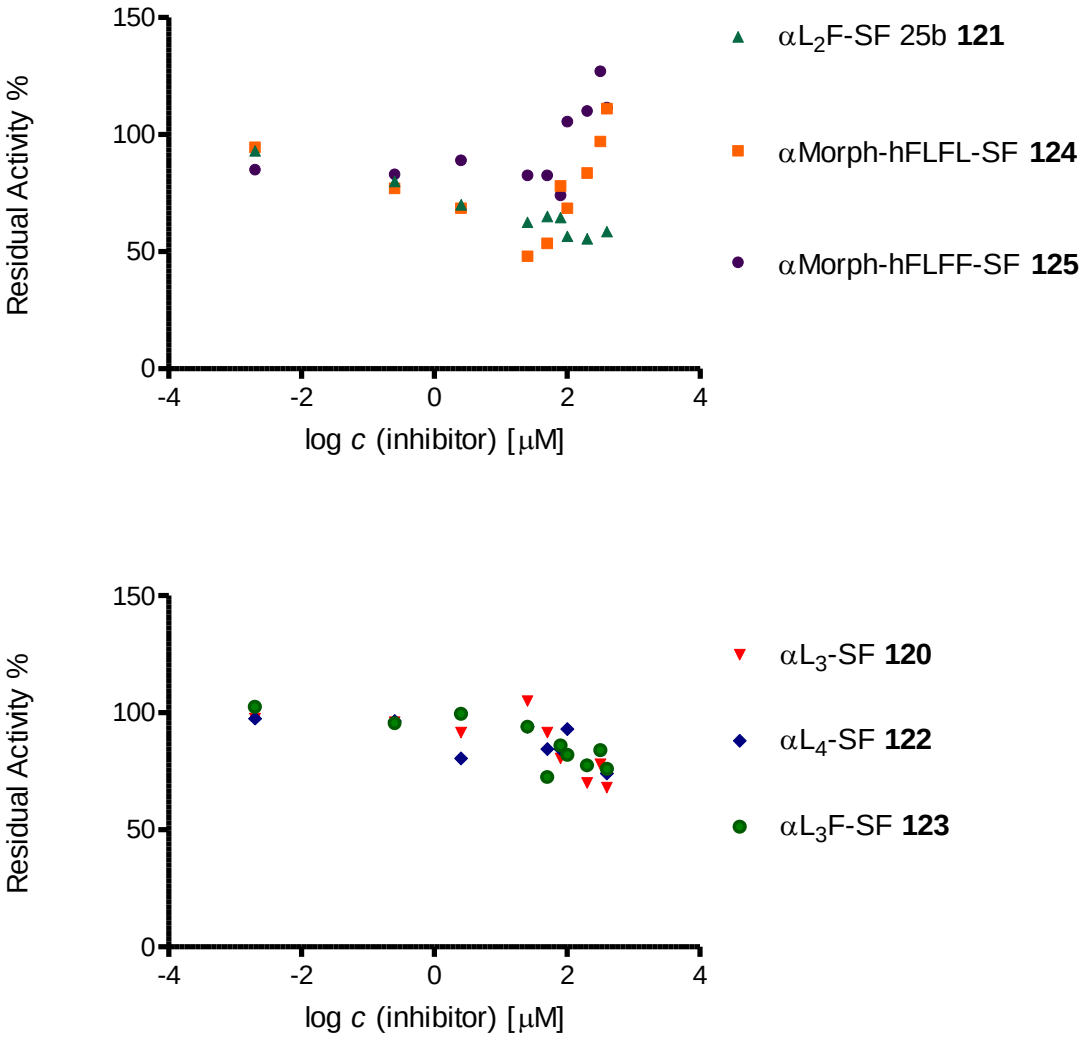

Figure 30 Inhibitory response of compounds **120-125** using 20% DMSO and 1h incubation time at 25 °C. No trend observed.

2.9 Summary

During the course of this work, several new amino acid derived sulfonyl fluorides have been synthesised containing the side chain of the amino acid in the alpha-position with respect to the sulfonyl fluoride moiety.

The preparation of these new molecules was achieved by both a racemic and a chiral synthesis, using either alkenes or natural amino acids as starting materials, which led to epoxides as synthons for shifting the side chain to the desired position. Efforts towards the optimisation of these syntheses were made and

significant progress was accomplished. This was of particular interest on the topic of the fluorination reaction.

The chemical reactivity of the α-substituted warheads was studied and compared with the previously described ß-substituted sulfonyl fluorides. Although the alpha sulfonyl fluorides **70** and **71** seemed to be chemically more reactive, this did not translate into more (bio)-active peptido sulfonyl fluorides after incorporation into peptide sequences.

Unfortunately, the poor solubility of the resulting αPSFs **120-125** (**Figure 31**) precluded a proper evaluation of their biological activity.

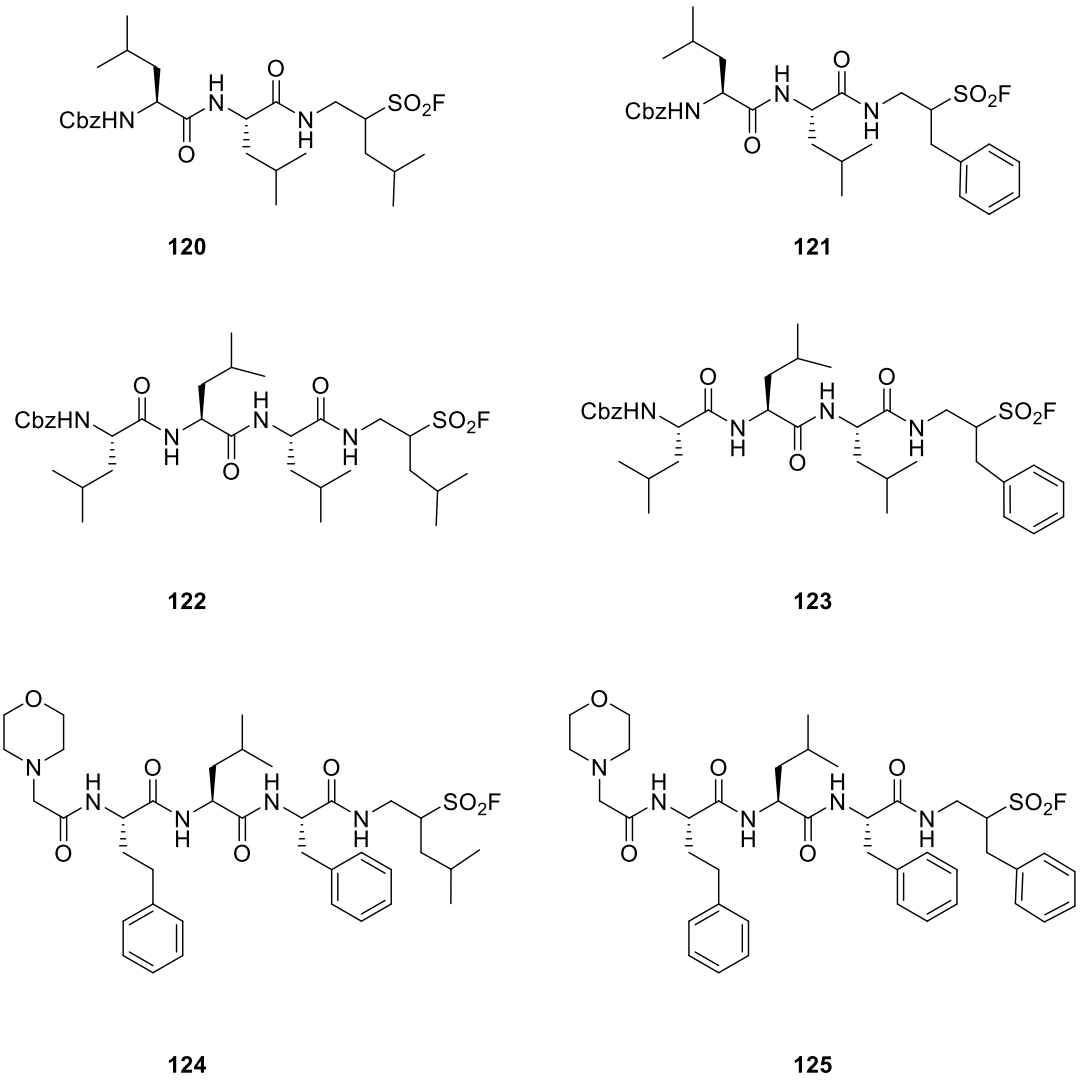

Figure 31 Summary of inhibitors **120-125**.

No significant differences were found between the α- and the ß-PSF during the buffer stability studies, showing all the tested PSFs a considerable aqueous stability.

3. Synthesis, Reactivity and Biological Evaluation of Vinyl Sulfonyl Fluorides

Part of the content of this chapter has been published:

Herrero Alvarez, N.; Brouwer, A. J.; Ciaffoni, A.; van de Langemheen, H.; Liskamp, R. M. J. "Proteasome inhibition by new dual warhead containing peptido vinyl sulfonyl fluoride" *Bioorganic Med. Chem.* **2016**, *24* (16), 3429–3435.

Very effective and selective proteasome inhibition has been achieved by inhibitors with 'dual' warheads. The FDA approval of Carfilzomib (**2**) and the development of OXN 0914 (**6**) have shown the unique advantages provided by containing two intrinsic electrophilic sites in one inhibitor. The capability of these inhibitors to exploit the bivalent character of the *N*-terminal threonine provides target selectivity and increased potency prevails over mono-electrophilic proteasome inhibitors. This set the stage for the investigation of new inhibitory strategies based on the employment of bivalent motifs.

Inspired by the dual warhead concept, vinyl sulfonyl fluorides (VSF) were designed as a new proteasome inhibitor class in which a Michael acceptor electrophilic trap is combined with a sulfonyl fluoride electrophile (**Scheme 43**). Both electrophilic traps may then interact by a double covalent binding with both nucleophilic amino and hydroxyl moieties of the *N*-terminal threonine residue present in the active site of the proteasome.

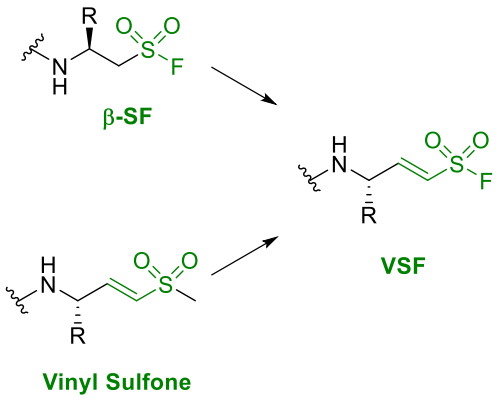

Scheme 43 Combination of ß-sulfonyl fluoride and vinyl sulfone moieties into the new vinyl sulfonyl fluoride warhead.

It was hypothesised that its molecular structure would allow a conjugate addition leading to a highly reactive sulfene intermediate upon release of the fluorine atom. The sulfene would then be attacked by the nucleophilic primary amine of the threonine residue in an intramolecular reaction leading to a seven-membered ring covalent adduct (**Scheme 44**).

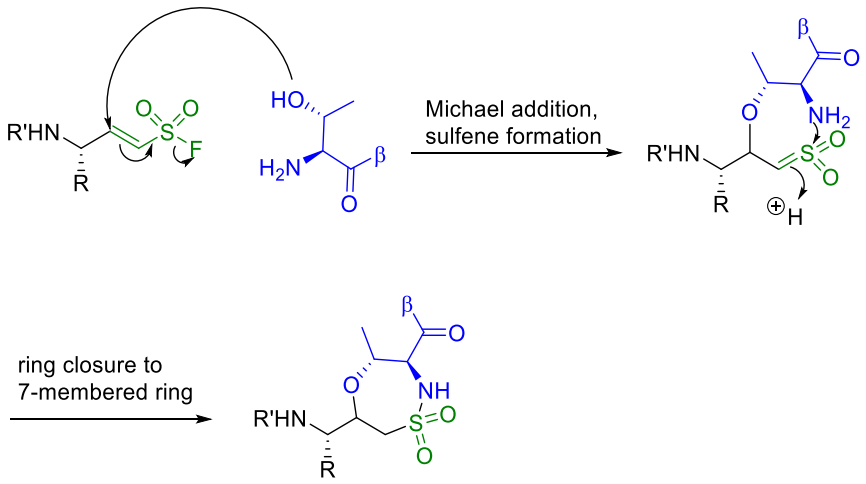

Scheme 44 Proposed mechanism for proteasomal inhibition by the vinyl sulfonyl fluoride warhead (VSF).

3.1 Aims of the Project

The aim of this project was to develop the vinyl sulfonyl fluoride warhead and to incorporate this new moiety into peptide sequences, leading to peptido vinyl sulfonyl fluorides (PVSF). The biological activity of these new PVSFs as potential peptidic proteasome inhibitors was subsequently evaluated. Understanding of the novel mechanism of action of this dual warhead system was pursued by performing a variety of reactivity studies in model systems (vide infra).

This chapter describes the synthesis of a Leucine-derived vinyl sulfonyl fluoride and the efforts to demonstrate the proposed inhibition mechanism (**Scheme 44**) *in vitro*. Importantly, the X-ray crystal structure of a peptido vinyl sulfonyl fluoride within the proteasomal active site revealed the formation of a seven-membered ring structure. Finally, the proteasomal inhibitory activity of two new compounds was quantified.

3.2 Synthesis of the Vinyl Sulfonyl Fluoride Warhead

The synthetic route towards the desired vinyl sulfonyl fluoride (**Scheme 45**) was designed by adapting a synthesis of vinyl aminosulfonic acids previously described by Gennari in 1994.[118]

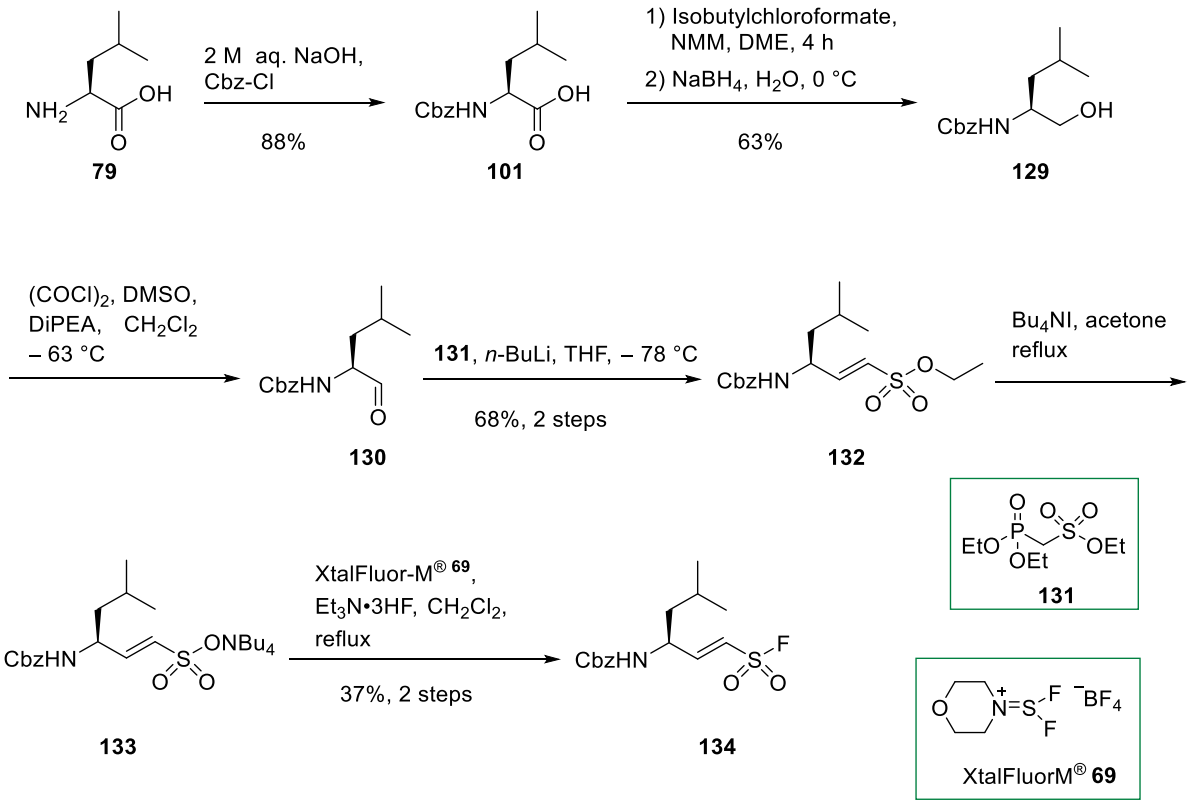

Scheme 45 Synthesis of Leucine-derived VSF **134**.

The sequence started with the Cbz-protection of L-Leucine **79** and subsequent reduction of Cbz-Leucine **101** to Cbz-Leucinol **129** was performed in a two-step process. First activation of the carboxylic acid with isobutyl chloroformate delivered the mixed anhydride which was then reduced to the corresponding alcohol using sodium borohydride. Although purification at this stage decreased the yield (63 %) compared to previous syntheses, improvement of the yield for the next steps was observed. Oxidation of the alcohol to the corresponding aldehyde **130** was performed by Swern oxidation. Cbz-Leucinal was then transformed into the ethyl vinylsulfonate **132** in a good yield (68 %) through a Wittig Horner

reaction, obtaining the *E* isomer (*J* = 15.0 Hz). The phosphonate reagent for the Wittig-Horner reaction **131** was prepared in two steps (**Scheme 46**). The commercially available methanesulfonyl chloride **135** was reacted with ethanol and NMM in CH_2Cl_2 to afford ethyl methanesulfonate **136.** Subsequent deprotonation with *n*-BuLi and reaction with diethylchlorophosphate **137** delivered the desired diethylphosphoryl methanesulfonate **131**. This phosphonate forms an stabilised ylid by conjugation and reacts with *E*-selectivity.

The ethyl ester was cleaved by treatment with tetrabutylammonium iodide in refluxing acetone, affording the respective tetrabutylammonium sulfonate **133**. The conversion of the sulfonate salt into the corresponding vinyl sulfonyl fluoride **134** was achieved by using XtalFluor-M® **69** in the presence of a catalytic amount of triethylamine trihydrofluoride acting as a fluoride source.

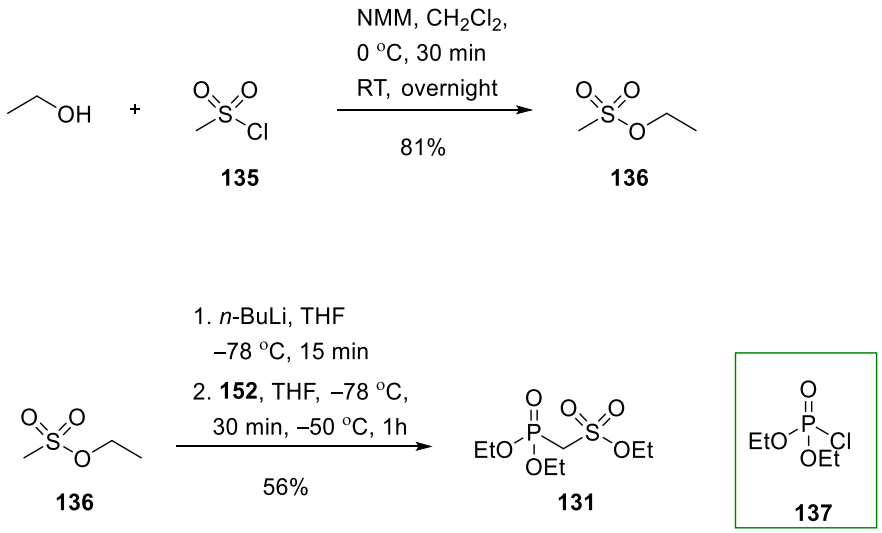

Scheme 46 Synthesis of the required Wittig-Horner reagent **131**.

Two potential PVSF proteasome inhibitors **138** and **139** were synthesised by removal of the Cbz-protecting group from VSF **134** with a 33% solution of HBr in acetic acid, followed by a coupling reaction with Cbz-Leu_2-OH **103** and Cbz-Leu_3-OH **107** using BOP and DiPEA in CH_2Cl_2 (**Scheme 47**). Compounds **138** and **139** were obtained after semi preparative reversed-phase HPLC purification in 26% and 33% yield respectively and were tested for their biological activities (see **Section 3.5**). In contrast with the inhibitors **120-125** (**Section 2.6.3**) compounds **138** and **139** were obtained as single diasteroisomers.

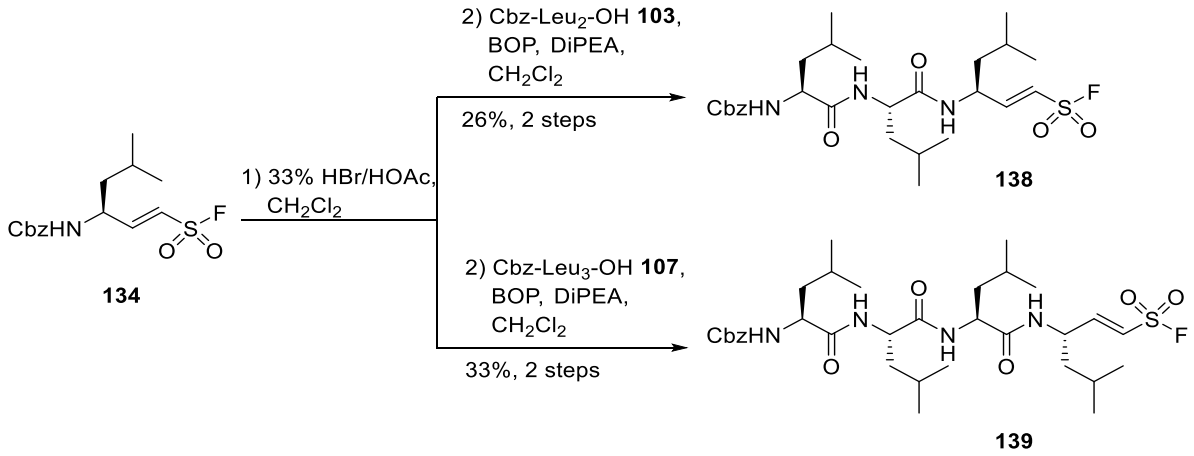

Scheme 47 Synthesis of peptido vinyl sulfonyl fluorides **138** and **139**.

3.3 Mechanistic Studies

To investigate whether the proposed formation within the enzyme of a seven-membered ring adduct **141** could be observed by chemo-synthesis, the reactivity of the vinyl sulfonyl fluoride **134** was studied *in vitro*. For this purpose the dipeptide H-Thr-Val-N(H)Me **140** was chosen as a model system of the threonine residue present in the catalytic site of the proteasome. Different base/solvent combinations were used and reactions evaluated by LC-MS analysis (**Table 8**).

Table 8 Model study: conditions and results.

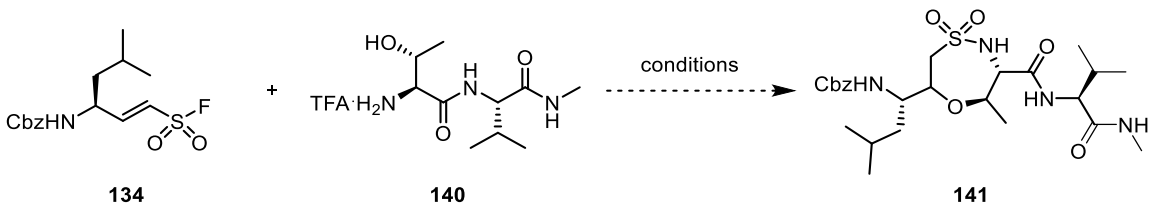

Entry	Solvent	Base(3 eq)	Formation of 141[(a)]
1	CH_2Cl_2	DBU	-
2	CH_3CN	DBU	-
3	CH_2Cl_2	NMM	traces
4	CH_2Cl_2	Et_3N	traces
5	CH_3CN	Et_3N	traces

a : LC-MS analysis of the crude mixture

Although the use of DBU resulted in an immediate decomposition of the VSF **134**, it was possible to observe two small peaks at *m/z* 541.4 and 563.5, corresponding to the $[M+H]^+$ and $[M+Na]^+$ masses of the 7-membered ring containing molecules **141** or **142**, when using Et_3N or NMM (**Figure 32**).

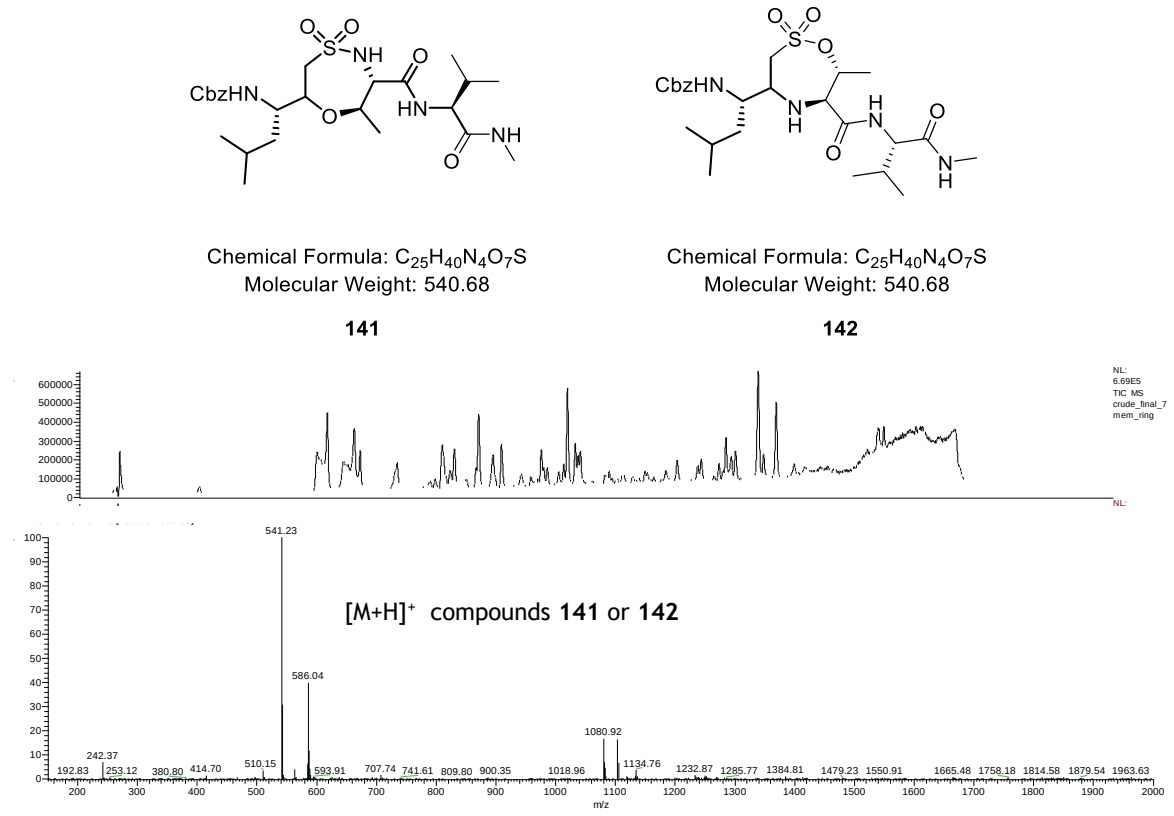

Figure 32 LC-MS chromatogram of the crude reaction mixture with the peaks corresponding to the $[M+H]^+$ and $[M+Na]^+$ mass value of structures **141** or **142**.

Additionally, two small peaks at *m/z* 561.3 and 587.3 were also detected, corresponding to the $[M+H]^+$ and $[M+Na]^+$ masses of a non-cyclic structure (**Figure 33**). Assuming that the Michael addition is the preferred reaction, the observed mass value could correspond to structures **143** or **144**. Unfortunately, these adducts were formed in trace amounts and all attempts to isolate them by column chromatography or semi-preparative HPLC failed. Attempts by varying the solvent (CH_2Cl_2 or MeCN) for the reaction were unsuccessful to increase product formation. The complexity of the mixture did not allow the identification or characterisation of the side products.

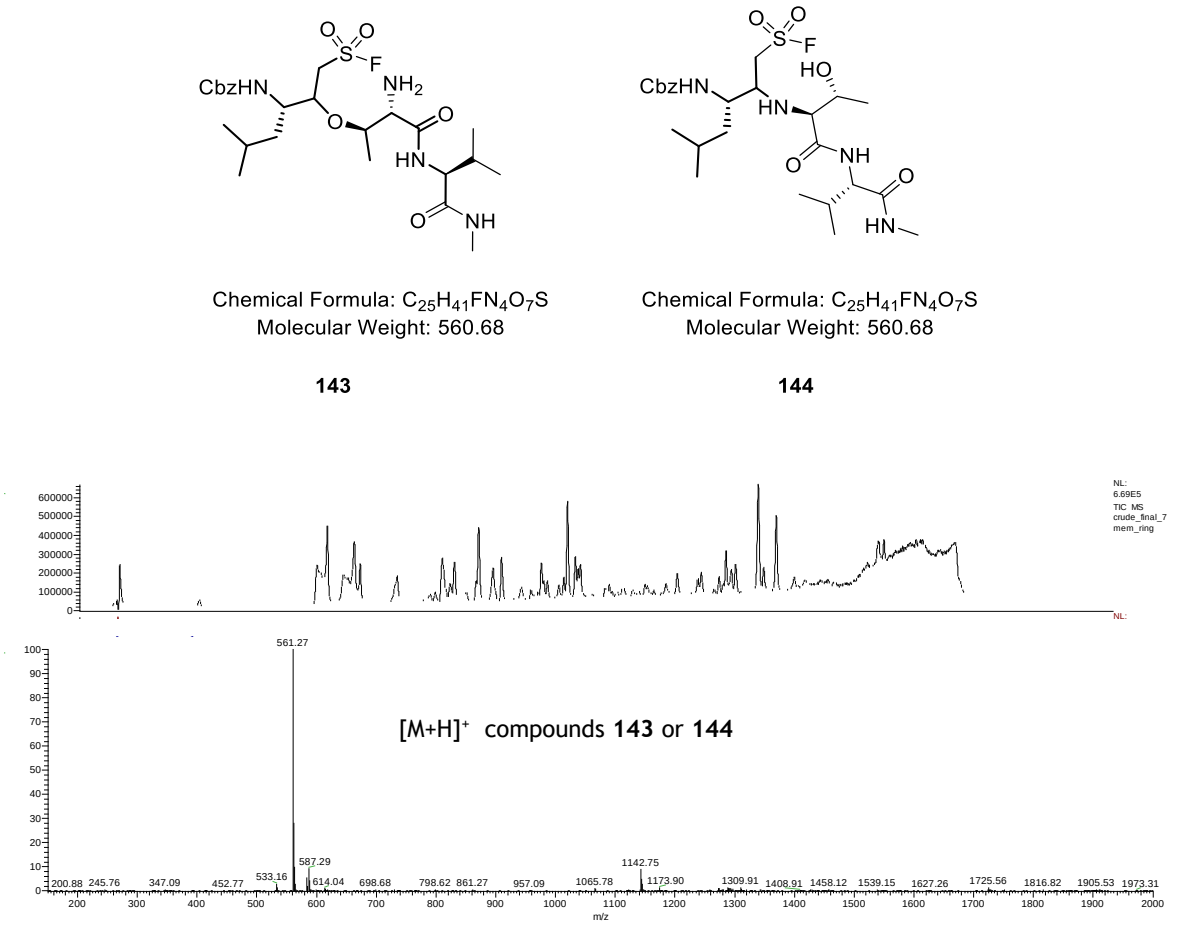

Figure 33 LC-MS chromatogram of the crude reaction mixture with the peaks corresponding to the $[M+H]^+$ and $[M+Na]^+$ mass value of structures **143** or **144**.

It is possible that an *in vitro* test reaction could give a false indication of the biological activity due the absence of other residues present in the catalytic site of the proteasome. This is especially important when considering the basic residues, which affect the relative nucleophilicity of the threonine nucleophiles in the enzyme and thereby determine the sequence of steps in the reaction. Whilst the proteasomal mechanism is characterised by the hydroxyl group being activated and reacting first, the higher nucleophilicity of the amino group in chemical systems would lead to the formation of different structures in this study. In addition, formation of a seven membered-ring is not a very favourable reaction from a chemosynthetic point of view.

In order to overcome these problems, it was decided to protect one of the nucleophiles to simplify the reaction conditions. As an attempt to mimic the

biological conditions and favour the performance of the first possible nucleophilic reaction by the hydroxyl group, the amine function was protected.

The Boc-protected dipeptide **145** was treated with NaH to deprotonate the hydroxyl and then reacted with VSF **134** (**Scheme 48**). Surprisingly, while a complete consumption of the VSF was observed, the dipeptide remained unreacted. It was thought that the released fluorine anion could be acting as an additional nucleophile in the system and interfering in the process.

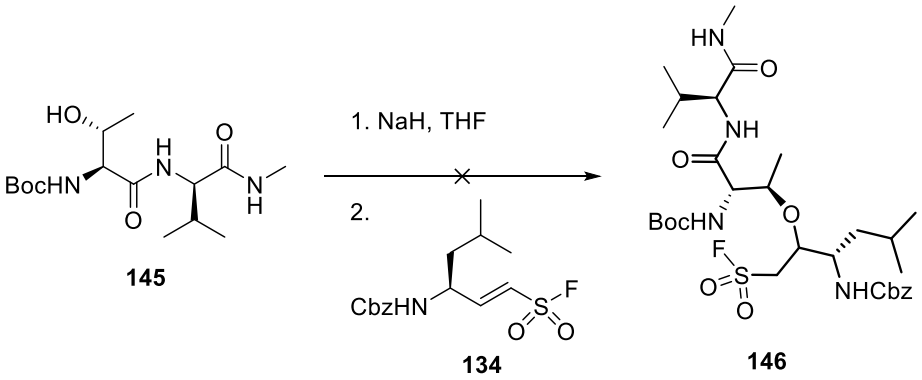

Scheme 48 Attempt of reaction between Boc-protected dipeptide **145** and VSF **134** using NaH as a base.

With this in mind, the same reaction was performed using CaH_2 as a base (**Scheme 49**), envisioning that the calcium cation could act as a fluorine scavenger and avoid some of the side reactions. Unfortunately, only unreacted dipeptide **145** was recovered at the end of the reaction.

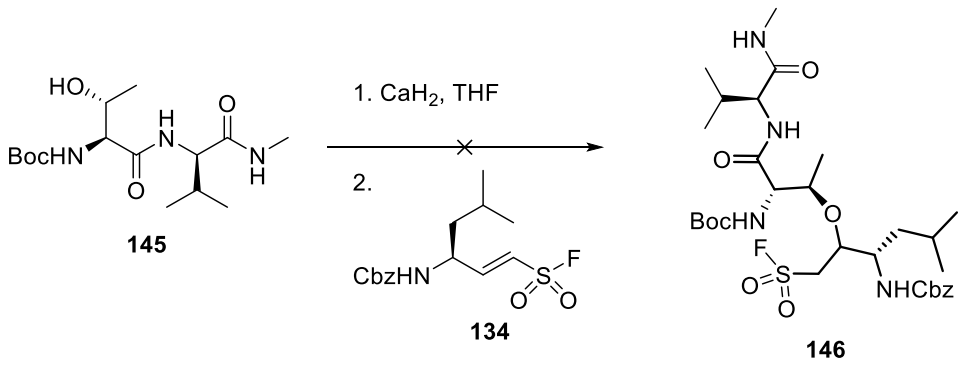

Scheme 49 Attempt of reaction between Boc-protected dipeptide **145** and VSF **134** using CaH_2 as a base.

3.3.1 Simple nucleophiles

Due to the difficulties encountered with the used model system and the failures of the previous approaches formation of the seven membered-ring **141** or **142** chemo-synthesis was no longer pursued. Instead it was decided to simplify the model of study and get some insight in the reactivity of VSF **134** with more simple nucleophiles. For this study solutions of VSF in CH_2Cl_2 were treated with an excess of different nucleophiles and stirred for 24 h (**Scheme 50**).

Firstly, the VSF **134** was reacted with piperidine, leading to a 2:3 ratio of the double substituted product **147** and the five-membered ring **148**. The unexpected five-membered ring was formed by attack of the Cbz-protected nitrogen on the sulfene intermediate generated upon attack of the piperidine to the Michael acceptor.

The reactivity of the VSF towards primary amines, which is the type of nucleophile present as the catalytic residue in the model system **140**, was then evaluated by reaction with benzylamine and methylamine. A disubstituted compound resulting from a Michael reaction and substitution at the sulfonyl fluoride moiety was expected. However, the disubstituted compounds **150** and **152** were only detected by LC-MS analysis and instead the ß-sultams **149** and **151** were the major products formed.

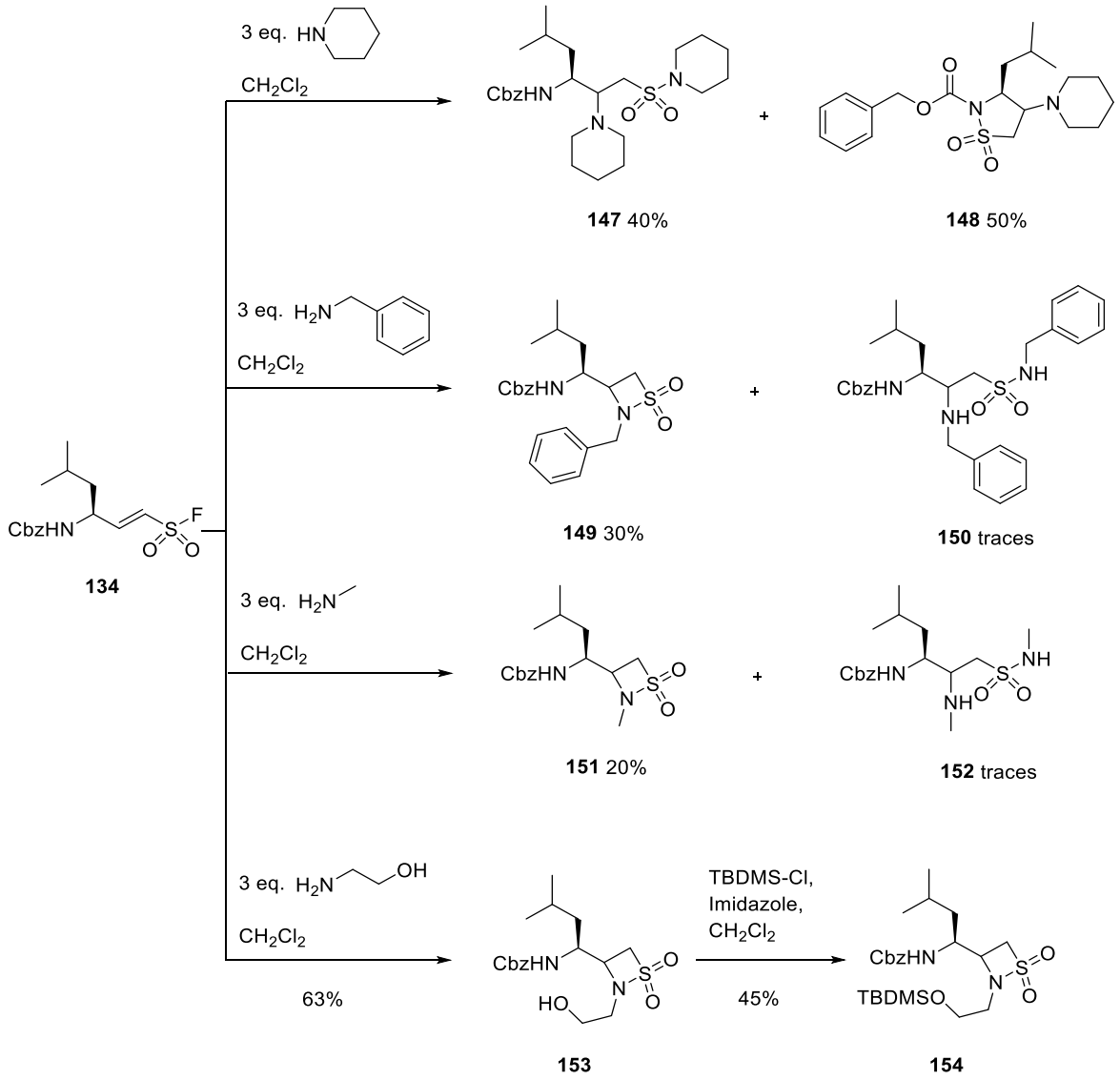

Scheme 50 Reactivity studies with VSF **134** and different nucleophiles. Yields are from isolated compounds after silica column chromatography.

Finally, moving forward to a bivalent nucleophile more similar to the active threonine, the VSF **134** was treated with ethanolamine. The reaction led to the clear formation of the ß-sultam **153** as the major product. To confirm that the alcohol functionality was unreacted in the formed product, the compound **153** was subjected to reaction with TBDMS-Cl in the presence of imidazole. The full conversion to the silyl ether **154** was consistent with the initial hypothesis.

3.3.2 Ethenesulfonyl fluoride

Treatment of ethenesulfonyl fluoride **155** (ESF) with amines has been used in the past among other strategies to synthesise β-sultam compounds **156** (**Scheme 51**).[119]

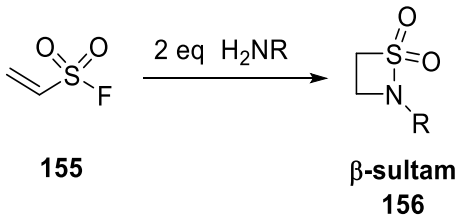

Scheme 51 Formation of β-sultams **156** with ESF **155** and primary amines.

Recently, ESF has been described as "the most perfect Michael acceptor ever found".[120] Kinetic studies of reactions of ESF with different nucleophiles were performed to quantify its electrophilicity. The study confirmed the high electrophilicity of the double bond, which reacts with a range of nitrogen, oxygen and carbon nucleophiles while the sulfonyl fluoride group remains unaffected when using equimolar amounts (**Scheme 52**).[120,121]

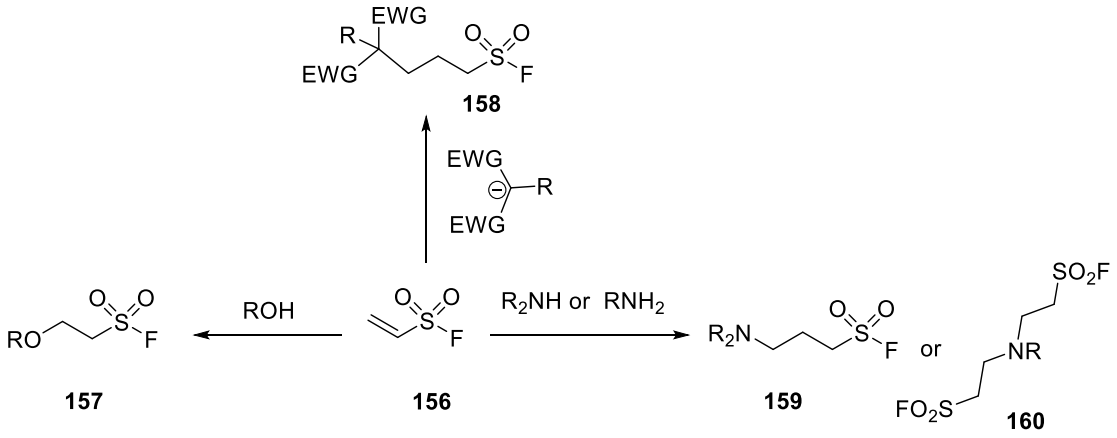

Scheme 52 Examples of the reactivity of ESF **156** with nitrogen, oxygen and carbon nucleophiles.

These results supported the observed reactivity of the VSF warhead. Consistent with the literature, the reaction mechanism of VSF towards nucleophiles was proposed (**Scheme 53**). The Michael acceptor is attacked by the nucleophile on

the ß-position, leading to a highly reactive sulfene intermediate, which immediately undergoes a second nucleophilic attack. When the second attack on the sulfene is performed intramolecularly by the introduced nucleophile molecule a cyclic structure results.

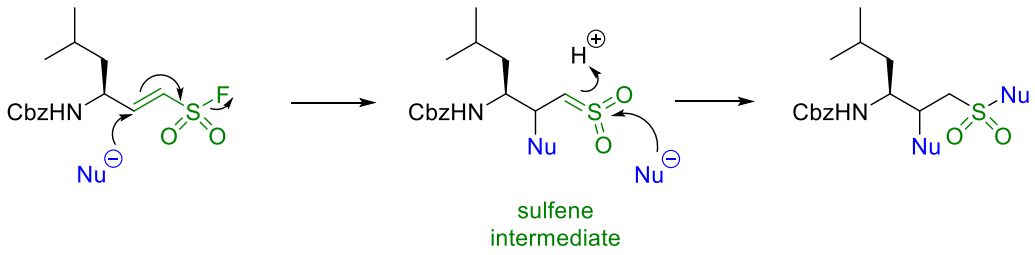

Scheme 53 Proposed reaction mechanism for the VSF **134** warhead.

Based on these findings it was decided to use the simple ethenesulfonyl fluoride **156** molecule as suitable models of our warhead unit for the test reactions.

As an attempt to reproduce the previous results ESF **156** was treated with ethanolamine. It was envisioned that opening of the ß-sultam **161** and formation of the seven-membered ring **162** could occur upon the attack of the hydroxyl group, deprotonated by treatment with NaH. Unfortunately, this reaction did not take place even when at refluxing temperature (**Scheme 55**). A possible explanation for this may be stereoelectronic factors due to the pseudorotation restriction of the four-membered ring. This results in a difficult angle of attack which makes unlikely the fission of the sulfonamide bond.[122]

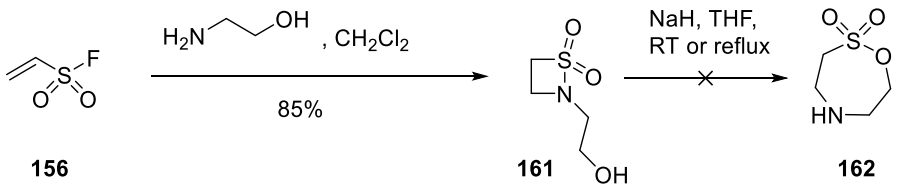

156 **161** **162**

Scheme 54 Reaction of ESF **156** with ethanolamine and attempt to open the ß-sultam **161** with NaH.

Additionally, reaction of ESF **156** with more biological substrates: *N*-methylated threonine **163** and *N*-methylated dipeptide **164,** as the initial model system, were attempted (**Scheme 55**). Nevertheless, the impossibility to dissolve substrates

163 and **164** in any of the utilised solvents (**Table 9**), even upon sonication, precluded the reactions to proceed and therefore the β-sultams **165** and **166** to be not formed.

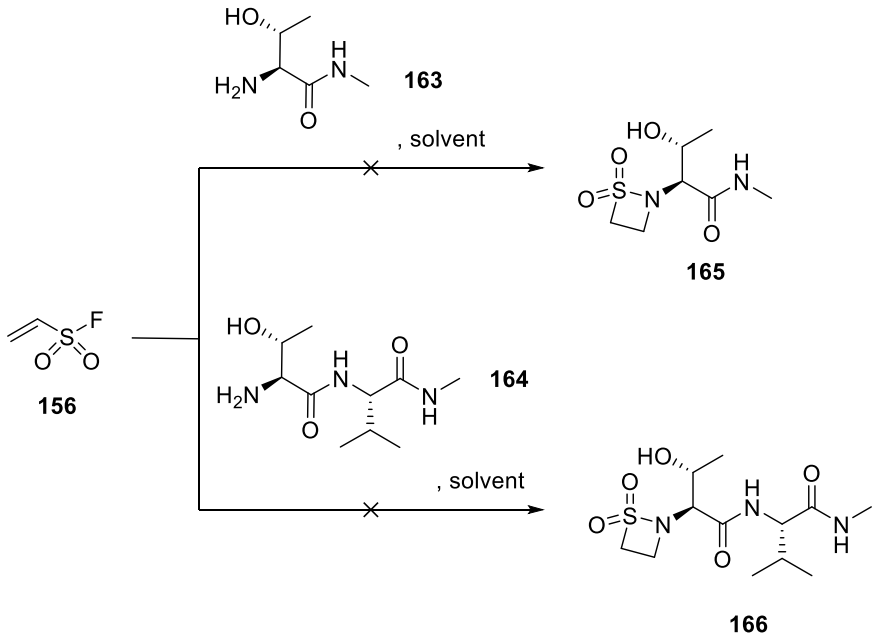

Scheme 55 Attempts to form β-sultam **165** and **166** by reaction of ESF **156** with *N*-methylated threonine **163** and *N*-methylated dipeptide **164.**

Table 9 Assayed solvents for the reaction of ESF with **156** with *N*-methylated threonine **163** and *N*-methylated dipeptide **164.**

Substrate	Solvent	Outcome
163 **164**	CH_2Cl_2	No dissolution
163 **164**	CH_3CN	No dissolution
163 **164**	EtOAC	No dissolution
163 **164**	THF	No dissolution
164	Ethanol	No dissolution
164	DMF	No dissolution
164	Methanol	No dissolution

3.4 Crystal Structure

As a part of our collaboration with Groll and coworkers, a crystallographic binding analysis of the peptido vinyl sulfonyl fluoride **139** in complex with the β5-subunit of the proteasome was conducted. Resolution of the X-ray structure at 2.3 Å revealed the formation of the 7-membered ring structure **167** at the proteasomal active site (**Figure 34**).

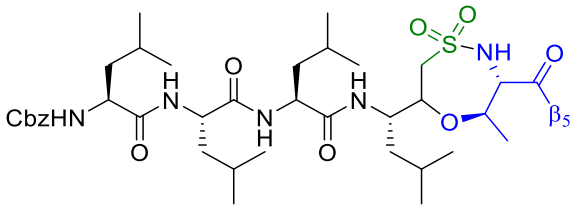

167

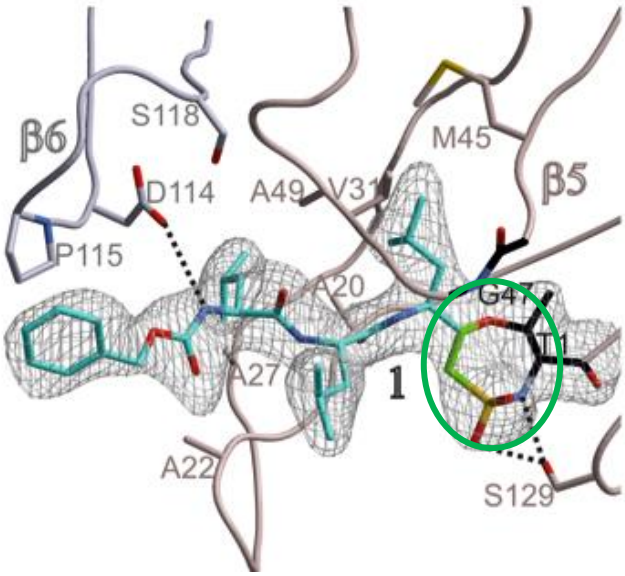

Figure 34 Crystal structure of Cbz-Leu$_4$-VSF **139** in complex with the β5 subunit of the proteasome obtained by Groll and co-workers. (Work unpublished)

The VSF warhead **134** was designed to provide two electrophiles that would react with the two nucleophiles of the *N*-terminal threonine. From a chemosynthesis point of view both 7-membered ring molecules **141** or **142** (**Figure 35**) could be formed, however, only molecule **141** was expected to be formed in the

proteasome. As proven by previous crystal structures of other inhibitors the hydroxyl group of the active threonine acts preferentially as the nucleophile due to the hydrogen bond activation, while the amino group only reacts in the presence of a second electrophile.[70]

Formation of the structure **167** within the enzyme is favoured not only by the hydrogen bonding network of the active centre but also by the interactions with the binding channels which prolong the residence time of the inhibitor while providing the optimal orientation for the reaction to occur. None of these interactions can be reproduce during the chemosynthesis which would explain the impossibility to isolate molecules **141** or **142**.

Satisfyingly the crystal structure confirmed the proposed inhibition mechanism of the VSF warhead and had an enormous biological value. The proof of the interaction between the two electrophiles of the VSF and the two nucleophiles of the *N*-terminal threonine validated the PVSF as a new class of proteasome inhibitors. This may provide exclusive possibilities in terms of duration and selectivity of the inhibition.

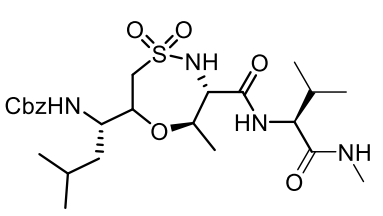

Chemical Formula: $C_{25}H_{40}N_4O_7S$
Molecular Weight: 540.68

141

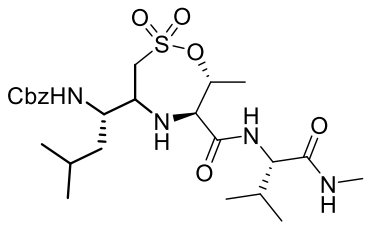

Chemical Formula: $C_{25}H_{40}N_4O_7S$
Molecular Weight: 540.68

142

Figure 35 7-membered ring molecules **141** and **142**.

3.5 Biological Evaluation

The inhibition of the proteasome activity by the peptido vinyl sulfonyl fluorides **138** and **139** and the previously synthesised PSF **30** and **32** was determined in a dose-response assay (**Figure 36**). For this purpose the hydrolysis of the fluorogenic substrate Suc-LLVY-AMC **126** was monitored at λ_{exc} = 360 and λ_{em} = 460 nm after incubation of the enzyme with the compounds in a range from 0.4 nM-8000 nM for 1h.

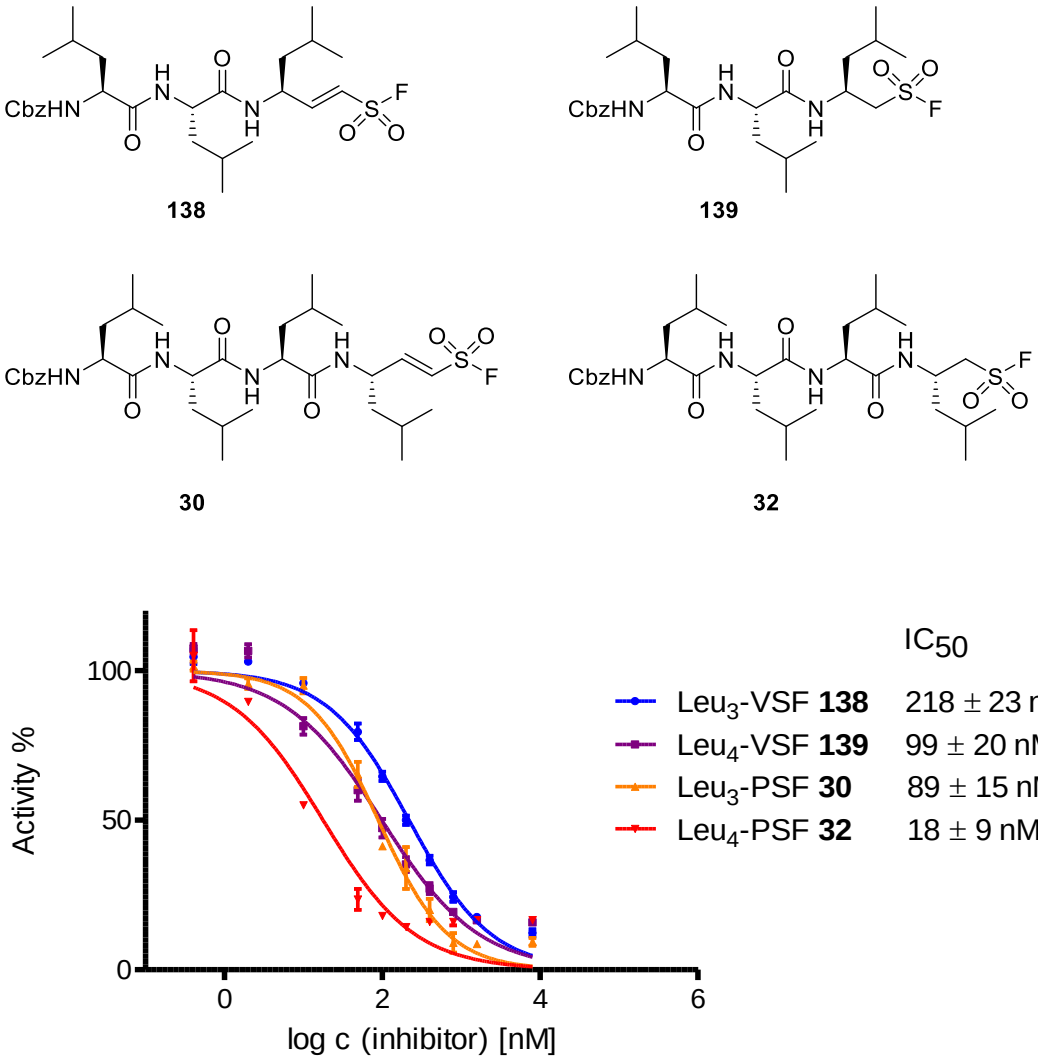

Figure 36 Inhibitory curves of human constitutive proteasome by PVSFs **138** and **139** and PSFs **30** and **32**.

PVSF showed a strong proteasome inhibition at the mid nanomolar range. IC_{50} values of 218 nM and 99 nM were obtained for compounds **138** and **139**, respectively. The obtained IC_{50} For PSFs **30** and **32** were consistent with literature

values.[97] Nevertheless, surprisingly the inhibitory activity of the PVSFs was diminished compared to PSFs **30** and **32**. Both PVSF and PSF benefit from elongated backbones as previously stated.[99]

These results could be due to the sulfonyl fluoride moiety of the VSF warhead **134** occupying a less favourable P1 position. Although the VSF may be more reactive than the ß-SF, it is more distant from the P1 side chain and this could lead to reduced potency. Therefore, potentially lower IC_{50} values may be obtained by evaluating different amino acid sequences with the vinyl sulfonyl fluoride dual warhead.

3.6 Summary

During the course of this work successful introduction of the vinyl sulfonyl fluoride moiety **134** into the amino acid L-Leucine was accomplished.

Although there was an indication of formation of the proposed seven membered-ring structure **141** by *in vitro* studies, this formation could not be unambiguously demonstrated. This was due to the impossibility of isolation and characterisation of the observed adducts. Possibly, formation of a seven-membered covalent adduct with the *N*-terminal threonine can only be achieved within the enzyme context due to the preorganised environment.

The encountered difficulties during the *in vitro* test reactions were addressed by using simplified models of study. Reactivity studies were conducted using the VSF warhead **134** and the ESF unit **156**. The obtained results were in agreement with literature.[86,120]

It was possible to resolve the crystal structure of the inhibitor **139** in complex with the ß5-subunit of the 20S proteasome at the resolution of 2.3 Å, which revealed the formation of the 7-membered ring. This finding proved the capability of the VSF warhead to exploit the bivalent character of the catalytic threonine which is the key to discriminate against other proteases and should therefore enhance the inhibitor selectivity.

Finally, the incorporation of the new electrophilic trap into peptide backbones led to very potent proteasome inhibitors which showed IC_{50} values of 218 nM and 99 nM, respectively.

4. Conclusions and Future Work

This work was dedicated to tune the structure of the sulfonyl fluoride warhead and to study the biochemical consequences of such modifications.

For this purpose two different types of sulfonyl fluoride containing molecules were synthesised and analysed: α-substituted sulfonyl fluorides and vinyl sulfonyl fluorides. Incorporation into peptide sequences resulted in two new types of inhibitors: α-PSF and PVSF (**Figure 37**).

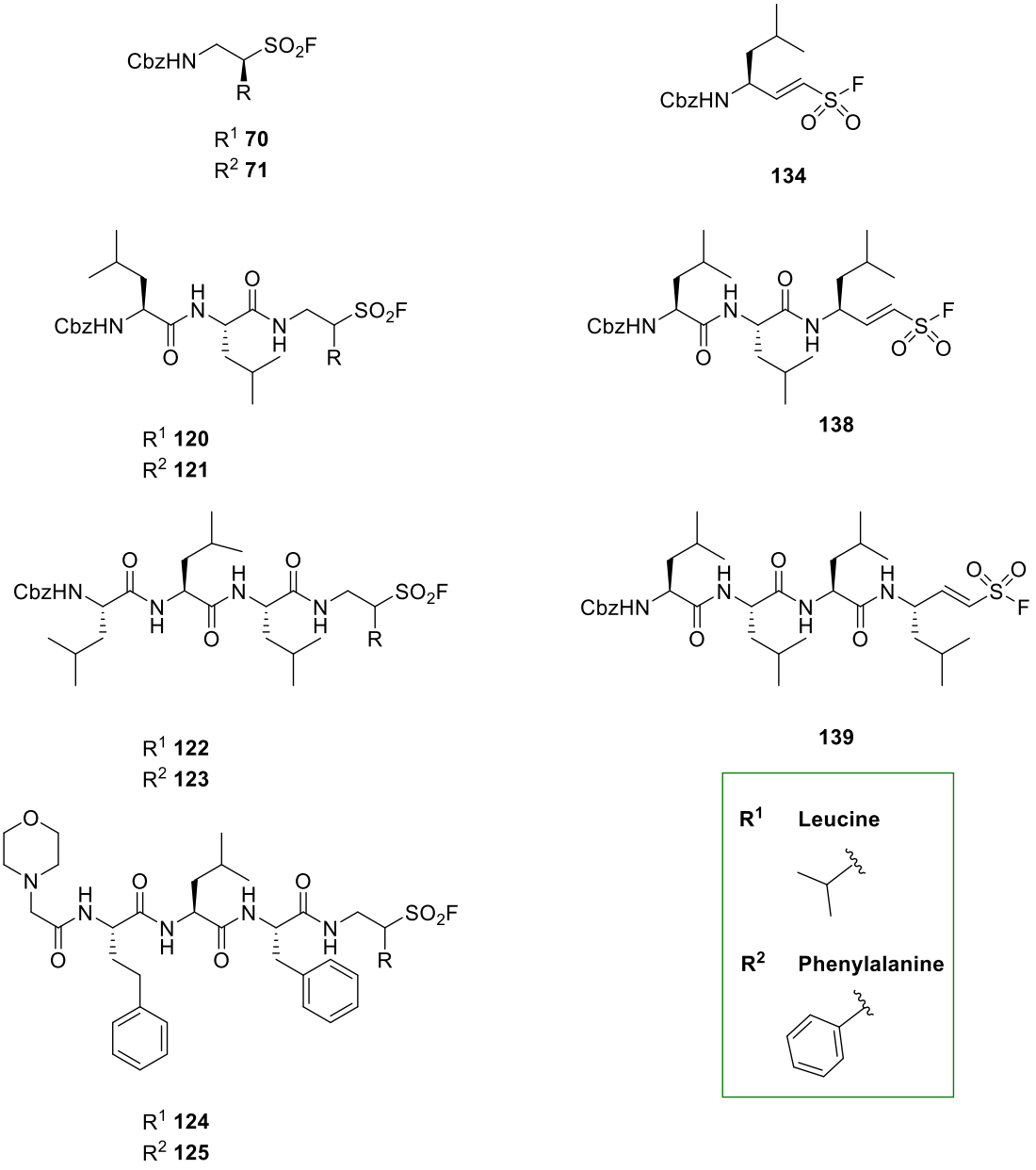

Figure 37 Overview of warheads **70**, **71** and **134** and inhibitors **120-125**, **138** and **139**.

Chemical reactivity and biological studies proved the sulfonyl fluoride electrophile to be very sensitive to the structural modifications. In fact the two new warheads exhibited remarkably different properties.

- α-SFs were chemically more stable than VSF.
- α-PSFs inhibitors were obtained as a mixture of diasteroisomers while PVSF did not show any racemisation or epimerisation issue.
- α-PSFs solubility problems precluded their biological evaluation whereas PVSF were easily tested and displayed a high inhibitory potency.

Additionally, these modifications decreased the inhibitory potency when compared to the previously synthesised ß-SF. This may be explained by the different alignments within the substrate biding pockets as a result of shifting the side chain residue or the electrophile to be attacked (**Figure 38**).

Regarding α-peptido sulfonyl fluorides, the near future research efforts will involve trying to improve the solubility for example by modifying or removing the N-terminal protecting group. An important part of the future work will be the exact determination of the racemisation causes and in which stage separation of the diastereoisomers should take place.

Future work for the PVSF will include the screening against off target proteases to test the selectivity of these inhibitors, with special attention to cysteine proteases, since they are known to react with Michael acceptors. Additionally, different peptide sequences will be screened in order to optimise the interactions with the substrate binding pockets.

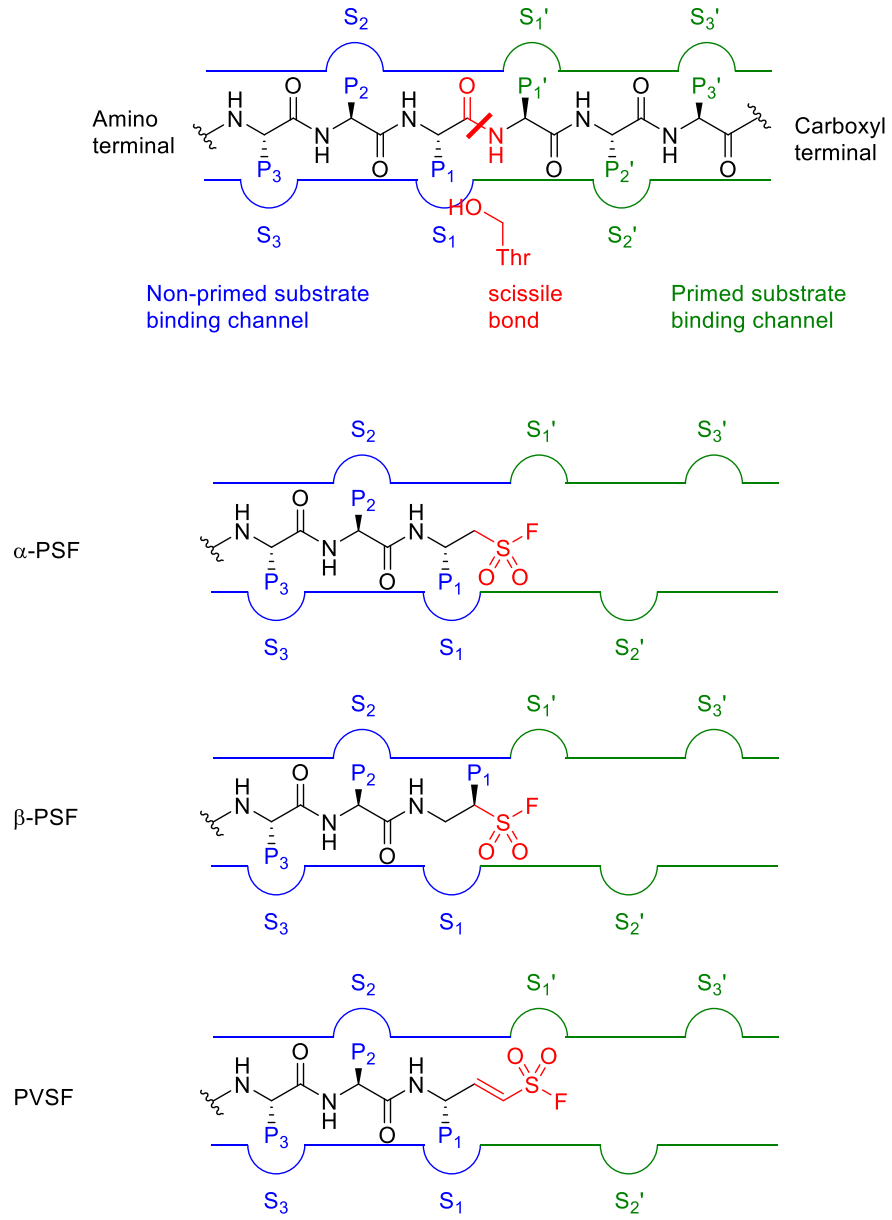

Figure 38 Alignments of α-PSFs, β-PSFs and VSF inside the substrate binding channel of the proteasome.

5. Experimental Section

General Experimental

All reagents were obtained from commercial sources and used without further purification unless specified otherwise. Air and/or moisture sensitive reactions were performed under an atmosphere of nitrogen in flame dried apparatus. Tetrahydrofuran (THF) and dichloromethane (CH_2Cl_2) were purified using a Pure-Solv™ 500 Solvent Purification System. Petroleum ether (PE) used for reactions and column chromatography was the 40–60 °C fraction. Ultra-pure water was obtained by using the water purification device Arium Comfort I.

Thin layer chromatography (TLC) was performed using Merck silica gel 60 glass plates F_{254}. TLC plates were visualised under UV light at λ = 254 nm and stained using the most appropriated solution (ninhydrin, anisaldehyde, bromocresol green or potassium permanganate). Flash column chromatography was performed with Silicaflash P60 gel (40–63 μm) from Silicycle (Canada) as solid support.

All ^1H NMR spectra were recorded on Bruker Avance III 400 MHz and 500 MHz spectrometers at ambient temperature. Data are reported as follows: chemical shift in ppm relative to $CDCl_3$ (7.26) on the δ scale, multiplicity (s = singlet, d = doublet, t = triplet, q = quartet, m = multiplet, br = broad, app. = apparent or a combination of these), coupling constant(s) *J* (Hz), integration and assignment. All ^{13}C NMR spectra were recorded on Bruker Avance III 400 MHz and 500 MHz spectrometers at 101 MHz and 126 MHz at ambient temperature and multiplicities were obtained using 2D data (HSQC, COSY) and DEPT sequence. Data are reported as follows: chemical shift in ppm relative to $CHCl_3$ (77.16) on the δ scale and assignment. All ^{19}F NMR spectra were recorded on Bruker Avance III 500 MHz spectrometer at 471 MHz at ambient temperature. Chemical shift is reported in ppm.

Optical rotations were recorded using an automatic polarimeter Autopol V.

High resolution mass spectra (HRMS) were recorded using positive chemical ionization (CI+) and positive ion impact (EI+) on Jeol MStation JMS-700 instrument; and positive or negative ion electrospray (ESI+/ESI-) techniques on a Bruker micrOTOF-Q instrument.

Analytical HPLC was performed on a Shimadzu Prominence instrument with a UV-detector operating at λ = 214 and 254 nm, using a Phenomenex column (Gemini, C4, 5 µm, 250 x 4.60 mm), (Gemini, C18, 5 µm, 250 x 4.60 mm) or a Dr. Maisch column (Reprosil Gold 200, C18, 5 µm, 250 x 4.60 mm) at a flow rate of 1 mL/min. The mobile phase was water/CH_3CN/TFA (95/5/0.1, v/v/v, buffer A) and water/CH_3CN/TFA (5/95/0.1, v/v/v, buffer B). Samples were dissolved in buffer A/B (1/2 or 1/3). Preparative HPLC was performed on an Agilent 1260 Infinity instrument using a Phenomenex column (Gemini, C18, 10 µm, 250 x 21.2 mm) at a flow rate of 12.5 mL/min, using the same buffers and sample preparation as described for the analytical HLPC. Analytical LC-MS was performed on a Thermo Scientific Dionex Ultimate 3000 LC system coupled to a Thermo Scientific LCQ Fleet™ Ion trap mass spectrometer using a Dr. Maisch column (Reprosil Gold 120, C18, 3 µm, 150 x 4mm) with a linear gradient of 1 mL/min. The mobile phase was water/CH_3CN/TFA (95/5/0.1, v/v/v, buffer A) and water/CH_3CN/TFA (5/95/0.1, v/v/v, buffer B). Samples were dissolved in buffer A/B (1/1 or 1/2). The UV absorption was monitored at λ = 214 and 254 nm over 10, 40 or 60 min.

Lyophilisation of peptides or building blocks from aqueous solutions and aqueous mixtures containing minor amounts of acetonitrile was performed using a Christ Alpha-2-4 lyophiliser equipped with a high vacuum pump.

Proteasome Enzymatic Assays were performed using the VIVAdetect™ 20S Proteasome Assay Kit PLUS (Viva bioscience, UK) and the Enzo Life Sciences® 20S Proteasome Assay Kit for Drug Discovery (Enzo Life Science, USA).

Fluorescence measurements were performed with a Clariostar microplate reader (BMG LABTECH, Germany).

(±)-*N*-benzyl amino alcohol 51

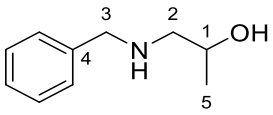

Chemical Formula: $C_{10}H_{15}NO$
Molecular Weight: 165.24

A solution of (±) propylene oxide **50** (0.14 mL, 1.0 mmol) and benzylamine (0.22 mL, 2.0 mmol) were dissolved in acetonitrile (6 mL). Calcium triflate (338 g, 1.0 mmol) was added and the reaction mixture stirred for 4 hours. Solvent was evaporated, water (5 mL) was added and the compound extracted with CH_2Cl_2 (3 × 5 mL). The combined organic phases were dried over $MgSO_4$, filtered and the solvent removed *in vacuo* to afford the desired compound **(±) 51** (140 mg, 0.85 mmol, 85%) as a colourless oil which did not require further purification.

^{1}H NMR (400 MHz, $CDCl_3$) δ 7.31 – 7.19 (m, 5H, CH-Ph), 3.72 (m, 3H, CH_2-C3, CH-C1), 2.40 (dd, 1H, CH_2-C2a), 2.07 (dd, 1H, CH_2-C2b), 1.05 (d, 3H, CH_3-C5)

Spectroscopic data are in accordance with literature.[100]

(*S*)-2-(phenylmethyl)-oxirane 53

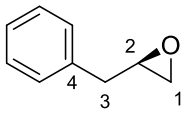

Chemical Formula: $C_9H_{10}O$
Molecular Weight: 134.18

Bromoalcohol **86**(10.7 g, 49.6 mmol) was dissolved in dry CH_2Cl_2 (150 mL) at RT and Cs_2CO_3 (35 g, 99 mmol) was added. The reaction mixture was stirred for 72 h and NMR of the crude showed the completion of the reaction. The mixture was filtered through celite and the epoxide containing solution was used directly in the next reaction.

^{1}H NMR (400 MHz, $CDCl_3$) δ 7.37 – 7.17 (m, 5H, CH-Ph), 3.21 – 3.14 (m, 1H, CH-C2), 2.91 (dd, *J* = 14.5, 5.4 Hz, 1H, CH_2-C1a), 2.88 – 2.84 (m, 1H, CH_2-C1b), 2.82 – 2.78 (m, 1H, CH_2-C3a), 2.55 (dd, *J* = 5.0, 2.7 Hz, 1H, CH_2-C3b).

Cbz-aminoalcohol 55

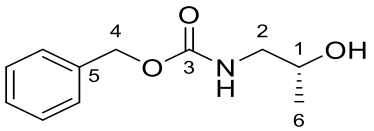

Chemical Formula: $C_{11}H_{15}NO_3$
Molecular Weight: 209.2450

(*R*)-1-amino-2-propanol **87** (1 g, 13.3 mmol) was dissolved in dry CH_2Cl_2 (50 mL) and cooled to 0 °C. Benzyl chloroformate (2.3 mL, 16 mmol) and Et_3N (9.3 mL, 66.5 mmol) were then added dropwise. The mixture was warmed to RT and the reaction stirred overnight. The mixture was neutralised by addition of a 1 M $KHSO_4$ aq. solution (50 mL) and the layers were separated. The organic phase was washed with a 1 M $KHSO_4$ aq. solution (2 x 50 mL), brine (2×50 mL), dried over $MgSO_4$, filtered and the solvent removed *in vacuo*. Purification by silica column chromatography (*n*-hex:EtOAc, 2:1) provided the desired compound **55** (2.22 g, 10.6 mmol, 80%) as a colourless oil.

^{1}H NMR (500 MHz, $CDCl_3$) δ 7.46 – 7.29 (m, 5H, CH-Ph), 5.18 (br s, 1H, NH), 5.13 (s, 2H, CH_2-C4), 4.00 – 3.92 (m, 1H, CH-C1), 3.37 (ddd, *J* = 13.5, 6.5, 3.0 Hz, 1H, CH_2-C2a), 3.09 (ddd, *J* = 13.5, 7.6, 5.4 Hz, 1H, CH_2- C2b), 2.04 (s, 1H, OH), 1.09 (d, *J* = 6.3 Hz, 3H, CH_3-C6).

^{13}C NMR (126 MHz, $CDCl_3$) δ 157.2 (CH-C3), 136.5 (C-C5), 128.6 (CH-Ph), 128.3 (CH-Ph), 128.2 (CH-Ph), 67.6 (CH-C1), 67.0 (CH_2-C4), 48.4 (CH_2-C2), 20.8 (CH_3-C6).

HRMS (ESI positive) calcd for $C_{11}H_{15}NNaO_3$ $[M+Na]^+$ 232.0944, found 232.0944.

(±)-Cbz-aminoalcohol 55

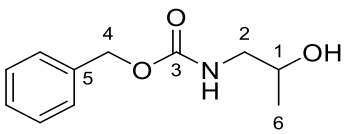

Chemical Formula: $C_{11}H_{15}NO_3$
Molecular Weight: 209.25

(±) Propylene oxide **50** (1.4 mL, 10 mmol) was added to a 30% aq. ammonia solution (200 mL) under vigorous stirring. The reaction was stirred at RT overnight. Evaporation of the solvent *in vacuo* and co-evaporation with $CHCl_3$ resulted in the corresponding amino alcohol **(±) 52**, which was dissolved in dry CH_2Cl_2 (35 mL) and

cooled to 0 °C. Benzyl chloroformate (1.7 mL, 12 mmol) and Et_3N (7 mL, 50 mmol) were then added dropwise. The mixture was warmed to RT and the reaction stirred overnight. The mixture was neutralised by addition of a 1 M $KHSO_4$ aq. solution (0 mL) and the layers were separated. The organic phase was washed with a 1 M $KHSO_4$ aq. solution (2 x 50 mL), brine (2 × 50 mL), dried over $MgSO_4$, filtered and the solvent removed *in vacuo*. Purification by silica column chromatography (EtOAc:*n*-hex, 2:8→4:6) afforded the desired compound **(±) 55** (1.6 g, 8 mmol, 80% over two steps) as a colourless oil.

(See compound **55** for data)

Cbz-aminoalcohol 56

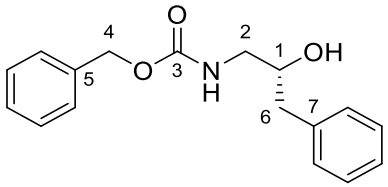

Chemical Formula: $C_{17}H_{19}NO_3$
Molecular Weight: 285.3430

The epoxide containing solution **53** was added to a 30% aq. ammonia solution (930 mL) under vigorous stirring. The reaction was stirred at RT overnight. Evaporation of the solvent *in vacuo* and co-evaporation with $CHCl_3$ resulted in the corresponding amino alcohol **54**, which was dissolved in dry CH_2Cl_2 (185 mL) and cooled to 0 °C. Benzyl chloroformate (8.5 mL, 60 mmol) and Et_3N (34 mL, 248 mmol) were added dropwise. The mixture was warmed to RT and the reaction stirred overnight. The mixture was neutralised by addition of a 1 M $KHSO_4$ aq. solution (100 mL) and the layers were separated. The organic phase was washed with a 1 M $KHSO_4$ aq. solution (2 x 100 mL) brine (2 × 100 mL), dried over $MgSO_4$, filtered and the solvent removed *in vacuo*. Purification by silica column chromatography (EtOAc:*n*-hex, 2:8→4:6) afforded the desired compound **92** (11.6 g, 39.1 mmol, 79% over three steps) as white crystals.

^{1}H NMR (400 MHz, $CDCl_3$) δ 7.43 – 7.10 (m, 10H, CH-Ph), 5.24 (br s, 1H, NH), 5.10 (s, 1H, CH_2-C4), 4.00 – 3.83 (m, 1H, CH-C1), 3.44 (ddd, *J* = 14.0, 6.9, 3.0 Hz, 1H, CH_2-C2a), 3.12 (ddd, *J* = 14.0, 7.6, 5.2 Hz, 1H, CH_2-C2b), 2.79 (dd, *J* = 13.7, 4.9 Hz, 1H, CH_2-C6a), 2.69 (dd, *J* = 13.7, 8.3 Hz, 1H, CH_2-C6b), 2.35 (br s, 1H, OH).

^{13}C NMR (126 MHz, $CDCl_3$) δ 136.2 (C-C5, C7), 129.2 (CH-Ph), 128.6 (CH-Ph), 128.4 (CH-Ph), 128.0 (CH-Ph), 126.6 (CH-Ph), 72.0 (CH-C1), 66.8 (CH_2-C4), 46.1 (CH_2-C2), 41.1 (CH_2-C6).

HRMS (ESI positive) calcd for $C_{17}H_{19}NNaO_3$ $[M+Na]^+$ 308.1257, found 308.1257.

$[\alpha]_D^{23}$ −1.3 (c 0.21, chloroform).

(±)-Cbz-aminoalcohol 56

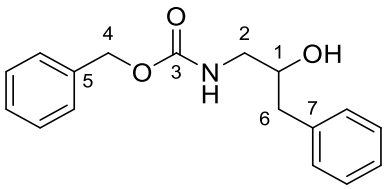

Chemical Formula: $C_{17}H_{19}NO_3$
Molecular Weight: 285.3430

(2,3-Epoxypropyl)benzene **53** (1.3 mL, 10 mmol) was added to a 30% aq. ammonia solution (200 mL) under vigorous stirring. The reaction was stirred at RT overnight. Evaporation of the solvent *in vacuo* and co-evaporation with $CHCl_3$ resulted in the corresponding amino alcohol **(±) 54**, which was dissolved in dry CH_2Cl_2 (35 mL) and cooled to 0 °C. Benzyl chloroformate (1.7 mL, 12 mmol) and Et_3N (7 mL, 50 mmol) were then added dropwise. The mixture was warmed to RT and the reaction stirred overnight. The mixture was neutralised by addition of a 1 M $KHSO_4$ aq. solution (0 mL) and the layers were separated. The organic phase was washed with a 1 M $KHSO_4$ aq. solution (2 x 50 mL), brine (2 × 50 mL), dried over $MgSO_4$, filtered and the solvent removed *in vacuo*. Purification by silica column chromatography (EtOAc:*n*-hex, 2:8→4:6) afforded the desired compound **56** (2.25 g, 7.9 mmol, 79% over two steps) as a white solid.

(See compound **56** for data)

Spectroscopic data are in accordance with literature.[123]

(±)-Cbz-mesylate 57

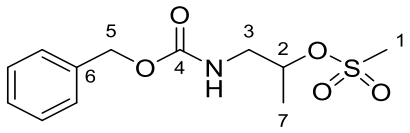

Chemical Formula: $C_{12}H_{17}NO_5S$
Molecular Weight: 287.33

(±) Cbz-amino alcohol **55** (1.04 g, 5 mmol) was dissolved in CH_2Cl_2 (20 mL) and cooled to 0 °C. Et_3N (0.85 mL, 5.75 mmol) and MsCl (0.45 mL) were added dropwise and the reaction mixture was stirred overnight. CH_2Cl_2 (20 mL) was added to the mixture and the organic phase was washed with a 1 M $KHSO_4$ aq. solution (2 x 20 mL), water (2 × 20 mL)and brine (2 × 20 mL). The combined organic layers ere dried over $MgSO_4$, filtered and the solvent removed *in vacuo*. Purification by silica column chromatography (acetone:CH_2Cl_2, 1:99→2:98) afforded the desired compound **57** (1.07g, 3.94 mmol, 79%) as a colourless oil.

^{1}H NMR (400 MHz, $CDCl_3$) δ 7.31 – 7.19 (m, 5H, CH-Ph), 5.12 (br s, 1H, NH), 5.04 (s, 2H, CH_2-C5), 4.79 (m, 1H, CH-C2), 3.42 (dd, 1H, CH_2-C3a), 3.22 (dd, 1H, CH_2-C3b), 2.89 (s, 3H, CH_3-C1), 1.18 (d, 3H, CH_3-C7).

Spectroscopic data are in accordance with literature.[103]

(±)-Cbz-mesylate 58

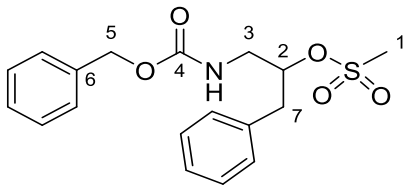

Chemical Formula: $C_{18}H_{21}NO_5S$
Molecular Weight: 363.43

(±) Cbz-amino alcohol **56** (593 mg, 2 mmol) was dissolved in CH_2Cl_2 (7 mL) and cooled to 0 °C. Et_3N (0.33 mL, 2.3 mmol) and MsCl (0.18 mL) were added dropwise and the reaction mixture was stirred overnight. CH_2Cl_2 (7 mL) was added to the mixture and the organic phase was washed with a 1 M $KHSO_4$ aq. solution (2 x 7 mL), water (2 × 7 mL)and brine (2 × 7 mL). The combined organic layers ere dried over $MgSO_4$, filtered and the solvent removed *in vacuo*. Purification by silica column chromatography (acetone:CH_2Cl_2, 2:98) afforded the desired compound **57** (470 mg, 1.29 mmol, 65%) as a colourless oil.

^{1}H NMR (400 MHz, $CDCl_3$) δ 7.30 – 7.16 (m, 10H, CH-Ph), 5.05 (s, 2H, CH_2-C5), 4.82 (m, 1H, CH-C2), 3.53 (dd, 1H, CH_2-C3a), 3.35 (dd, 1H, CH_2-C3b), 2.97 (m, 2H, CH_2-C7), 2.39 (s, 3H, CH_3-C1).

Cbz-thioacetate 59

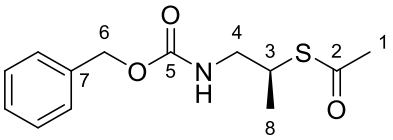

Chemical Formula: $C_{13}H_{17}NO_3S$
Molecular Weight: 267.34

To a solution of triphenylphosphine (5.5 g, 21 mmol) in dry THF (25 mL) at −10 °C was added a solution of diisopropyl azodicarboxylate (4.2 mL, 21 mmol) in dry THF (12 mL) dropwise. The resulting mixture was stirred at −10 °C for 30 minutes. A solution of Cbz-protected amino alcohol **55** (2.2 g, 10.6 mmol) and thioacetic acid (1.5 mL, 21 mmol) in dry THF (25 mL) was then added dropwise. The reaction mixture was stirred at −10 °C overnight. After evaporation of THF *in vacuo*, triphenylphosphine oxide was precipitated by adding a cold 1:1 mixture of EtOAc and PE. The mixture was filtered, the solvent removed *in vacuo* and the crude purified by silica column chromatography (*n*-hex:CH_2Cl_2, 1:1→2:8) affording the desired thioacetate **59** (2.2 g, 8.1 mmol, 76%) as a yellow oil.

^{1}H NMR (500 MHz, $CDCl_3$) δ 7.32 – 7.13 (m, 5H, CH-Ph), 5.09 – 4.97 (m, 2H, CH_2-C6), 4.96 – 4.86 (m, 1H, NH), 3.61 – 3.52 (m, 1H, CH-C3), 3.35 (app dt, J = 14.0, 5.7 Hz, 1H, CH_2-C4a), 3.20 (ddd, J = 14.0, 7.6, 6.3 Hz, 1H, CH_2- C4b), 2.21 (s, 3H, CH_3-C1), 1.21 (d, *J* = 7.1 Hz, 3H, CH_3-C8).
^{13}C NMR (126 MHz, $CDCl_3$) δ 195.5 (C-C2), 156.3 (C-C5), 136.3 (C-C7), 128.4 (CH-Ph), 128.0 (CH-Ph), 66.7 (CH_2-C6), 46.1 (CH_2-C4), 39.7 (CH-C3), 30.6 (CH_3-C1), 18.0 (CH_3-C8).
HRMS (EI positive) calcd for $C_{13}H_{17}NO_3S$ $[M+H]^+$ 267.0929, found 267.0933.

Cbz-thioacetate 60

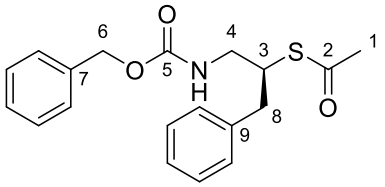

Chemical Formula: $C_{19}H_{21}NO_3S$
Molecular Weight: 343.44

To a solution of triphenylphosphine (8.8 g, 33.6 mmol) in dry THF (40 mL) at −10 °C was added a solution of diisopropyl azodicarboxylate (6.6 mL, 33.6 mmol) in dry THF (20 mL) dropwise. The resulting mixture was stirred at −10 °C for 30 minutes. A solution of Cbz-protected amino alcohol **56** (4.8 g, 16.8 mmol) and thioacetic acid (2.3 mL, 33.6 mmol) in dry THF (40 mL) was then added dropwise. The reaction mixture was stirred at −10 °C overnight. After evaporation of THF *in vacuo*, triphenylphosphine oxide was precipitated by adding a cold 1:1 mixture of EtOAc and PE. The mixture was filtered, the solvent removed *in vacuo* and the crude purified by silica column chromatography (*n*-hex:CH_2Cl_2, 95:5→50:50) affording the desired thioacetate **60** (3.11 g, 9.05 mmol, 54%) as a yellow oil.

^{1}H NMR (500 MHz, CDCl3) δ 7.44 – 7.16 (m, 10H, CH-Ph), 5.20 – 5.11 (m, 2H, CH_2-C6), 5.05 – 4.95 (m, 1H, NH), 3.91 (dddd, J = 7.7, 7.2, 7.1, 5.2 Hz, 1H, CH-C3), 3.55 (ddd, J = 14.2, 5.4, 5.2 Hz, 1H, CH_2-C4a), 3.40 (app dt, J = 14.2, 7.1, Hz, 1H, CH_2-C4b), 2.99 (dd, J = 14.1, 7.2 Hz, 1H, CH_2-C8a), 2.92 (dd, J = 14.1, 7.7 Hz, 1H, CH_2-C8b), 2.32 (s, 3H, CH_3-C1).

^{13}C NMR (126 MHz, $CDCl_3$) δ 195.5 (C-C2), 156.5 (C-C5), 137.9 (C-C7, C9), 129.3 (CH-Ph), 128.6 (CH-Ph), 128.6 (CH-Ph), 128.3 (CH-Ph), 126.9 (CH-Ph), 67.0 (CH_2-C6), 46.2 (CH_2-C4), 44.4 (CH-C3), 38.5 (CH_2-C8), 30.9 (CH_3-C1).

HRMS (ESI positive) calcd for $C_{19}H_{21}NNaO_3S$ $[M+Na]^+$ 366.1134, found 366.1130.

$[\alpha]_D^{23}$ +3.6 (c 0.25, chloroform).

(±) Cbz-thioacetate 60

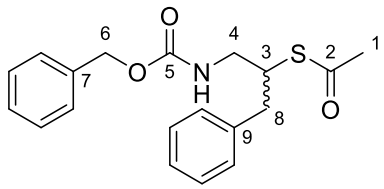

Chemical Formula: $C_{19}H_{21}NO_3S$
Molecular Weight: 343.44

The general procedure was followed on a 10 mmol scale resulting in the desired product (1.40 g, 4 mmol, 40%) as a yellow oil.

(See compound **60** for data)

Bromohydrin 62

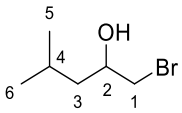

Chemical Formula: $C_6H_{13}BrO$
Molecular Weight: 181.07

4-methyl-1-pentene (0.25 mL, 2 mmol) and NBS (356 mg, 2 mmol) were dissolved in water (0.8 mL). The reaction was stirred overnight. The mixture was extracted with Et_2O (2 × 4 mL). The combined organic layers were washed a 10% Na_2SO_3 aq. solution (2 × 4 mL), dried over $MgSO_4$, filtered and the solvent removed *in vacuo* to afford compound **62** (109 mg, 0.6 mmol, 30%) which did not required further purification.

^{1}H NMR (400 MHz, CDCl3) δ 3.81 – 3.72 (m, 1H, CH-C2), 3.45 (dd, 1H, CH_2-C1a), 3.30 (dd, 1H, CH_2-C1b), 1.76 (m, 1H, CH-C4), 1.42 (dd, 1H, CH_2-C3a), 1.25 (dd, 1H, CH_2-C3b), 0.88 (m, 6H, CH_3-C5, C6).

Spectroscopic data are in accordance with literature.[103]

(*S*)-2-(2-methylpropyl)-oxirane 63

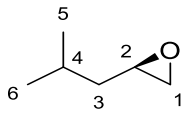

Chemical Formula: $C_6H_{12}O$
Molecular Weight: 100.16

Bromoalcohol **82** (6.6 g, 30 mmol) was dissolved in dry CH_2Cl_2 (90 mL) at RT and Cs_2CO_3 (21.2 g, 60 mmol) was added. The reaction mixture was stirred for 72 h. The mixture was filtered through celite and the epoxide containing solution was used directly in the next reaction.

^{1}H NMR (400 MHz, $CDCl_3$) δ 2.89 (dddd, *J* = 6.6, 5.4, 4.0, 2.8 Hz, 1H, CH-C2), 2.72 (dd, *J* = 5.1, 4.0 Hz 1H, CH_2-C1a), 2.40 (dd, *J* = 5.1, 2.8 Hz, 1H, CH_2-C1b), 1.86 – 1.74 (m, 1H, CH-C4), 1.46 – 1.28 (m, 2H, CH_2-C3), 0.96 (d, *J* = 6.7, 3H, CH_3-C5), 0.94 (d, *J* = 6.7, 3H, CH_3-C6).
Spectroscopic data are in accordance with literature.[124]

(±)-2-(2-methylpropyl)-oxirane 63

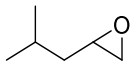

Chemical Formula: $C_6H_{12}O$
Molecular Weight: 100.16

m-CPBA (5.3 g, 24 mmol) was dissolved in CH_2Cl_2 (140 mL) and added to a solution of 4-methyl-1-pentene (2.5 mL, 20 mmol) in CH_2Cl_2 (40 mL) and the reaction mixture stirred at RT overnight. NMR of the crude showed the completion of the reaction. The mixture was filtered and the reaction quenched by addition of a 10% $Na_2S_2O_3$ aq. solution (200 mL). The layers were separated and the organic phase washed with a 1 M $NaHCO_3$ aq. solution (1 × 200 mL), brine (1 × 200 mL), dried over $MgSO_4$ and filtered. The epoxide containing solution was used directly in the next reaction.

(See compound **63** for data)

Cbz-aminoalcohol 65

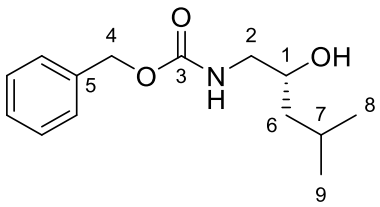

Chemical Formula: $C_{14}H_{21}NO_3$
Molecular Weight: 251.3260

The epoxide containing solution **63** was added to a 30% aq. ammonia solution (600 mL) under vigorous stirring. The reaction was stirred at RT overnight. Evaporation of the solvent *in vacuo* and co-evaporation with $CHCl_3$ resulted in the corresponding amino alcohol **64**, which was dissolved in dry CH_2Cl_2 (110 mL) and cooled to 0 °C. Benzyl chloroformate (5.1 mL, 36 mmol) and Et_3N (21 mL, 150 mmol) were then added dropwise. The mixture was warmed to RT and the reaction stirred overnight. The mixture was neutralised by addition of a 1 M $KHSO_4$ aq. solution (100 mL) and the layers were separated. The organic phase was washed with a 1 M $KHSO_4$ aq. solution (2 x 100 mL), brine (2 × 100 mL), dried over $MgSO_4$, filtered and the solvent removed *in vacuo*. Purification by silica column chromatography (EtOAc: *n*-hex, 5:95→30:70) afforded the desired compound **65** (4.8 g, 19.2 mmol, 64% over three steps) as a yellow oil.

^{1}H NMR (500 MHz, $CDCl_3$) δ 7.39 – 7.29 (m, 5H, CH-Ph), 5.18 – 5.06 (m, 3H, NH, CH_2-C4), 3.80 –3.69 (m, 1H, CH-C1), 3.39 (ddd, *J* = 14.0, 6.7, 3.0 Hz, 1H, CH_2-C2a), 3.05 (ddd, *J* = 14.0, 7.7, 5.3 Hz, 1H, CH_2-C2b), 1.96 (br s, 1H, OH), 1.80 – 1.73 (m, 1H, CH-C7), 1.39 (ddd, *J* = 13.5, 8.9, 5.8 Hz, 1H, CH_2-C6a), 1.23 (ddd, *J* = 13.5, 8.5, 4.3 Hz, 1H, CH_2-C6b), 0.93 (d, *J* = 6.6 Hz, 3H, CH_3-C8), 0.91 (d, *J* = 6.6 Hz, 3H, CH_3-C9).

^{13}C NMR (126 MHz, $CDCl_3$) δ 157.2 (C-C3), 136.5 (C-C5), 128.6 (CH-Ph), 128.3 (CH-Ph), 128.2 (CH-Ph), 69.6 (CH_2-C4), 67.0 (CH-C1), 47.5 (CH_2-C2), 43.9 (CH_2-C6), 24.6 (CH-C7), 23.4 (CH_3-C8), 22.2 (CH_3-C9).

HRMS (ESI positive) calcd for $C_{14}H_{21}NNaO_3$ $[M+Na]^+$ 274.1414, found 274.1414.

$[\alpha]_D^{23}$ −5.5 (c 0.77, chloroform).

(±) Cbz-aminoalcohol 65

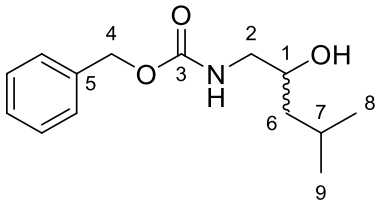

Chemical Formula: $C_{14}H_{21}NO_3$
Molecular Weight: 251.33

The general procedure was followed on a 10 mmol scale resulting in the desired product (2.50 g, 9.1 mmol, 91%)as a yellow oil.

(See compound **65** for data)

Cbz-thioacetate 66

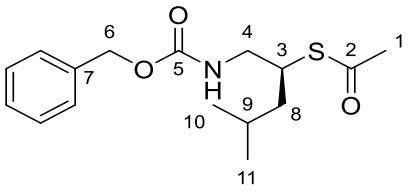

Chemical Formula: $C_{16}H_{23}NO_3S$
Molecular Weight: 309.42

To a solution of triphenylphosphine (10 g, 38.4 mmol) in dry THF (45 mL) at −10 °C was added a solution of diisopropyl azodicarboxylate (7.5 mL, 38.4 mmol) in dry THF (23 mL) dropwise. The resulting mixture was stirred at −10 °C for 30 minutes. A solution of Cbz-protected amino alcohol **65** (4.8 g, 19.2 mmol) and thioacetic acid (12.7 mL, 38.4 mmol) in dry THF (45 mL) was then added dropwise. The reaction mixture was stirred at −10 °C overnight. After evaporation of THF *in vacuo*, triphenylphosphine oxide was precipitated by adding a cold 1:1 mixture of EtOAc and PE. The mixture was filtered, the solvent removed *in vacuo* and the crude purified by silica column chromatography (*n*-hex:CH_2Cl_2, 6:4→2:8) affording the desired compound **66** (4.2 g, 13.6 mmol, 71%) as a yellow oil.

^{1}H NMR (400 MHz, $CDCl_3$) δ 7.44 – 7.29 (m, 5H, CH-Ph), 5.20 – 5.02 (m, 2H, CH_2-C6), 4.98 (br s, 1H, NH), 3.72 – 3.62(m, 1H, CH-C3), 3.46 (app dt, *J* = 14.0, 4.8 Hz, 1H, CH_2-C4a), 3.32 (app dt, *J* = 14.0, 7.0 Hz, 1H, CH_2-C4b), 2.31 (s, 3H, CH_3-C1), 1.77 – 1.72 (m, 1H, CH-C9), 1.47 – 1.38 (m, 2H, CH_2-C8), 0.92 (d, *J* = 6.6 Hz, 3H, CH_3-C10), 0.87 (d, *J* = 6.6 Hz, 3H, CH_3-C11).

^{13}C NMR (126 MHz, $CDCl_3$) δ 195.7 (C-C2), 156.3 (C-C5), 136.4 (C-7), 128.4 (CH-Ph), 128.0 (CH-Ph), 66.6 (CH_2-C6), 45.5 (CH_2-C4), 43.1 (CH-C3), 40.4 (CH_2-C8), 30.6 (CH_3-C1), 25.4 (CH-C9), 22.7 (CH_3-C10), 21.7 (CH_3- C11).

HRMS (ESI positive) calcd for $C_{16}H_{23}NNaO_3S$ $[M+Na]^+$ 332.1282, found 332.1291.

$\mathbf{[\alpha]_D^{23}}$ +1.5 (c 0.45, chloroform).

(±) Cbz-thioacetate 66

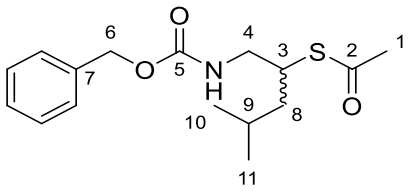

Chemical Formula: $C_{16}H_{23}NO_3S$
Molecular Weight: 309.42

The general procedure was followed on a 5 mmol scale resulting in the desired product (718 mg, 2.45 mmol, 49%) as a yellow oil.

(See compound **66** for data)

Cbz-sulfonate salt 67

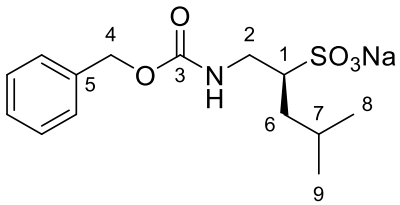

Chemical Formula: $C_{14}H_{20}NNaO_5S$
Molecular Weight: 337.37

Thioacetate **66** (1.6 g, 4.7 mmol) was dissolved in acetic acid (15 mL) and a 30% aq. H_2O_2 solution (5 mL) was added. The reaction was stirred at RT overnight. NaOAc (425 mg, 5.2 mmol) was added and the mixture stirred at RT for 1 h. Co-evaporation with DMF was repeated until the excess of peroxides was removed (checked with starch iodide paper) and lyophilisation of the residual water resulted in the desired sulfonate salt **67** as an off-white solid. No further purification was performed.

HRMS (ESI positive) calcd for $C_{14}H_{20}NNaO_5S$ $[M+Na]^+$ 360.0852, found 360.0843.

(±) Cbz-sulfonate salt 67

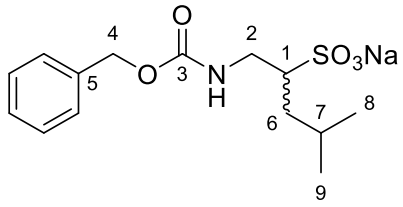

Chemical Formula: $C_{14}H_{20}NNaO_5S$
Molecular Weight: 337.37

The general procedure was followed on a 2.3 mmol scale resulting in the desired product (764 mg, 2.2 mmol, 97%) as a white solid.

(See compound **67** for data)

Cbz-sulfonate salt 68

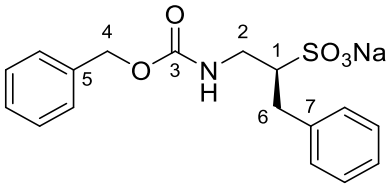

Chemical Formula: $C_{17}H_{18}NNaO_5S$
Molecular Weight: 371.38

Thioacetate **60** (4.2 g, 13.6 mmol) was dissolved in acetic acid (50 mL) and a 30% aq. H_2O_2 solution (18 mL) was added. The reaction was stirred at RT overnight. NaOAc (1.2 g, 15 mmol) was added and the mixture stirred at RT for 1 h. Co-evaporation with DMF was repeated until the excess of peroxides was removed (checked with starch iodide paper) and lyophilisation of the residual water resulted in the desired sulfonate salt **68** as an off-white solid. No further purification was performed.

HRMS (ESI positive) calcd for $C_7H_{18}NNaO_5S$ $[M+Na]^+$ 394.0696, found 394.0693.

(±) Cbz-sulfonate salt 68

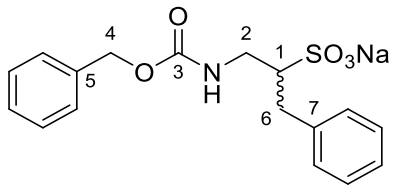

Chemical Formula: $C_{17}H_{18}NNaO_5S$
Molecular Weight: 371.38

The general procedure was followed on a 2 mmol scale resulting in the desired product (630 mg, 1.7 mmol, 84%) as a white solid.

(See compound **68** for data)

Cbz-sulfonyl fluoride 70

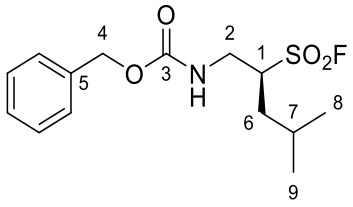

Chemical Formula: $C_{14}H_{20}FNO_4S$
Molecular Weight: 317.38

Procedure 1: The crude sulfonate salt **67** (1 g, 2.9 mmol) was dissolved in dry CH_2Cl_2 (150 mL). XtalFluor-M **69** (1.26 g, 5.22 mmol) and $NEt_3{\cdot}3HF$ (20 µL, 0.12 mmol) were added and the reaction was stirred under a nitrogen atmosphere at reflux overnight. Evaporation of the solvent *in vacuo* and purification of the crude product by silica column chromatography (EtOAc:*n*-hex, 5:95→30:70) afforded the desired sulfonyl fluoride **70** (100 mg, 0.32 mmol, 11%) as a colourless oil followed by the sulfonate methyl ester **90** (395 mg, 1.2 mmol, 42%) as a yellow oil.

Procedure 2: The crude sulfonate salt **67** (300 mg, 0.94 mmol) was dissolved in dry DCE (45 mL). XtalFluor-M **69** (353 mg, 1.45 mmol) and $NEt_3{\cdot}3HF$ (6 µL, 0.03 mmol) were added and the reaction was stirred under a nitrogen atmosphere at reflux overnight. Evaporation of the solvent *in vacuo* and purification of the crude product by silica column chromatography (EtOAc:*n*-hex, 0:1→2:8) afforded the desired sulfonyl fluoride **70** (60 mg, 0.19 mmol, 24%) as a colourless oil.

Procedure 3: The crude tetrabutylammonium sulfonate salt **92** (300 mg, 0.54 mmol) was dissolved in dry DCE (25 mL). XtalFluor-M (236 mg, 0.97 mmol) and

$NEt_3 \cdot 3HF$ (4 µL, 0.02 mmol) were added and the reaction was stirred under a nitrogen atmosphere at reflux overnight. Evaporation of the solvent *in vacuo* and purification of the crude product by silica column chromatography (EtOAc:*n*-hex, 0:1→2:8) afforded the desired sulfonyl fluoride **70** (100 mg, 0.31 mmol, 57%) as a colourless oil.

^{1}H NMR (500 MHz, $CDCl_3$) δ 7.33 – 7.15 (m, 5H, CH-Ph), 5.26 (br s, 1H, NH), 5.08 (d, *J* = 12.1 Hz, 1H, CH_2-C4a), 5.02 (d, *J* = 12.1 Hz, 1H, CH_2-C4b), 3.72 (ddd, *J* = 12.4, 6.9, 2.2 Hz, 1H, CH_2-C2a), 3.56 – 3.44 (m, 2H, CH_2-C2b, CH-C1), 1.90 – 1.79 (m, 1H, CH-C7), 1.79 –1.70 (m, 1H, CH_2-C6a), 1.56 (ddd, *J* = 14.2, 8.8, 5.4 Hz, 1H, CH_2-C6b), 0.89 (d, *J* = 6.5 Hz, 3H, CH_3-C8), 0.88 (d, *J* = 6.5 Hz, 3H, CH_3-C9).
^{13}C NMR (126 MHz, $CDCl_3$) δ 156.4 (C-C3), 136.1 (C-C5), 128.7 (CH-Ph), 128.4 (CH-Ph), 128.2 (CH-Ph), 67.3 (CH_2-C4), 61.6 (d, *J* = 9.4 Hz, CH-C1), 40.1 (CH_2-C2), 35.6 (CH-C6), 25.3 (CH-C7), 22.8 (CH_3-C8), 21.5 (CH_3-C9).
^{19}F NMR (471 MHz, $CDCl_3$) δ 48.38 (s).
HRMS (ESI positive) calcd for $C_{14}H_{20}FNO_4S$ $[M+H]^+$ 317.1097, found 317.1101.

$[\alpha]_D^{33}$ −2.1 (c 2, chloroform).

(±) Cbz-sulfonyl fluoride 70

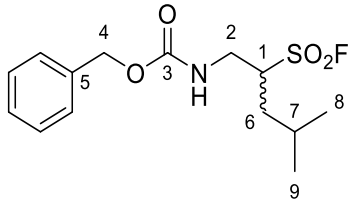

Chemical Formula: $C_{14}H_{20}FNO_4S$
Molecular Weight: 317.38

The general procedure was followed on a 1 mmol scale resulting in the desired product (160 mg, 0.5 mmol, 51%) as a colourless oil

(See compound **70** for data)

Cbz-sulfonyl fluoride 71

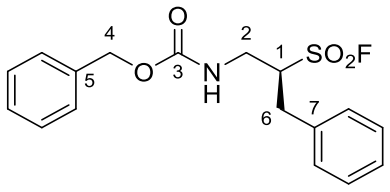

Chemical Formula: $C_{14}H_{20}FNO_4S$
Molecular Weight: 317.38

Procedure 1: The crude sulfonate salt **68** (1 g, 2.7 mmol) was dissolved in dry CH_2Cl_2 (140 mL). XtalFluor-M **69** (1.18 g, 4.86 mmol) and $NEt_3{\cdot}3HF$ (20 µL, 0.12 mmol) were added and the reaction was stirred under a nitrogen atmosphere at reflux overnight. Evaporation of the solvent *in vacuo* and purification of the crude product by silica column chromatography (EtOAc:*n*-hex, 5:95→30:70) afforded the desired sulfonyl fluoride **71** (140 mg, 0.40 mmol, 15%) as a colourless oil followed by the sulfonate methyl ester **91** (400 mg, 1.1 mmol, 41%) as a yellow oil.

Procedure 2: The crude sulfonate salt **68** (300 mg, 0.85 mmol) was dissolved in dry DCE (45 mL). XtalFluor-M (353 mg, 1.45 mmol) and $NEt_3{\cdot}3HF$ (6 µL, 0.03 mmol) were added and the reaction was stirred under a nitrogen atmosphere at reflux overnight. Evaporation of the solvent *in vacuo* and purification of the crude product by silica column chromatography (EtOAc:*n*-hex, 0:10→2:8) afforded the desired sulfonyl fluoride **71** (70 mg, 0.20 mmol, 25%) as a solid.

^{1}H NMR (500 MHz, $CDCl_3$) δ 7.38 – 7.06 (m, 10H, CH-Ph), 5.17 (br s, 1H, NH), 5.06 – 4.94 (m, 2H, CH_2-C4), 3.94 – 3.84 (m, 1H, CH-C1), 3.65 (ddd, *J* = 14.7, 6.2, 3.0 Hz, 1H, CH_2-C2a), 3.52 (app dt, *J* = 14.7, 6.9 Hz, 1H, CH_2-C2b), 3.34 (dd, *J* = 14.4, 4.6 Hz, 1H, CH_2-C6a), 2.93 (dd, *J* = 14.4, 9.5 Hz, 1H, CH_2-C6b).
^{13}C NMR (126 MHz, $CDCl_3$) δ 156.0 (C-C3), 135.9 (C-C5), 134.5 (C-C7), 129.1 (CH-Ph), 129.0 (CH-Ph), 128.6 (CH-Ph), 128.3 (CH-Ph), 128.1 (CH-Ph), 127.8 (CH-Ph), 67.2 (CH_2-C4), 63.9 (d, *J* = 8.8 Hz, CH-C1), 39.5 (CH_2-C2), 33.1 (CH_2-C6).
^{19}F NMR (471 MHz, $CDCl_3$) δ 50.56 (s).
HRMS (ESI positive) calcd for $C_{17}H_{18}FNNaO_4S$ $[M+Na]^+$ 374.0833, found 374.0828.

$\mathbf{[\alpha]_D^{33}}$ +31.2 (c 0.6, chloroform).

(±) Cbz-sulfonyl fluoride 71

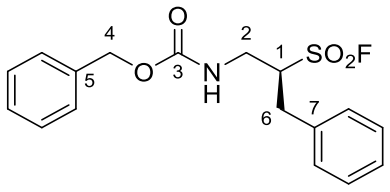

Chemical Formula: $C_{14}H_{20}FNO_4S$
Molecular Weight: 317.38

The general procedure was followed on a 1.4 mmol scale resulting in the desired product (236 mg, 0.6 mmol, 48%) as a white solid.

(See compound **71** for data)

(*S*)-Ethyl-2-bromo-4-methylpentanoate 81

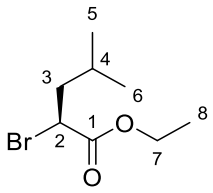

Chemical Formula: $C_8H_{15}BrO_2$
Molecular Weight: 223.1100

L-Leucine **79** (13.2 g, 100 mmol) and KBr (41.6 g, 350 mmol) were dissolved in a 2.5 M H_2SO_4 aq. solution (130 mL) at 0 °C and $NaNO_2$ (8.9 g, 130 mmol) was added over 2 h. The reaction mixture was warmed to RT and stirred for 72 h. The mixture was extracted with EtOAc (3 × 300 mL). The combined organic extracts were washed with brine (1 × 300 mL), dried over $MgSO_4$, filtered and removed *in vacuo*, affording (*S*)-2-bromo-4-methylpentanoic acid **80** which was used directly in the next reaction without further purification. The α-bromo acid (17.6 g, 90.0 mmol) was dissolved in a mixture of EtOH (230 mL) and conc. H_2SO_4 (3 mL) and stirred at reflux overnight. Removal of the solvent *in vacuo* and purification by silica column chromatography (PE:CH_2Cl_2, 9:1) afforded the desired compound **81** (11.1 g, 50 mmol, 50% over 2 steps) as a colourless oil.

^{1}H NMR (500 MHz, $CDCl_3$) δ 4.29 – 4.18 (m, 3H, CH-C2, CH_2-C7), 1.96 – 1.84 (m, 2H, CH_2-C3), 1.82 – 1.70 (m, 1H, CH-C4), 1.29 (t, *J* = 7.1 Hz, 3H, CH_3-C8), 0.95 (d, *J* = 6.6 Hz, 3H, CH_3-C5), 0.90 (d, *J* = 6.6 Hz, 3H, CH_3-C6).
^{13}C NMR (126 MHz, $CDCl_3$) δ 169.9 (C-C1), 61.7 (CH-C2), 44.6 (CH_2-C7), 43.3 (CH_2-C3), 26.2 (CH-C4), 22.2 (CH_3-C5), 21.4 (CH_3-C6), 13.8 (CH_3-C8).

HRMS (CI iso-butane) calcd for $C_8H_{16}O_2Br$ $[M+H]^+$ 223.0334, found 223.0325.

$[\alpha]_D^{20}$ −35.8 (c 2.4, chloroform).

Spectroscopic data are in accordance with literature.[108]

(*S*)-2-bromo-4-methyl-1-pentanol 82

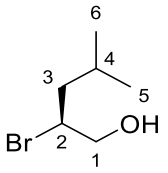

Chemical Formula: $C_6H_{13}BrO$
Molecular Weight: 181.0730

To a solution of **81** (11.1 g, 50 mmol) in dry THF (180 mL) at RT was added $NaBH_4$ (4.7 g, 125 mmol) and LiCl (5.2 g, 125 mmol). After stirring for 10 min, EtOH (290 mL) was added and the reaction mixture was stirred overnight. During the reaction additional dry THF (75 mL) was added to achieve adequate stirring. The reaction was cooled to 0 °C and quenched by slow addition of a saturated aq. NH_4Cl solution (250 mL). The layers were separated and the aqueous phase was extracted with EtOAc (3 × 300 mL). The combined organic extracts were dried over $MgSO_4$, filtered and solvent removed *in vacuo*. Purification by silica column chromatography (*n*-hex:CH_2Cl_2, 4:6) afforded the desired bromoalcohol **82** (6.6 g, 30 mmol, 60%) as a colourless oil.

^{1}H NMR (500 MHz, $CDCl_3$) δ 4.14 (dddd, *J* = 10.2, 7.0, 4.2, 4.2 Hz, 1H, CH-C2), 3.75 (dd, *J* = 12.4, 4.2 Hz, 1H, CH_2-C1a), 3.66 (dd, *J* = 12.4, 7.0 Hz, 1H, CH_2-C1b), 2.20 (br s, 1H, OH), 1.87 – 1.79 (m, 1H, CH-C4), 1.75 (ddd, *J* = 14.6, 10.2, 5.0 Hz, 1H, CH_2-C3a), 1.50 (ddd, *J* = 14.6, 8.9, 4.2 Hz, 1H, CH_2-C3b), 0.89 (d, *J* = 6.6 Hz, 3H, CH_3-C5), 0.84 (d, *J* = 6.6 Hz, 3H, CH_3-C6).
^{13}C NMR (126 MHz, $CDCl_3$) δ 67.7 (CH_2-C1), 58.6 (CH-C2), 43.7 (CH_2-C3), 26.3 (CH-C4), 23.0 CH_3-C5), 21.3 (CH_3-C6).
HRMS not recorded, sample does not ionise.

$[\alpha]_D^{20}$ −41.8 (c 0.7, chloroform). **lit** $[\alpha]_D^{22}$ −41.9 (c 1.346, MeOH).

(*S*)-Ethyl-2-bromo-3-phenylpropionate 85

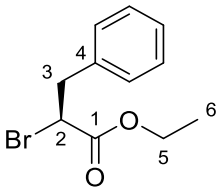

Chemical Formula: $C_{11}H_{13}BrO_2$
Molecular Weight: 257.1270

L-Phenylalanine **83** (16.5 g, 100 mmol) and KBr (41.6 g, 350 mmol) were dissolved in a 2.5 M H_2SO_4 aq. solution (130 mL) at 0 °C and $NaNO_2$ (8.9 g, 130 mmol) was added over 2 h. The reaction mixture was warmed to RT and stirred for 72 h. The mixture was extracted with EtOAc (3 × 300 mL). The combined organic extracts were washed with brine (1 × 300 mL), dried over $MgSO_4$, filtered and removed *in vacuo*, affording (*S*)-2-bromo-benzenepropanoic acid **84** which was used directly in the next reaction without further purification. The α-bromo acid (22.0 g, 96.2 mmol) was dissolved in a mixture of EtOH (250 mL) and conc. H_2SO_4 (4 mL) and stirred at reflux overnight. Removal of the solvent *in vacuo* and purification by silica column chromatography (*n*-hex:CH_2Cl_2, 4:1) afforded the desired compound **85** (16.9 g, 65.7 mmol, 66% over 2 steps) as colourless oil.

^{1}H NMR (400 MHz, $CDCl_3$) δ 7.36 – 7.13 (m, 5H, CH-Ph), 4.38 (dd, *J* = 8.5, 7.1 Hz, 1H, CH-C2), 4.26 – 4.15 (m, 2H, CH_2-C5), 3.49 (dd, *J* = 14.1, 8.5 Hz, 1H, CH_2-C3a), 3.27 (dd, *J* = 14.1, 7.1 Hz, 1H, CH_2-C3b), 1.25 (t, *J* = 7.1 Hz, 3H, CH_3-C6).

^{13}C NMR (126 MHz, $CDCl_3$) δ 169.5 (C-C1), 136.9 (C-C4), 129.3 (CH-Ph), 128.7 (CH-Ph), 127.4 (CH-Ph), 62.1 (CH-C2), 45.6 (CH_2-C5), 41.2 (CH_2-C3), 13.8 (CH_3-C6).

HRMS (ESI positive) calcd for $C_{11}H_{13}NaO_2Br$ $[M+Na]^+$ 278.9982, found 278.9991.

$\mathbf{[\alpha]_D^{20}}$ −8.0 (c 3.7, chloroform). $\mathbf{[\alpha]_D^{22}}$ +0.9 (c 0.632, MeOH).

Spectroscopic data are in accordance with literature.[108]

(*S*)-2-bromo-benzenepropanol 86

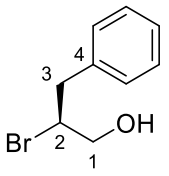

Chemical Formula: $C_9H_{11}BrO$
Molecular Weight: 215.0900

To a solution of **85** (16.9 g, 65.7 mmol) in dry THF (240 mL) at RT was added $NaBH_4$ (6.2 g, 165 mmol) and LiCl (6.9 g, 165 mmol). After stirring for 10 min, EtOH (380 mL) was added and the reaction mixture was stirred overnight. During the reaction additional dry THF (150 mL) was added to achieve adequate stirring. The reaction was cooled to 0 °C and quenched by slow addition of a saturated aq. NH_4Cl solution (300 mL). The layers were separated and the aqueous phase was extracted with EtOAc (3 × 400 mL). The combined organic extracts were dried over $MgSO_4$, filtered and solvent removed *in vacuo*. Purification by silica column chromatography (*n*-hex:CH_2Cl_2, 2:8) afforded the desired product **86** (10.7 g, 49.6 mmol, 75%) as a colourless oil.

^{1}H NMR (500 MHz, $CDCl_3$) δ 7.37 – 7.24 (m, 5H, CH-Ph), 4.36 (dddd, *J* = 7.5, 7.5, 6.0, 3.7 Hz, 1H, CH-C2), 3.86 (ddd, *J* = 12.5, 6.5, 3.7 Hz, 1H, CH_2-C1a), 3.77 (ddd, *J* = 12.5, 6.5, 6.0 Hz, 1H, CH_2-C1b), 3.29 (dd, *J* = 14.2, 7.5 Hz, 1H, CH_2-C3a), 3.21 (dd, *J* = 14.2, 7.5 Hz, 1H, CH_2-C3b), 2.03 (t, *J* = 6.5 Hz, 1H, OH).

^{13}C NMR (126 MHz, $CDCl_3$) δ 138.0 (C-C4), 129.6 (CH-Ph), 129.0 (CH-Ph), 127.4 (CH-Ph), 66.4 (CH_2-C1), 59.2 (CH-C2), 41.7 (CH_2-C3).

HRMS (EI positive) calcd for $C_9H_{11}OBr$ $[M+H]^+$ 213.9993, found 213.992.

$[\alpha]_D^{20}$ −19.3 (c 0.9, chloroform). **lit** $[\alpha]_D^{20}$ −22.6 (c 5, chloroform).

Spectroscopic data are in accordance with literature.[125]

Cbz-sulfonate salt 88

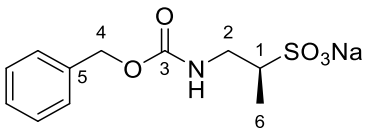

Chemical Formula: $C_{11}H_{14}NNaO_5S$
Molecular Weight: 295.28

Thioacetate **59** (2.16 g, 8.1 mmol) was dissolved in acetic acid (25 mL) and a 30% aq. H_2O_2 solution (9 mL) was added. The reaction was stirred at RT overnight. NaOAc (730 mg, 8.9 mmol) was added and the mixture stirred at RT for 1 h. Co-evaporation with DMF was repeated until the excess of peroxides was removed (checked with starch iodide paper) and lyophilisation of the residual water resulted in the desired sulfonate salt **88** as an off-white solid. No further purification was performed.

HRMS (ESI negative) calcd for $C_{11}H_{14}NO_5S$ $[M-H]^-$ 272.0598, found 272.0578.

Cbz-sulfonyl fluoride 89

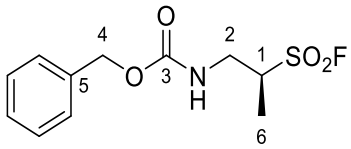

Chemical Formula: $C_{14}H_{20}FNO_4S$
Molecular Weight: 317.38

The crude sulfonate salt **88** (1.4 g, 5 mmol) was dissolved in dry DCE (200 mL). XtalFluor-*M* (2.1 g, 8.5 mmol) and $NEt_3 \cdot 3HF$ (59 µL, 0.4 mmol) were added and the reaction was stirred under a nitrogen atmosphere at reflux overnight. Evaporation of the solvent *in vacuo* and purification of the crude product by silica column chromatography (EtOAc:*n*-hex, 4:6) afforded the desired sulfonyl fluoride **89** (230 mg, 0.89 mmol, 29%) as a yellow oil.

^{1}H NMR (500 MHz, $CDCl_3$) δ 7.37 – 7.16 (m, 5H, CH-Ph), 5.30 – 5.18 (br s, 1H, NH), 5.11 – 5.00 (m, 2H, CH_2-C4), 3.72 – 3.55 (m, 3H, CH-C1, CH_2-C2), 1.47 (d, *J* = 6.9 Hz, 3H, CH_3-C6).

^{13}C NMR (126 MHz, $CDCl_3$) δ 156.4 (C-C3), 136.0 (C-C5), 128.7 (CH-Ph), 128.5 (CH-Ph), 128.2 (CH-Ph), 67.4 (CH_2-C4), 58.3 (d, *J* = 11.7 Hz, CH-C1), 41.6 (CH_2-C2), 12.8 (CH_3-C6).

^{19}F NMR (471 MHz, $CDCl_3$) δ 46.10 (s).

HRMS (ESI positive) calcd for $C_{11}H_{14}FNNaO_4S$ $[M+Na]^+$ 298.0520, found 298.0506.

$[\alpha]_D^{33}$ +16.8 (c 0.6, chloroform).

Cbz-sulfonate methyl ester 90

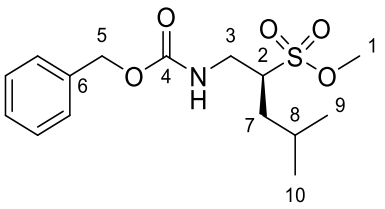

Chemical Formula: $C_{15}H_{23}NO_5S$
Molecular Weight: 329.4110

^{1}H NMR (400 MHz, $CDCl_3$) δ 7.46 – 7.21 (m, 5H, CH-Ph), 5.48 (t, *J* = 6.2 Hz, 1H, NH), 5.21 – 5.01 (m, 2H, CH_2-C5), 3.86 (s, 3H, CH_3-C1), 3.68 (ddd, *J* = 15.1, 6.2, 3.0 Hz, 1H, CH_2-C3a), 3.59 – 3.51 (m, 1H, CH_2-C3b), 3.30 (app ddt, *J* = 12.5, 7.6, 3.0 Hz, 1H, CH-C2), 1.90 – 1.79 (m, 1H, CH-C8), 1.72 (ddd, *J* = 12.5, 9.0, 4.3 Hz, 0H, CH_2-C7a), 1.55 (ddd, *J* = 14.3, 9.0, 5.4 Hz, 1H, CH_2-C7b), 0.95 (d, *J* = 6.5 Hz, 3H, CH_3-C9), 0.93 (d, *J* = 6.5 Hz, 3H, CH_3-C10).

^{13}C NMR (126 MHz, $CDCl_3$) δ 156.3 (C-C4), 136.2 (C-C6), 128.6 (CH-Ph), 128.3 (CH-Ph), 128.1 (CH-Ph), 67.0 (CH_2-C5), 59.0 (CH-C2), 55.1 (CH_3-C1), 39.9 (CH_2-C3), 35.4 (CH_2-C7), 25.2 (CH-C8), 23.0 (CH_3-C9), 21.5 (CH_3-C10).

HRMS (ESI positive) calcd for $C_{15}H_{23}NNaO_5S$ $[M+Na]^+$ 352.1189, found 352.1179.

Cbz-sulfonate methyl ester 91

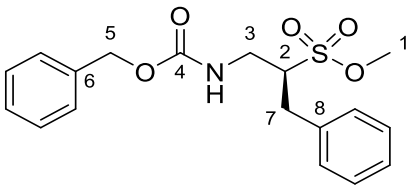

Chemical Formula: $C_{18}H_{21}NO_5S$
Molecular Weight: 363.4280

^{1}H NMR (400 MHz, $CDCl_3$) δ 7.40 – 7.12 (m, 10H, CH-Ph), 5.47 (t, *J* = 5.5 Hz, 1H, NH), 5.05 (s, 2H, CH_2-C5), 3.76 (s, 3H, CH_3-C1), 3.62 – 3.48 (m, 3H, CH_2-C3, CH-C2), 3.30 (dd, *J* = 14.3, 4.0 Hz, 1H, CH_2-C7a), 2.89 (dd, *J* = 14.3, 8.3 Hz, 1H, CH_2-C7b).

^{13}C NMR (126 MHz, $CDCl_3$) δ 156.1 (C-C4), 138.3 (C-C8), 136.5 (C-C6), 129.0 (CH-Ph), 128.7 (CH-Ph), 128.4 (CH-Ph), 128.3 (CH-Ph), 127.80 (CH-Ph), 127.2 (CH-Ph), 67.0 (CH_2-C5), 61.6 (CH-C2), 55.4 (CH_3-C1), 39.5 (CH_2-C3), 33.1 (CH_2-C7).

HRMS (ESI positive) calcd for $C_{18}H_{21}NNaO_5S$ $[M+Na]^+$ 386.1033, found 386.1041.

Cbz-sulfonate salt 92

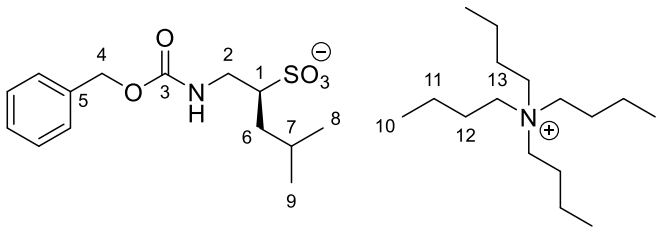

Chemical Formula: $C_{30}H_{56}N_2O_5S$
Molecular Weight: 556.8470

Sulfonate ester **90** (395 mg, 1.2 mmol) was dissolved in acetone (25 mL) and tetrabutylammonium iodide (450 mg, 1.2 mmol) was added. The reaction was stirred at reflux overnight. Evaporation of the solvent *in vacuo* provided the compound **92** (660 mg, 1.2 mmol, quant) as a yellow oil. The salt did not require any further purification and was used directly in the next step.

^{1}H NMR (500 MHz, $CDCl_3$) δ 7.39 – 7.21 (m, 5H, CH-Ph), 6.67 (s, 1H, NH), 5.15 – 4.99 (m, 2H, CH_2-C4), 3.71 (ddd, *J* = 13.7, 5.6, 2.4 Hz, 1H, CH_2-C2a), 3.40 (ddd, *J* = 13.7, 8.2, 4.9 Hz, 1H, CH_2-C2b), 3.32 – 3.26 (m, 8H, CH_2-C13), 2.82 (app td, *J* = 10.5, 8.2, 2.4 Hz, 1H, CH-C1), 1.83 – 1.74 (m, 2H, CH_2-C6a, CH-C7), 1.69 – 1.58

(m, 9H, CH_2-C6b, C12), 1.50 –1.37 (m, 8H, CH_2-C11), 1.00 (t, *J* = 7.3 Hz, 12H, CH_3-C10), 0.91 (d, *J* = 5.8 Hz, 3H, CH_3-C8), 0.89 (d, *J* = 5.8 Hz, 3H, CH_3-C9).

^{13}C NMR (126 MHz, $CDCl_3$) δ 156.6 (C-C3), 135.1 (C-C5), 128.3 (CH-Ph), 127.9 (CH-Ph), 127.7 (CH-Ph), 66.1 (CH_2-C4), 59.0 (CH_2-C13), 57.2 (CH-C1), 40.8 (CH_2-C2), 36.6 (CH_2-C6), 25.3 (CH-C7), 24.1 (CH_2-C12), 23.7 (CH_3-C8), 21.5 (CH_3-C9), 19.8 (CH_2-C11), 13.7 (CH_3-C10).

HRMS (ESI negative) calcd for $C_{14}H_{20}NO_5S$ $[M-H]^-$ 314.1068, found 314.0981.

(*S*)-Ethyl-2-bromo-3-hydroxypropionate 95

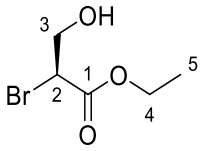

Chemical Formula: $C_5H_9BrO_3$
Molecular Weight: 197.0280

L-Serine **93** (12.6 g, 105 mmol) and KBr (50.0 g, 119 mmol) were dissolved in a 1.25 M H_2SO_4 aq. solution (250 mL) at 0 °C and $NaNO_2$ (13.2 g, 192 mmol) was added at over 2 h. The reaction mixture was warmed to RT and stirred for 48 h. The mixture was extracted with EtOAc (4 × 300 mL). The combined organic extracts were washed with brine (1 × 300 mL), dried over $MgSO_4$, filtered and removed *in vacuo*, affording the corresponding bromo acid **94** which was used directly in the next reaction without further purification. The α-bromo acid **95** (16.5 g, 98.0 mmol) was dissolved in a mixture of EtOH (350 mL) and conc. H_2SO_4 (6 mL) and stirred at reflux overnight. Removal of the solvent *in vacuo* and purification by silica column chromatography (CH_2Cl_2) afforded the desired compound **109** (11.9 g, 60.0 mmol, 50% over 2 steps) as a yellow oil.

^{1}H NMR (500 MHz, $CDCl_3$) δ 4.27 (dd, *J* = 7.5, 5.4 Hz, 1H, CH-C2), 4.20 (q, *J* = 7.1 Hz, 2H, CH_2-C4), 3.98 (ddd, *J* = 12.5, 7.5, 6.5 Hz, 1H, CH_2-C3a), 3.87 (ddd, *J* = 12.5, 6.9, 5.4 Hz, 1H, CH_2-C3b), 2.80 – 2.70 (br s, 1H, OH), 1.25 (t, *J* = 7.1 Hz, 3H, CH_3-C5).

^{13}C NMR (101 MHz, $CDCl_3$) δ 169.0 (C-C1), 63.8 (CH_2-C3), 62.4 (CH_2-C4), 44.6 (CH-C2), 13.9 (CH_3-C5).

HRMS (ESI positive) calcd for $C_5H_9NaO_3Br$ $[M+Na]^+$ 218.9627, found 218.9630.

TPDPS-(*S*)-Ethyl-2-bromo-3-hydroxypropionate 96

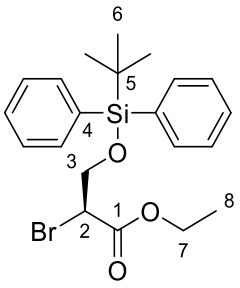

Chemical Formula: $C_{21}H_{27}BrO_3Si$
Molecular Weight: 435.4330

α-bromo ester **95** (300 mg, 1.52 mmol) and imidazole (124 mg, 1.82 mmol) were dissolved in dry CH_2Cl_2 (10 mL) and the mixture cooled to 0 °C. TBDPS-Cl (0.43 mL, 1.82 mmol) was added dropwise and the reaction mixture was warmed to RT and stirred overnight. The mixture was diluted with CH_2Cl_2 and washed with brine (1 × 50 mL). The organic phase was dried over $MgSO_4$, filtered and solvent removed *in vacuo*. The crude product was purified by silica column chromatography (CH_2Cl_2:*n*-hex, 0:10→2:8) affording the desired compound **96** (430 mg, 0.99 mmol, 66%) as a colourless oil.

^{1}H NMR (500 MHz, $CDCl_3$) δ 7.62 –7.57 (m, 4H, Ph), 7.40 – 7.30 (m, 6H, Ph), 4.23 – 4.15 (m, 3H, CH-C2, CH_2-C7), 4.05 (dd, *J* = 10.3, 8.7 Hz, 1H, CH_2-C3a), 3.84 (dd, *J* = 10.3, 5.6 Hz, 1H, CH_2-C3b), 1.24 (t, *J* = 7.2 Hz, 3H, CH_3-C8), 0.96 (s, 9H, CH_3-C6).

TPDPS-(*S*)-2-bromo-3-hydroxypropanol 97

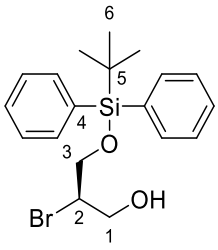

Chemical Formula: $C_{19}H_{25}BrO_2Si$
Molecular Weight: 393.3960

To a solution of **96** (430 mg, 0.99 mmol) in dry THF (5 mL) at RT was added $NaBH_4$ (93 mg, 2.5 mmol) and LiCl (105 mg, 2.5 mmol). After stirring for 10 min, EtOH (6 mL) was added and the reaction mixture was stirred overnight. The reaction was cooled to 0 °C and quenched by slow addition of a saturated aq. NH_4Cl solution

(15 mL). The layers were separated and the aqueous phase was extracted with EtOAc (3 × 25 mL). The combined organic extracts were washed with brine (1 × 25 mL), dried over $MgSO_4$, filtered and solvent removed *in vacuo*. The desired bromoalcohol **97** (320 mg, 0.81 mmol, 82%) was obtained as a colourless oil and did not require any further purification.

^{1}H NMR (500 MHz, $CDCl_3$) δ 7.62 –7.57 (m, 4H, CH-Ph), 7.42 – 7.27 (m, 6H, CH-Ph), 4.11 – 4.02 (m, 1H, CH-C2), 3.96 – 3.79 (m, 3H, CH_2-C1, C3), 2.02 (t, *J* = 6.8 Hz, 1H, OH), 1.00 (s, 9H, CH_3-C6).

^{13}C NMR (101 MHz, $CDCl_3$) δ 135.6, 135.5 (C-C4), 132.9 (CH-Ph), 132.7 (CH-Ph), 130.0(CH-Ph), 129.9(CH-Ph), 127.9(CH-Ph), 127.8 (CH-Ph), 65.3 (CH_2-C1), 64.7 (CH_2-C3), 55.2 (CH-C2), 26.8 (CH_3-C6), 19.3 (C-C5).

HRMS (ESI positive) calcd for $C_{19}H_{25}NaO_2SiBr$ $[M+Na]^+$ 415.0699, found 415.0687.

Piperidine substituted compound from 71

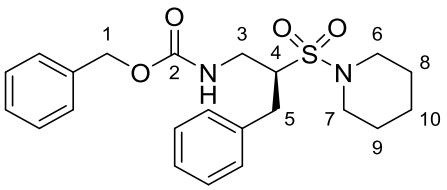

Chemical Formula: $C_{22}H_{28}N_2O_4S$
Molecular Weight: 416.54

Cbz-Phe-SO_2F **71** (30 mg, 0.085 mmol) was dissolved in CH_2Cl_2 (1 mL) at RT and piperidine (18 µL, 0.187 mmol) was added. The reaction mixture was stirred for 24h. After evaporation of the solvent *in vacuo* the crude material was purified by silica column chromatography (*n*-hex:CH_2Cl_2, 3:7) affording the substituted compound (25 mg, 0.06mmol, 70%) as a colourless oil.

^{1}H NMR (500 MHz, $CDCl_3$) δ 7.43 – 7.16 (m, 10H, CH-Ph), 5.55 (br s, 1H, NH), 5.13 – 5.05 (m, 2H, CH_2-C1), 3.56 (app t, *J* = 5.4 Hz, 2H, CH_2-C3), 3.36 – 3.20 (m, 6H, CH_2-C6, C7, C5a, CH-C4), 2.85 (dd, *J* = 14.1, 10.3 Hz, 1H, CH_2-C5b), 1.68 – 1.52 (m, 5H, CH_2-C8, C9, C10).

^{13}C NMR (101 MHz, $CDCl_3$) δ 156.3 (C-C4), 136.8 (C-Ph), 136.5 (C-Ph), 129.1 (CH-Ph), 129.0 (CH-Ph), 128.6, 128.2 (CH-Ph), 127.3 (CH-Ph), 66.9 (CH_2-C1), 62.6 (CH-C4), 47.0 (CH_2-C6, C7), 39.4 (CH_2-C3), 33.2 (CH_2-C5), 26.1 (CH_2-C8, C9), 23.9 (CH_2-C10).

HRMS (ESI positive) calcd for $C_{22}H_{28}N_2NaO_4S$ $[M+Na]^+$ 439.1662, found 439.1648.

Benzylamine substituted compound from 71

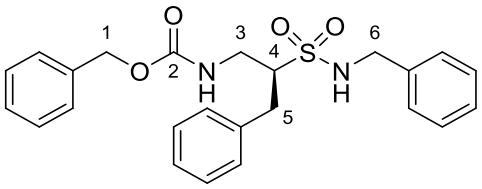

Chemical Formula: $C_{24}H_{26}N_2O_4S$
Molecular Weight: 438.54

Cbz-Phe-SO_2F **71** (30 mg, 0.085 mmol) was dissolved in CH_2Cl_2 (1 mL) at RT and benzyl amine (20 µL, 0.187 mmol) was added. The reaction mixture was stirred for 24h. After evaporation of the solvent *in vacuo* the crude material was purified by silica column chromatography (*n*-hex:CH_2Cl_2, 1:1) affording the substituted compound (10 mg, 0.023 mmol, 27%) as a colourless oil.

^{1}H NMR (400 MHz, $CDCl_3$) δ 7.43 – 7.09 (m, 15H, CH-Ph), 5.43 (t, *J* = 6.3 Hz, 1H, NH), 5.16 – 5.03 (m, 2H, CH_2-C1), 4.64 (t, *J* = 6.1 Hz, 1H, NH), 4.26 (dd, *J* = 14.1, 6.1 Hz, 1H, CH_2-C6a), 4.10 (dd, *J* = 14.1, 6.1 Hz, 1H, CH_2-C6b), 3.65 (ddd, *J* = 15.0, 6.3, 2.3 Hz, 1H, CH_2-C3a), 3.50 (ddd, *J* = 15.0, 6.3, 6.3 Hz, 1H, CH_2-C3b), 3.31 – 3.20 (m, 2H, CH_2-C5a, CH-C4), 2.92 –2.80 (m, 1H, CH_2-C5b).

^{13}C NMR (101 MHz, $CDCl_3$) δ 156.6 (C-C2), 136.7 (C-Ph), 136.4 (C-Ph), 129.2 (CH-Ph), 129.0 (CH-Ph), 128.7 (CH-Ph), 128.3 (CH-Ph), 128.2 (CH-Ph), 127.4 (CH-Ph), 67.1 (CH_2-C1), 63.7 (CH-C4), 47.6 (CH_2-C6), 39.7 (CH_2-C3), 33.5 (CH_2-C5).

HRMS (ESI positive) calcd for $C_{24}H_{26}N_2NaO_4S$ $[M+Na]^+$ 461.1505, found 461.1489.

Piperidine substituted compound from 70

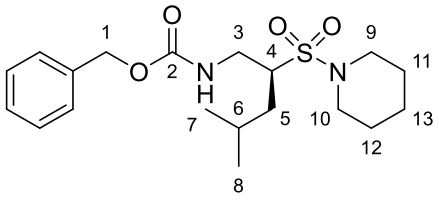

Chemical Formula: $C_{19}H_{30}N_2O_4S$
Molecular Weight: 382.52

Cbz-Leu-SO_2F **70** (26 mg, 0.08 mmol) was dissolved in CH_2Cl_2 (1 mL) at RT and piperidine (18 µL, 0.18 mmol) was added. The reaction mixture was stirred for 24h. After evaporation of the solvent *in vacuo* the crude material was purified by silica column chromatography (*n*-hex:CH_2Cl_2, 1:1→3:7) affording the substituted compound (22 mg, 0.057mmol, 72%) as an off-white solid.

^{1}H NMR (500 MHz, $CDCl_3$) δ 7.43 – 7.26 (m, 5H, CH-Ph), 5.64 (t, *J* = 6.2 Hz 1H, NH), 5.13 (d, *J* = 12.3 Hz, 1H, CH_2-C1a), 5.09 (d, *J* = 12.3 Hz, 1H, CH_2-C1b), 3.64 (ddd, *J* = 14.9, 6.2, 3.0 Hz, 1H, CH_2-C3a), 3.51 (ddd, *J* = 14.9, 7.5, 6.2 Hz,, 1H, CH_2-C3b), 3.28 (br s, 4H, CH_2-C9, C10), 3.05 (app dt, *J* = 7.5, 3.0 Hz, 1H, CH-C4), 1.84 – 1.74 (m, 1H, CH-C6), 1.67 – 1.55 (m, 5H, CH_2-C11, C12, C13), 1.56 – 1.41 (m, 2H, CH_2-C5), 0.94 (d, *J* = 6.6 Hz, 3H, CH_3-C7), 0.92 (d, *J* = 6.6 Hz, 3H, CH_3-C8).

^{13}C NMR (126 MHz, $CDCl_3$) δ 156.4 (C-C2), 136.5 (C-Ph), 128.5 (CH-Ph), 128.1 (CH-Ph), 128.0 (CH-Ph), 66.8 (CH_2-C1), 59.9 (CH-C4), 47.0 (CH_2-C9, C10), 39.5 (CH_2-C3), 35.3 (CH_2-C5), 26.0 (CH_2-C11, C12), 25.2 (CH-C6), 23.8 (CH_2-C13), 23.4 (CH_3-C7), 21.5 (CH_3-C8).

HRMS (ESI positive) calcd for $C_{19}H_{30}N_2NaO_4S$ $[M+Na]^+$ 405.1818, found 405.1816.

Piperidine substituted compound from 27c

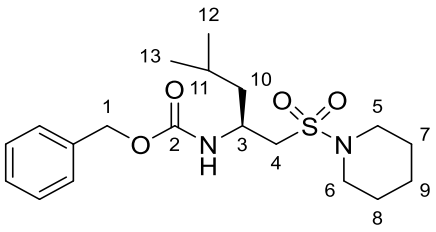

Chemical Formula: $C_{19}H_{30}N_2O_4S$
Molecular Weight: 382.52

Cbz-Leu-SO_2F **27c** (30 mg, 0.09 mmol) was dissolved in CH_2Cl_2 (1 mL) at RT and piperidine (21 µL, 0.21 mmol) was added. The reaction mixture was stirred for 24h. After evaporation of the solvent *in vacuo* the crude material was purified by silica column chromatography (*n*-hex:CH_2Cl_2, 1:1→3:7), affording the substituted compound (16 mg, 0.042mmol, 47%) as an off-white solid.

^{1}H NMR (400 MHz, Chloroform-*d*) δ 7.40 – 7.23 (m, 5H, CH-Ph), 5.23 (d, *J* = 8.9 Hz, 1H, NH), 5.15 – 5.05 (m, 2H, CH_2-C1), 4.11 (app td, *J* = 8.9, 5.2 Hz, 1H, CH-C3), 3.24 – 3.12 (m, 5H, CH_2-C4a, C5, C6), 3.04 (dd, *J* = 14.1, 5.2 Hz, 1H, CH_2-C4b), 1.75 – 1.46 (m, 9H, CH_2-C7, C8, C9, C10, CH-C11), 0.94 (d, *J* = 6.1 Hz, 3H, CH_3-C12), 0.92 (d, *J* = 6.1 Hz, 3H, CH_3-C13).

^{13}C NMR (101 MHz, $CDCl_3$) δ 155.7 (C-C2), 136.4 (C-Ph), 128.5 (CH-Ph), 128.1 (CH-Ph), 128.0 (CH-Ph), 66.7 (CH_2-C1), 52.3 (CH_2-C4), 46.5 (CH_2-C5, C6), 46.2 (CH-C3), 42.8 (CH_2-C10), 25.5 (CH_2-C7, C8), 24.9 (CH-C11), 23.7 (CH_2-C9), 22.9 (CH_3-C12), 21.8 (CH_3-C13).

HRMS (ESI positive) calcd for $C_{19}H_{30}N_2NaO_4S$ $[M+Na]^+$ 405.1818, found 405.1821.

Cbz-Leucine 101

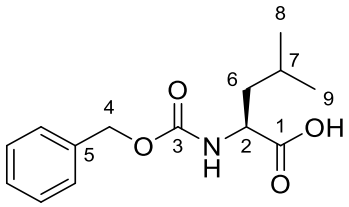

Chemical Formula: $C_{14}H_{19}NO_4$
Molecular Weight: 265.31

L-Leucine **79** (7.9 g, 60 mmol) was dissolved in a 2 M NaOH aq. solution (30 mL, 60 mmol) and cooled to 0 °C. Benzyl chloroformate (8.5 mL, 66 mmol) and a 2 M NaOH aq. solution (33 mL, 66 mmol) were simultaneously added dropwise to the mixture. After 1 h the mixture was warmed to RT and the reaction was stirred overnight. EtOAc (100 mL) was added and the mixture was acidified to pH 2 with a 1 M $KHSO_4$ aq. solution (100 mL). The layers were separated and the aqueous phase was extracted with EtOAc (3 x 200 mL). The combined organic extracts were washed with brine (1 x 200 mL), dried over $MgSO_4$, filtered and the solvent removed *in vacuo*, to afford the product **101** as a colourless oil (14 g, 53 mmol, 88%).

^{1}H NMR (500 MHz, $CDCl_3$) δ 9.73 (br s, 1H, COOH), 7.36 – 7.29 (m, 5H, CH-Ph), 5.21 (d, J = 9.1 Hz, 1H, NH), 5.12 – 5.06 (m, 2H, CH_2-C4), 4.42 (app td, J = 9.1, 4.9 Hz, 1H, CH-C2), 1.82 – 1.72 (m, 1H, CH-C7), 1.70– 1.59 (m, 1H, CH_2-C6a), 1.56 (ddd, J = 13.6, 9.4, 4.9 Hz, 1H, CH_2-C6b), 0.96 (m, 6H, CH_3-C8, C9).

^{13}C NMR (126 MHz, $CDCl_3$) δ 177.9 (C-C1), 156.0 (C-C3), 136.0 (C-C5), 128.4 (CH-Ph), 128.1 (CH-Ph), 127.9 (CH-Ph), 67.0 (CH_2-C4), 52.3 (CH-C2), 41.3 (CH_2-C6), 24.7 (CH-C7), 22.7(CH_3-C8), 21.6 (CH_3-C9).

HRMS (CI iso-butane) calcd for $C_{14}H_{20}NO_4$ $[M+H]^+$ 266.1392, found 266.1393.

Spectroscopic data are in accordance with literature.[53]

Cbz-Leu-Leu-OMe 102

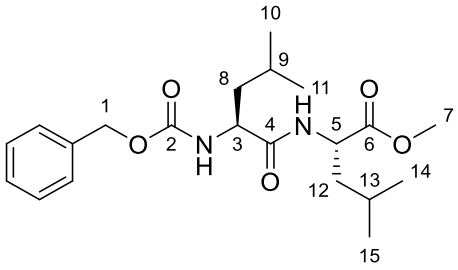

Chemical Formula: $C_{21}H_{32}N_2O_5$
Molecular Weight: 392.50

L-Leucine **79** (3.93 g, 30 mmol) was dissolved in MeOH (30 mL) and cooled to 0 °C. $SOCl_2$ (2.17 mL, 30 mmol) was added dropwise and the reaction mixture was warmed to RT and stirred overnight. The solvent was removed *in vacuo* to deliver HCl·H-Leu-OMe ester **100** (5.4 g, quant.) as a white solid.

HCl·H-Leu-OMe ester **100** (2.72 g, 15 mmol) and Cbz-Leu-OH **101** (3.98 g, 15 mmol) were dissolved in CH_2Cl_2 (600 mL) and BOP reagent (6.96 g, 15.75 mmol) and DiPEA (5.7 mL, 31.5 mmol) added. The reaction was stirred at RT overnight. The solvent was removed *in vacuo* and the residue dissolved in EtOAc (500 mL). The mixture was neutralised by addition of a 1 M $KHSO_4$ aq. solution (500 mL). The layers were separated and the organic phase was washed with a 1 M $KHSO_4$ aq. solution (2 × 500 mL), brine (1 × 300 mL), dried over $MgSO_4$, filtered and the solvent removed *in vacuo*. The crude material was purified by silica column chromatography (*n*-hex:EtOAc, 6:1→3:1) to afford the desired compound **102** (4.62 g, 12 mmol, 80%) as a white solid.

^{1}H NMR (400 MHz, $CDCl_3$) δ 7.41 – 7.26 (m, 5H, CH-Ph), 6.46 (d, *J* = 8.6 Hz, 1H, NH next to C5), 5.29 (d, *J* = 8.5 Hz, 1H, NH next to C3), 5.10 (s, 2H, CH_2-C1), 4.59 (app td, *J* = 8.6, 5.1 Hz, 1H, CH-C5), 4.23 (app td, *J* = 8.5, 4.9 Hz, 1H, CH-C3), 3.72 (s, 3H, CH_3-C7), 1.79 – 1.45 (m, 6H, CH_2-C8, C12, CH-C9, C13), 1.00 – 0.86 (m, 12H, CH_3-C10, C11, C14, C15).
^{13}C NMR (101 MHz, $CDCl_3$) δ 173.6 (C-C4), 172.4 (C-C6), 156.6 (C-C2), 136.6 (C-Ph), 128.9 (CH-Ph), 128.6 (CH-Ph), 128.4 (CH-Ph), 67.5 (CH_2-C1), 53.8 (CH-C3), 52.7 (CH_3-C7), 51.1 (CH-C5), 41.9 (CH_2-C8), 41.8 (CH_2-C12), 25.2 (CH-C9), 25.0 (CH-C13), 23.3 (CH_3-C10), 23.2 (CH_3-C11), 22.5 (CH_3-C14), 22.3 (CH_3-C15).

HRMS (ESI positive) calcd for $C_{21}H_{32}N_2NaO_5$ $[M+Na]^+$ 415.2203, found 415.2184.

Spectroscopic data are in accordance with literature.[53]

Cbz-Leu-Leu-OH 103

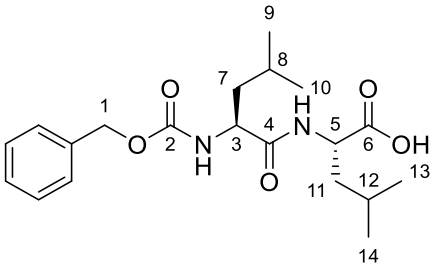

Chemical Formula: $C_{20}H_{30}N_2O_5$
Molecular Weight: 378.47

Cbz-Leu-Leu-OMe **102** (4.62 g, 12 mmol) was dissolved in dioxane (91 mL), MeOH (32 mL) and a 2 M NaOH aq. solution (7 mL) were added and the reaction was stirred at RT overnight. The mixture was acidified to pH 2 with a 1 M $KHSO_4$ aq. solution and solvents were removed *in vacuo*. EtOAc was added (250 mL) and the layers were separated. The aqueous phase was extracted with EtOAc (2 × 250 mL) and the combined organic extracts were washed with water (1 × 500 mL) and brine (1 × 300 mL), dried over $MgSO_4$, filtered and the solvent removed *in vacuo* to afford in the desired compound **103** (4.30 g, 95%) as a white solid.

^{1}H NMR (400 MHz, $CDCl_3$) δ 7.41 – 7.21 (m, 5H, CH-Ph), 6.64 (d, *J* = 8.0 Hz, 1H, NH next to C5), 5.42 (d, *J* = 8.3 Hz, 1H, NH next to C3), 5.10 (s, 2H, CH_2-C1), 4.56 (app td, *J* = 8.0, 5.0 Hz, 1H, CH-C5), 4.32 – 4.16 (m, 1H, CH-C3), 1.76 – 1.46 (m, 6H, CH_2-C7, C11, CH-C8, C12), 0.92 (m, 12H, CH_3-C9, C10, C13, C14).

^{13}C NMR (101 MHz, $CDCl_3$) δ 175.7 (C-C6), 172.4 (C-C4), 156.3 (C-C2), 128.4 (CH-Ph), 128.1 (CH-Ph), 127.8 (CH-Ph), 67.0 (CH_2-C1), 53.2 (CH-C3), 50.8 (CH-C5), 40.8 (CH_2-C7, C11), 24.7 (CH-C8), 24.4 (CH-C12), 22.6 (CH_3-C9), 21.8 (CH_3-C10), 21.6 (CH_3-C13, C14).

HRMS (ESI positive) calcd for $C_{20}H_{30}N_2NaO_5$ $[M+Na]^+$ 401.2047, found 401.2033.

Spectroscopic data are in accordance with literature.[53]

Cbz-Leu-Leu-Leu-OMe 106

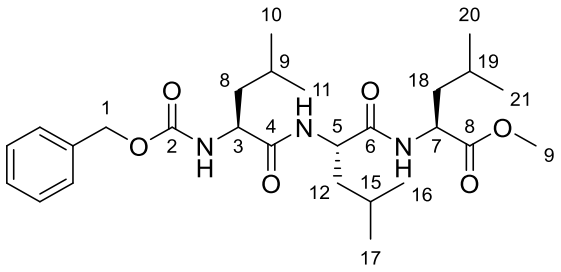

Chemical Formula: $C_{27}H_{43}N_3O_6$
Molecular Weight: 505.66

L-Leucine **79** (3.93 g, 30 mmol) was dissolved in MeOH (30 mL) and cooled to 0 °C. $SOCl_2$ (2.17 mL, 30 mmol) was added dropwise and the reaction mixture was warmed to RT and stirred overnight. The solvent was removed *in vacuo* to deliver HCl·H-Leu-OMe ester **100** (5.4 g, quant.) as a white solid.

HCl·H-Leu-OMe ester **100** (2.72 g, 15 mmol) and Boc-Leu-OH **104** (3.46 g, 15 mmol) were dissolved in CH_2Cl_2 (600 mL) and BOP reagent (6.96 g, 15.75 mmol) and DiPEA (5.7 mL, 31.5 mmol) added. The reaction was stirred at RT overnight. The solvent was removed *in vacuo* and the residue dissolved in EtOAc (500 mL). The mixture was neutralised by addition of a 1 M $KHSO_4$ aq. solution (500 mL). The layers were separated and the organic phase was washed with a 1 M $KHSO_4$ aq. solution (2 × 500 mL) and brine (1 × 500 mL), dried over $MgSO_4$ and filtered. Evaporation of the solvent *in vacuo* afforded Boc-Leu-Leu-OMe **105** (4.30 g, 12mmol, 80%) as a white solid.

Boc-Leu-Leu-OMe **105** (4.30 g, 12 mmol) was dissolved in CH_2Cl_2 (50 mL) at RT and TFA (50 mL) added. The mixture was stirred for 2 h. After evaporation of the solvent *in vacuo* and co-evaporation with $CHCl_3$ (3×50 mL), the crude TFA-salt was directly dissolved in CH_2Cl_2 (480 mL) and Cbz-Leu-OH **101** (3.18 g, 12 mmol), BOP reagent (5.57 g, 12.6 mmol) and DiPEA (4.4 mL, 25.2 mmol) were added. The reaction was stirred at RT overnight. The solvent was removed *in vacuo* and the residue dissolved in EtOAc (500 mL). The mixture was neutralised by addition of a 1 M $KHSO_4$ aq. solution (500 mL). The layers were separated and the organic phase was washed with a 1 M $KHSO_4$ aq. solution (2 × 500 mL) and brine (1 × 500 mL), dried over $MgSO_4$, filtered and the solvent removed *in vacuo*. The crude material was purified by silica column chromatography (*n*-hex:EtOAc, 5:1→2:1) to afford the desired compound **106** (5.15 g, 10.2 mmol, 85%) as an off-white solid.

^{1}H NMR (400 MHz, $CDCl_3$) δ 7.41 – 7.27 (m, 5H, CH-Ph), 6.55 (d, *J* = 8.2 Hz, 1H, NH), 6.44 (d, *J* = 8.2 Hz, 1H, NH), 5.25 (d, *J* = 8.1 Hz, 1H, NH), 5.10 (s, 2H, CH_2-C1), 4.58 (td, *J* = 8.2, 4.8 Hz, 1H, CH-C5), 4.46 (td, *J* = 8.2, 6.0 Hz, 1H, CH-C7), 4.25 – 4.13 (m, 1H, CH-C3), 3.72 (s, 3H, CH_3-C9), 1.78 – 1.42 (m, 9H, CH_2-C8, C12, C18, CH-C9, C15, C19), 1.01 – 0.78 (m, 18H, CH_3-C10, C11, C16, C17, C20, C21).
^{13}C NMR (101 MHz, $CDCl_3$) δ 173.0 (C-C4), 172.2 (C-C6), 171.4 (C-C8), 156.2 (C-C2), 136.1 (C-Ph), 128.6 (CH-Ph), 128.3 (CH-Ph), 128.0 (CH-Ph), 67.1 (CH_2-C1), 53.4 (CH-C3), 52.3 (CH_3-C9), 51.6 (CH-C7), 50.7 (CH-C5), 41.3, 40.6 (CH_2-C10, C14, C18), 24.7 (CH-C11, C15, C19), 22.8, 22.7, 22.1, 21.9, 21.8 (CH_3-C12, C13, C16, C17, C20, C21).

HRMS (ESI positive) calcd for $C_{27}H_{43}N_3NaO_6$ $[M+Na]^+$ 528.3044, found 528.3014.

Spectroscopic data are in accordance with literature.[126]

Cbz-Leu-Leu-Leu-OH 107

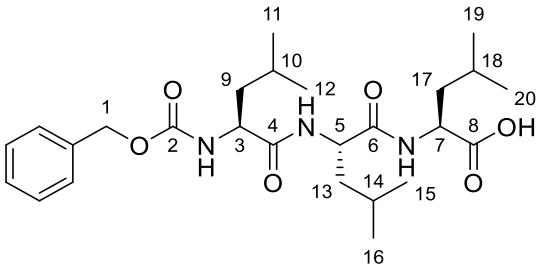

Chemical Formula: $C_{26}H_{41}N_3O_6$
Molecular Weight: 491.63

Cbz-Leu-Leu-Leu-OMe **106** (5.15 g, 10.2 mmol) was dissolved in dioxane (84 mL), MeOH (30 mL) and a 4 M NaOH aq. solution (12 mL) were added and the reaction was stirred at RT overnight. The mixture was acidified to pH 2 with a 1 M $KHSO_4$ aq. solution and solvents were removed *in vacuo*. EtOAc was added (250 mL) and the layers were separated. The aqueous phase was extracted with EtOAc (1 × 250 mL) and the combined organic extracts were washed with water (1 × 500 mL) and brine (1 × 300 mL), dried over $MgSO_4$, filtered and the solvent removed *in vacuo* to afford the desired compound **107** (4.76 g, 9.7 mmol, 95%) as a white solid.

^{1}H NMR (500 MHz, $CDCl_3$) δ 7.39 – 7.22 (m, 5H, CH-Ph), 7.07 (br s, 1H, NH), 5.56 (br s, 1H, NH), 5.10 (d, *J* = 12.1 Hz, 1H, CH_2-C1a), 5.05 (d, *J* = 12.1 Hz, 1H, CH_2-C1b), 4.62 – 4.42 (m, 2H, CH-C5, C7), 4.29 – 4.18 (m, 1H, CH-C3), 1.76 – 1.46 (m,

9H, CH_2-C9, C13, C17, CH-C10, C14, C18), 0.93 – 0.83 (m, 18H, CH_3-C111, C12, C15, C16, C19, C20).

^{13}C NMR (126 MHz, $CDCl_3$) δ 175.2 (C-C8), 172.9 (C-C4), 172.3 (C-C6), 156.5 (C-C2), 136.0 (C-Ph), 128.6 (CH-Ph), 128.3 (CH-Ph), 128.0 (CH-Ph), (CH-Ph), 67.2 (CH_2-C1), 53.7 (CH-C3), 52.0 (CH-7), 51.0 (CH-C5), 41.2 (CH_2-C9), 40.8 (CH_2-C13), 40.6 (CH_2-C17), 24.8 (CH-C10), 24.7 (CH-C14), 24.6 (CH-C18), 22.8 (CH_3-C11), 22.7 (CH_3-C12), 22.1 (CH_3-C15), 21.9 (CH_3-C16), 21.7 (C19, C20).

HRMS (ESI positive) calcd for $C_{26}H_{41}N_3NaO_6$ $[M+Na]^+$ 514.2888, found 514.2865.

Morph-hPhe-Leu-Phe-OH 116

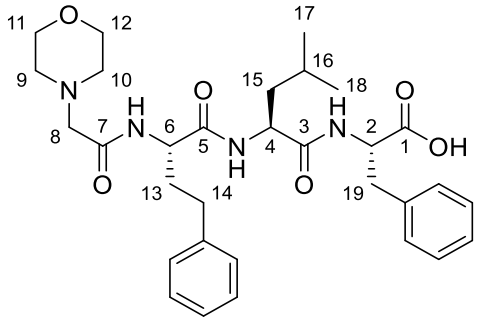

Chemical Formula: $C_{31}H_{42}N_4O_6$
Molecular Weight: 566.70

2-Cl-Tritylchloride resin (3g) and Fmoc-Phe-OH **108** (775 mg, 2 mmol) were suspended in CH_2Cl_2 (50 mL) and DiPEA (0.35 mL, 2 mmol) was added to the mixture. After 5 min another portion of DiPEA (0.52 mL, 2.5 mmol) was added and the reaction mixture stirred at RT overnight. Remaining 2-Cl-tritylchloride on the resin was capped by addition of MeOH (5 mL) and DiPEA (1.2 mL) were added to the mixture which was stirred for 30 min. The mixture was then transferred to a plastic solid phase synthesis syringe and washed with CH_2Cl_2 (3 × 15 mL), MeOH (3 × 15 mL) and Et_2O (3 × 15 mL). The resin was dried *in vacuo* for 3 h, affording the crude product Fmoc-Phe-resin **109** (3.82 g, 0.82 mmol, 41%). The resin was shaken with 20% piperidine in DMF (2 × 10 mL) for 15 min. The deprotected resin was washed with DMF (3 × 15 mL) and CH_2Cl_2 (3 × 15 mL) and suspended in DMF (30 mL). Fmoc-Leu-OH **110** (870 mg, 2.46 mmol), HCTU reagent (1.02g, 2.46 mmol) and DiPEA (0.4 mL, 2.46 mmol) were added and the reaction mixture shaken overnight. The deprotection sequence was repeated and the resin **11** was suspended in DMF (30 mL) and shaken with Fmoc-hPhe-OH **112** (1 g, 2.46 mmol),

HCTU reagent (1.02g, 2.46 mmol) and DiPEA (0.4 mL, 2.46 mmol) overnight. The deprotection sequence was repeated and the resin **113** was capped with 2-morpholino acetic acid **114** (500 mg, 5.5 mmol), HCTU reagent (1.02g, 2.46 mmol) and DiPEA (0.4 mL, 2.46 mmol) in DMF (30 mL) overnight. Finally, the peptide was cleaved from the resin **115** by treatment with 30% HFIP in CH_2Cl_2 (30 mL) at RT for 30 min. The resin was washed with CH_2Cl_2 (3 × 30 mL) and the solvent removed *in vacuo*. The residue was dissolved in a 1:1 mixture of water and *t*-BuOH (30 mL) and freeze dried. The crude product was purified by preparative HPLC (0%B to 80%B-buffer in 60 min) affording the desired compound **116** (382 mg, 0.67 mmol, 81% over 7 steps) as a white solid.

^{1}H NMR (500 MHz, $CDCl_3$) δ 9.21 (br s, 1H, NH), 8.43 (d, *J* = 8.0 Hz, 1H, NH), 7.57 (d, *J* = 7.5 Hz, 1H, NH), 7.32 – 6.98 (m, 10H, Ph), 4.66 (dt, *J* = 14.0, 7.5 Hz, 1H, CH-C4), 4.38 (dt, *J* = 14.0, 8.0 Hz, 1H, CH-C6), 4.26 (app dt, *J* = 13.2, 6.2 Hz, 1H, CH-C2), 4.01 (d, *J* = 15.8 Hz, 1H, CH_2-C8a), 3.92 (br s, 4H, CH_2-C11, C12), 3.81 (d, *J* = 15.8 Hz, 1H, CH_2-C8b), 3.33 (br s, 4H, CH_2-C9, C10), 3.22 (dd, *J* = 13.8, 6.2 Hz, 1H, CH_2-C19a), 2.97 (dd, *J* = 13.8, 9.2 Hz, 1H, CH_2-C19b), 2.81 – 2.71 (m, 1H, CH_2-C14a), 2.71 – 2.61 (m, 1H, CH_2-C14b), 2.15 – 1.99 (m, 2H, CH_2-C13), 1.49 – 1.40 (m, 1H, CH-C16), 1.39 – 1.23 (m, 2H, CH_2-C15), 0.76 (d, *J* = 6.0 Hz, 3H, CH_3-C17), 0.72 (d, *J* = 6.0 Hz, 3H, CH_3-C18).

^{13}C NMR (126 MHz, $CDCl_3$) δ 174.6 (C-C1), 173.2 (C-C5), 172.8 (C-C3), 164.4 (C-C7), 140.2 (C-Ph), 136.4 (C-Ph), 129.3 (CH-Ph), 128.6 (CH-Ph), 128.5 (CH-Ph), 128.4 (CH-Ph), 126.9 (CH-Ph), 126.4 (CH-Ph), , 63.4 (CH_2-C11, C12), 57.5 (CH_2-C8), 55.9 (CH-C2), 53.9 (CH-C4), 53.5 (CH-C6), 53.0 (CH_2-C9, C10), 40.4 (CH_2-C15), 37.5 (CH_2-C13), 33.6 (CH_2-C14), 32.2 (CH_2-C19), 24.7 (CH-C16), 22.5 (CH_3-C17), 21.6 (CH_3-C18).

HRMS (ESI positive) calcd for $C_{31}H_{42}N_4NaO_6$ $[M+Na]^+$ 589.2997, found 589.2976.

t_R = 36.3 min (Gemini column C18, 10 µm, 250 x 21.2 mm, 30B to 100B in 80 min).

Spectroscopic data are in accordance with literature.[99]

General coupling procedure

The Cbz-protected sulfonyl fluoride **70** or **71** was treated with a 1:1 mixture of a 30% HBr/HOAc solution:CH_2Cl_2 at RT for 1 h. After evaporation of the solvents *in vacuo*, the crude product was dissolved in water, stirred with Dowex-Cl resin (60 mg/0.1 mmol crude product) for 10 min and freeze dried, affording the deprotected salt. The salt was dissolved in THF and treated with Zn powder (2 eq) at RT for 30 min generating the free amine *in situ*. The solution was filtered and added to a mixture of the peptide backbone **103**, **107** or **116** (1 eq), DCC (1.1 eq) and HOBt-Cl (1.1 eq) in THF, which had been previously pre-activated for 10 min. The reaction was stirred at RT overnight. After removal of the solvent *in vacuo*, the crude product was dissolved in buffer A:B (1:3) and purified by preparative HPLC affording the desired compound.

Cbz-Leu-Leu-[Leu-SO_2F] 120

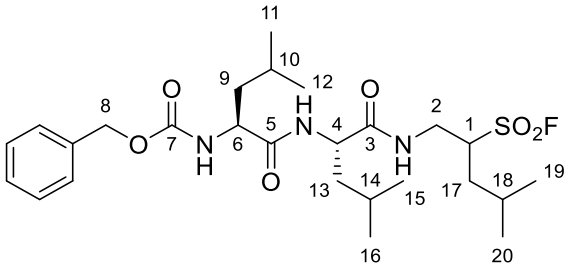

Chemical Formula: $C_{26}H_{42}FN_3O_6S$
Molecular Weight: 543.70

The general procedure was followed on a 0.157 mmol scale delivering the desired product **120** as a 2.5:1 mixture of diasteroisomers (15 mg, 0.027 mmol, 18%) as a white solid.

^{1}H NMR (400 MHz, $CDCl_3$) δ 7.40 – 7.30 (m, 5H, CH-Ph, CH-Ph*), 7.13 (s, 0.7H, NH), 6.95 (s, 0.3H, NH*), 6.47 (d, *J* = 8.0 Hz, 0.3H, NH*), 6.41 (d, *J* = 8.0 Hz, 0.7H, NH), 5.18 – 5.08 (m, 3H, NH, NH*, CH_2-C8, CH_2-C8*), 4.50 – 4.35 (m, 1H, CH-C4, CH-C4*), 4.18 – 4.09 (m, 1H, CH-C6, CH-C6*), 3.83 – 3.69 (m, 1.7H, CH_2-C2a, CH_2-C2a*, CH-C1), 3.65 – 3.48 (m, 1.3H, CH_2-C2b, CH_2-C2b*, CH-C1*), 1.97 – 1.43 (m, 9H, CH_2-C9, C13, C17, CH-C10 C14, C18, CH_2-C9*, C13*, C17*, CH-C10*, C14*, C18*), 1.05 – 0.84 (m, 18H, CH_3-C11, C12, C15, C16, C19, C20, CH_3-C11*, C12*, C15*, C16*, C19*, C20*).

^{13}C NMR (101 MHz, $CDCl_3$) δ 172.6, 172.4, 172.3 (C-C5, C3, C-C5*, C3*), 156.8 (C-C7, C-C7*), 135.9 (C-Ph*), 135.8 (C-Ph), 128.6, 128.4, 128.3, 128.2, 128.1 (CH-Ph, CH-Ph*)), 67.6 (CH_2-C8), 67.4 (CH_2-C8*), 61.0 (d, *J* = 9.4 Hz, CH-C1*), 60.5 (d, *J* = 9.7 Hz, CH-C1) 54.2 (CH-6), 53.9 (CH-C6*), 52.0 (CH-C4*), 51.7 (CH-C4), 40.7, 40.2, 40.1 (CH_2-C9, C13, CH_2-C9*, C13*), 38.7 (CH_2-C2, C2*), 35.9(CH_2-C17, CH_2-C17*), 25.3, 24.9, 24.8, 24.7 (CH-C10, C14, C18, CH-C10*, C14*, C18*), 22.9, 22.7, 21.7, 21.6, 21.5, 21.4 (CH_3-C11, C12, C15, C16, C19, C20).

^{19}F NMR (377 MHz, $CDCl_3$) δ 48.8, 48.4 (2 s).

HRMS (ESI positive) calcd for $C_{26}H_{42}FN_3NaO_6S$ $[M+Na]^+$ 566.2671, found 566.2647.

t_R = 53.8 min (Gemini column C18, 10 µm, 250 x 21.2 mm, 0B to 100B in 80 min).

Cbz-Leu-Leu-[Phe-SO_2F] 121

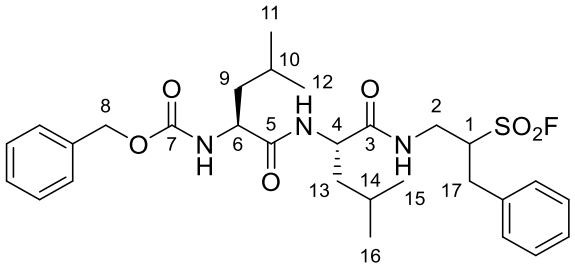

Chemical Formula: $C_{29}H_{40}FN_3O_6S$
Molecular Weight: 577.71

The general procedure was followed on a 0.14 mmol scale to afford the desired product **121** (10 mg, 0.017 mmol, 12%) as a 4:1 mixture of diasteroisomers as a white solid.

^{1}H NMR (500 MHz, $CDCl_3$) δ 7.35 – 7.22 (m, 10.2H, CH-Ph, CH-Ph*, NH*), 7.08 – 7.00 (br s, 0.8H, NH), 6.80 (br s, 0.2H, NH*), 6.30 (br s, 1H, NH, NH*), 5.17 – 5.09 (m, 2H, CH_2-C8, CH_2-C8*), 5.08 – 5.03 (br s, 0.8H, NH), 4.36 (m, 1H,CH-C4, CH-C4*), 4.09 (m, 1.6H, CH-C6, CH-C1), 3.91 (m, 0.4H, CH-C6*, C1*), 3.73 (m, 1H, CH_2-C2a, CH_2-C2a*), 3.56 (app dt, *J* = 14.6, 7.0 Hz, 1H, CH_2-C2b, CH_2-C2b*), 3.39 (dd, *J* = 14.5, 4.9 Hz, 1H, CH_2-C17a, CH_2-C17a*), 2.99 (dd, *J* = 14.5, 9.3 Hz, 1H, CH_2-C17b, CH_2-C17b*), 1.79 – 1.42 (m, 6H, CH_2-C9, C13, CH-C10, C14, CH_2-C9*, C13*, CH-C10*, C14*), 0.97 – 0.85 (m, 12H, CH_3-C11, C12, C15, C16, CH_3-C11*, C12*, C15*, C16*).

^{13}C NMR (101 MHz, $CDCl_3$) δ 172.5, 172.2 (C-C4, C6, C-C4*, C6*), 156.8 (C-C7, C-C7*), 135.8, 135.7 , 134.6 (C-Ph, C-Ph*), 129.1, 129.0, 128.6, 128.4, 128.2, 128.1, 127.7 (CH-Ph, CH-Ph*), 67.6 (CH_2-C8), 67.4 (CH_2-C8*), 63.4 (CH-C1*), 62.8 (d, *J* = 8.6 Hz, CH-C1), 54.2 (CH-C6, CH-C6*), 51.9 (CH-C4*), 51.7 (CH-C4), 40.6, 40.2, 40.0 (CH_2-C9, C13, CH_2-C9*, C13*), 38.2 (CH_2-C2), 37.9 (CH_2-C2*), 33.4 (CH_2-C17, CH_2-C17*), 24.9, 24.8, 24.7 (CH-C10, C14, CH-C10*, C14*), 22.9, 21.7, 21.5 (CH_3-C11, C12, C15, C16, CH_3-C11*, C12*, C15*, C16*).

^{19}F NMR (377 MHz, $CDCl_3$) δ 51.3, 50.8 (2 s).

HRMS (ESI positive) calcd for $C_{29}H_{40}FN_3NaO_6S$ $[M+Na]^+$ 600.2514, found 600.2492.

t_R = 44.0 min (Gemini column C18, 10 µm, 250 x 21.2 mm, 10B to 100B in 80 min).

Cbz-Leu-Leu-[Phe-SO_2F] 121

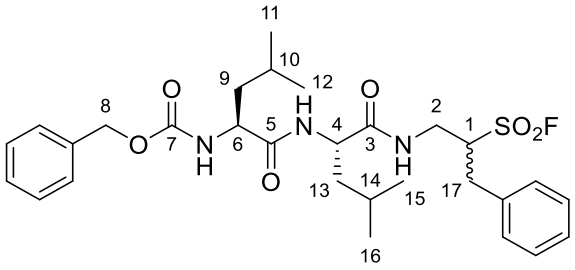

Chemical Formula: $C_{29}H_{40}FN_3O_6S$
Molecular Weight: 577.7124

(±)-Cbz-protected sulfonyl fluoride **71** (50 mg, 0.14 mmol) was dissolved in with a 1:1 mixture of a 30% HBr/HOAc solution:CH_2Cl_2 (8 mL) at RT and the mixture stirred for 1 h. After evaporation of the solvents *in vacuo*, the crude material was dissolved in water (4 mL), stirred with Dowex-Cl resin (70 mg) for 10 min and freeze dried to afford the deprotected salt. The salt was added to a mixture of Cbz-Leu_2-OH **103** (49 mg, 0.13 mmol), BOP (61 mg, 0.14 mmol) and DiPEA (48 µL, 0.27 mmol) in CH_2Cl_2 (4 mL). The reaction mixture was stirred at RT overnight. Solvent was removed *in vacuo* and the crude material was dissolved in EtOAc (25 mL) and a 1 M $KHSO_4$ aq. solution (25 mL) was added. The layers were separated and the organic phase was washed with a 1 M $NaHCO_3$ aq. solution (1 x 25 mL) and brine (1 x 25 mL), dried over $MgSO_4$, filtered and the solvent removed *in vacuo*. The crude product was dissolved in buffer A:B (1:3) and purified by preparative HPLC (30B to 100B in 80 min) affording the desired compound **121** (12 mg, 0.021 mmol, 15%) as a 1.2:1mixture of diasteroisomers as a white solid.

^{1}H NMR (400 MHz, $CDCl_3$) δ 7.35 – 7.22 (m, 0H, CH-Ph, CH-Ph*), 7.17 (d, *J* = 6.0 Hz, 0.55H, NH), 6.70 (d, *J* = 7.9 Hz, 0.45H, NH*), 6.64 (d, *J* = 7.9 Hz, 0.45H, NH*), 5.42 (d, *J* = 6.9 Hz, 0.55H, NH), 5.38 (d, *J* = 6.9 Hz, 1H, NH, NH*), 5.17 – 5.01 (m, 2H, CH_2-C8, CH_2-C8*), 4.41 (td, *J* = 8.8, 5.3 Hz, 1H, CH-C4, CH-C4*), 4.21 – 4.10 (m, 0.55H, CH-C6), 4.07 – 4.02 (m, 1H, CH-C1, CH-C6*), 3.96 – 3.90 (m, 0.45H, CH-C1*), 3.75 – 3.62 (m, 1H, CH_2-C2a, CH_2-C2a*), 3.56 (app dt, *J* = 14.6, 7.0 Hz, 1H, CH_2-C2b, CH_2-C2b*), 3.35 (app dt, *J* = 14.5, 5.6 Hz, 1H, CH_2-C17a, CH_2-C17a*), 2.99 (dd, *J* = 14.5, 9.3 Hz, 1H, CH_2-C17b, CH_2-C17b*), 1.79 – 1.42 (m, 6H, CH_2-C9, C13, CH-C10, C14, CH_2-C9*, C13*, CH-C10*, C14*), 0.97 – 0.78 (m, 12H, CH_3-C11, C12, C15, C16, CH_3-C11*, C12*, C15*, C16*).

^{13}C NMR (101 MHz, $CDCl_3$) δ 172.5, 172.2 (C-C5, C3, C-C5*, C3*), 156.8, 156.6 (C-C7, C-C7*), 135.8, 135.7, 134.6 (C-Ph, C-Ph*), 129.1, 129.0, 128.6, 128.4, 128.2, 128.1, 128.0, 127.8, 127.7 (CH-Ph, CH-Ph*), 67.7 (CH_2-C8), 67.4 (CH_2-C8*), 63.36 (d, *J* = 8.8 Hz, CH-C1*), 62.83 (d, *J* = 8.6 Hz, CH-C1), 54.2 (CH-C6), 53.8 (CH-C6*), 51.9 (CH-C4*), 51.7 (CH-C4), 40.7, 40.6, 40.2, 40.0 (CH_2-C9, C13, CH_2-C9*, C13*), 38.2 (CH_2-C2*), 37.9 (CH_2-C2), 33.4 (CH_2-C17, CH_2-C17), 24.9, 24.8, 24.7, 24.6 (CH-C10, C14, CH-C10*, C14*), 22.9, 22.8, 21.8, 21.7, 21.6, 21.5 (CH_3-C11, C12, C15, C16, CH_3-C11*, C12*, C15*, C16*).

^{19}F NMR (377 MHz, $CDCl_3$) δ 51.3, 50.8 (2 s).

HRMS (ESI positive) calcd for $C_{29}H_{40}FN_3NaO_6S$ $[M+Na]^+$ 600.2514, found 600.2490.

t_R = 44.1 min (Gemini column C18, 10 µm, 250 x 21.2 mm, 10B to 100B in 80 min).

Cbz-Leu-Leu-[Leu-SO_2F] 120

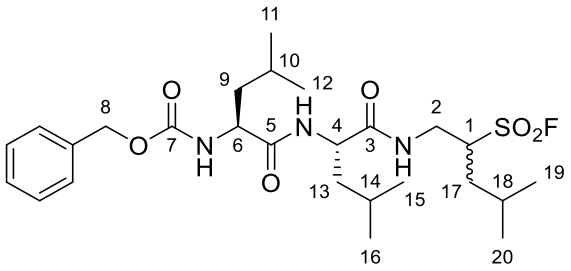

Chemical Formula: $C_{26}H_{42}FN_3O_6S$
Molecular Weight: 543.70

(±)-Cbz-protected sulfonyl fluoride **70** (50 mg, 0.14 mmol) was dissolved in with a 1:1 mixture of a 30% HBr/HOAc solution:CH_2Cl_2 (8 mL) at RT and the mixture stirred for 1 h. After evaporation of the solvents *in vacuo* , the crude material was dissolved in water (4 mL), stirred with Dowex-Cl resin (70 mg) for 10 min and freeze dried to afford the deprotected salt. The salt was added to a mixture of Cbz-Leu_2-OH **103** (49 mg, 0.13 mmol), BOP (61 mg, 0.14 mmol) and DiPEA (48 µL, 0.27 mmol) in CH_2Cl_2 (4 mL) and the reaction mixture was stirred at RT overnight. Solvent was removed *in vacuo* and the crude material was dissolved in EtOAc (25 mL) and a 1 M $KHSO_4$ aq. solution (25 mL) was added. The layers were separated and the organic phase was washed with a 1 M $NaHCO_3$ aq. solution (1 x 25 mL) and brine (1 x 25 mL), dried over $MgSO_4$, filtered and the solvent removed *in vacuo*. The crude product was dissolved in buffer A:B (1:3) and purified by preparative HPLC (30B to 100B in 80 min) affording the desired compound **120** (10 mg, 0.018 mmol, 13%) as a mixture of a 1:3 mixture of diasteroisomers.

^{1}H NMR (400 MHz, $CDCl_3$) δ 7.43 – 7.24 (m, 5H, CH-Ph, CH-Ph*), 7.10 (s, 0.25H, NH), 6.88 (Br s, 0.75H, NH*), 6.40 (d, *J* = 7.9 Hz, 0.75H, NH*), 6.35 (d, *J* = 7.9 Hz, 0.25H, NH), 5.19 – 5.04 (m, 3H, NH, CH_2-C8, NH*, CH_2-C8*), 4.50 – 4.35 (m, 1H, CH-C4, CH-C4*), 4.19 – 4.05 (m, 1H, CH-C6, CH-C6*), 3.86 – 3.71 (m, 1.5H, CH_2-C2, CH_2-C2a*, CH-1), 3.66 – 3.50 (m, 1.5H, CH_2-C2b*, CH-1*), 1.97 – 1.44 (m, 9H, CH_2-C9, C13, C17, CH-C10 C14, C18, CH_2-C9*, C13*, C17,* CH-C10* C14*, C18*), 1.03 – 0.87 (m, 18H, CH_3-C11, C12, C15, C16, C19, C20, CH_3-C11*, C12*, C15*, C16*, C19*, C20*).

^{13}C NMR (101 MHz, $CDCl_3$) δ 172.6, 172.4, 172.3 (C-C5, C3, C-C5*, C3*), 156.8 (C-C7, C-C7*), 135.9 (C-Ph*), 135.8 (C-Ph), 128.6, 128.5, 128.4, 128.2, 128.1 (CH-Ph, CH-Ph*), 67.6 (CH_2-C8), 67.4 (CH_2-C8*), 61.0 (d, *J* = 9.4 Hz, CH-C1*), 60.5 (d, *J* = 9.7 Hz, CH-C1) 54.2 (CH-C6*), 53.9 (CH-C6), 52.0 (CH-C4*), 51.7 (CH-C4), 40.7,

40.2, 40.1 (CH_2-C9, C13, CH_2-C9*, C13*), 38.7 (CH_2-C2), 38.4 (CH_2-C2*), 35.9 (CH_2-C17, CH_2-C17*), 25.3, 25.2, 24.9, 24.8, 24.7 (CH-C10, C14, C18, CH-C10*, C14*, C18*), 23.0, 22.9, 22.7, 22.6, 21.7, 21.5, 21.4 (CH_3-C11, C12, C15, C16, C19, C20, CH_3-C11*, C12*, C15*, C16*, C19*, C20*).

^{19}F NMR (377 MHz, $CDCl_3$) δ 48.8, 48.4 (2 s).

HRMS (ESI positive) calcd for $C_{26}H_{42}FN_3NaO_6S$ $[M+Na]^+$ 566.2671, found 566.2648.

t_R = 53.8 min (Gemini column C18, 10 µm, 250 x 21.2 mm, 0B to 100B in 80 min).

Cbz-Leu-Leu-Leu-[Leu-SO_2F] 122

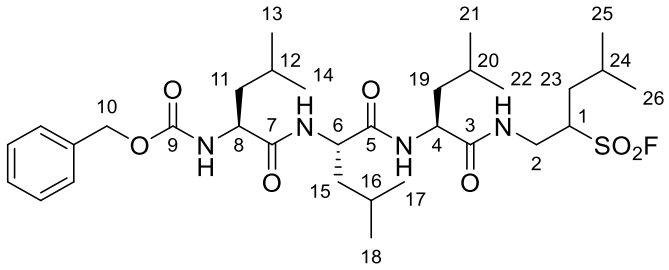

Chemical Formula: $C_{32}H_{53}FN_4O_7S$
Molecular Weight: 656.86

The general procedure was followed on a 0.17 mmol scale to afford the desired product **122** (15 mg, 0.023 mmol, 14%) as a 4:1 mixture of diasteroisomers as a white solid.

^{1}H NMR (500 MHz, $CDCl_3$) δ 7.43 – 7.28 (m, 6H, CH-Ph, NH, CH-Ph*, NH*), 7.17 (br s, 0.2H, NH*), 6.95 (d, *J* = 7.7 Hz, 1H, NH, NH*), 6.46 (br s, 0.8H, NH), 5.21 – 5.05 (m, 3H, NH, CH_2-C10, NH*, CH_2-C10*), 4.45 – 4.37 (m, 1H, CH-C6, CH-C6*), 4.29 – 4.22 (m, 1H, CH-C4, CH-C4*), 4.12 (app dt, *J* = 17.0, 8.5 Hz, 1H, CH-C8, CH-C8*), 3.82 – 3.71 (m, 2H, CH_2-C2a, CH-C1, CH_2-C2a*, CH-C1*), 3.69 – 3.63 (m, 0.2H, CH_2-C2b *), 3.58 – 3.49 (m, 0.8H, CH_2-C2b), 1.98 – 1.44 (m, 12H, CH_2-C11, C15, C19, C23, CH-C12, C16, C20, C24, CH_2-C11, C15, C19, C23, CH-C12*, C16*, C20*, C24*), 1.03 – 0.81 (m, 24H, CH_3-C13, C14, C17, C18, C21, C22, C25, C26, CH_3-C13*, C14*, C17*, C18*, C21*, C22*, C25*, C26*).

^{13}C NMR (126 MHz, $CDCl_3$) δ 173.4, 173.1, 171.8 (C-C7, C5, C3, C-C7*, C5*, C3*), 156.9 (C-C9, C-C9*) , 135.6 (C-Ph, C-Ph*), 128.7, 128.6, 128.0 (CH-Ph, CH-Ph*), 67.6 (CH_2-C10, CH_2-C10*), 60.2 (d, *J* = 8.1 Hz, CH-C1), 54.7 (CH-C8, CH-C8*), 53.4

(CH-C4, CH-C4*), 52.1, 51.9 (CH-C6, CH-C6*), 40.6, 39.9, 39.8, (CH_2-C11, C15, C19, CH_2-C11*, C15*, C19*), 39.1 (CH_2-C2, CH_2-C2*), 36.1 (CH_2-C23, CH_2-C23*), 25.4, 25.3, 25.01, 24.9, 24.8 (CH-C12, C16, C20, C24, CH-C12*, C16*, C20*, C24*), 23.2, 23.0, 22.9, 22.6, 21.6, 21.5, 21.1 (CH_3-C13, C14, C17, C18, C21, C22, C25, C26, CH_3-C13*, C14*, C17*, C18*, C21*, C22*, C25*, C26*).

^{19}F NMR (471 MHz, $CDCl_3$) δ 49.7, 48.7 (2 s).

HRMS (ESI positive) calcd for $C_{32}H_{53}FN_4NaO_7S$ $[M+Na]^+$ 679.3511, found 679.3474.

t_R = 26.3 min (Gemini column C18, 10 µm, 250 x 21.2 mm, 30B to 100B in 80 min).

Cbz-Leu-Leu-Leu-[Phe-SO_2F] 123

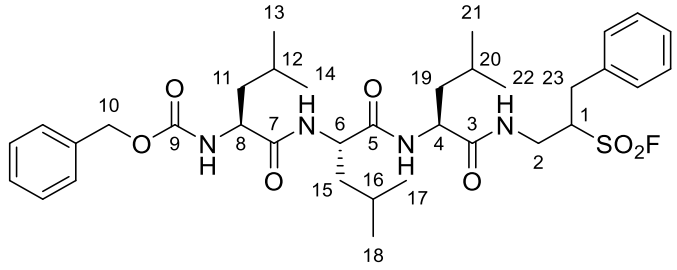

Chemical Formula: $C_{35}H_{51}FN_4O_7S$
Molecular Weight: 690.87

The general procedure was followed on a 0.19 mmol scale to afford the desired product **123** (13 mg, 0.019 mmol, 10%) as a 3:1 mixture of diasteroisomers as a white solid.

^{1}H NMR (500 MHz, $CDCl_3$) δ 7.38 – 7.16 (m, 11H, CH-Ph, NH, CH-Ph*, NH*), 7.03 (br s, 1H, NH, NH*), 6.54 (br s, 1.25H, NH, NH*, NH*), 5.19 (d, *J* = 7.4 Hz, 0.75H, NH), 5.17-5.10 (s, 2H, CH_2-C10, CH_2-C10*), 4.46 – 4.35 (m, 1H, CH-C6, CH-C6*), 4.30 – 4.23 (m, 1H, CH-C4, CH-C4*), 4.17 – 4.12 (m, 1H, CH-C8, CH-C8*), 4.12 – 4.07 (m, 0.75H, CH-C1), 4.05 – 3.99 (m, 0.25H, CH-C1*), 3.74 – 3.67 (m, 1H, CH_2-C2a, CH_2-C2a*), 3.63 – 3.53 (m, 1H, CH_2-C2b, CH_2-C2b*), 3.35 (dd, *J* = 14.5, 5.3 Hz, 1H, CH_2-C23a, CH_2-C23a*), 3.06 (dd, *J* = 14.5, 8.3 Hz, 0.75H, CH_2-C23b), 2.99 (m, 0.25H, CH_2-C23b*), 1.92 – 1.39 (m, 9H, CH_2-C11, C15, C19, CH-C12, C16, C20, CH_2-C11*, C15*, C19*, CH-C12*, C16*, C20*), 0.95 – 0.83 (m, 18H, CH_3-C13, C14, C17, C18, C21, C22, CH_3-C13*, C14*, C17*, C18*, C21*, C22*).

^{13}C NMR (126 MHz, $CDCl_3$) δ 173.4, 173.1, 171.9 (C-C7, C5, C3, C-C7*, C5*, C3*), 156.8 (C-C9, C-C9*), 135.6, 134.9 (C-Ph, C-Ph*), 129.2, 128.9, 128.7, 128.6, 128.0,

127.5 (CH-Ph, CH-Ph*), 67.5 (CH_2-C10, CH_2-C10*), 62.7 (d, *J* = 7.7 Hz, CH-C1), 54.6 (CH-C8, CH-C8*), 53.0 (CH-C4, CH-C4*), 52.0 (CH-C6, CH-C6*), 40.8, 40.0, 39.8 (CH_2-C11, C15, C19, CH_2-C11*, C15*, C19*), 38.6 (CH_2-C2, CH_2-C2*), 33.4 (CH_2-C23, CH_2-C23*), 25.0, 24.9, 24.8 (CH-C12, C16, C20, CH-C12*, C16*, C20*), 23.2, 22.9, 22.8, 21.8, 21.6, 21.2 (CH_3-C13, C14, C17, C18, C21, C22, CH_3-C13*, C14*, C17*, C18*, C21*, C22*).

^{19}F NMR (471 MHz, $CDCl_3$) δ 52.5, 51.6 (2 s).

HRMS (ESI positive) calcd for $C_{35}H_{51}FN_4NaO_7S$ $[M+Na]^+$ 713.3355, found 713.3322.

t_R = 27.8 min (Gemini column C18, 10 µm, 250 x 21.2 mm, 30B to 100B in 80 min).

Morph-hPhe-Leu-Phe-[Leu-SO_2F] 124

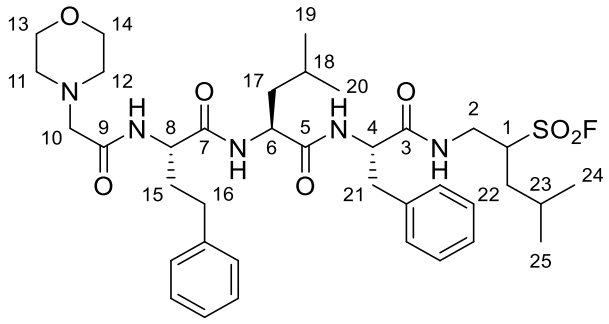

Chemical Formula: $C_{37}H_{54}FN_5O_7S$
Molecular Weight: 731.93

The general procedure was followed on a 0.13 mmol scale to afford the desired product **124** (20 mg, 0.027 mmol, 21%) as a white solid. No ratio of diasteroisomers could be calculated.

^{1}H NMR (600 MHz, $CDCl_3$) δ 8.69 (br s, 3H, NH), 7.36 – 6.89 (m, 10H, CH-Ph), 4.78 (m, 3H, CH- C4, C6, C8), 3.93 – 3.45 (m, 9H, CH_2-C13, C14, CH_2-C10, CH_2-C2, CH-C1), 3.28 – 2.89 (m, 6H, CH_2-C11, C12, CH_2-C21), 2.55 (s, 2H, CH_2-C16), 2.17 – 1.71 (m, 5H, CH_2-C15, CH_2-C22, CH-C23), 1.57 (m, 3H, CH_2-C17, CH-C18), 1.01 – 0.89 (m, 6H, CH_3-C24, C25), 0.84 (d, *J* = 5.6 Hz, 3H, CH_3-C19), 0.80 (d, *J* = 5.6 Hz, 3H, CH_3-C20).

^{13}C NMR (151 MHz, $CDCl_3$) δ 172.7, 172.1, 171.7, 165.3 (C-C3, C5, C7, C9) , 140.6, 136.6 (C-Ph), 129.3, 128.8, 128.6, 128.5, 128.3, 127.1, 126.5 (CH-Ph), 64.0 (CH_2-C13, C14), 61.0 (d, *J* = 8.1 Hz, CH-C1), 58.2 (CH_2-C10), 54.6, 53.7 (CH-C4, C6), 53.6 (CH_2-C11, C12), 52.3 (CH-C8), 41.7(CH_2-C17) , 38.9 (CH_2-C2), 38.1 (CH_2-C21),

36.3 (CH_2-C22), 33.4 (CH_2-C15), 32.2 (CH_2-C16), 25.5, 25.0, (CH-C18, C23), 22.8, 22.6, 22.4, 21.6 (CH_3-C19, C20, C24, C25).

^{19}F NMR (471 MHz, $CDCl_3$) δ 49.7 (s).

HRMS (ESI positive) calcd for $C_{37}H_{55}FN_5O_7S$ $[M+H]^+$ 732.3801, found 732.3765.

t_R = 26.8 min (Gemini column C18, 10 µm, 250 x 21.2 mm, 30B to 100B in 80 min).

Morph-hPhe-Leu-Phe-[Phe-SO_2F] 125

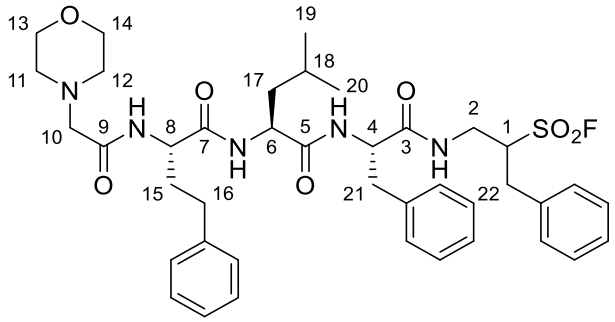

Chemical Formula: $C_{37}H_{54}FN_5O_7S$
Molecular Weight: 731.93

The general procedure was followed on a 0.12 mmol scale to afford the desired product **125** (10 mg, 0.013 mmol, 11%) as a white solid. No ratio of diasteroisomers could be calculated.

^{1}H NMR (600 MHz, $CDCl_3$) δ 7.37 – 6.99 (m, 15H, CH-Ph), 4.66 (br s, 2H, CH-C8,) 4.42 (br s, 1H, CH-C4), 3.98 (br s, 1H, CH-C1), 3.83 (m, 8H, CH_2-C13, C14, CH_2-C10, CH_2-C2) 3.33 – 2.87 (m, 8H, CH_2-C22, CH_2-C11, C12, CH_2-C21), 2.65 – 2.59 (m, 2H, CH_2-C16), 2.05 (dd, *J* = 13.2, 6.3 Hz, 1H, CH_2-C15b), 1.96 (app p, *J* = 7.5, 7.0 Hz, 1H, CH_2-C15b), 1.48 (br s, 3H, CH_2-C17, CH-C18), 0.83 (d, *J* = 5.0 Hz, 3H, CH_3-C19), 0.79 (d, *J* = 5.0 Hz, 3H, CH_3-C20).

^{13}C NMR (151 MHz, $CDCl_3$) δ 173.0, 172.8, 172.1, 172.0 (C-C3, C5, C7, C9), 140.5, 136.7, 136.6, 134.8 (C-Ph), 129.42, 129.3, 129.2, 129.2, 129.1, 128.8, 128.7, 128.5, 128.4, 127.9, 127.1, 126.5 (CH-Ph), 64.6, 64.4(CH2-C13, C14), 63.1 (d, *J* = 8.2 Hz, CH-C1), 59.0 (CH_2-C10), 54.5, 53.8 (CH-C4, C6), 53.2 (CH_2-C11, C12), 52.9 (CH-C8), 40.8 (CH_2-C17), 38.4 (CH_2-C2), 37.4 (CH_2-C21), 33.70 (CH_2-C22), 33.4 (CH_2-C15), 32.2 (CH_2-C16), 24.9 (CH-C18), 22.7, 21.9 (CH_3-C19,C20)

^{19}F NMR (471 MHz, $CDCl_3$) δ 51.7 (s).

HRMS (ESI positive) calcd for $C_{40}H_{53}FN_5O_7S$ $[M+H]^+$ 766.3644, found 766.3608.

t_R = 27.8 min (Gemini column C18, 10 µm, 250 x 21.2 mm, 30B to 100B in 80 min).

Cbz-Leucinol 129

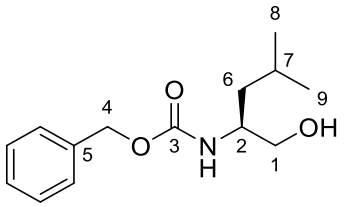

Chemical Formula: $C_{14}H_{21}NO_3$
Molecular Weight: 251.33

Cbz-Leucine **101** (12.9 g, 48.8 mmol) was dissolved in dry DME (50 mL) and cooled to 0 °C. NMM (5.40 mL, 48.8 mmol) and isobutylchloroformate (6.40 mL, 48.8 mmol) were slowly added and the mixture was stirred at RT for 3h. The resultant white precipitate was removed by filtration over celite. The residue was washed with DME (3 x 10 mL) and the collected filtrate was cooled to 0 °C. $NaBH_4$ (2.77 g, 73.2 mmol) was dissolved in water (25 mL) separately and slowly added. When gas evolution ceased the reaction was quenched with water (500 mL). DME was removed *in vacuo* and CH_2Cl_2 (300 mL) was added. The layers were separated and the aqueous phase was extracted with CH_2Cl_2 (2 x 300 mL). The combined organic extracts were dried over $MgSO_4$, filtered and the solvent removed *in vacuo*. The crude material was purified by silica column chromatography (CH_2Cl_2) to afford the desired compound **129** (7.8 g, 31 mmol, 63%) as a colourless oil.

^{1}H NMR (500 MHz, $CDCl_3$) δ 7.38 – 7.29 (m, 5H, CH-Ph), 5.10 (s, 2H, CH_2-C4), 4.77 (d, *J* = 7.0 Hz, 1H, NH), 3.84-3.76 (m, 1H, CH-C2), 3.66 (dd, *J* = 11.3, 3.7 Hz, 1H, CH_2-C1a), 3.58-3.52 (m, 1H, CH_2-C1b), 2.37 (br s, 1H, OH), 1.66 – 1.58 (m, 1H, CH-C7), 1.39 – 1.28 (m, 2H, CH_2-C6), 0.93 (d, *J* = 6.5 Hz, 6H, CH_3-C8, C9).

^{13}C NMR (126 MHz, $CDCl_3$) δ 156.9 (C-C3), 136.5 (C-C5), 128.6 (CH-Ph), 128.3 (CH-Ph), 128.2 (CH-Ph), 66.9 (CH_2-C4), 66.1 (CH_2-C1), 51.6 (CH-C2), 40.6 (CH_2-C6), 24.9 (CH-C7), 23.2 (CH_3-C8), 22.3 (CH_3-C9).

HRMS (CI iso-butane) calcd for $C_{14}H_{22}NO_3$ $[M+H]^+$252.1600, found 252.1602.

Spectroscopic data are in accordance with literature.[127]

Cbz-Leucinal 130

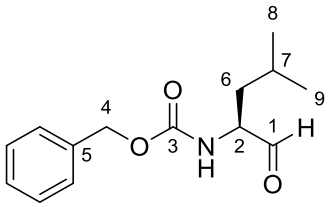

Chemical Formula: $C_{14}H_{19}NO_3$
Molecular Weight: 249.31

Oxalyl chloride (4.4 mL, 51 mmol) was dissolved in dry CH_2Cl_2 (75 mL) and cooled to −63 °C. A solution of DMSO (7.30 mL, 102 mmol) in dry CH_2Cl_2 (12 mL) was added dropwise over 20 min. A solution of Cbz-Leucinol **129** (7.8 g, 31 mmol) in dry CH_2Cl_2 (20 mL) was subsequently added dropwise over 20 min, and the mixture was stirred at −63 °C for 30 min. A solution of DIPEA (32.0 mL, 186 mmol) in dry CH_2Cl_2 (7 mL) was then added dropwise over 20 min. After 30 min, the mixture was warmed to RT and water (10 mL) was added under vigorous stirring. The biphasic mixture was poured into Et_2O (175 mL) and the layers were separated. The organic phase was washed with a 1 M $KHSO_4$ aq. solution (2 x 50 mL) and the aqueous phase was extracted with Et_2O (1 x 50 mL). The combined organic extracts were dried over $MgSO_4$, filtered and the solvent removed *in vacuo* to afford the crude product **130** (7.9 g, 30 mmol, 97%) as a yellow oil. The compound was used in the next reaction without further purification.

^{1}H NMR (500 MHz, $CDCl_3$) δ 9.59 (s, 1H, CH-C1), 7.38 – 7.31 (m, 5H, CH-Ph), 5.25 (d, *J* = 7.4 Hz, 1H, NH), 5.11 (s, 2H, CH_2-C4), 4.33 (ddd, *J* = 9.4, 7.4, 4.8 Hz, 1H, CH-C2), 1.77 – 1.60 (m, 1H, CH-C7), 1.68 (ddd, *J* = 13.5, 8.6, 4.8 Hz, 1H, CH_2-C6a), 1.42 (ddd, *J* = 13.5, 9.4, 5.5 Hz, 1H, CH_2-C6b), 0.98 (d, *J* = 6.7 Hz, 3H, CH_3-C8), 0.96 (d, *J* = 6.7 Hz, 3H, CH_3-C9).

^{13}C NMR (126 MHz, $CDCl_3$) δ 199.8 (CH-C1), 156.3 (C-C3), 136.2 (C-C5), 128.6 (CH-Ph), 128.3 (CH-Ph), 128.2 (CH-Ph), 67.2 (CH_2-C4), 58.9 (CH-C2), 38.2 (CH_2-C6), 24.7 (CH-C7), 23.1 (CH_3-C8), 22.0 (CH_3-C9).

HRMS (CI iso-butane) calcd for $C_{14}H_{20}NO_3$ $[M+H]^+$250.1443, found 250.1445.

Spectroscopic data are in accordance with literature.[128]

Diethylphosphoryl methanesulfonate 131

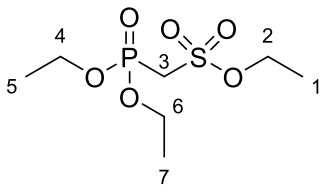

Chemical Formula: $C_7H_{17}O_6PS$
Molecular Weight: 260.2408

Ethyl methanesulfonate **136** (10 g, 80 mmol) was dissolved in dry THF (200 mL) and cooled to −78 °C before the addition of *n*-BuLi (2.5 M in hexanes, 35 mL, 89 mmol) over 30 min. After 15 min, diethylchlorophosphate **137** (6.5 mL, 45 mmol) was added and the solution was stirred for 30 min before cooling to −50 °C and stirring for 1 h. The mixture was removed *in vacuo* and the residue diluted with water (100 mL) and extracted with CH_2Cl_2 (3 x 120 mL). The layers were separated and the combined organic extracts were dried over $MgSO_4$, filtered and the solvent removed *in vacuo*. Purification of the crude material by silica column chromatography (PE:EtOAc, 1:1) afforded the product **131** (6.5 g, 25 mmol, 56%) as a colourless oil.

^{1}H NMR (500 MHz, $CDCl_3$) δ 4.36 (q, J = 7.1 Hz, 2H, CH_2-C2), 4.23 – 4.13 (m, 4H, CH_2-C6, C4), 3.69 (d, $^2J_{PH}$ = 17.2 Hz, 2H, CH_2-C3), 1.38 (t, J = 7.1 Hz, 3H, CH_3-C1), 1.32 (t, J = 7.1 Hz, 6H, CH_3-C5, C7).

^{13}C NMR (126 MHz, $CDCl_3$) δ 68.3 (CH_2-C2), 63.7 (CH_2-C4, C6), 47.8 (d, J = 140.0 Hz, CH_2-C3), 16.3 (CH_3-C5), 16.2 (CH_3-C7), 15.0 (CH_3-C1).

HRMS (CI iso-butane) calcd for $C_7H_{18}O_6PS$ $[M+H]^+$ 261.0562, found 261.0561.

Spectroscopic data are in accordance with literature.[129]

Cbz-Leucine inspired vinyl sulfonate 132

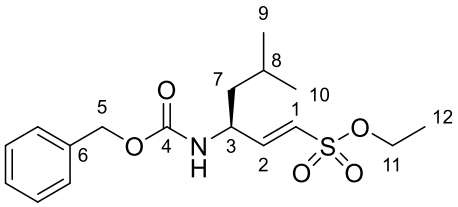

Chemical Formula: $C_{17}H_{25}NO_5S$
Molecular Weight: 355.4490

Diethylphosphoryl methanesulfonate **131** (6.5 g, 25 mmol) was dissolved in dry THF (100 mL) and cooled to −78 °C. *n*-BuLi (2.5 M in hexanes, 10.5 mL, 26.2 mmol) was slowly added and the mixture was stirred for 20 min. A solution of Cbz-Leucinal **130** (7.5 g, 30 mmol) in dry THF (25 mL) was then added and the mixture stirred for an additional 45 min before warming to RT and stirring overnight. Solvent was removed *in vacuo* and the residue was treated with water (450 mL) and extracted with CH_2Cl_2 (3 x 450 mL). The layers were separated and the combined organic extracts were dried over $MgSO_4$, filtered and the solvent removed *in vacuo*. Purification of the crude material by silica column chromatography (PE:EtOAc, 4:1) afforded the desired product **132** (6.1 g, 17 mmol, 68%) as a yellow oil.

^{1}H NMR (500 MHz, $CDCl_3$) δ 7.39 – 7.32 (m, 5H, CH-Ph), 6.79 (dd, *J* = 15.2, 5.3 Hz, 1H, CH-C2), 6.30 (dd, *J* = 15.2, 1.3 Hz, 1H, CH-C1), 5.10 (s, 2H, CH_2-C5), 4.79 (d, *J* = 7.8 Hz, 1H, NH), 4.49 – 4.41 (m, 1H, CH-C3), 4.13 (q, *J* = 6.8 Hz, 2H, CH_2-C11), 1.74 – 1.64 (m, 1H, CH-C8), 1.44 (dd, *J* = 7.2 Hz, 7.2 Hz, 2H, CH_2-C7), 1.35 (t, *J* = 6.8 Hz, 3H, CH_3-C12), 0.94 (d, *J* = 6.6 Hz, 6H, CH_3-C9, C10).

^{13}C NMR (126 MHz, $CDCl_3$) δ 155.6 (C-C4), 148.6 (CH-C2), 136.2 (C-C6), 128.7 (CH-Ph), 128.4 (CH-Ph), 128.2 (CH-Ph), 124.6 (CH-C1), 67.2 (CH_2-C5), 67.1 (CH_2-C11), 50.1 (CH-C3), 43.2 (CH_2-C7), 24.8 (CH-C8), 22.8 (CH_3-C9), 22.0 (CH_3-C10), 14.9 (CH_3-C12).

HRMS (ESI negative) calcd for $C_{17}H_{24}NO_5S$ $[M-H]^-$ 354.1381, found 354.1366.

Cbz-Leucine inspired vinyl sulfonate salt 133

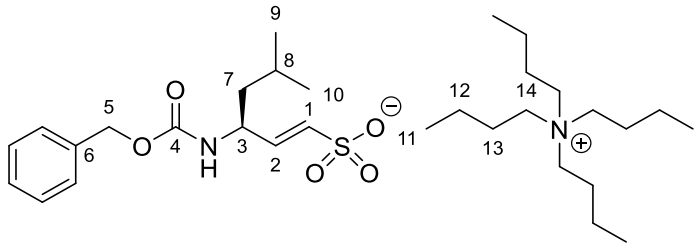

Chemical Formula: $C_{31}H_{56}N_2O_5S$
Molecular Weight: 568.8580

Sulfonate ester **132** (6.1 g, 17 mmol) was treated with tetrabutylammonium iodide (6.3 g, 17 mmol) in refluxing acetone and the reaction mixture was stirred overnight. The solvent was removed *in vacuo* to afford the desired compound **133** (11.3 g) as a yellow oil. The salt was directly used in the next step without further purification.

^{1}H NMR (400 MHz, $CDCl_3$) δ 7.37 – 7.28 (m, 5H, CH-Ph), 6.48 (dd, J = 15.3, 1.1 Hz, 1H, CH-C1), 6.40 (dd, J = 15.3, 4.6 Hz, 1H, CH-C2), 5.10 (d, J = 6.1 Hz, 1H, CH_2-C5a),5.05 (d, J = 6.1 Hz, 1H, CH_2-C5b), 4.61 (d, J = 9.1 Hz, 1H, NH), 4.40 – 4.34 (m, 1H, CH-C3), 3.34 – 3.26 (m, 8H, CH_2-C14), 1.72 – 1.60 (m, 9H, CH_2-C13, CH-C8), 1.50 – 1.35 (m, 10H, CH_2-C12, C7), 1.00 (t, J = 7.3 Hz, 12H, CH_3-C11), 0.91 – 0.84 (m, 6H, CH_3-C9, C10).

^{13}C NMR (126 MHz, $CDCl_3$) δ 155.4 (C-C4), 136.4 (C-C5), 134.5 (CH-C1), 133.8 (CH-C2), 128.3 (CH-Ph), 127.8 (CH-Ph), 66.4 (CH_2-C5), 58.8 (CH_2-C14), 49.3 (CH-C3), 44.3 (CH_2-C7), 24.4 (CH-C8), 24.0 (CH_2-C13), 22.6 (CH_3-C9), 22.1 (CH_3-C10), 19.6 (CH_2-C12), 13.5 (CH_3-C11).

HRMS (ESI negative) calcd for $C_{15}H_{20}NO_5S$ $[M-H]^-$ 326.1068, found 326.1055.

Cbz-Leucine inspired vinyl sulfonyl fluoride 134

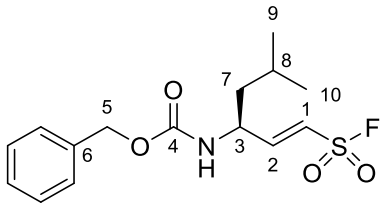

Chemical Formula: $C_{15}H_{20}FNO_4S$
Molecular Weight: 329.3864

Sulfonate salt **133** (4.8 g, 8.5 mmol) was dissolved in dry CH_2Cl_2 (170 mL), XtalFluor- M **69** (3.72 g, 15.3 mmol) and $Et_3N{\cdot}3HF$ (59 µL, 0.36 mmol) were added and the reaction was stirred at reflux overnight. The solvent was removed *in vacuo* and the crude product was purified by silica column chromatography (CH_2Cl_2:PE, 2:1) to afford the desired compound **134** (720 mg, 2.18 mmol, 26%) as a white solid.

^{1}H NMR (500 MHz, $CDCl_3$) δ 7.41 – 7.33 (m, 5H, CH-Ph), 7.06 (dd, *J* = 15.0, 4.7 Hz, 1H, CH-C2), 6.49 (d, *J* = 15.0 Hz, 1H, CH-C1), 5.12 (s, 2H, CH_2-C5), 4.72 (d, *J* = 7.1 Hz, 1H, NH), 4.57 – 4.50 (m, 1H, CH-C3), 1.76 – 1.65 (m, 1H, CH-C8), 1.47 (dd, J = 7.3 Hz, 7.3 Hz, 2H, CH_2-C7), 0.96 (d, J = 6.6 Hz, 6H, CH_3-C9, C10).

^{13}C NMR (126 MHz, $CDCl_3$) δ 155.8 (C-C4), 153.7 (CH-C2), 136.2 (C-C5), 129.0 (CH-Ph), 128.8 (CH-Ph), 128.6 (CH-Ph), 122.3 (d, *J* = 27.7 Hz, CH-C1), 67.8 (CH_2-C5), 50.5 (CH-C3), 43.1 (CH_2-C7), 25.1 (CH-C8), 23.1 (CH_3-C9), 22.2 (CH_3-C10).

^{19}F NMR (471 MHz, $CDCl_3$) δ 60.40 (s)

HRMS (ESI negative) calcd for $C_{15}H_{19}FNO_4S$ $[M-H]^-$ 328.1024, found 328.1017.

Melting point: 120 °C.

Ethyl methanesulfonate 136

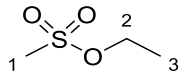

Chemical Formula: $C_3H_8O_3S$
Molecular Weight: 124.1540

Ethanol (6.40 mL, 110 mmol) was dissolved in dry CH_2Cl_2 (400 mL) and the solution was cooled to 0 °C. NMM (22.0 mL, 200 mL) and methanesulfonyl chloride **135** (7.70 mL, 100 mmol) were added and the mixture was stirred for 30 min. The mixture was then warmed to RT and the reaction stirred overnight. CH_2Cl_2 (200 mL) was added and the resulting mixture was washed with a 1 M $KHSO_4$ aq. solution (200 mL). The layers were separated and the organic phase was washed with water (200 mL), dried over $MgSO_4$, filtered and the solvent removed *in vacuo* to afford the desired compound **136** (10 g, 80 mmol, 81%) as a colourless oil.

^{1}H NMR (500 MHz, $CDCl_3$) *δ* 4.23 (q, *J* = 7.1 Hz, 2H, CH_2-C2), 2.94 (s, 3H, CH_3-C1), 1.34 (t, *J* = 7.1 Hz, 3H, CH_3-C3).

^{13}C NMR (126 MHz, $CDCl_3$) δ 66.4 (CH_2-C2), 37.3 (CH_3-C1), 14.9 (CH_3-C3).

HRMS (CI iso-butane) calcd for $C_3H_9O_3S$ $[M+H]^+$ 125.0272, found 125.0270.

Spectroscopic data are in accordance with the commercially available compound (Sigma-Aldrich).

Double substituted VSF 147

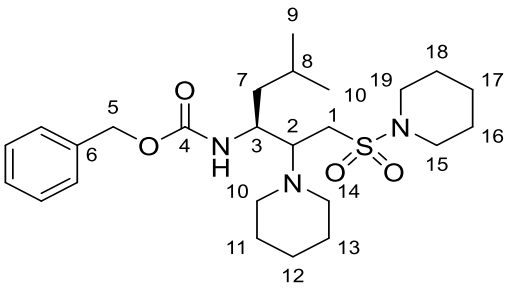

Chemical Formula: $C_{25}H_{41}N_3O_4S$
Molecular Weight: 479.6800

Vinyl sulfonyl fluoride **134** (30 mg, 0.1 mmol) was dissolved in dry CH_2Cl_2 (2 mL) and treated with piperidine (32 µL, 0.3 mmol). The reaction was stirred at RT overnight. Solvent was removed *in vacuo* and the crude material was purified by silica column chromatography (*n*-hex:EtOAc, 8:1→5:1) to afford the double-

substituted product **147** (20 mg, 0.04 mmol, 40%) followed by the five-membered ring **148** (20 mg, 0.05 mmol, 50%) both as off-white oils.

^{1}H NMR (500 MHz, $CDCl_3$) δ 7.39 – 7.28 (m, 5H, CH-Ph), 5.20 – 5.09 (m, 2H, NH, CH_2-C5a), 5.04 (d, *J* = 12.4 Hz, 2H, CH_2-C5b), 3.81 (app qd, *J* = 10.4, 2.6 Hz, 1H, CH-C3), 3.12 – 3.01 (m, 5H, CH_2-C1a, C15, C19), 2.94 (ddd, *J* = 8.9, 6.1, 2.6 Hz, 1H, CH-C2), 2.78 (dd, *J* = 14.0, 6.1 Hz, 1H, CH_2-C1b), 2.57 (ddd, *J* = 11.0, 7.0, 3.5 Hz, 2H, CH_2-C10a, C14a), 2.33 (ddd, *J* = 11.0, 6.8, 3.4 Hz, 2H, CH_2-C10b, C14b), 1.77 – 1.70 (m, 2H, CH_2-C7a, CH-C8), 1.70 – 1.64 (m, 10H, CH_2-C11, C12, C13, C16, C18), 1.42 (app p, *J* = 5.9 Hz, 2H, CH_2-C17), 1.31 – 1.20 (m, 1H, CH_2-C7b), 0.92 (d, *J* = 6.3 Hz, 6H, CH_3-C9, C10).

^{13}C NMR (126 MHz, $CDCl_3$) δ 156.9 (C-C4), 136.8 (CH_2-C6), 128.6 (CH-Ph), 128.1 (CH-Ph), 128.0 (CH-Ph), 66.7 (CH_2-C5), 64.4 (CH-C2), 51.1 (CH-C3), 50.2 (CH_2-C10, C14), 46.7 (CH_2-C15, C19), 44.0 (CH_2-C7), 43.4 (CH_2-C1), 26.4 (CH_2-C16, C18), 25.5 (CH_2-C11, C13), 24.9 (CH-C8), 24.7 (CH_2-C17), 23.9 (CH_2-C12), 23.8 (CH_3-C9), 21.8 (CH_3-C10).

HRMS (ESI positive) calcd for $C_{25}H_{41}N_3NaO_4S$ $[M+Na]^+$ 502.2710, found 502.2685.

Five-membered ring 148

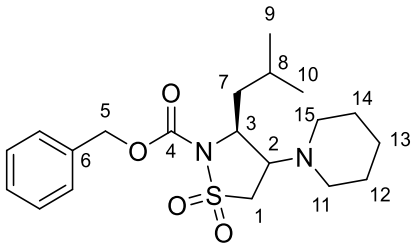

Chemical Formula: $C_{20}H_{30}N_2O_4S$
Molecular Weight: 394.5300

^{1}H NMR (500 MHz, $CDCl_3$) δ 7.44 – 7.29 (m, 5H, CH-Ph), 5.37 – 5.23 (m, 2H, CH_2-C5), 4.26 (app dt, *J* = 9.6, 3.1 Hz, 1H, CH-C3), 3.49 (d, *J* = 6.5 Hz, 2H, CH_2-C1), 3.34 (td, *J* = 6.5, 3.1 Hz, 1H, CH-C2), 2.56 – 2.50 (m, 2H, CH_2-C12a, C14a), 2.49 – 2.43 (m, 2H, CH_2-C12b, C14b), 1.70 – 1.62 (m, 2H, CH_2-C7a, CH-C8), 1.60 – 1.52 (m, 5H, CH_2-C7b, C11, C15), 1.43 (app dt, *J* = 8.8, 4.4 Hz, 2H, CH_2-C13), 0.94 (d, *J* = 6.2 Hz, 6H, CH_3-C9), 0.92 (d, *J* = 6.2 Hz, 6H, CH_3-C10).

^{13}C NMR (126 MHz, $CDCl_3$) δ 150.8 (C-C4), 135.4 (C-C6), 128.9 (CH-Ph), 128.7(CH-Ph), 128.2 (CH-Ph), 69.0 (CH_2-C5), 63.4 (CH-C2), 57.9 (CH-C1), 50.6, 49.4 (CH_2-

C12, C14), 43.8 (CH_2-C1), 26.4 (CH_2- C11, C15), 25.1 (CH-C18), 24.5 (CH_2-C13), 23.7 (CH_3-C9), 22.1 (C10).

HRMS (ESI positive) calcd for $C_{20}H_{30}N_2NaO_4S$ $[M+Na]^+$ 417.1818, found 417.1798.

ß-sultam 149

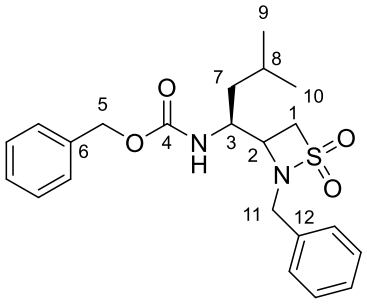

Chemical Formula: $C_{22}H_{28}N_2O_4S$
Molecular Weight: 416.5360

VSF **134** (50 mg, 0.15 mmol) was dissolved in CH_2Cl_2 (3 mL) and treated with benzylamine (50 µL, 0.45 mmol). The reaction was stirred at RT overnight. The solvent was removed *in vacuo* and the crude material was purified by silica column chromatography (*n*-hex:EtOAc, 6:1→4:1) to afford the major (10 mg, 0.02 mmol, 16%) followed by the minor (3 mg, 0.007 mmol, 5%) diasteroisomer of the ß-sultam **149** as colourless oils.

Major isomer

^{1}H NMR (500 MHz, CDCl3) δ 7.43 – 7.22 (m, 10H, Ph), 5.15 (d, *J* = 12.3 Hz, 1H, CH_2-C5a), 5.05 (d, *J* = 12.3 Hz, 1H, CH_2-C5b), 4.43 (d, *J* = 14.5 Hz, 1H, CH_2-C11a), 4.32 (d, *J* = 8.2 Hz, 1H, NH), 4.10 (d, *J* = 14.5 Hz, 1H, CH_2-C11b), 4.02 (dd, *J* = 12.6, 8.3 Hz, 1H, CH_2-C1a),3.90 – 3.87 (m, 1H, CH-C3), 3.86 (dd, *J* = 12.6, 6.2 Hz, 1H, CH_2-C1b), 3.34 – 3.25 (m, 1H, CH-C2), 1.62 – 1.52 (m, 1H, CH-C8), 1.19 (dd, *J* = 8.6, 4.4 Hz, 2H, CH_2-C7), 0.84 (d, *J* = 6.7 Hz, 3H, CH_3-C9), 0.82 (d, *J* = 6.7 Hz, 3H, CH_3-C10).

^{13}C NMR (126 MHz, CDCl3) δ 150.0 (C-C4), 134.7 (C-C6, C12), 128.9 (CH-Ph), 128.6 (CH-Ph), 128.4 (CH-Ph), 128.0 (CH-Ph), 67.2 (CH_2-C5) 59.0 (CH_2-C1), 50.9 (CH-C2), 50.0 (CH-C3, CH_2-C11), 39.4 (CH_2-C7), 24.5 (CH-C8), 23.1 (CH3-C9), 21.3 (CH3-C10).

HRMS (ESI positive) calcd for $C_{22}H_{28}N_2NaO_4S$ $[M+Na]^+$ 439.1662, found 439.1645.

ß-sultam 151

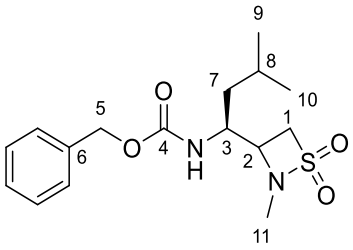

Chemical Formula: $C_{16}H_{24}N_2O_4S$
Molecular Weight: 340.4380

VSF **134** (50 mg, 0.15 mmol) was dissolved in dry CH_2Cl_2 (3 mL) and treated with methylamine (22 µL, 0.45 mmol). The reaction was stirred at RT overnight. The solvent was removed *in vacuo* and the crude material was purified by silica column chromatography (*n*-hex:EtOAc, 4:1) to provide the ß-sultam **151** (10 mg, 0.03 mmol, 20%) as a 3:1 mixture of diasteroisomers as a yellow oil.

^{1}H NMR (500 MHz, Chloroform-*d*) δ 7.40 – 7.12 (m, 5H, CH-Ph, Ph*), 5.26 – 4.80 (m, 3H, CH_2-C5, C5*, NH, NH*), 4.06 – 3.89 (m, 1H, CH-C3*, CH_2-C1a), 3.89 – 3.75 (m, 1.75H, CH-C3, CH_2-C1b, C1a*), 3.66 (dd, *J* = 12.6, 8.5 Hz, 0.25H, CH_2-C1b*), 3.10 (ddd, *J* = 8.5, 6.0, 2.7 Hz, 0.25H, CH-C2*), 3.03 – 2.93 (m, 0.75H, CH-C2), 2.67 (s, 0.75H, CH_3-C11*), 2.65 (s, 2.25H, CH_3-C11), 1.68 – 1.55 (m, 1H, CH-C8, C8*), 1.36 (ddd, *J* = 13.8, 10.6, 4.9 Hz, 0.25H, CH_2-C7a*), 1.26 – 1.01 (m, 1.75H, CH_2-C7b*, C7), 0.89 – 0.82 (m, 6H, CH_3-C9, C10, C9*, C10*).

^{13}C NMR (126 MHz, $CDCl_3$) δ 156.6 (C-C4*), 156.5 (C-C4), 136.4 (C-C6*), 136.2 (C-C6), 128.6 (CH-Ph, CH-Ph*), 128.3 (CH-Ph, CH-Ph*), 128.2, 127.8 (CH-Ph, CH-Ph*), 67.1 (CH_2-C5), 66.9 (CH_2-C5*), 59.9 (CH_2-C1), 58.9 (CH_2-C1*), 52.6 (CH-C2), 52.0 (CH-C2*), 50.6 (CH-C3), 49.7 (CH-C3*), 42.3 (CH_2-C7*), 40.0 (CH_2-C7), 33.6 (CH_3-C11*), 31.6 (CH_3-C11), 24.9, 24.7 (CH-C8, CH-C8*), 23.3, 23.2, 21.7, 21.5 (CH_3-C9, C10, C9*, C10*).

HRMS (ESI positive) calcd for $C_{16}H_{24}N_2NaO_4S$ $[M+Na]^+$ 363.1349, found 363.1333.

ß-sultam 153

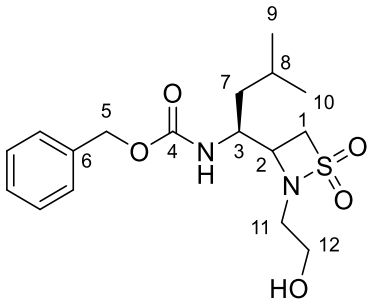

Chemical Formula: $C_{17}H_{26}N_2O_5S$
Molecular Weight: 370.4640

VSF **134** (100 mg, 0.3 mmol) was dissolved in CH_2Cl_2 (6 mL) and treated with ethanolamine (55 µL, 0.9 mmol). The reaction was stirred at RT overnight. The solvent was removed *in vacuo* and the crude material was purified by silica column chromatography (*n*-hex:EtOAc, 2:1) to give ß-sultam **153** (70 mg, 0.19 mmol, 63%) as a 2.3:1 mixture of diasteroisomers as a colourless oil.

^{1}H NMR (500 MHz, $CDCl_3$) δ 7.39 – 7.28 (m, 5H, CH-Ph, CH-Ph*), 5.60 – 5.48 (m, 0.3H, NH*), 5.38 (br s, 0.7H, NH), 5.12 – 4.99 (m, 2H, CH_2-C5, CH_2-C5*), 4.13 – 4.05 (m, 1.3H,CH-C3, C3*,CH_2-C1a*), 4.04 – 3.90 (m, 2.4H, CH-C2, C2*, CH_2-C1), 3.89 – 3.80 (m, 0.3H, CH_2-C1b*), 3.71 – 3.51 (m, 3H, CH_2-C11a, CH_2-C12, CH_2-C11a*, CH_2-C12*), 3.25 – 3.10 (m, 1H, CH-C2, C2*), 2.96 – 2.89 (m, 1H, CH_2-C11b, C11b*), 1.72 – 1.63 (m, 1H, CH-C8, CH-C8*), 1.43 (ddd, *J* = 13.6, 10.9, 4.6 Hz, 0.3H, CH_2-C7a*).1.23 – 1.07 (m, 1.7H,CH_2-C7, CH_2-C7b*), 0.94 – 0.88 (m, 6H, CH_3-C9, C10, CH_3-C9*, C10*).

^{13}C NMR (126 MHz, $CDCl_3$) δ 157.3 (C-C4), 156.6 (C-C4*), 136.1 (C-C6*), 136.0 (C-C6), 128.4 (CH-Ph, CH-Ph*), 128.1(CH-Ph, CH-Ph*), 127.8(CH-Ph, CH-Ph*), 127.7 (CH-Ph, CH-Ph*), 67.1 (CH_2-C5), 66.9 (CH_2-C5*), 60.7 (CH_2-C12, C12*), 57.6 (CH_2-C1, CH_2-C1*), 50.8 (CH-C2*), 50.0 (CH-C2) , 49.9 (CH-C3, C3*), 49.4, (CH_2-C11, CH_2-C11*), 41.4 (CH_2-C7*), 39.9 (CH_2-C7), 24.7, (CH-C8*) 24.6 (CH-C8), 23.1, 23.0, 21.4 (CH_3-C9, C10, CH_3-C9*, C10*).

HRMS (ESI positive) calcd for $C_{17}H_{26}N_2NaO_5S$ $[M+Na]^+$ 393.1455, found 393.1440.

Silil protected ß-sultam 154

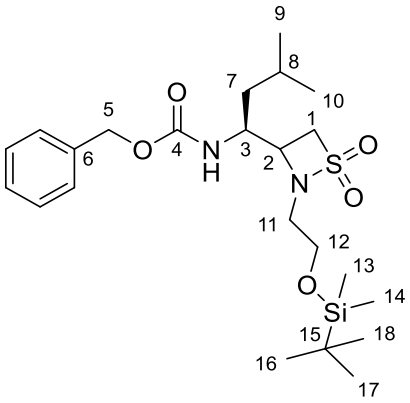

Chemical Formula: $C_{23}H_{40}N_2O_5SSi$
Molecular Weight: 484.7270

ß-sultam **153** (70 mg, 0.19 mmol) was dissolved in dry CH_2Cl_2 (5 mL) and treated with imidazole (26 mg, 0.38 mmol) and TBDMSCl (57 mg, 0.38 mmol).The reaction was stirred at RT overnight. The mixture was diluted with CH_2Cl_2 (10 mL) and washed with brine (10 mL). The layers were separated and the aqueous phase was extracted with CH_2Cl_2 (10 mL). The combined organic extracts were dried over $MgSO_4$, filtered and the solvent removed *in vacuo*. Purification of the crude product by silica column chromatography (*n*-hex:EtOAc, 11:1→7:1) afforded the minor (5 mg, 0.01 mmol, 5%) followed by the major (36 mg, 0.07 mmol, 37%) diasteroisomer of the ß-sultam **154** as colourless oils.

Major isomer

^{1}H NMR (500 MHz, $CDCl_3$) δ 7.31 – 7.18 (m, 5H, CH-Ph), 5.33 (d, *J* = 9.1 Hz, 1H, NH), 5.11 – 4.97 (m, 2H, CH_2-C5), 3.98 – 3.89 (m, 2H, CH_2-C1a, CH-C3), 3.76 (dd, *J* = 12.7, 6.1 Hz, 1H, CH_2-C1b), 3.74 – 3.62 (m, 2H, CH_2-C12), 3.50 – 3.41 (m, 1H, CH_2-C11a), 3.35 – 3.26 (m, 1H, CH-C2), 2.84 (ddd, *J* = 14.4, 6.7, 4.5 Hz, 1H, CH_2-C11b), 1.68 – 1.58 (m, 1H, CH-C8), 1.45 – 1.32 (m, 1H, CH_2-C7a), 1.23 – 1.10 (m, 1H, CH_2-C7b), 0.87 (d, *J* = 6.7 Hz, 6H, CH_3-C9, C10), 0.82 (s, 9H, CH_3-C16, C17, C18), 0.01 (s, 3H, CH_3-C13), 0.00 (s, 3H, CH_3-C14).

^{13}C NMR (126 MHz, $CDCl_3$) δ 156.2 (C-C4), 136.4 (C-C6), 128.5 (CH-Ph), 128.1 (CH-Ph), 127.9 (CH-Ph), 66.8 (CH_2C5), 62.7 (CH_2-C12), 58.6 (CH_2-C1), 51.4 (CH-C2), 49.9 (CH-C3), 48.5 (CH_2-C11), 38.2 (CH_2-C7), 26.0 (CH_3-C16, C17, C18), 24.6 (CH-C8), 23.5 (CH_3-C9), 21.4 (CH_3-C10), 18.4 (C-C15), -5.4 (CH_3-C13, C14).

HRMS (ESI positive) calcd for $C_{23}H_{40}N_2NaO_5SSi$ $[M+Na]^+$ 507.2319, found 507.2298.

Minor isomer

^{1}H NMR (500 MHz, $CDCl_3$) δ 7.31 – 7.15 (m, 5H, CH-Ph), 5.25 – 5.18 (br s, 1H, NH), 5.06 (d, *J* = 12.2 Hz, 1H, CH_2-C5a), 5.03 (d, *J* = 12.2 Hz, 1H, CH_2-C5b),3.96 (dd, *J* = 12.7, 8.2 Hz, 1H, CH_2-C1a), 3.88 – 3.81 (m, 1H, CH-C3), 3.76 (dd, *J* = 12.7, 5.8 Hz, 1H, CH_2-C1b), 3.71 – 3.62 (m, 2H, CH_2-C12), 3.48 (dt, *J* = 14.0, 4.5 Hz, 1H, CH_2-C11a), 3.34 – 3.29 (m, 1H, CH-C2), 2.80 (ddd, *J* = 14.0, 7.3, 5.4 Hz, 1H, CH_2-C11b), 1.64 – 1.53 (m, 1H, CH-C8), 1.49 – 1.41 (m, 1H, CH_2-C7a), 1.25 – 1.12 (m, 1H, CH_2-C7b), 0.85 (d, *J* = 6.8 Hz, 6H, CH_3-C9, C10), 0.80 (s, 9H, CH_3- C16, C17, C18), 0.01 (s, 3H, CH_3-C13), 0.00 (s, 3H, CH_3-C14).

^{13}C NMR (126 MHz, $CDCl_3$) δ 156.8 (C-C4), 136.5 (C-C6), 128.6 (CH-Ph), 128.2 (CH-Ph), 127.9 (CH-Ph), 67.1 (CH_2- C5), 62.2 (CH_2-C12), 59.8 (CH_2-C1), 50.8 (CH-C2), 50.3 (CH-C3), 49.6 (CH_2-C11), 42.4 (CH_2-C7), 26.0 (CH_3- C16, C17, C18), 25.0 (CH-C8), 23.4 (CH_3-C9), 21.7 (CH_3-C10), 18.5 (C-C15), -5.2 (CH_3- C13, C14).

ß-sultam 161

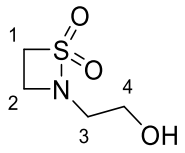

Chemical Formula: $C_4H_9NO_3S$
Molecular Weight: 151.1800

Ethensulfonyl fluoride **156** (150 µL, 1.8 mmol) was dissolved in CH_2Cl_2 (8 mL) and treated with ethanolamine (326 µL, 5.4 mmol). The reaction was stirred at RT for 2 h. The solvent was removed *in vacuo* and the crude material was purified by silica column chromatography (EtOAc:CH_2Cl_2, 1:1,) to afford the ß-sultam **161** (200 mg, 1.3 mmol, 72%) as a colourless oil.

^{1}H NMR (500 MHz, $CDCl_3$) δ 4.13 (t, *J* = 6.6 Hz, 2H, CH_2-C1), 3.78 (dt, *J* = 4.2, 4.2, 4.2 Hz, 2H, CH_2-C4), 3.30 (t, *J* = 6.6 Hz, 2H, CH_2-C2), 3.26 – 3.21 (m, 2H, CH_2-C3), 2.10 (br s, 1H, OH).

^{13}C NMR (126 MHz, $CDCl_3$) δ 60.4 (CH_2-C4), 57.8 (CH_2-C1), 49.2 (CH_2-C3), 36.2 (CH_2-C2).

HRMS (ESI positive) calcd for $C_4H_9NNaO_3S$ $[M+Na]^+$ 174.0202, found 174.0195.

Biological activity evaluation

Enzymatic activity was determined by monitoring the inhibition of the hydrolysis of the fluorogenic substrate Suc-LLVY-AMC **126** at RT for 1 h. Fluorescence was measured at λ_{exc} = 360, λ_{em} = 460 nm. Point-measurements were performed after 1 h incubation of the enzyme with the inhibitors on a shaker, previous to substrate addition. Assays were performed in 96-wells CORNING half area plates using a final volume of 50 µL. The assays were performed in duplicates with three repetitions. The inhibitory activities of compounds were expressed as IC_{50} values. The values were obtained by plotting the percentage of enzymatic activity against the logarithm of the inhibitor concentrations.

The experimental data were fitted to the equation:

$$\%\ \text{Residual Activity} = \frac{100}{1 + 10^{((\text{LogIC50} - \text{Log}c\ (\text{inhibitor}))* \text{ Hill Slope})}}$$

using GraphPad Prism software version 5.

Compounds 120-125

Inhibition of the proteasome by compounds **120-125** was determined with an Enzo Life Sciences® 20S Proteasome Assay Kit for Dug Discovery. The enzyme solution (12.5 nM) was prepared by dilution of the supplied 20S proteasome (1 mg/mL) in assay buffer (50 mM Tris/HCl, pH 7.5, 25 mM KCl, 10 mM NaCl, 1 mM $MgCl_2$). A 37.5 mM stock solution of the substrate was made by dissolving Suc-LLVY-AMC **126** (500 µg) in DMSO. This was diluted with assay buffer, resulting in a 375 µM substrate solution. DMSO was used for the inhibitor stock solution (4 mM) and the corresponding dilutions.

Procedure 1: To each well in a typical assay it was added enzyme solution (10 µL), inhibitor solution (5 µL), substrate solution (10 µL) and buffer (25 µL). Final concentrations in the wells were: enzyme: 2.5 nM; substrate: 75 µM; inhibitor: 0.002, 0.25, 2.5, 25, 50, 75, 100, 200, 300 and 400 µM. Epoxomicin (**29**) was used as reference inhibitor. For the positive controls DMSO was added instead of inhibitor solution, thereby maintaining a final concentration of 10% DMSO per well.

Procedure 2: To each well in a typical assay it was added enzyme solution (10 µL), inhibitor solution (5 µL), substrate solution (10 µl), buffer (20 µL) and extra DMSO (5 µL). Final concentrations in the wells were: enzyme: 2.5 nM; substrate: 75 µM; inhibitor: 0.002, 0.25, 2.5, 25, 50, 75, 100, 200, 300 and 400 µM. Epoxomicin (**29**) was used as reference inhibitor. For the positive controls DMSO was added instead of inhibitor solution, thereby maintaining a final concentration of 20% DMSO per well.

Experimental data could not be fit to the equation.

Compounds 138, **139**, **30** and **32**

Inhibition of the proteasome by compounds **138**, **139**, **30** and **32** was determined with a VIVAdetect™ 20S Proteasome Assay Kit PLUS. The enzyme solution (25 nM) was prepared by dilution of the supplied 20S proteasome (1 mg/mL) in VIVA buffer. A 10 mM stock solution of the substrate was made by dissolving Suc-LLVY-AMC **126** (500 µg) in DMSO, this was diluted with VIVA buffer, resulting in a 100 µM substrate solution. DMSO was used for the inhibitor stock solution (500 µM) and the corresponding dilutions. To each well in a typical assay it was added enzyme solution (5 µL), inhibitor solution (4 µL), substrate solution (5 µl) and buffer (36 µL). Final concentrations in the wells were: enzyme: 2.5 nM; substrate: 100 µM; inhibitor: 0.4, 2, 10, 50, 100, 200, 400, 800, 1600 and 8000 nM. MG 132 (**28**) was used as reference inhibitor. For the positive controls DMSO was added instead of inhibitor solution, thereby maintaining a final concentration of 9% DMSO per well.

	Leu_3-VSF 138	Leu_4-VSF 139	Leu_3-PSF 30	Leu_4-PSF 32
log(inhibitor) vs. normalized response -- Variable slope				
Best-fit values				
LogIC50	2.339	1.994	1.950	1.251
HillSlope	-0.8372	-0.7070	-0.9853	-0.7479
IC50	218.3	98.52	89.06	17.82
Std. Error				
LogIC50	0.02227	0.04302	0.03518	0.1005
HillSlope	0.03850	0.05145	0.07623	0.09885
95% Confidence Intervals				
LogIC50	2.294 to 2.384	1.907 to 2.080	1.877 to 2.022	1.043 to 1.458
HillSlope	-0.9145 to -0.7600	-0.8104 to -0.6037	-1.142 to -0.8286	-0.9519 to -0.5439
IC50	196.9 to 241.9	80.75 to 120.2	75.40 to 105.2	11.05 to 28.74
Goodness of Fit				
Degrees of Freedom	53	52	26	24
R^2	0.9780	0.9445	0.9757	0.9079
Absolute Sum of Squares	1398	3531	898.5	2808
Sy.x	5.137	8.241	5.879	10.82
Number of points				
Analyzed	55	54	28	26

Buffer stability studies

The aqueous stability of the peptido sulfonyl fluorides **120-125** was determined in phosphate buffered saline (PBS) at pH 6.5, 7.4 and 8.0. The compounds were dissolved in DMSO to a final concentration of 500 μM. 90 μL of stock solution was added to 910 μL of the different buffer systems; giving a final percentage of DMSO of 9%. The degree of hydrolysis under these conditions was monitored by analytical HPLC over 12 h. First measurement (time = 0 h) was taken as the reference peak and the remaining percentage of inhibitor was plotted against the time.

6. References

(1) Powers, J. C.; Asgian, J. L.; Ekici, Ö. D.; James, K. E. *Chem. Rev.* **2002**, *102* (12), 4639–4750.

(2) Babine, R. E.; Bender, S. L. *Chem. Rev.* **1997**, *97* (5), 1359–1472.

(3) Dash, C.; Kulkarni, A.; Dunn, B.; Rao, M. *Crit. Rev. Biochem. Mol. Biol.* **2003**, *38* (2), 89–119.

(4) Hedstrom, L. *Chem. Rev.* **2002**, *102* (12), 4501–4523.

(5) Bachovchin, D. A.; Cravatt, B. F. *Nat. Rev. Discov.* **2012**, *11* (1), 52–68.

(6) Leung, Donmienne; Abbenante, Giovanni; Fairlie, D. P. *J.Med.Chem.* **2000**, *43* (3), 305–341.

(7) Schweitzer, A.; Aufderheide, A.; Rudack, T.; Beck, F.; Pfeifer, G.; Plitzko, J. M.; Sakata, E.; Schulten, K.; Förster, F.; Baumeister, W. *Proc. Natl. Acad. Sci. U. S. A.* **2016**, *113* (28), 7816–7821.

(8) Śledź, P.; Baumeister, W. *Annu. Rev. Pharmacol. Toxicol.* **2016**, *56*, 191–209.

(9) Bhattacharyya, S.; Yu, H.; Mim, C.; Matouschek, A. *Nat. Rev. Mol. Cell Biol.* **2014**, *15* (2), 122–133.

(10) Bedford, L.; Lowe, J.; Dick, L. R.; Mayer, R. J.; Brownell, J. E. *Nat. Rev. Drug Discov.* **2011**, *10* (1), 29–46.

(11) Hershko, A.; Ciechanover, A. *Annu. Rev. Biochem.* **1992**, *61*, 761–807.

(12) Weissman, A. M.; Shabek, N.; Ciechanover, A. *Nat. Rev. Mol. Cell Biol.* **2011**, *12* (9), 605–620.

(13) Ciechanover, A. *EMBO J.* **1998**, *17* (24), 7151–7160.

(14) Myung, J.; Kim, K. B.; Crews, C. M. *Med. Res. Rev.* **2001**, *21* (4), 245–273.

(15) Schulman, B. a; Wade Harper, J. *Nat. Rev. Mol. Cell Biol.* **2009**, *10* (5), 319–331.

(16) Hershko, A.; Ciechanover, A. *J. Biosci.* **2006**, *31* (March), 137–155.

(17) Ardley, H. C.; Robinson, P. A. *Essays Biochem.* **2005**, *4*, 15–30.

(18) Voges, D.; Zwickl, P.; Baumeister, W. *Annu. Rev. Biochem.* **1999**, *68*, 1015–1068.

(19) Finley, D. *Annu. Rev. Biochem.* **2009**, *78*, 477–513.

(20) Rosenzweig, R.; Osmulski, P. a; Gaczynska, M.; Glickman, M. H. *Nat. Struct. Mol. Biol.* **2008**, *15* (6), 573–580.

(21) Löwe, J.; Stock, D.; Jap, B.; Zwickl, P.; Baumeister, W.; Huber, R. *Science*

1995, *268* (5210), 533–539.

(22) Groll, M.; Clausen, T. *Curr. Opin. Struct. Biol.* **2003**, *13* (6), 665–673.

(23) Groll, M.; Ditzel, L.; Löwe, J.; Stock, D.; Bochtler, M.; Bartunik, H. D.; Huber, R. *Nature* **1997**, *386* (6624), 463–471.

(24) Borissenko, L.; Groll, M. *Biol. Chem.* **2007**, *388* (9), 947–955.

(25) Groll, M.; Nazif, T.; Huber, R.; Bogyo, M. *Chem. Biol.* **2002**, *9* (5), 655–662.

(26) Gibbard, S.; Levy, E. H.; Lunine, J. I. *Nature* **1995**, *378* (6557), 592–595.

(27) Seemüller, E.; Lupas, A.; Baumeister, W. *Nature* **1996**, *382* (6590), 468–470.

(28) Marques, A. J.; Palanimurugan, R.; Mafias, A. C.; Ramos, P. C.; Dohmen, R. J. *Chem. Rev.* **2009**, *109* (4), 1509–1536.

(29) Huber, E. M.; Heinemeyer, W.; Li, X.; Arendt, C. S.; Hochstrasser, M.; Groll, M. *Nat. Commun.* **2016**, *7*, 1–10.

(30) Borissenko, L.; Groll, M. *Chem. Rev.* **2007**, *107* (3), 687–717.

(31) Xin, B. T.; De Bruin, G.; Huber, E. M.; Besse, A.; Florea, B. I.; Filippov, D. V.; Van Der Marel, G. A.; Kisselev, A. F.; Van Der Stelt, M.; Driessen, C.; Groll, M.; Overkleeft, H. S. *J. Med. Chem.* **2016**, *59* (15), 7177–7187.

(32) Dahlmann, B.; Ruppert, T.; Kuehn, L.; Merforth, S.; Kloetzel, P. M. *J. Mol. Biol.* **2000**, *303* (5), 643–653.

(33) Groettrup, M.; Schmidtke, G. *Drug Discov. Today* **1999**, *4* (2), 63–71.

(34) Hewitt, E. W. *Immunology* **2003**, *110* (2), 163–169.

(35) Groettrup, M.; Kirk, C. J.; Basler, M. *Nat. Rev. Immunol.* **2010**, *10* (1), 73–78.

(36) Kimura, H.; Caturegli, P.; Takahashi, M.; Suzuki, K. *J. Immunol. Res.* **2015**, *2015*.

(37) Huber, E. M.; Basler, M.; Schwab, R.; Heinemeyer, W.; Kirk, C. J.; Groettrup, M.; Groll, M. *Cell* **2012**, *148* (4), 727–738.

(38) Murata, S.; Sasaki, K.; Kishimoto, T.; Niwa, S.; Hayashi, H.; Takahama, Y.; Tanaka, K. *Science (80-.).* **2007**, *316* (5829), 1349–1353.

(39) Adams, J.; Behnke, M.; Chen, S.; Cruickshank, A. A.; Dick, L. R.; Grenier, L.; Klunder, J. M.; Ma, Y. T.; Plamondon, L.; Stein, R. L. *Bioorganic Med. Chem. Lett.* **1998**, *8* (4), 333–338.

(40) Rews, C. R. M. C.; Meng, L.; Mohan, R.; Kwok, B. H.; Elofsson, M.; Sin, N.; Crews, C. M. *Proc. Natl. Acad. Sci. U. S. A.* **1999**, *96* (18), 10403–10408.

(41) Orlowski, R. Z. *Cell Death Differ.* **1999**, *6* (4), 303–313.

(42) Nencioni, a; Grünebach, F.; Patrone, F.; Ballestrero, A.; Brossart, P.

Leukemia **2007**, *21*, 30–36.

(43) Spataro, V.; Norbury, C.; Harris, A. *Br. Joumal Cancer* **1998**, *77* (3), 448–455.

(44) McBride, W. H.; Iwamoto, K. S.; Syljuasen, R.; Pervan, M.; Pajonk, F. *Oncogene* **2003**, *22* (37), 5755–5773.

(45) Almond, J. B.; Cohen, G. M. *Leukemia* **2002**, *16* (4), 433–443.

(46) Chauhan, D.; Hideshima, T.; Anderson, K. C. *Annu. Rev. Pharmacol. Toxicol.* **2005**, *45* (1), 465–476.

(47) Guzman, M. L.; Swiderski, C. F.; Howard, D. S.; Grimes, B. A.; Rossi, R. M.; Szilvassy, S. J.; Jordan, C. T. *Proc. Natl. Acad. Sci. U. S. A.* **2002**, *99* (25), 16220–16225.

(48) Nalepa, G.; Rolfe, M.; Harper, J. W. *Nat. Rev. Drug Discov.* **2006**, *5* (7), 596–613.

(49) Chen, F.; Liu, Y.; Yang, C.; Yang, C. *IOVS* **2012**, *53* (7), 3682–3694.

(50) Gräwert, M. A.; Groll, M. *Chem. Commun.* **2012**, *48* (10), 1364–137.

(51) Huber, E. M.; Groll, M. *Angew. Chemie - Int. Ed.* **2012**, *51* (35), 8708–8720.

(52) Puente, X. S.; Sánchez, L. M.; Overall, C. M.; López-Otín, C. *Nat. Rev. Genet.* **2003**, *4* (7), 544–558.

(53) Verdoes, M.; Florea, B. I.; van der Linden, W. a; Renou, D.; van den Nieuwendijk, A. M. C. H.; van der Marel, G. a; Overkleeft, H. S. *Org. Biomol. Chem.* **2007**, *5* (9), 1416–1426.

(54) Singh, J.; Petter, R. C.; Baillie, T. A.; Whitty, A. *Nat. Rev. Drug Discov.* **2011**, *10* (4), 307–317.

(55) Stein, M. L.; Cui, H.; Beck, P.; Dubiella, C.; Voss, C.; Krüger, A.; Schmidt, B.; Groll, M. *Angew. Chemie - Int. Ed.* **2014**, *53* (6), 1679–1683.

(56) Kisselev, A. F.; Van Der Linden, W. A.; Overkleeft, H. S. *Chem. Biol.* **2012**, *19* (1), 99–115.

(57) Groll, M.; Berkers, C. R.; Ploegh, H. L.; Ovaa, H. *Structure* **2006**, *14* (3), 451–456.

(58) Verdoes, M.; Florea, B. I.; Menendez-Benito, V.; Maynard, C. J.; Witte, M. D.; van der Linden, W. A.; van den Nieuwendijk, A. M. C. H.; Hofmann, T.; Berkers, C. R.; van Leeuwen, F. W. B.; Groothuis, T. A.; Leeuwenburgh, M. A.; Ovaa, H.; Neefjes, J. J.; Filippov, D. V.; van der Marel, G. A.; Dantuma, N. P.; Overkleeft, H. S. *Chem. Biol.* **2006**, *13* (11), 1217–1226.

(59) Groll, M.; Kim, K. B.; Kairies, N.; Huber, R.; Crews, C. M. *J. Am. Chem. Soc.* **2000**, *122* (6), 1237–1238.

(60) Gräwert, M. A.; Gallastegui, N.; Stein, M.; Schmidt, B.; Kloetzel, P.-M.;

Huber, R.; Groll, M. *Angew. Chemie Int. Ed.* **2011**, *50* (2), 542–544.

(61) Chauhan, D.; Hideshima, T.; Anderson, K. C. *Br. J. Cancer* **2006**, *95* (8), 961–965.

(62) Anderson, K. C. *Hematology* **2000**, *2000* (1), 147–165.

(63) Ma, M. H.; Yang, H. H.; Parker, K.; Manyak, S.; Friedman, J. M.; Altamirano, C.; Wu, Z.; Borad, M. J.; Frantzen, M.; Roussos, E.; Neeser, J.; Mikail, A.; Adams, J.; Sjak-Shie, N.; Vescio, R. a; Berenson, J. R. *Clin. Cancer Res.* **2003**, *9* (3), 1136–1144.

(64) Altun, M.; Galardy, P. J.; Shringarpure, R.; Hideshima, T.; LeBlanc, R.; Anderson, K. C.; Ploegh, H. L.; Kessler, B. M. *Cancer Res.* **2005**, *65* (17), 7896–7901.

(65) Demo, S. D.; Kirk, C. J.; Aujay, M. A.; Buchholz, T. J.; Dajee, M.; Ho, M. N.; Jiang, J.; Laidig, G. J.; Lewis, E. R.; Parlati, F.; Shenk, K. D.; Smyth, M. S.; Sun, C. M.; Vallone, M. K.; Woo, T. M.; Molineaux, C. J.; Bennett, M. K. *Cancer Res.* **2007**, *67* (13), 6383–6391.

(66) Hideshima, T.; Richardson, P.; Chauhan, D.; Palombella, V. J.; Elliott, P. J.; Adams, J.; Anderson, K. C. *Cancer Res.* **2001**, *61* (7), 3071–30766.

(67) Adams, J.; Kauffman, M. *Cancer Invest.* **2004**, *22* (2), 304–311.

(68) Argyriou, A. A.; Iconomou, G.; Kalofonos, H. P.; Argyriou, A. A.; Iconomou, G.; Iconomou, G.; Kalofonos, H. P.; Kalofonos, H. P. *Blood* **2008**, *112* (5), 1593–1599.

(69) Ruschak, A. M.; Slassi, M.; Kay, L. E.; Schimmer, A. D. *JNCI J. Natl. Cancer Inst.* **2011**, *103* (13), 1007–1017.

(70) Harshbarger, W.; Miller, C.; Diedrich, C.; Sacchettini, J. *Structure* **2015**, *23* (2), 418–424.

(71) McBride, A.; Klaus, J. O.; Stockerl-Goldstein, K. *Am. J. Health. Syst. Pharm.* **2015**, *72* (5), 353–360.

(72) Azab, A. K.; Muz, B.; Ghazarian, R.; Ou, M.; Luderer, M.; Kusdono, H. *Drug Des. Devel. Ther.* **2016**, *10*, 217.

(73) Shirley, M. *Drugs* **2016**, *76* (3), 405–411.

(74) Lin, E. H. B.; Von Korff, M.; Peterson, D.; Ludman, E. J.; Ciechanowski, P.; Katon, W. *Am. J. Manag. Care* **2014**, *20* (11), 887–893.

(75) Moreau, P.; Richardson, P. G.; Cavo, M.; Orlowski, R. Z.; Miguel, F. S.; Palumbo, A. *Blood* **2015**, *120* (5), 947–960.

(76) Schrader, J.; Henneberg, F.; Mata, R. A.; Tittmann, K.; Schneider, T. R.; Stark, H.; Bourenkov, G.; Chari, A. *Science (80-.).* **2016**, *353* (6299), 594–598.

(77) Ja, S.; Groll, M.; Huber, R.; Wolf, D. H.; Heinemeyer, W. *J. Mol. Biol* **1999**, *291*, 997–1013.

(78) Britton, M.; Lucas, M. M.; Downey, S. L.; Screen, M.; Pletnev, A. A.; Verdoes, M.; Tokhunts, R. A.; Amir, O.; Goddard, A. L.; Pelphrey, P. M.; Wright, D. L.; Overkleeft, H. S.; Kisselev, A. F. *Chem. Biol.* **2009**, *16* (12), 1278–1289.

(79) Sierra, H.; Cordova, M.; Chen, C.-S. J.; Rajadhyaksha, M. *J. Invest. Dermatol.* **2015**, *135* (2), 612–615.

(80) de Bruin, G.; Huber, E. M.; Xin, B.; van Rooden, E. J.; Al-Ayed, K.; Kim, K.; Kisselev, A. F.; Driessen, C.; van der Stelt, M.; van der Marel, G. A.; Groll, M.; Overkleeft, H. S. *J. Med. Chem.* **2014**, *57* (14), 6197–6209.

(81) Kemp, D. K. M. and A. *Nature* **1954**, *173*, 33–34.

(82) Fahrney, D. E.; Gold, A. M. *J. Am. Chem. Soc.* **1963**, *85* (7), 997–1000.

(83) Acta, B.; Chemistry, C. *Biochim. Biophys. Acta - Mol. Cell Res.* **1976**, *439*, 194–205.

(84) Lively, M. O.; Powers, J. C. *Biochim. Biophys. Acta* **1978**, *525*, 171–179.

(85) Narayanan, A.; Jones, L. H. *Chem. Sci.* **2015**, *6* (5), 2650–2659.

(86) Dong, J.; Krasnova, L.; Finn, M. G.; Barry Sharpless, K. *Angew. Chemie - Int. Ed.* **2014**, *53* (36), 9430–9448.

(87) Kiang, T.; Zare, R. N. *J. Chem. Soc. Chem. Commun.* **1980**, No. 24, 1228–1229.

(88) Kice, J. L.; Lunney, E. A. *J. Org. Chem.* **1975**, *40* (14), 2125–2127.

(89) Landini, D.; Maia, A.; Rampoldi, A. *J. Org. Chem.* **1989**, *54* (11), 328–332.

(90) Pal, P. K.; Wechter, W. J.; Colman, R. F. *Biochemistry* **1975**, *14* (4), 707–715.

(91) Gushwa, N. N.; Kang, S.; Chen, J.; Taunton, J. *J. Am. Chem. Soc.* **2012**, *134* (50), 20214–20217.

(92) Alapafuja, S. O.; Nikas, S. P.; Bharathan, I. T.; Shukla, V. G.; Nasr, M. L.; Bowman, A. L.; Zvonok, N.; Li, J.; Shi, X.; Engen, J. R.; Makriyannis, A. *J. Med. Chem.* **2012**, *55* (22), 10074–10089.

(93) Baraldi, P. G.; Cacciari, B.; Moro, S.; Romagnoli, R.; Ji, X.; Jacobson, K. A.; Gessi, S.; Borea, P. A.; Spalluto, G. *J. Med. Chem.* **2001**, *44* (17), 2735–2742.

(94) Grimster, N. P.; Connelly, S.; Baranczak, A.; Dong, J.; Krasnova, L. B.; Sharpless, K. B.; Powers, E. T.; Wilson, I. A.; Kelly, J. W. *J. Am. Chem. Soc.* **2013**, *135* (15), 5656–5668.

(95) Brouwer, A. J.; Ceylan, T.; Linden, T. v d; Liskamp, R. M. J. *Tetrahedron Lett.* **2009**, *50* (26), 3391–3393.

(96) Brouwer, A. J.; Ceylan, T.; Jonker, A. M.; Linden, T. Van Der; Liskamp, R. M. J. *Bioorganic Med. Chem.* **2011**, *19* (7), 2397–2406.

(97) Brouwer, A. J.; Jonker, A.; Werkhoven, P.; Kuo, E.; Li, N.; Gallastegui, N.; Kemmink, J.; Florea, B. I.; Groll, M.; Overkleeft, H. S.; Liskamp, R. M. J. *J. Med. Chem.* **2012**, *55* (24), 10995–11003.

(98) Tschan, S.; Brouwer, A. J.; Werkhoven, P. R.; Jonker, A. M.; Wagner, L.; Knittel, S.; Aminake, M. N.; Pradel, G.; Joanny, F.; Liskamp, R. M. J.; Mordmuller, B. *Antimicrob. Agents Chemother.* **2013**, *57* (8), 3576–3584.

(99) Dubiella, C.; Cui, H.; Gersch, M.; Brouwer, A. J.; Sieber, S. A.; Krüger, A.; Liskamp, R. M. J.; Groll, M. *Angew. Chemie - Int. Ed.* **2014**, *53* (44), 11969–11973.

(100) Cepanec, I.; Litvic, M.; Mikuldas, H.; Bartolincic, A.; Vinkovic, V. *ChemInform* **2003**, *34* (29), 23–28.

(101) Mori, A.; Miyakawa, Y.; Ohashi, E.; Haga, T.; Maegawa, T.; Sajiki, H. *Org. Lett.* **2006**, *8* (15), 3279–3281.

(102) Bernotas, R. C.; Cube, R. V. *Synth. Commun.* **1990**, *20* (8), 1209–1212.

(103) Xu, J.; Xu, S. *Synthesis (Stuttg).* **2004**, No. 2, 276–282.

(104) Veitía, M. S.-I.; Brun, P. L.; Jorda, P.; Falguières, A.; Ferroud, C. *Tetrahedron: Asymmetry* **2009**, *20* (18), 2077–2089.

(105) Meng, F.; Chen, N.; Xu, J. *Sci. China Chem.* **2012**, *55* (12), 2548–2553.

(106) L'Heureux, A.; Beaulieu, F.; Bennett, C.; Bill, D. R.; Clayton, S.; LaFlamme, F.; Mirmehrabi, M.; Tadayon, S.; Tovell, D.; Couturier, M. *J. Org. Chem.* **2010**, *75* (10), 3401–3411.

(107) Zurwerra, D.; Gertsch, J.; Altmann, K.-H. *Org. Lett.* **2010**, *12* (10), 2302–2305.

(108) Tan, D. Q.; Younai, A.; Pattawong, O.; Fettinger, J. C.; Cheong, P. H.-Y.; Shaw, J. T. *Org. Lett.* **2013**, *15* (19), 5126–5129.

(109) Govek, S. P.; Overman, L. E. *Tetrahedron* **2007**, *63* (35), 8499–8513.

(110) Monge, D.; Daza, S.; Bernal, P.; Fernández, R.; Lassaletta, J. M. *Org. Biomol. Chem.* **2013**, *11* (2), 326–335.

(111) Brouwer, A. J.; Herrero Álvarez, N.; Ciaffoni, A.; van de Langemheen, H.; Liskamp, R. M. J. *Bioorg. Med. Chem.* **2016**, *24* (16), 3429–3435.

(112) Toro, A.; Nowak, P.; Deslongchamps, P. *J. Am. Chem. Soc.* **2000**, *122* (18), 4526–4527.

(113) Baxter, N. J.; Rigoreau, L. J. M.; Laws, A. P.; Page, M. I.; December, R. V. *J. Am. Chem. Soc.* **2000**, No. 122, 3375–3385.

(114) Ballistreri, F. P.; Cantone, A.; Maccarone, E.; Tomaselli, G. A.; Tripolone,

M. *J. Chem. Soc. Perkin Trans. 2* **1981**, No. 3, 438–441.

(115) Mikołajczyk, M. *Phosphorous Sulfur Relat. Elem.* **1986**, *27* (1–2), 31–42.

(116) Tantry, S. J.; Ananda, K.; Suresh Babu, V. V. *Indian J. Chem.* **2002**, *41* (5), 1028–1031.

(117) Gallastegui, N.; Groll, M. Dohmen, R. J., Scheffner, M., Eds.; Methods in Molecular Biology; Humana Press: Totowa, NJ, 2012; Vol. 832, pp 373–390.

(118) Gennari, C.; Salom, B.; Potenza, D.; Williams, A. *Angew. Chemie Int. Ed. English* **1994**, *33* (20), 2067–2069.

(119) Champseix, A.; Chanet, J.; Etienne, A.; Le Berre, A.; Masson, J.; Napierala, C.; Vessiere, R. *Bull. Soc. Chim. Fr.* **1985**, *3*, 463–472.

(120) Chen, Q.; Mayer, P.; Mayr, H. *Angew. Chemie Int. Ed.* **2016**, *55* (41), 12664–12667.

(121) Krutak, J. J.; Burpitt, R. D.; Moore, W. H.; Hyatt, J. A. *J. Org. Chem.* **1979**, *44* (22), 3847–3858.

(122) Page, M. I.; Laws, A. P. *Tetrahedron* **2000**, *56* (31), 5631–5638.

(123) Nagendra, G.; Madhu, C.; Vishwanatha, T. M.; Sureshbabu, V. V. *Tetrahedron Lett.* **2012**, *53* (38), 5059–5063.

(124) Mori, K. *Tetrahedron* **1976**, *32*, 1101–1106.

(125) Arrigo, P. D.; Lattanzio, M.; Fantoni, G. P.; Servi, S. *Tetrahedron: Asymmetry* **1998**, *9*, 4021–4026.

(126) Tian, J.; Gao, W.; Zhou, D.; Zhang, C. *Org. Lett.* **2012**, *14*, 3020–3023.

(127) Kumar, G. D. K.; Baskaran, S. *J. Org. Chem.* **2005**, *70*, 4520–4523.

(128) Burckhardt, P. E.; Waespe-sartevil, N. *Helv. Chim. Acta* **1983**, *66* (38), 450–465.

(129) Dichlorphosphiny, R. Von; Fild, M.; Rieck, H. *Chem. Ber.* **1980**, *113*, 142–151.

7. Appendices

NMR and LC-MS Spectra of Selected Compounds

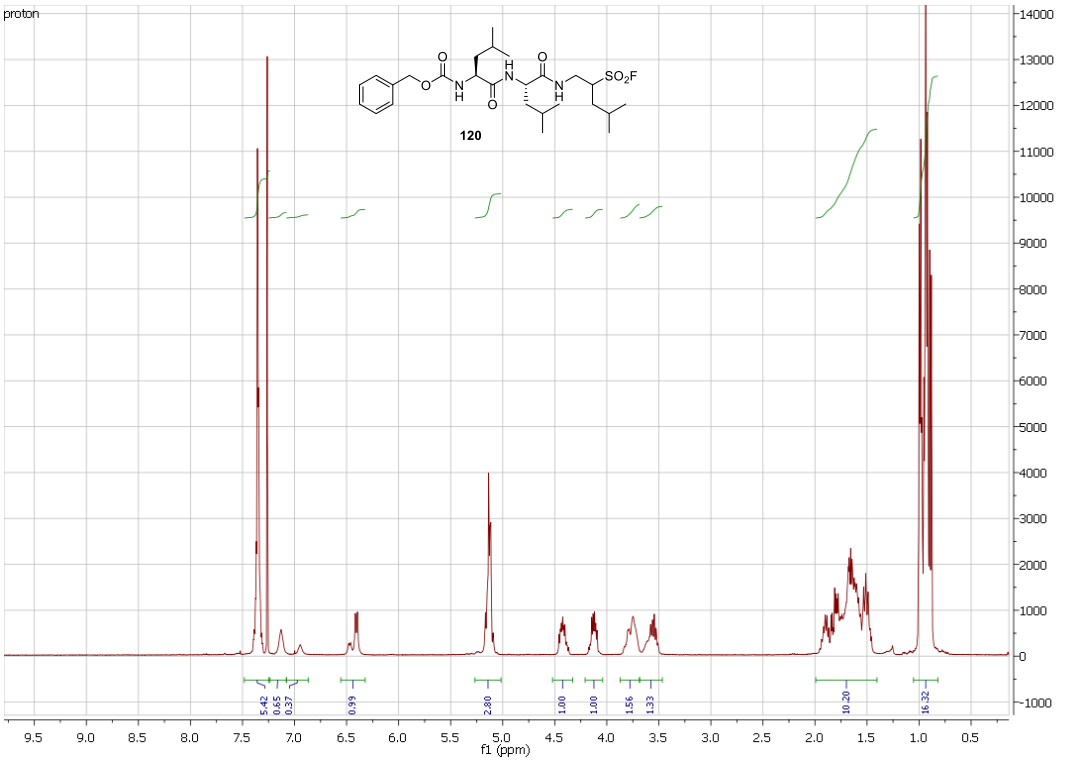

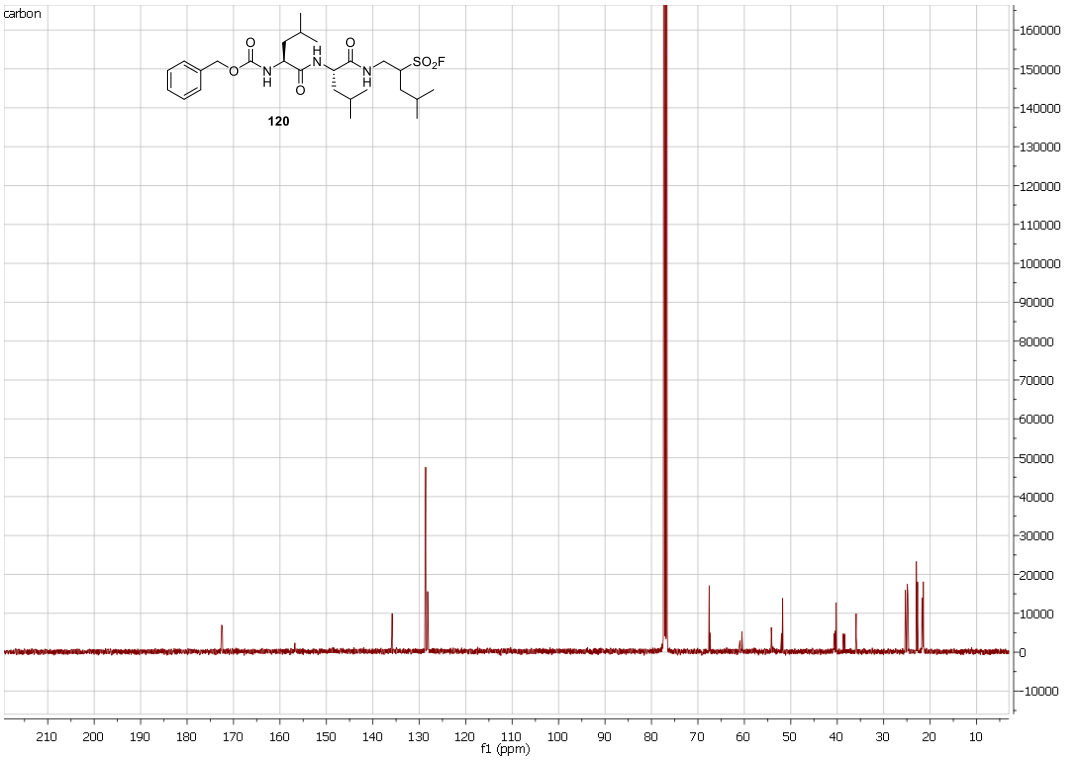

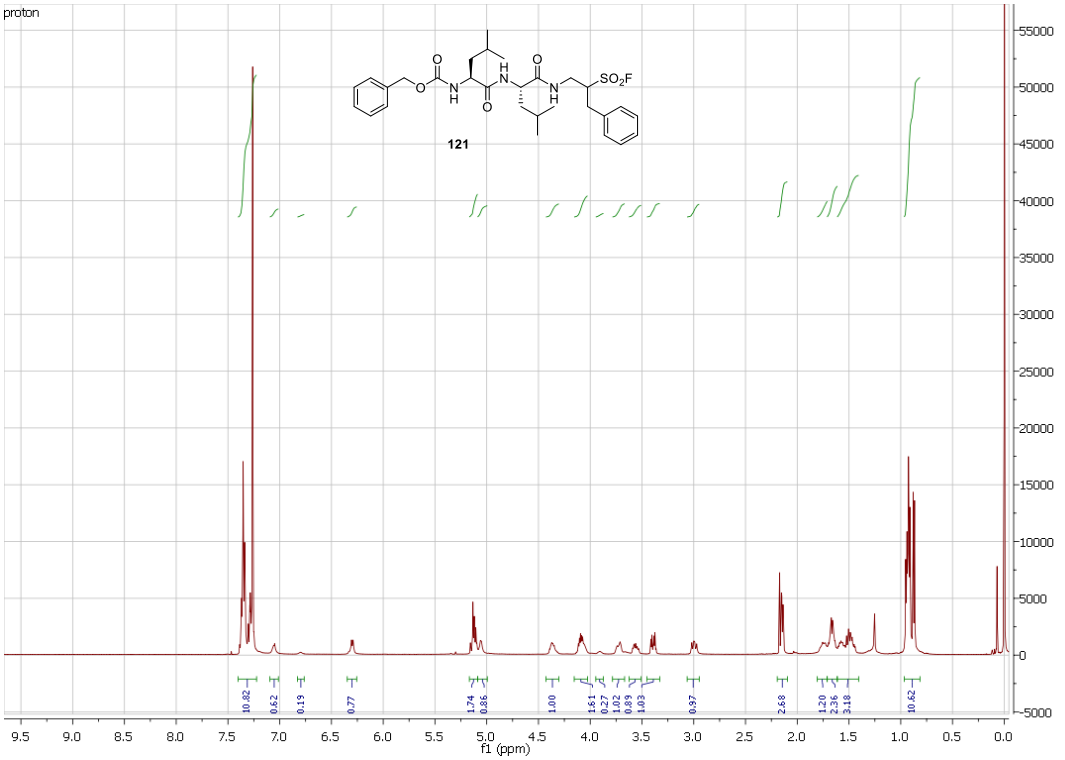
proton
121
f1 (ppm)

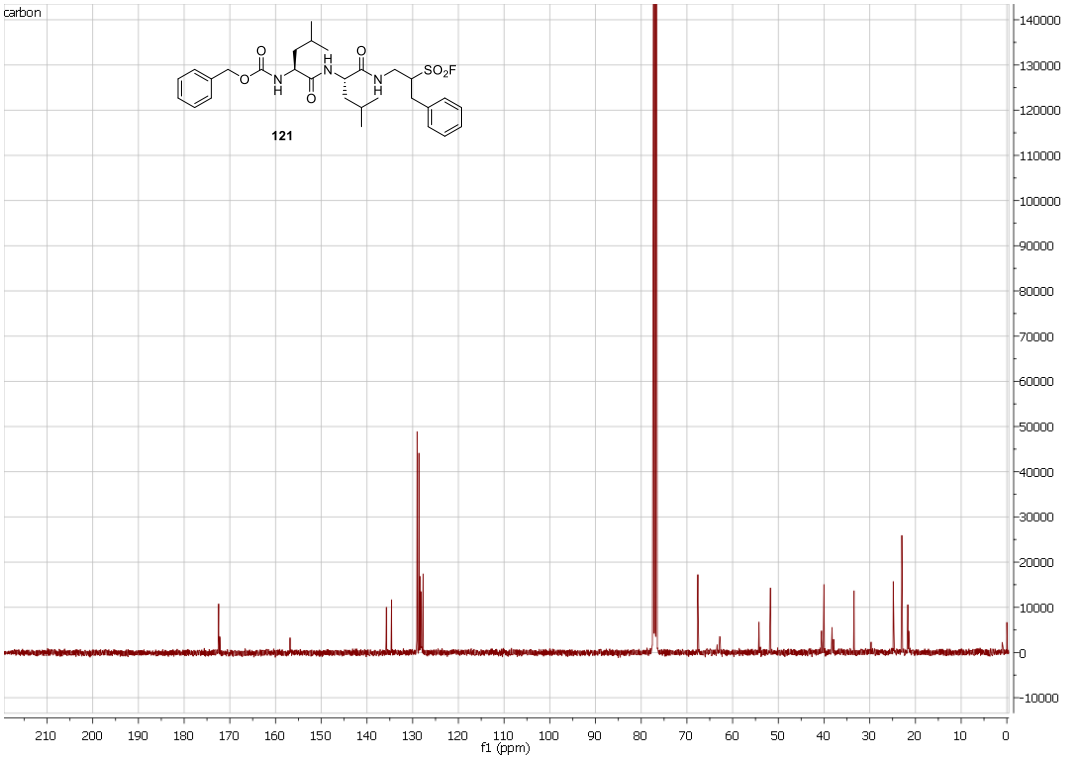
carbon
121
f1 (ppm)

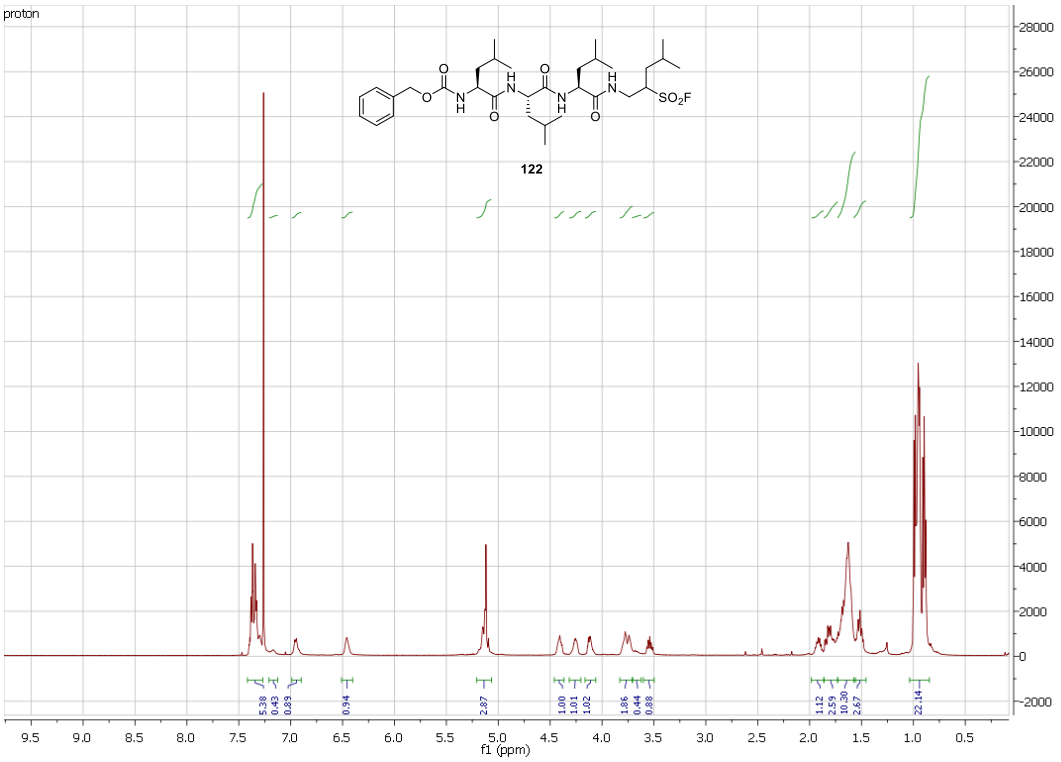
proton
122
f1 (ppm)

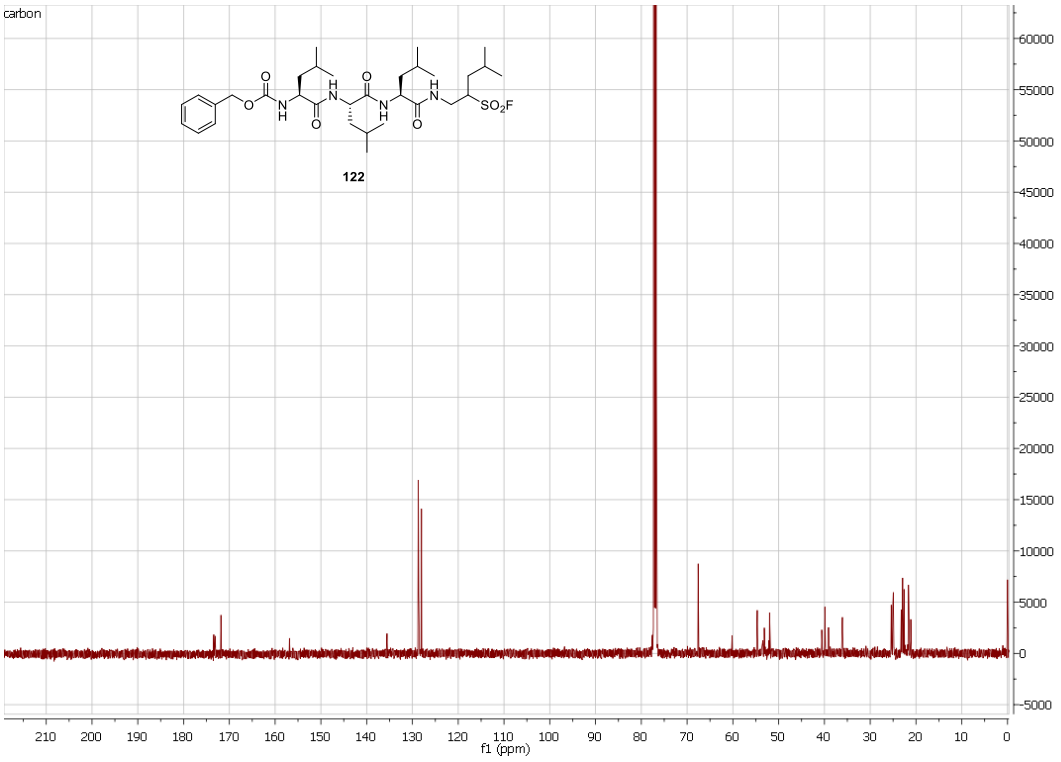
carbon
122
f1 (ppm)

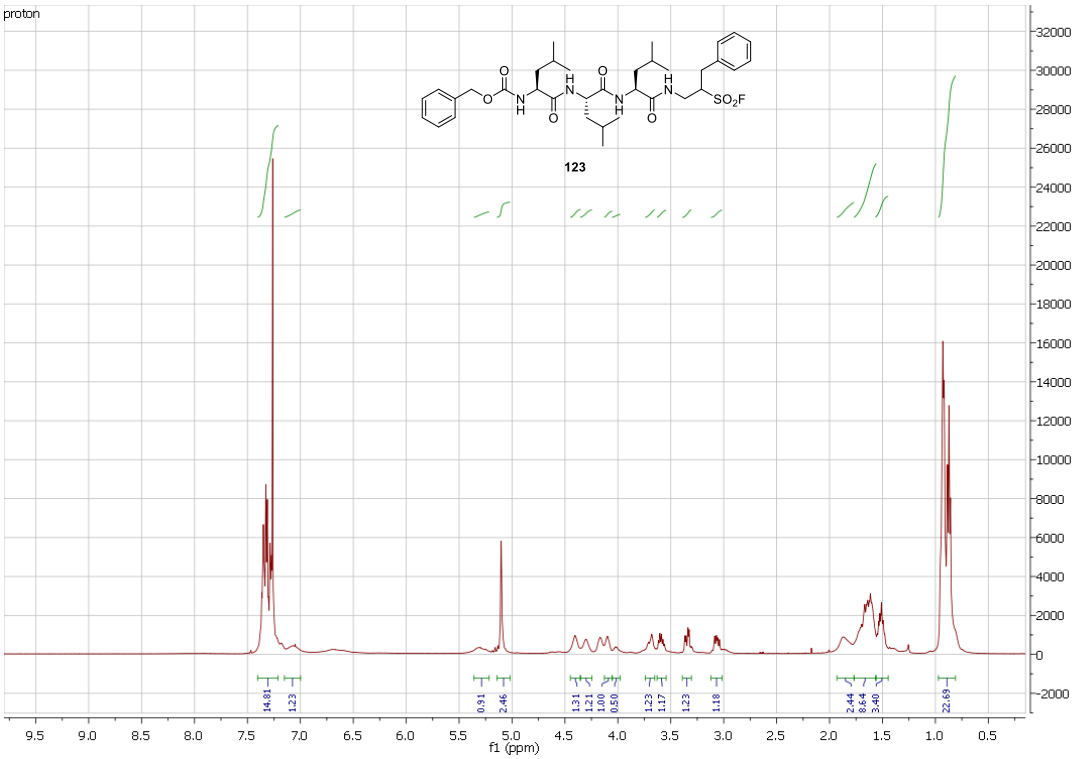
proton
123
f1 (ppm)

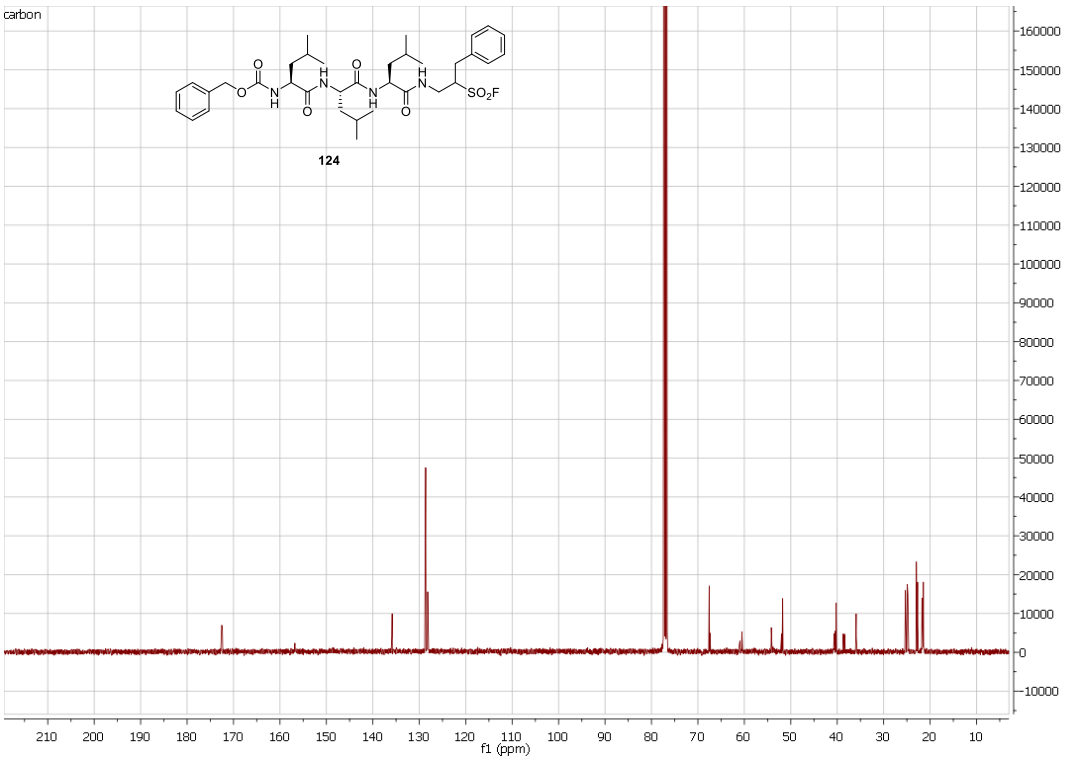
carbon
124
f1 (ppm)

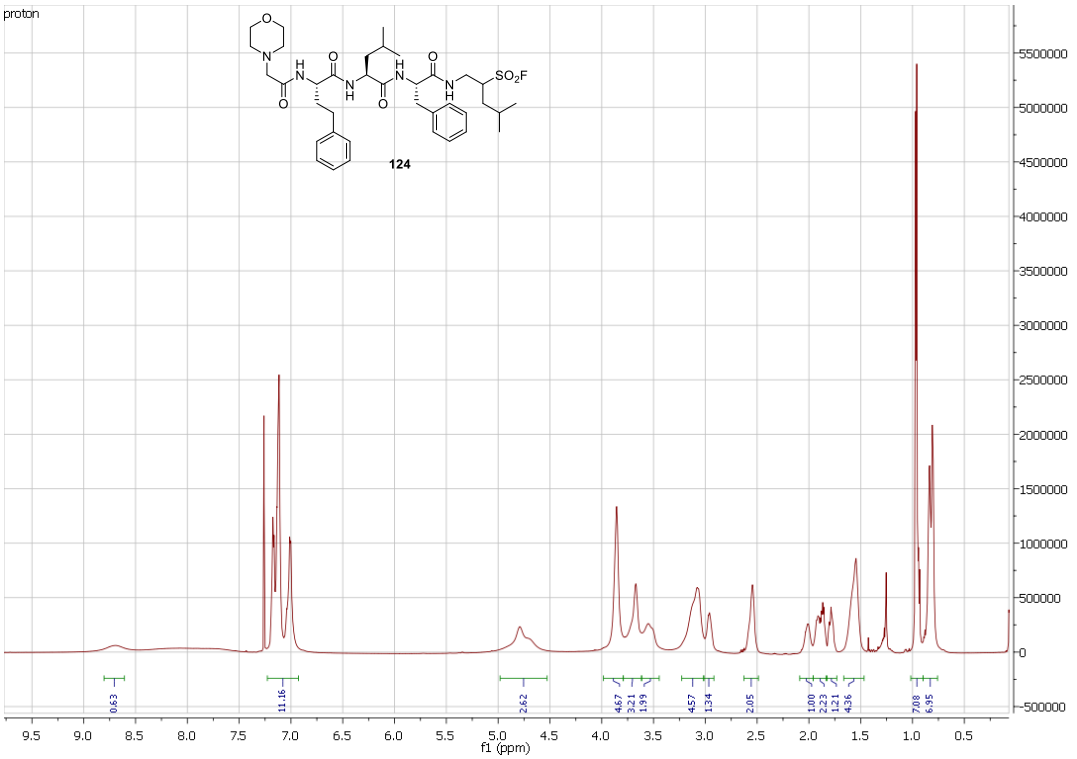
proton
124
f1 (ppm)

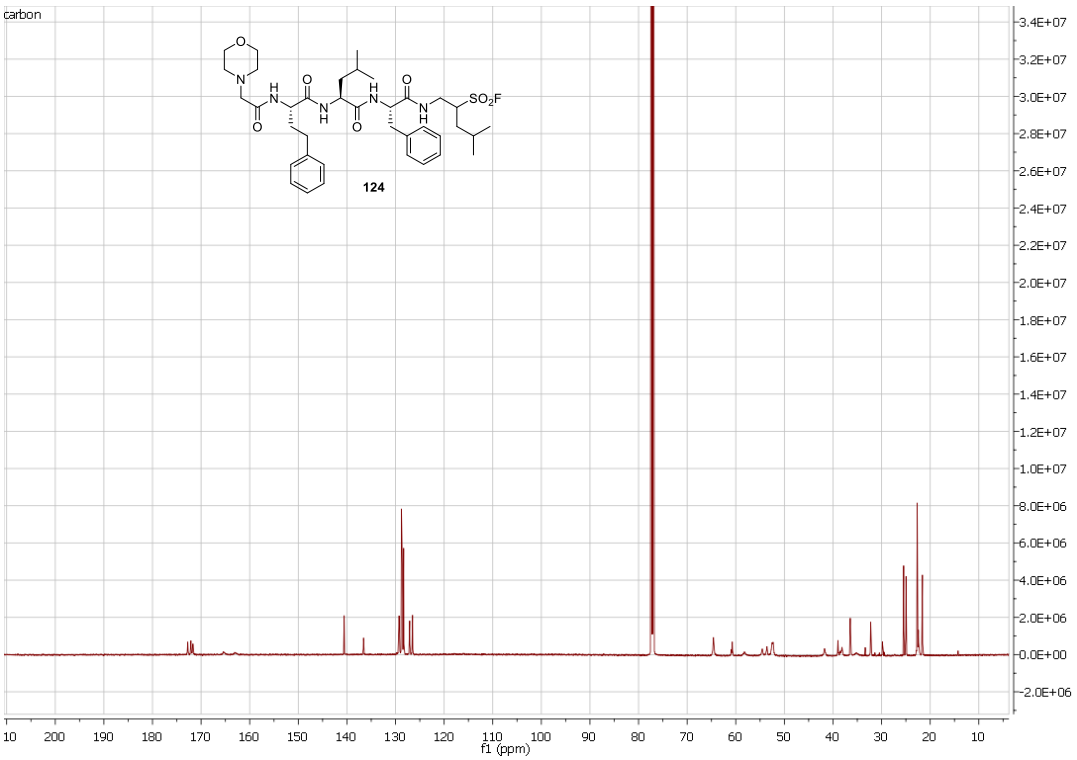
carbon
124
f1 (ppm)

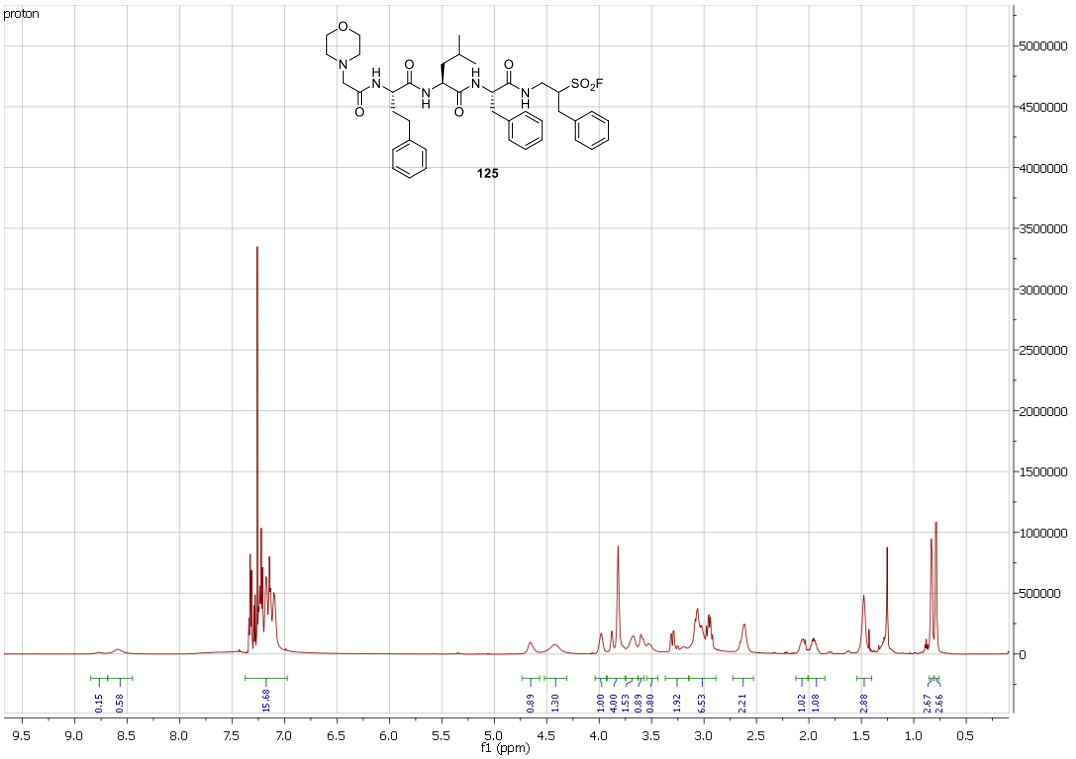
proton
125
f1 (ppm)

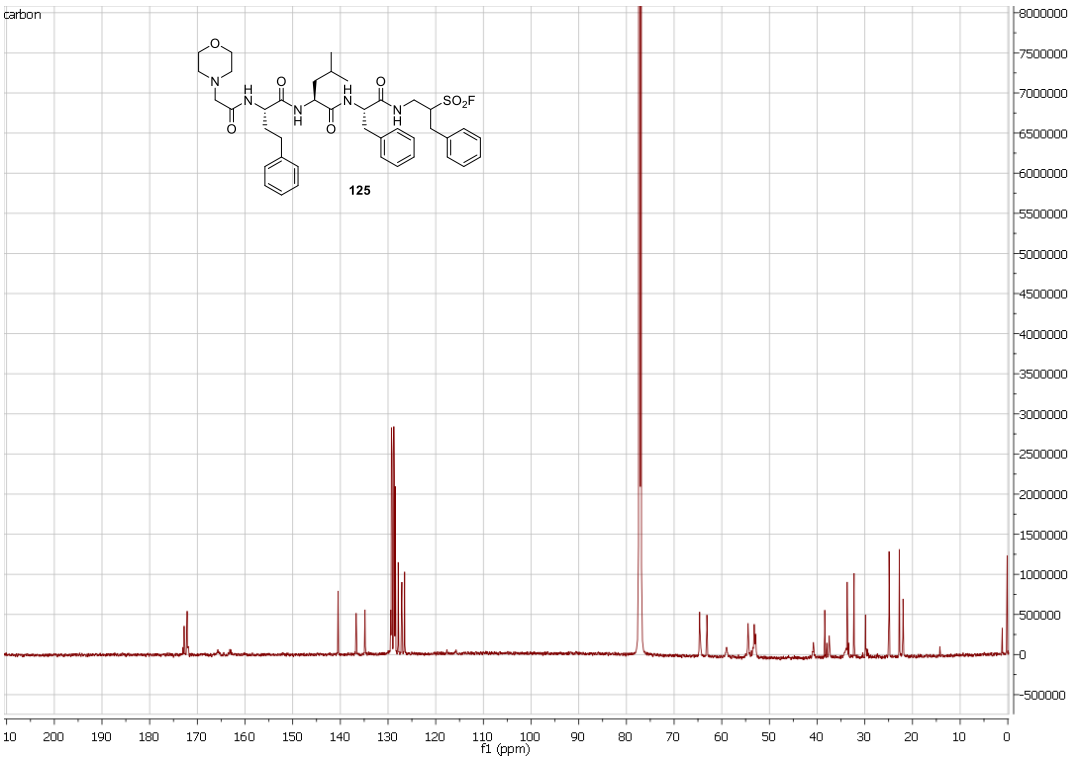
carbon
125
f1 (ppm)

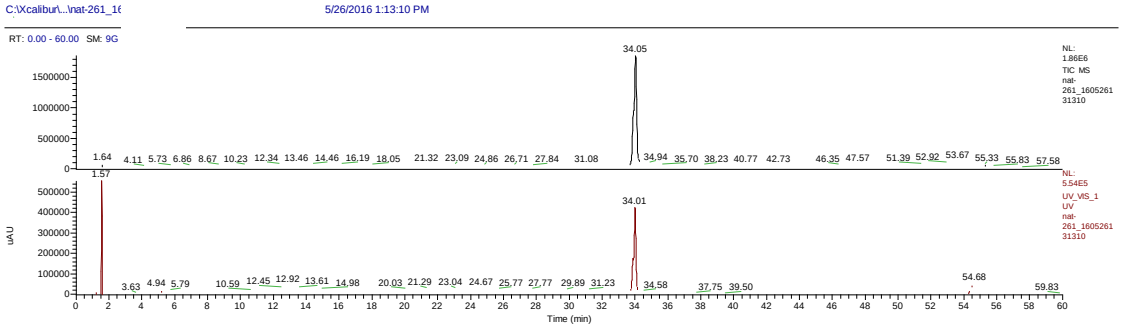
C:\Xcalibur\...\nat-261_16
5/26/2016 1:13:10 PM
RT: 0.00 - 60.00 SM: 9G
NL: 1.86E6 TIC MS nat-261_1605261 31310
NL: 5.54E5 UV_VIS_1 UV nat-261_1605261 31310
uAU
Time (min)

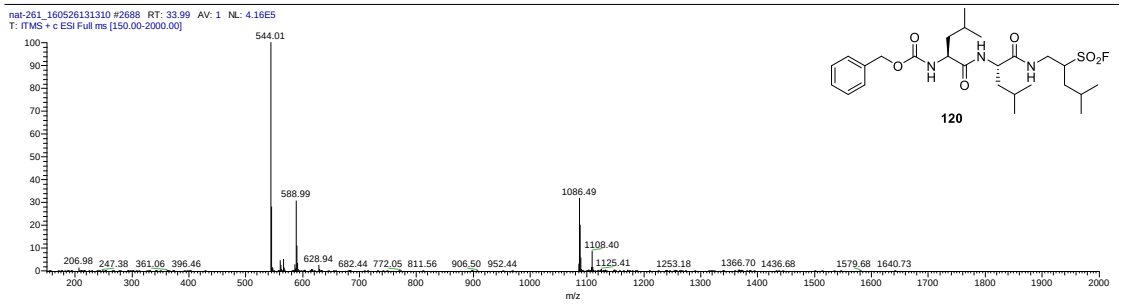
nat-261_160526131310 #2688 RT: 33.99 AV: 1 NL: 4.16E5
T: ITMS + c ESI Full ms [150.00-2000.00]
544.01
588.99
1086.49
1108.40
m/z

120

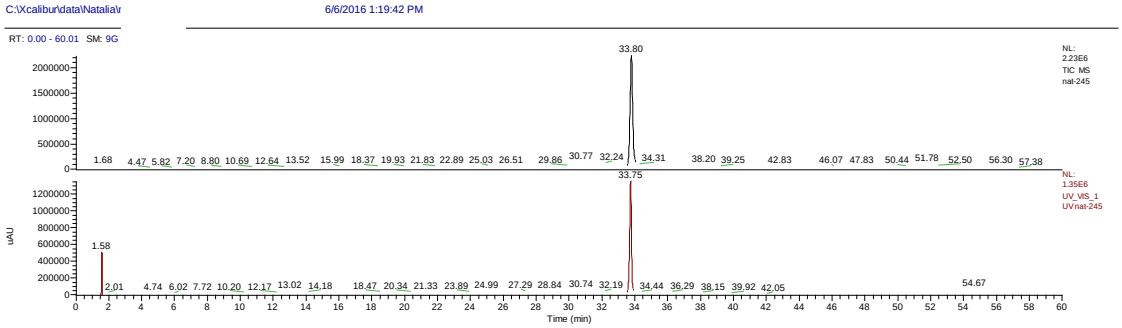
C:\Xcalibur\data\Natalia\r
6/6/2016 1:19:42 PM
RT: 0.00 - 60.01 SM: 9G
NL: 2.23E6 TIC MS nat-245
NL: 1.35E6 UV_VIS_1 UV nat-245
uAU
Time (min)

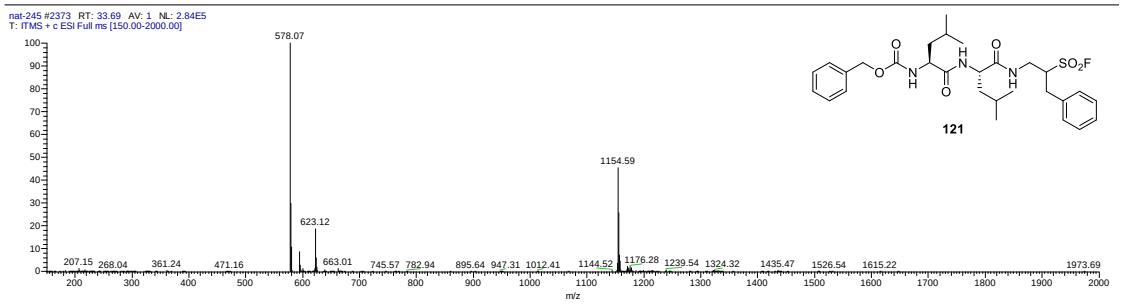
nat-245 #2373 RT: 33.69 AV: 1 NL: 2.84E5
T: ITMS + c ESI Full ms [150.00-2000.00]
578.07
623.12
1154.59
m/z

121

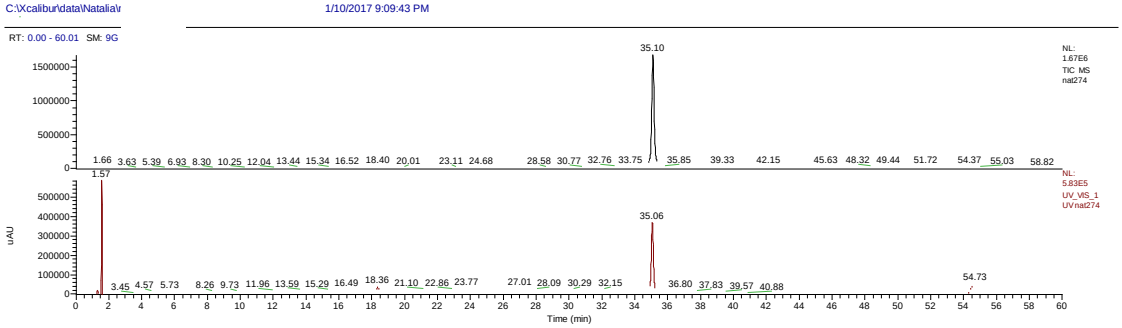
C:\Xcalibur\data\Natalia\r
1/10/2017 9:09:43 PM
RT: 0.00 - 60.01 SM: 9G
NL: 1.67E6 TIC MS nat274
NL: 5.83E5 UV_VIS_1 UV nat274
uAU
Time (min)

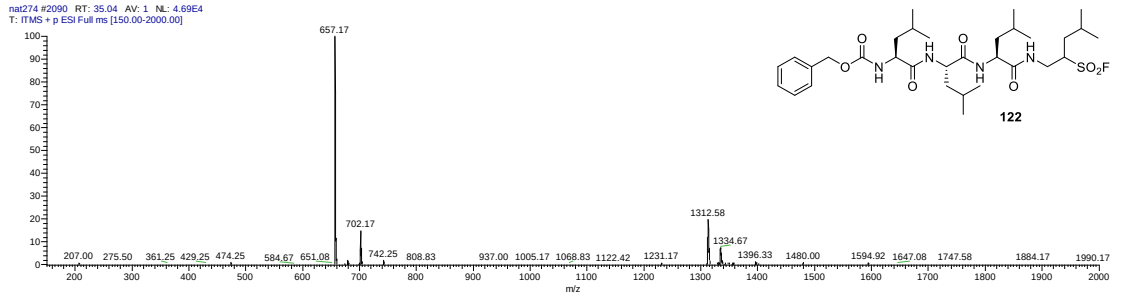
nat274 #2090 RT: 35.04 AV: 1 NL: 4.69E4
T: ITMS + p ESI Full ms [150.00-2000.00]
657.17
702.17
1312.58
1334.67
m/z

122

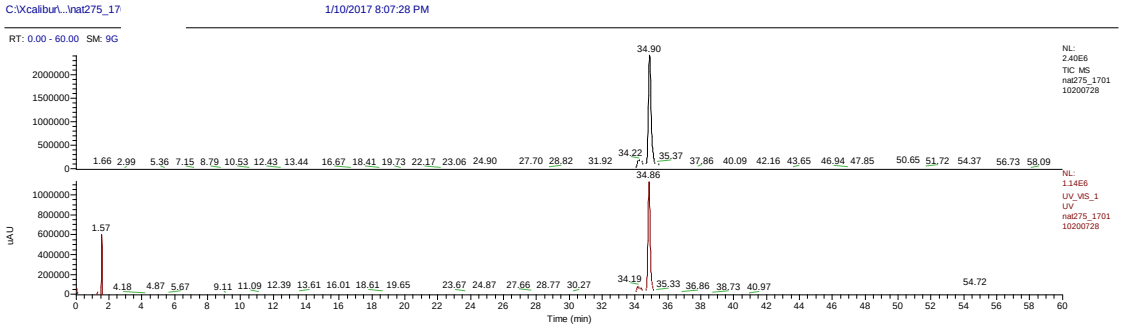
C:\Xcalibur\...\nat275_17
1/10/2017 8:07:28 PM
RT: 0.00 - 60.00 SM: 9G
34.90
NL: 2.40E6 TIC MS nat275_1701 10200728
34.86
NL: 1.14E6 UV_VIS_1 UV nat275_1701 10200728
1.57
uAU
Time (min)

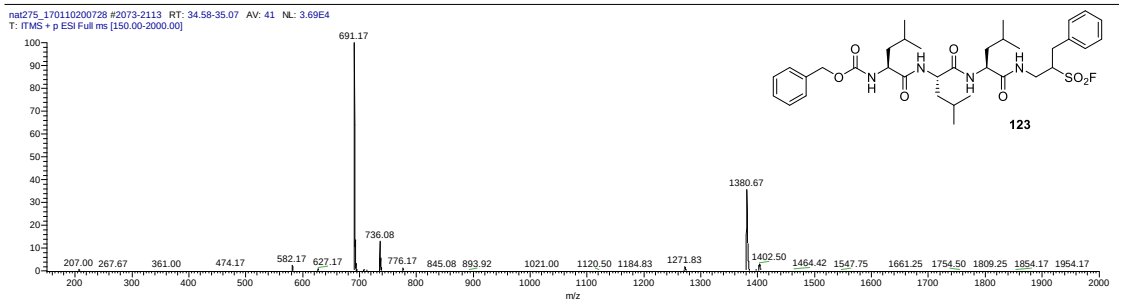
nat275_170110200728 #2073-2113 RT: 34.58-35.07 AV: 41 NL: 3.69E4
T: ITMS + p ESI Full ms [150.00-2000.00]
691.17
736.08
1380.67
m/z

123

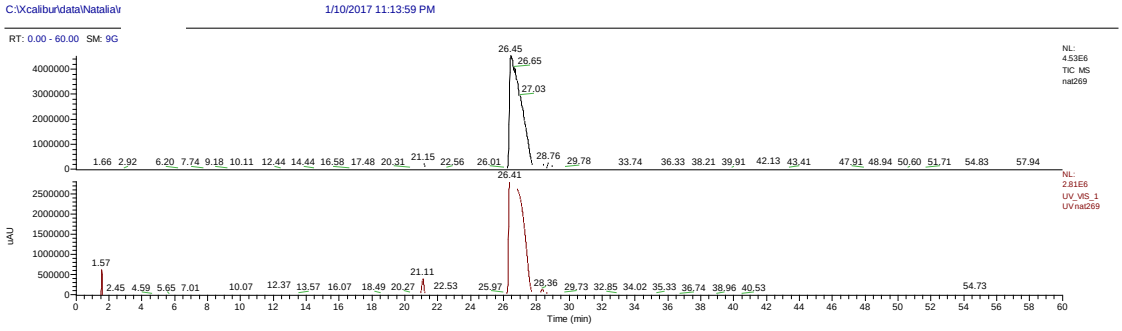
C:\Xcalibur\data\Natalia\v
1/10/2017 11:13:59 PM
RT: 0.00 - 60.00 SM: 9G
26.45
NL: 4.53E6 TIC MS nat269
26.41
NL: 2.81E6 UV_VIS_1 UVnat269
1.57
uAU
Time (min)

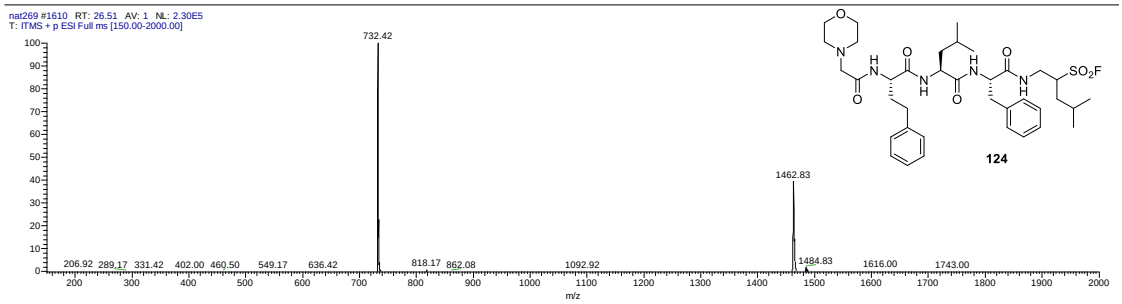
nat269 #1610 RT: 26.51 AV: 1 NL: 2.30E5
T: ITMS + p ESI Full ms [150.00-2000.00]
732.42
1462.83
m/z

124

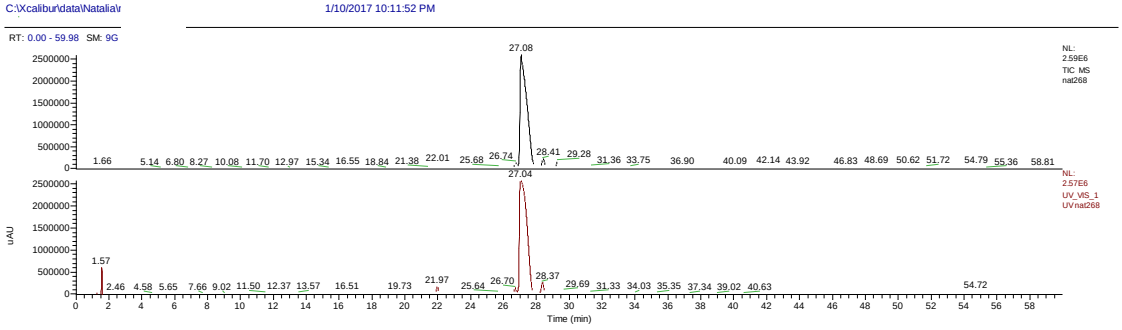
C:\Xcalibur\data\Natalia\v
1/10/2017 10:11:52 PM
RT: 0.00 - 59.98 SM: 9G
27.08
NL: 2.59E6 TIC MS nat268
27.04
NL: 2.57E6 UV_VIS_1 UVnat268
1.57
uAU
Time (min)

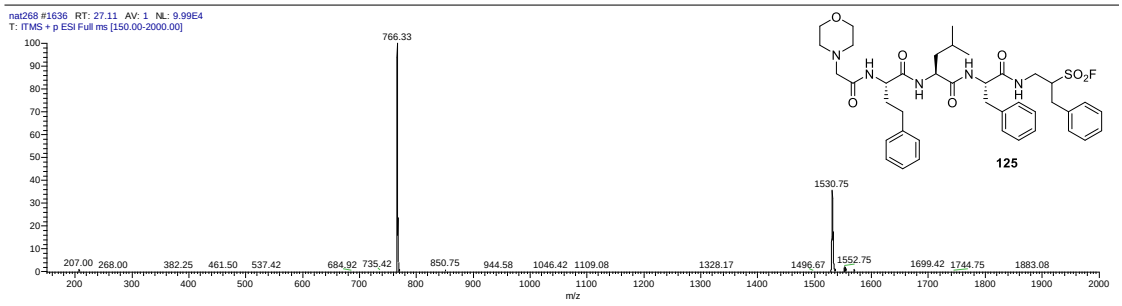
nat268 #1636 RT: 27.11 AV: 1 NL: 9.99E4
T: ITMS + p ESI Full ms [150.00-2000.00]
766.33
1530.75
m/z

125